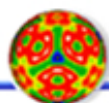
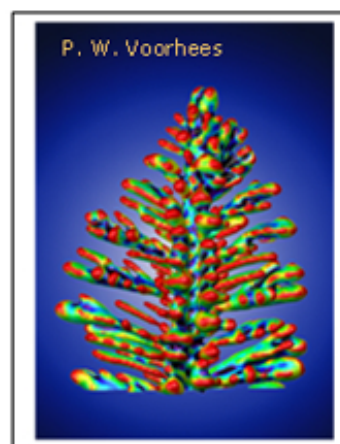
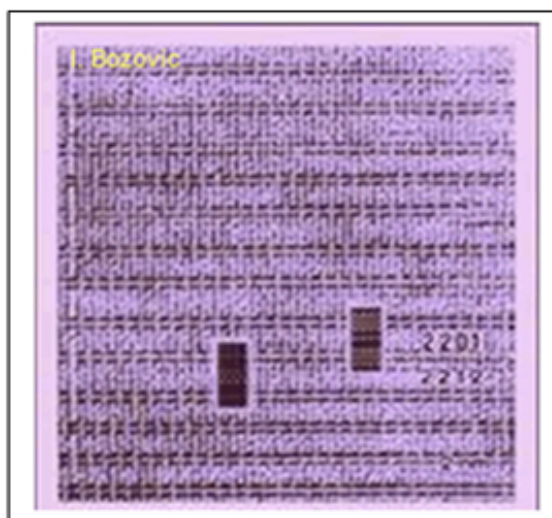
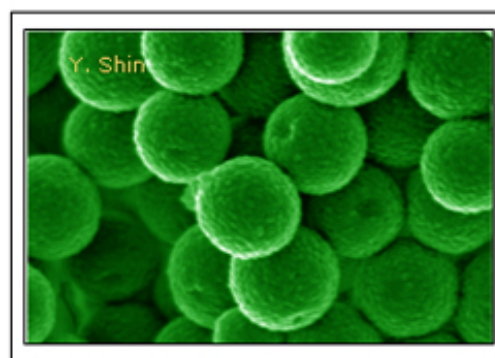
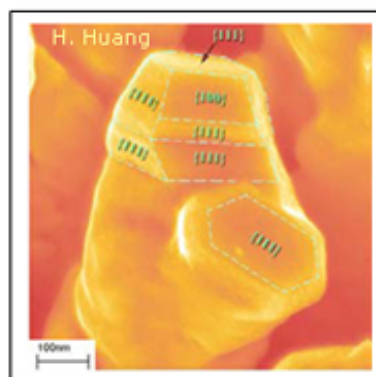
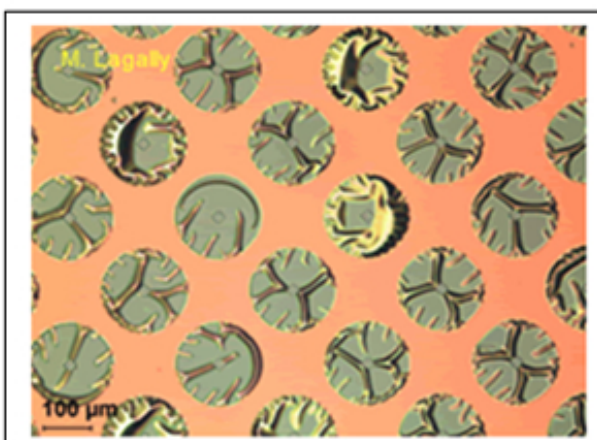


FUNDAMENTAL SYNTHESIS RESEARCH CHALLENGES FOR 21ST CENTURY MATERIALS: MECHANISM AND METHODS

CONTRACTORS MEETING - 2007

Baltimore Marriott Hunt Valley Inn, July 8-11, 2007



Office of Basic Energy Sciences
Division of Materials Sciences and Engineering

Office of
Science
U.S. DEPARTMENT OF ENERGY

On the Cover:

Top Left: Optical image of a strained three-layer Si (110) nanomembrane in the process of release from the silicon-on-insulator (SOI) substrate. Patterned etchant access holes, seen at the center of each circle, allow observation of the etch front around the release holes and the edges of the membrane. The released portions (green) are rippled because of the lateral expansion of the released parts of the membrane during strain sharing.

Courtesy: Max Lagally (University of Wisconsin)

Bottom Left: TEM image of an artificial superlattice synthesized by molecular beam epitaxy. The superlattice is formed by alternating layers of Bi₂Sr₂CuO₆ and Bi₂Ca₂Cu₂O₈ compounds. The hetero-interfaces are atomically sharp. The film was superconducting with a high critical temperature ($T_c = 85$ K).

Courtesy: Ivan Bozovic (Brookhaven National Laboratories)

Top Right: Science-based design of nanorod branching: a $\langle 110 \rangle$ Cu nanorod branches into Yshape as a result of three-dimensional Ehrlich-Schwoebel barrier, geometrical shadowing, and twin formation.

Courtesy: Hanchen Huang (Rensselaer Polytechnic Institute)

Center Right: Hydrothermal dehydration of concentrated aqueous fructose solution in a closed system at 125 degrees Celsius forms non-polar carbon nanospheres via a spontaneous selfassembly process analogous to that by which a detergent emulsifies a mixture of oil and water.

Courtesy: Yongsoon Shin (Pacific Northwest National Laboratories)

Bottom Right: Three-dimensional reconstruction of a free-growing aluminum dendrite in an aluminum-copper eutectic liquid. Solid denotes the aluminum dendrite while the eutectic is transparent. The interface of the dendrite is colored according to its local mean curvature.

Courtesy: Peter Voorhees (Northwestern University)

Table of Contents

Forward	v
Agenda	ix
Poster List	xiv
Invited Speaker Presentation	1
Paul F. McMillan, U College London: Stable vs. Metastable Routes to New Materials via High Pressure Synthesis	3
Session I: Structural and Chemical Complexity	5
Gang Chen, MIT: High Throughput Screening of Nanostructured Hydrogen Storage Materials ...	7
Anand Bhattacharya, ANL: Digital Synthesis: A Pathway to Emergent States at Interfaces of Complex Oxides	11
B. Chu, Stony Brook U: Polymer-Assisted Formation of Nanostructured Transition Metal Clusters and Crystals	15
Cedomir Petrovic, BNL: Bulk Materials Synthesis and Characterization	19
Martin Greven, Stanford: Growth and Study of Mercury-Based High-Temperature Superconductors	25
Alexandra Navrotsky, UC-Davis: Thermochemistry of Anion Defect and Charge Coupled Substitutions in Fluorite and Perovskite Based Materials	29
I. Bozovic, BNL: Synthesis of Atomically Smooth Films of Cuprate Superconductors and Related Oxides	33
T. A. Lograsso, Ames: Rational Growth, Control and Manipulation of Novel Materials	37
John M. Tranquada, BNL: Neutron Scattering: Growth of Large Single-Crystal Samples	41
Poster Session I: Structural and Chemical Complexity	
Ying Liu, Penn State: Odd-Parity, Spin-Triplet Superconductivity in Sr_2RuO_4 and the Physics of Ruthenates in $Sr_{n+1}Ru_nO_{3n+1}$ Series: Single Crystals, Eutectic Systems, and Thin Films	47
L. L. Jones, Ames: Materials Preparation Center	51
Vijay John, Tulane: The Molecular Design Basis for Hydrogen Storage in Clathrate Hydrates ..	55

G. S. Nolas, U South Florida: A Fundamental Study of Type II Clathrate Materials	59
Rafael Muñoz-Espí, Stony Brook U: Effect of Polyethers on the Structure of Polyoxometalates and Derived Oxides.....	63
Poster Session II: Defect-Controlled Synthesis	
Jeff Drucker, Arizona State: Science of Nanowire Epitaxy	65
Hongbo Zeng, UC: Properties of Surfaces and Films Over Large Length and Time Scales	69
Michael Nastasi, LANL: Ion Enhanced Synthesis of Materials.....	73
Eric Chason, Brown U: Determining and Controlling the Fundamental Mechanisms of Sputter Ripple Formation	77
S. A. Scott, U Wisconsin-Madison: Strain Engineered Si-Based Nanomembranes: Ultra-Thin, Transferable, and Flexible Single-Crystal Si.....	81
Session II: Defect-Controlled Synthesis	85
Maria C. Tamargo, CCNY: Use of Nano-Islands (with Dopant and “Codopant”) for Improved Doping in Wide-Bandgap Semiconductors	87
Max G. Lagally, U Wisconsin-Madison: Silicon-Based Nanomembranes, Nanoribbons, and Quantum Dots.....	91
Scott A. Chambers, PNNL: Fundamental Studies of Doping and Properties Modification in Oxide Semiconductor Epitaxial Films	95
Yaoyu Pang, U Texas: Self-Assembled Surface Patterns in Epitaxial Thin Films	99
Session III: Precision Nanoscale Synthesis	103
Xiaogang Peng (invited speaker), U Arkansas: Controlled Synthesis of Colloidal Nanocrystals: From Size, Shape, Bandgap, to Doping.....	105
S. S. Wong, BNL: Synthesis and Characterization of Novel Nanomaterials	107
A. W. Castleman, Jr., Penn State: Superatoms and Metal-Semiconductor Motifs for Cluster Materials	111
Judy Wu, U Kansas: Material Science and Physics at a Nanoscale	115
Hanchen Huang, RPI: From New Kinetic Barrier to Nanorods Design.....	119

M. L. Simpson, ORNL: Tuning Structure and Function of Carbon Nanofiber and Metal Nanoparticles in a Controlled Co-Synthesis Process.....123

D. B. Geohegan, ORNL: In Situ Time-Resolved Measurements of Carbon Nanotube and Nanohorn Growth127

Feng Liu, U Utah: From Nanomechanical Science to Nanofabrication Technology: A New Route Towards Nanotube Synthesis.....129

Poster Session III: Precision Nanoscale Synthesis

R. E. Schaak, Texas A&M: Low Temperature Synthesis Routes to Intermetallic Superconductors.....135

Michael J. Aziz, Harvard: Nanoscale Morphology Evolution Under Ion Irradiation139

Zhili Xiao, Northern Illinois U: One-Dimensional Mesostructures of NbSe₂ and NbN Superconductors.....145

R. Paiella, Boston U: Plasmonic Dispersion Engineering for Light-Emission Efficiency Enhancement.....149

S. J. Peppernick, Penn State: Investigations into the Electronic and Magnetic Behavior of Semiconductor-Transition Metal Clusters via Velocity Map Imaging.....153

P. J. Roach, Penn State: Al₄H₇⁻: A Resilient Building Block for Aluminum Hydrogen Cluster Materials155

Poster Session IV: Hybrid Materials and Assembly

Stephen Hudson, Clemson: Asymmetric Hybrid Nanoparticles.....157

Paul Gourley, SNL: Artificially Structured Semiconductors for Biophotonics161

David J. Norris, U Minnesota: Modification of Thermal Emission via Metallic Photonic Crystals165

B. G. Potter, Jr., U Arizona: Photo-Directed Molecular Assembly of Multifunctional Inorganic Materials169

G. Kane Jennings, Vanderbilt: Surface-Initiated Ionomer Films Based on Modified Poly(n-alkylnorbornene)s173

J. A. Libera, ANL: Spatially Controlled Atomic Layer Deposition in Porous Supports.....177

Poster Session V: Tools for Synthesis and Novel Approaches

George Scherer, Princeton: Stress in Confined Fluids.....179

P. W. Voorhees, Northwestern U: The Evolution of Topologically Complex Structures:
Coarsening of Dendritic Mixtures183

Ivan Petrov, UIUC: Self-Organized Nanostructured Superhard Materials187

R. E. Napolitano, Ames: Solidification Dynamics and Selection Principles.....191

Session IV: Hybrid Materials and Assembly.....195

Michael J. Pellin, ANL: Hybrid Nanoscale Synthesis and Assembly Using Atomic Layer
Deposition.....197

Gregory J. Exarhos, PNNL: Carbohydrate Templates for Engineering Nanostructures201

Bruce C. Bunker, SNL: Active Assembly of Dynamic and Adaptable Materials.....205

Anna C. Balazs, U Pittsburgh: Combing with Light to Create Defect-Free, Hierarchically
Ordered Polymeric Materials.....209

Paul Chaikin (invited speaker), NYU: Self-Replication with Colloids.....213

Session V: Tools for Synthesis and Novel Approaches.....215

Stephen H. Garofalini, Rutgers: Atomistic Structure, Strength, and Kinetic Properties of
Intergranular Films in Ceramics217

T. A. Lograsso, Ames: Rational Growth, Control and Manipulation of Novel Materials.....221

Brent Fultz, Cal Tech: Vibrational Entropy Studies Using Inelastic Neutron Scattering225

Karl Ludwig, Jr., Boston U: Real-Time X-Ray Studies of Surface and Thin Film Processes229

G. B. Stephenson, ANL: *In Situ* Synchrotron X-Ray Studies of Growth and Ferroelectricity in
Ultrathin Perovskite Films233

Author Index.....237

Participants.....241

Foreword

The synthesis of new and higher quality materials is a first and critical step for increasing our understanding of outstanding scientific issues and for the discovery of intriguing new phenomena. The 20th century has shown that the synthesis of optimized materials has been the foundation for almost all technological advancement and consequently significant economic impact. The 21st century presents new challenges such as the structural and chemical complexity of high performance materials, the design of defect controlled and defect tolerant materials, exploring the promise of nanostructured materials, and understanding hybrid organic/inorganic/bio materials. This meeting focuses on the fundamental understanding of the methods and mechanisms in the synthesis of these 21st century materials.

These materials challenges bear a direct connection to priority research directions and grand challenges that were recently identified in the DOE Basic Research Needs (BRN) Workshop Series on Energy. The Office of Basic Energy Sciences BRN Workshop series reports can be found at the following website: <http://www.sc.doe.gov/bes/reports/list.html>. This series of workshops have included BRN to Assure a Secure Energy Future, BRN in Superconductivity, BRN for Solar Energy Utilization, BRN for Solid-State Lighting, BRN for the Hydrogen Economy and BRN for Advanced Nuclear Materials.

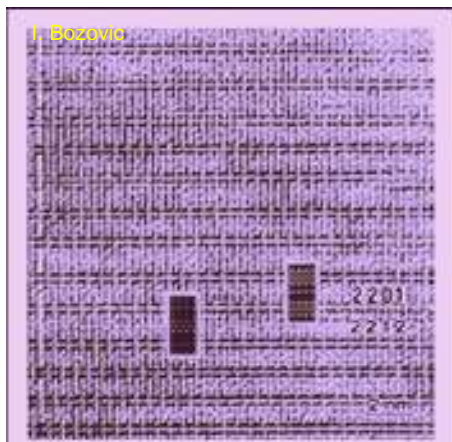
We hope you enjoy the meeting.
Sincerely,

Bonnie Gersten (Program Manager)
Tim Fitzsimmons (Program Manager)
Maria Tamargo (Chair)
Jim Misewich (Chair)

Program Sessions:

- I. [Structural and Chemical Complexity](#)
- II. [Defect-controlled Synthesis](#)
- III. [Precision Nanoscale Synthesis](#)
- IV. [Hybrid Materials and Assembly](#)
- V. [Tools for Synthesis and Novel Approaches](#)
- VI. [Post-deadline Session](#)

[I. Structural and Chemical Complexity:](#)



Background: Many of the materials that have recently been discovered to have outstanding physical properties also are characterized by a chemical or structural complexity. For example, many extreme physical properties are found in the transition metal oxide family of materials. This includes the highest temperature superconductors in

the cuprates, colossal magnetoresistance in the manganates, very high ferroelectricity and piezoelectricity in the titanates, and high thermopower in the cobaltates. In another interesting example, multiferroic ferrite oxide materials can display simultaneous ferromagnetism and ferroelectric behavior. Some of these technologically interesting materials have elaborate unit cells that contain many elements and have many phases. The complexity, density of phases, polytypes, and other issues present ongoing and new challenges for synthesis science.

Examples include:

- Complex oxides
- Semiconductors, including direct bandgap materials
- Multiferroics
- Hydrogen storage materials
- Multiphase metallics

Proposed Grand Challenge: There is a need to be able to synthesize high quality samples of known complex materials in order to enable experiments that will clarify our understanding of such materials. A potential second grand challenge in complex materials is the need for rapid synthesis (and characterization) of new samples for materials exploration and discovery.

II. Defect-controlled Synthesis:



Background: Defects in materials often play a significant role in determining important physical properties of that material. For example defect nature and density can affect the transport of charge in semiconductors. Additionally, trap sites can affect the recombination of electrons and holes in optoelectronic materials, and defects play a role in the critical properties of superconductors. Recent advances in materials synthesis have enabled unprecedented control of defect nature and densities in important materials sets, but there is still a need for new methods and strategies to extend

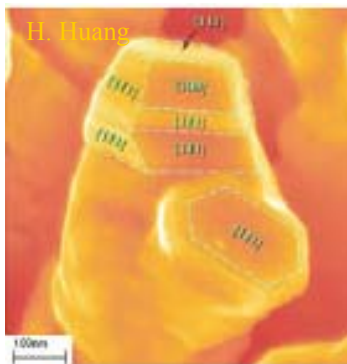
control over a broader range of materials and scales. Among the various synthesis techniques, Molecular Beam Epitaxy offers unique opportunities due to its non-equilibrium nature. By providing atomic level control of the deposition process, one can modify and control the defect structure and its properties, produce low defect density heterointerfaces, and engineer the bandstructure of novel complex materials.

Examples include:

- Dislocation free nanowires
- Single crystals
- Strain/stress engineering techniques in thin films
- Nanostressors, Non-equilibrium doping

Proposed Grand Challenge: To develop methods and strategies for the synthesis of materials with no defects or controlled defect densities in a wide variety of materials (including both organic and inorganic) and scales (from nanoscale to bulk crystals).

III. Precision Nanoscale Synthesis:



Background: Low dimensional materials that enhance quantum confinement effects in one or more dimensions have shown remarkable promise for impact on a number of technologies. For example, it has been demonstrated that a single quasi-1-d carbon nanotube when used as the channel material in a field effect transistor can perform with exceptional characteristics on a scale well below the projected limits for conventional silicon semiconductor devices. Another exciting recent example is the use of 0-d materials (semiconductor quantum dots) to enhance the impact ionization rate and convert a single photo-excitation into multiple excitons (electron-hole pairs), which might have a potential to significantly impact solar energy conversion. However these examples also illustrate the limitations of nanoscale materials: nanomaterial synthesis reproducibility, and the interface between the nanomaterial and the macroscopic world. For example, despite the fact that carbon nanotubes are composed of a single element, the carbon nanotube samples currently available contain a mixture of semi-conducting and metallic nanotubes because current synthesis techniques produce a large diversity of nanotube structures. And the lack of uniformity in size and spatial distribution of semiconductor quantum dots continue to hinder their practical applications.

Examples include:

- Solid state synthesis of nanomaterials
- Nanomaterial cloning
- Clusters (“superatoms”)
- Volmer-Weber growth

Proposed Grand Challenge: There is a need to develop strategies and techniques to synthesize nanomaterials with reproducible structures and chemical composition. There is also another synthesis and processing challenge to produce reproducible, well-characterized interfaces between nanomaterials and the macroscopic world.

IV. Hybrid Materials and Assembly:



Background: Great progress has been made in the quality and understanding of inorganic materials as witnessed by the silicon semiconductor revolution of the 20th century. Recently direct bandgap inorganic semiconductors have also been explored (such as III-V and II-VI materials) for light emission properties. The search for high efficiency light emitting materials has also explored the use of organic materials (OLEDs) to generate optical output. An area of potential opportunity is at the organic/inorganic interface, where perhaps the best properties of each material might be exploited. The “organic” materials that offer interesting promise include bio-materials, where nature has adapted to make remarkable materials with

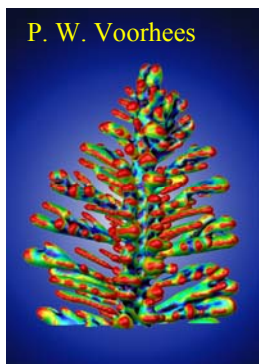
important physical properties in a wide variety of areas from catalysis to the harvesting of light. In addition, a full realization of the promise of self-assembly and directed-assembly techniques is likely to require the use of organic components that play a role in the assembly of inorganic building blocks, either as ligands that control interactions between components, or as templates for assembly.

Examples include:

Organic/inorganic heterostructures
Bio-integration
Templated Self-assembly

Proposed Grand Challenge: To understand the interface between organic (or bio-materials) with inorganic materials so that hybrid materials can be produced and understood to enhance certain functions.

V. Tools for Synthesis and Novel Approaches:



Background: Historically, advanced tools for determining material composition and structure have often helped improve the quality of materials synthesis. For example, the advent of electron diffraction helps molecular beam epitaxy scientists to “count” atomic layers as they are growing (RHEED) and sensitive mass spectrometries (including ion scattering mass spectrometry) have enabled a better understanding of the composition of the layers. In addition, novel techniques and associated tools can be used to synthesize material phases or structures that are not normally accessible. One example would be the use of new high pressure tools to increase oxygen content in transition metal oxide materials. Finally, computation is rapidly advancing to the state where it can play a role in the synthesis of new materials or help to improve the quality of synthesis of important materials. This session will focus on new tools and novel approaches for control and understanding of synthetic processes.

Examples include:

Ion beam processing
Inelastic neutron scattering
Synthesis of volatile materials
Computational tools

Proposed Grand Challenge: To improve the quality of materials synthesis and to enhance the search for new materials.

VI. Post-deadline Session

This session is reserved for significant late-breaking results in each of the categories listed above. The deadline will be June 22 for submission of abstracts. A very limited number of abstracts will be accepted for oral presentation in a special session of the meeting.

**Fundamental Synthesis Research Challenges for
21st Century Materials: Mechanism and Methods**
Sponsored by the U.S. Department of Energy, Office of Basic Energy Sciences
July 8-11, 2007

Agenda

Sunday, July 8, 2007

- 3:00 - 6:00pm Registration
- 5:00 - 6:00 Reception
- 6:00 - 7:00 ***** Dinner *****
- 7:30 - 8:20 *Introductory Remarks*
Harriet Kung (20 min)
Director, Division of Materials Science and Engineering
Bonnie Gersten/ Tim Fitzsimmons (10 min)
Program Managers, Synthesis and Processing Science
Maria Tamargo/ Jim Misewich (10 min each)
City College of New York/ Brookhaven National Laboratory
- 8:20 - 9:00pm **Invited Speaker** - Paul McMillan
Professor of Solid State Chemistry
University College London
*Stable vs Metastable Routes to New Materials via High
Pressure Synthesis*

Monday, July 9, 2007

- 7:00 - 8:00am ***** Breakfast *****
- Session I** **Structural and Chemical Complexity**
Chair: G.S. Nolas, University of South Florida
- 8:30 - 9:00 Gang Chen, Massachusetts Institute of Technology
*High Throughput Screening of Nanostructured Hydrogen
Storage Materials*
- 9:00 - 9:30 Anand Bhattacharya, Argonne National Laboratory
*Digital Synthesis: A Pathway to Emergent States at
Interfaces of Complex Oxides*

- 9:30 - 10:00 Ben Chu, Stony Brook University
Polymer-Assisted Formation of Nanostructured Transition Metal Clusters and Crystals
- 10:00 - 10:30 ***** Coffee Break *****
- 10:30 - 11:00 Cedomir Petrovic, Brookhaven National Laboratory
Bulk Materials Synthesis and Characterization
- 11:00 - 11:30 Martin Greven, Stanford University
Growth and Study of Mercury-Based High-Temperature Superconductors
- 11:30 - 12:00pm Alexandra Navrotsky, University of California at Davis
Thermochemistry of Anion Defect and Charge Coupled Substitutions in Fluorite and Perovskite Based Materials
- 12:00 - 1:00 ***** Lunch Break *****
- 1:00 - 1:30 Ivan Bozovic, Brookhaven National Laboratory
Synthesis of Atomically Smooth Films of Cuprate Superconductors and Related Oxides
- 1:30 - 2:00 P.C. Canfield, Ames Laboratory
Rational Growth, Control and Manipulation of Novel Materials
- 2:00 - 2:30 John Tranquada, Brookhaven National Laboratory
Neutron Scattering: Growth of Large Single-Crystal Samples
- 2:30 - 3:30 **Poster Session -**
I. Structural and Chemical Complexity
II. Defect-Controlled Synthesis
- 3:30-4:00 ***** Coffee Break *****
- Session II** **Defect-Controlled Synthesis**
Chair: Jeff Drucker, Arizona State University
- 4:00 - 4:30 Maria Tamargo, City College of New York
Use of Nano-Islands (with Dopant and “Codopant”) for Improved Doping in Wide-Bandgap Semiconductors

- 4:30 - 5:00 Max Lagally, University of Wisconsin-Madison
Silicon-Based Nanomembranes, Nanoribbons, and Quantum Dots
- 5:00 - 5:30 Scott Chambers, Pacific Northwest National Laboratory
Fundamental Studies of Doping and Properties Modification in Oxide Semiconductor Epitaxial Films
- 5:30 - 6:00 Rui Huang, University of Texas
Self-Assembled Surface Patterns in Epitaxial Thin Films
- 6:00 - 7:30 ***** Dinner Break *****
- 7:30 - 8:30 **Postdeadline Session 1**
Chair: Vijay John, Tulane University
- 8:30 - 10:00 **Discussions and Interactions (Cash Bar)**
Posters remain up

Tuesday, July 10, 2007

- 7:00 - 8:00am ***** Breakfast *****
- Session III** **Precision Nanoscale Synthesis**
Chair: Michael Aziz, Harvard School of Engineering and Applied Sciences
- 8:30 - 9:00am **Invited Speaker:** Xiaogang Peng, University of Arkansas
Controlled Synthesis of Colloidal Nanocrystals: From Size, Shape, Bandgap, to Doping
- 9:00 - 9:30 Stanislaus Wong, Stony Brook University
Synthesis and Characterization of Novel Nanomaterials
- 9:30 - 10:00 A.W. Castleman, Jr., Pennsylvania State University
Superatoms and Metal-Semiconductor Motifs for Cluster Materials
- 10:00 - 10:30 ***** Coffee Break *****
- 10:30 - 11:00 Judy Wu, University of Kansas
Material Science and Physics at a Nanoscale

- 11:00 - 11:30 Hanchen Huang, Rensselaer Polytechnic Institute
From New Kinetic Barrier to Nanorods Design
- 11:30 - 12:00pm M.L. Simpson, Oak Ridge National Laboratory
Tuning Structure and Function of Carbon Nanofiber and Metal Nanoparticles in a Controlled Co-Synthesis Process
- 12:00 - 1:00 ***** Lunch Break *****
- 1:00 - 1:30 D.B. Geohegan, Oak Ridge National Laboratory
In Situ Time-Resolved Measurements of Carbon Nanotube and Nanohorn Growth
- 1:30 - 2:00 Feng Liu, University of Utah
From Nanomechanical Science to Nanofabrication Technology: A New Route towards Nanotube Synthesis
- 2:00 - 3:00 **Poster Session**
III. Precision Nanoscale Synthesis
IV. Hybrid Materials and Assembly
V. Tools for Synthesis and Novel Approaches
- 3:00 - 3:30 ***** Coffee Break *****
- Session IV** **Hybrid Materials and Assembly**
Chair: Paul Gourley, Sandia National Laboratories
- 3:30 - 4:00pm Michael Pellin, Argonne National Laboratory
Hybrid Nanoscale Synthesis and Assembly using Atomic Layer Deposition
- 4:00 - 4:30 Gregory Exarhos, Pacific Northwest National Laboratory
Carbohydrate Templates for Engineering Nanostructures
- 4:30 - 5:00 Bruce Bunker, Sandia National Laboratory
Active Assembly of Dynamic and Adaptable Materials
- 5:00 - 5:30 Anna Balazs, University of Pittsburgh
Combining with Light to Create Defect-Free, Hierarchically Ordered Polymeric Materials
- 5:30 - 6:00pm **Invited Speaker:** Paul Chaikin, New York University
Self-Replication with Colloids

6:00 - 7:30 ***** Dinner Break *****

7:30 - 8:30 **Postdeadline Session 2**
Chair: T. A. Lograsso, Ames Laboratory

8:30 - 10:00pm **Discussions and Interactions (Cash Bar)**
Posters remain up

Wednesday, July 11, 2007

7:30 - 8:30am ***** Breakfast *****

Session V **Tools for Synthesis and Novel Approaches**
Chair: P.W. Voorhees, Northwestern University

8:30 - 9:00am Stephen Garofalini, Rutgers University
Atomistic Structure, Strength, and Kinetic Properties of Intergranular Films in Ceramics

9:00 - 9:30 T.A. Lograsso, Ames Laboratory
Rational Growth, Control and Manipulation of Novel Materials

9:30 - 10:00 ***** Coffee Break *****

10:00 - 10:30 Brent Fultz, California Institute of Technology
Vibrational Entropy Studies Using Inelastic Neutron Scattering

10:30 - 11:00 Karl F. Ludwig, Jr., Boston University
Real-Time X-ray Studies of Surface and Thin Film Processes

11:00 - 11:30 G.B. Stephenson, Argonne National Laboratory
In Situ Synchrotron X-ray Studies of Growth and Ferroelectricity in Ultrathin Perovskite Films

11:30 - 11:45 Closing Remarks

11:45 ***** Lunch and Adjourn *****

POSTER LIST

I. Structural and Chemical Complexity Posters:

Ying Liu, Pennsylvania State University
Odd-parity, Spin-triplet Superconductivity in Sr_2RuO_4 and the Physics of Ruthenates in $Sr_{n+1}Ru_nO_{3n+1}$ Series: Single Crystals, Eutectic Systems, and Thin Films

L. Jones, Ames Laboratory
Materials Preparation Center

Vijay John, Tulane University
The Molecular Design Basis for Hydrogen Storage in Clathrate Hydrates

G.S. Nolas, University of South Florida
A Fundamental Study of Type II Clathrate Materials

Rafael Muñoz-Espí, (student) Stony Brook University
Effect of Polyethers on the Structure of Polyoxometalates and Derived Oxides

II. Defect-Controlled Synthesis Posters:

Jeff Drucker, Arizona State University
Science of Nanowire Epitaxy

Hongbo Zeng (student), University of California
Properties of Surfaces and Films over Large Length and Time Scales

Michael Nastasi, Los Alamos National Laboratory
Ion Enhanced Synthesis of Materials

Eric Chason, Brown University
Determining and Controlling the Fundamental Mechanisms of Sputter Ripple Formation

Yaoyu Pang, Sanjay Banarjee (student), and Rui Haung, University of Texas at Austin
Self-assembled surface patterns in epitaxial thin films

Shelley Scott (student) and Max Lagally, University of Wisconsin-Madison
Strain engineered Si-based nanomembranes: ultra-thin, transferable, and flexible single-crystal Si

III. Precision Nanoscale Synthesis Posters:

R.E. Schaak, Texas A&M University
Low Temperature Synthesis Routes to Intermetallic Superconductors

Michael Aziz, Harvard School of Engineering and Applied Sciences
Nanoscale Morphology Evolution under Ion Irradiation

Zhili Xiao, Northern Illinois University
One-dimensional Mesostructures of NbSe₂ and NbN Superconductors

R. Paiella, Boston University
Plasmonic Dispersion Engineering for Light-Emission Efficiency Enhancement

S.J. Peppernick (student) and A.W. Castleman, Jr., Pennsylvania State University
Investigations into the Electronic and Magnetic Behavior of Semiconductor Transition Metal Clusters via Velocity Map Imaging

P. J. Roach (student), W. H. Woodward, and A.W. Castleman, Jr., Pennsylvania State University ; A.C. Reber (student) and S.N. Khanna, Virginia Commonwealth University
Al₄H₇⁻: A Resilient Building Block for Aluminum Hydrogen Cluster Materials

Roberto Paiella, Boston University
Plasmonic Dispersion Engineering for Light-Emission Efficiency Enhancement

IV. Hybrid Materials and Assembly Posters:

George Chumanov, Clemson University
Asymmetric Hybrid Nanoparticles

Paul Gourley, Sandia National Laboratory
Artificially Structured Semiconductors for Biophotonics

Andreas Stein, University of Minnesota
Modification of Thermal Emission via Metallic Photonic Crystals

B.G. Potter, Jr., University of Arizona
Photo-Directed Molecular Assembly of Multifunctional Inorganic Materials

Brad Berron (student), Vanderbilt University
Surface-Initiated Ionomer Films Based on Modified Poly(n-alkylnorbornene)s

Joseph Libera (student) and Michael Pellin, Argonne National Laboratory
Spatially Controlled Atomic Layer Deposition in Porous Supports

V. Tools for Synthesis and Novel Approaches Posters:

George Scherrer, Princeton University
Stress in Confined Fluids

P.W. Voorhees, Northwestern University

The Evolution of Topologically Complex Structures: Coarsening of Dendritic Mixtures

Ivan Petrov, University of Illinois at Urbana-Champaign
Self-organized Nanostructured Superhard Materials

R.E. Napolitano, Ames Laboratory
Solidification Dynamics and Selection Principles

Invited Speaker Presentation

Paul McMillan, University College London

This page is intentionally blank

Title: Stable vs. Metastable Routes to New Materials *via* High Pressure Synthesis

Author: **Paul F. McMillan**, *Department of Chemistry and Materials Chemistry Centre, University College London, 20 Gordon Street, London WC1H 0AJ, UK*

Abstract:

We use a combination of diamond anvil cell and "large volume" press techniques to synthesise new materials at high pressure and high temperature conditions, and to carry out *in situ* studies of their structure and properties. Our current work is focused on: (i) transition metal nitrides and carbides (high hardness; metallic; superconductors); (ii) main group nitride and oxynitride spinels (wide bandgap; high hardness); light element solids including icosahedral B₆O-B₆N solid solutions and both layered and dense C-N-H solids (potentially superhard materials, with variable bandgap, and potentially new intercalation reactions). We use the P and T variables to explore and "tune" both stable and metastable transformations and reactions. Chemically designed precursors are used to access a wide range of metastable states and to form composite materials. We also explore the metastably compressed amorphous state to generate new materials.

This page is intentionally blank

Session I

Structural and Chemical Complexity

Session Chair: G.S. Nolas, University of South Florida

This page is intentionally blank

High Throughput Screening of Nanostructured Hydrogen Storage Materials

Gang Chen and Mildred S. Dresselhaus
Massachusetts Institute of Technology, Cambridge, MA 02139

Costas P. Grigoropoulos and Samuel S. Mao
University of California at Berkeley, Berkeley, CA 94720

Xiaodong Xiang
Intematix Corporation, Fremont, CA 94538

Taofang Zeng
North Carolina State University, Raleigh, NC 27695

1. PROGRAM SCOPE

The project aims at developing nanostructured metastable hydride materials that are capable of storing hydrogen with both chemisorption and physisorption mechanisms, and with fast sorption and desorption kinetics, and good heat transfer characteristics. These goals are to be achieved through combining a high throughput combinatorial materials search with fundamental studies to identify high capacity hydrogen storage materials with fast sorption and desorption kinetics. The following targets have been identified:

- Destabilize metal hydrides using nanostructures synthesized by laser pyrolysis and sol-gel chemistry.
- Development of a high throughput screening method for nanostructured metastable metal and complex hydrides using combinatorial materials discovery principles.
- Development of nanoporous hydride materials with integrated chemisorption and physisorption through synthesis of nanocomposite materials with fine-tuning of the process conditions.
- Development of materials characterization techniques which are compatible with the combinatorial synthesis.
- Development of models and simulations for the fundamental understanding of size effects on the thermodynamics, kinetics of hydrogen sorption and desorption, and heat transfer in nanostructured hydrogen storage materials.

2. RECENT PROGRESSES

2.1 Synthesis

Our materials strategies are to synthesis nanophased materials using combinatorial methods and explore methods to scale up the materials while improving their thermodynamic and kinetic properties.

Combinatorial synthesis: Using Intematix's combinatorial tool, we extended our combinatorial synthesis approach using laser pyrolysis to successfully generate ternary samples (Al-Mg-Ni, Fe-Ni-Co, Li-Al-Ti, Ca-B-Ni). This promotes fast screening process by making samples which contain continuous composition changes of each element and allow for

determination of the most promising metal hydrides. Figure 1 shows an example of Al-Mg-Ni library.

Mesoporous silica scaffolds for enhanced MgH_2 release kinetics and improved thermodynamics: Magnesium hydride (MgH_2) powders and several other types of metal nanoparticles (20~100 nm) have been successfully incorporated into nanoporous silica aerogels. We have modified a well-established aerogel synthesis route to eliminate residual water after hydrolysis and have greatly minimized MgH_2 dehydrogenation by rapid condensation and solvent exchanges. Nanoparticles used to catalyze MgH_2 decomposition have been incorporated into the gels. We have developed a new synthesis procedure for these selected metal nanoparticles employed in metal displacement reduction. The resulting aerogels are heavily loaded with MgH_2 powder.

2.2 Materials Characterization

The materials characterization effort includes developing fast screening tools for combinatorially synthesized samples, detailed characterization on promising samples, and mechanistic studies. Detailed characterization using standard methods such as X-ray, gravimetric measurements, BET, etc. are being carried out on MgH_2 -based nanoporous samples [Fig.2].

Fast Screening Techniques: We are developing several techniques for fast screening of samples. One is based on reflectivity measurement. The metallic and hydrogenated states of metal hydrides have different optical properties. In-situ reflectivity measurements have been used to characterize the reflectivity change of the prepared ternary samples during H_2 charging. The reflectivity study of the sample when exposed to hydrogen is used to determine absorption temperature and kinetics and to give qualitative estimate of

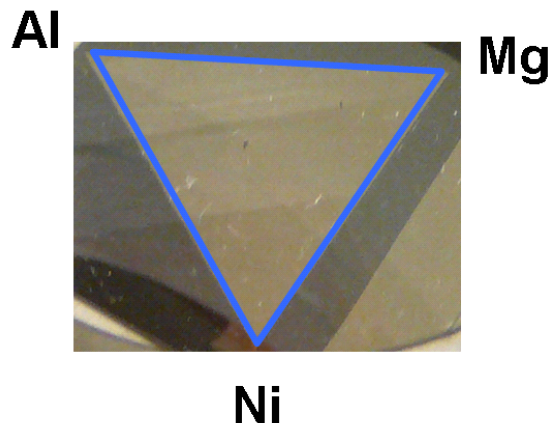


Figure 1: Example of Al-Mg-Ni ternary library generated at Intematix.

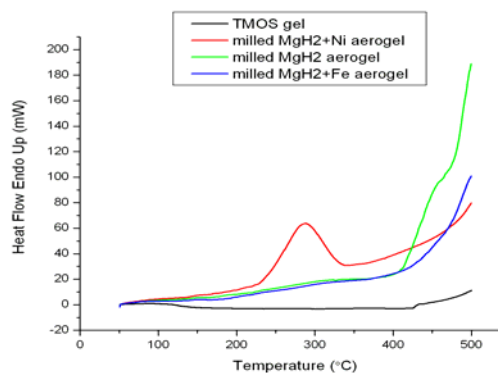


Figure 2 DSC results on MgH_2 embedded in aerogel. The use of silica nanoporous scaffold and nanostructured MgH_2 facilitates MgH_2 decomposition at lower temperatures than MgH_2 alone.

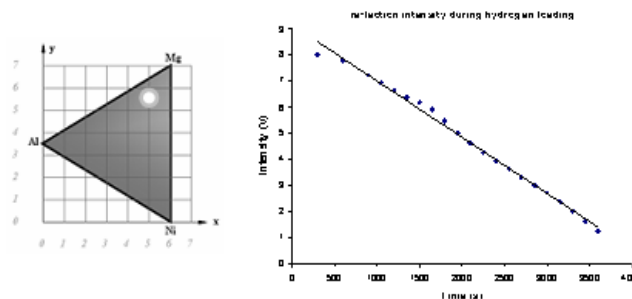


Figure 3 IR reflectivity measurements can be used to study kinetics of the reaction. In situ IR reflectivity measurement of the Mg-Al-Ni sample during H_2 charging at RT, 300 psi H_2 (the right plot). The left picture shows the sample position on X-Y stages.

the sorption capacity [Fig.3]. We are also developing a pump and probe set-up for characterizing the thermal conductivity and specific heat of combinatorially synthesized materials.

TEM Experiments: To experimentally investigate size effects on thermodynamic properties, we are currently carrying out TEM based experiment on ball milled MgH_2 . In order to verify that excess energy due to excess volume in deformed regions of the metal hydrides, we use a TEM sample holder that has been modified to provide real time temperature control of the sample (300K to 800K). The study of the dehydration reaction under the TEM allows us to follow in real-time the dehydration reaction and to determine the effect on the release temperature of the particle size, the grain size and the concentration and nature of the defects.

2.3 Modeling

We are developing models that explore size effects on thermodynamic, kinetic, and heat transfer properties of nanostructured hydrogen storage materials, and use the models to refine our experimental approaches. The size effects on kinetic and heat transfer characteristics are projected to system level to evaluate their impacts on systems. In the case of MgH_2 , we identified that mass transfer through the powder does not significantly limit absorption kinetics for particle diameters 10 μm and larger, although it becomes as significant as heat transfer for particles 100 nm and smaller. This analysis is useful to establish practical design considerations to ensure proper thermal management and adequate gas flow for actual hydrogen storage systems.

We are engaged in modeling the size effects on the thermodynamics and kinetics for physisorption and chemisorption. Efficient hydrogen storage materials should have a small enthalpy of formation. We investigated the effect of surface energy, grain boundary energy and the presence of metastable hydride phase (such as $\gamma\text{-MgH}_2$) and found that they could not be responsible for the observed reduction of the enthalpy of formation in metal hydrides that have been subject to high energy treatments. We hypothesized that excess enthalpy present in highly deformed regions could be responsible for the observed reduction and we proposed a thermodynamic model that can reproduce observations.

3. FUTURE PLANS

We will continue the effort of high throughput material screening to identify Mg, Li and Ca based alloys that may have high capacity of hydrogen storage, and explore ways to synthesis promising materials into nanoparticle form and incorporating them to nanoporous templates for increased kinetics and improved thermodynamics properties. We will test different combination of catalysts including carbon nanotubes, bimetals in the MgH_2 and increase the loading ratio of MgH_2 in aerogels.

We will continue to refine fast screening methods that match combinatorial synthesis and perform TEM experiments to further understand the relation between structure, enthalpy, kinetics and release temperature in metal MgH_2 .

We plan to pursue our thermodynamic investigation of the effect of lattice deformations and structural defects on enthalpy of formation while looking at possible ways to promote lattice deformations only in the hydrided phase as to lower the enthalpy of formation. Such investigation will be centered on Mg based hydrides and performed using DFT and molecular dynamics through the quantum-espresso package. We are developing Monte Carlo simulations of thermal transport in powdered hydride materials. These simulations will combine phonon and

molecular gas transport in order to properly characterize the size effects for hydride powders, and their implications for thermal management.

4. PUBLICATIONS

Journal Publications

1. V. Bérubé, G. Radtke, M. Dresselhaus, G. Chen, Size effects on the hydrogen storage properties of nanostructured metal hydrides: A review, *Int J Energy Research*, in press, 2007.
2. C. Wu, T. Zeng, Size-Tunable Synthesis of Metallic Nanoparticles in a Continuous and Steady-Flow Reactor, *Chemistry of Materials*, vol. 19, pp. 123-125, 2007.
3. S. S. Mao, X. Chen, A. Hunt, X.Zhang, Hydrogen Sorption in Nanoporous Metal-Inorganic Networks, submitted, 2006.
4. C. Wu, B. P. Mosher, T. Zeng, Rapid Synthesis of Gold and Platinum Nanoparticles Using Metal Displacement Reduction with Sonomechanical Assistance, *Chemistry of Materials*, vol. 18, pp. 2925-2928, 2006.

Selected Conference Presentations

1. B. P. Mosher, C. Wu, S. S. Mao, G. Chen, and T. Zeng, Investigation of Hydrogen Storage and Absorption/Release Kinetics in Nanocomposite Metal Hydride and Nanoscaffolds, MRS Spring Meeting, San Francisco, April 2006.
2. B. P. Mosher, C. Wu, S. S. Mao, G. Chen, T. Zeng, Nanoscaffolding Metal Hydrides for Enhanced H₂ Storage, MRS Spring Meeting, San Francisco, April 2006.
3. M. S. Rogers, S. S. Mao, C. P. Grigoropoulos, Pulsed laser deposition of nanoparticles with nano- and femtosecond pulses, SPIE Photonics West, San Jose, CA, January 23-25, 2007 .
4. V. Berube, G. Radtke, G. Chen, M. Dresselhaus, Thermodynamic Study of Nanoscale Metal Hydride for Hydrogen Storage, MRS Fall Meeting, Boston, MA, November 27-December 1, 2006 .
5. S. Barcelo, C. Dong, J. Chiou, J. Guo, S. Mao, Soft X-ray Emission and Absorption Spectra of Nickel Magnesium Hydride, presented at Energy Nanotechnology International Conference, MIT, June 25-28, 2006.
6. V. Berube, G. Radtke, M. Dresselhaus, G. Chen, Thermodynamic Study of Nanoscale Metal Hydrides for Hydrogen Storage, presented at Energy Nanotechnology International Conference, MIT, June 25-28, 2006..
7. K. R. Carrington, X. Chen, A. Hunt, S. S. Mao, Characterization of Hydrogen Storage Capacity of Silica Aerogel, presented at Energy Nanotechnology International Conference, MIT, June 25-28, 2006.
8. M. S. Rogers, S. S. Mao, C. P. Grigoropoulos, June 25-28, 2006, Hydrogen Storage of Mg-Ni Prepared by Pulsed Laser Deposition, presented at Energy Nanotechnology International Conference, MIT.
9. G. Chen, June 25 2006, Hydrogen Storage, tutorial at the Energy Nanotechnology
10. M. Dresselhaus, Keynote talk at European Materials Research (EMRS), Nice, France, May 31, 2006.
11. M. Dresselhaus, Basic Energy Sciences Workshop on Hydrogen, Washington DC, May 18, 2006.

Digital Synthesis: A Pathway to Emergent States at Interfaces of Complex Oxides.

Anand Bhattacharya, Samuel D. Bader (Center For Nanoscale Materials and Materials Science Division, Argonne National Laboratory) and J. N. Eckstein (Department of Physics, University of Illinois at Urbana - Champaign).

Program Scope:

Compelling questions in materials physics arise in doped complex oxides, with the emergence of novel states of condensed matter that possess strikingly different properties from their parent compounds. Competing interactions within these materials give rise to a variety of different ground states that have distinct broken symmetries, giving rise to the rich phase diagrams that are the hallmark of strongly correlated systems. When materials with distinct ground states that are chemically and structurally compatible are brought into intimate proximity, new states of condensed matter will emerge at their interfaces due to correlations involving charge, spin, strain, dimensional confinement and artificially broken symmetries, with attributes that are qualitatively different from the those of the constitutive parts. The disorder inherent to conventional doping can profoundly influence emergent behavior in complex oxides, and the challenge of separating the effects of disorder from the ‘intrinsic’ physics is critical to our understanding of these collective states. We use ozone-assisted oxide MBE to implement a strategy that we choose to call Digital Synthesis. Within this scheme, materials are synthesized by interleaving integer unit cells of transition metal perovskites, where the *A*-site in a given layer is populated by a single cation. For example, $\text{La}_{2/3}\text{Sr}_{1/3}\text{MnO}_3$ may be synthesized as a superlattice of $(\text{LaMnO}_3)_{2n}(\text{SrMnO}_3)_n$. With these strategies, we will explore systems where the charge transfer or ‘doping’ occurs exclusively at well-ordered interfaces, along with other reconstructions associated with lattice and spin degrees of freedom. Furthermore, these emergent interfacial states are particularly susceptible to gate-electric fields, because their restricted dimensionality enables a relatively small capacitively induced charge to create large changes in carrier density in the interfacial region. Our techniques will allow us to engineer the transparency of interfaces to charge and spin, and to create structures where symmetries are broken artificially. Specifically, we will target four areas: (i) *interfacial collective states* that arise out of magnetic and electronic reconstruction at interfaces, (ii) *electric field-effect gating* of magnetic and superconducting properties at interfaces, (iii) *proximity induced quantum coherence*, tackling the predictions of a new class of triplet superconductivity in proximity *F/S/F* structures, and (iv) *tailored multifunctional materials*, with multiferroic properties by using artificially broken symmetries within superlattices that allow for the simultaneous occurrence of ferromagnetism and ferroelectricity, and the cross-couplings between these order parameters.

Recent Progress:

Within the last year, we have synthesized and characterized ordered analogues of $\text{La}_{1-x}\text{Sr}_x\text{MnO}_3$ for $x=0.33$ and $x=0.67$ in superlattices of $(\text{LaMnO}_3)_{2n}(\text{SrMnO}_3)_n$ for $n=1-5$, and $(\text{LaMnO}_3)_m(\text{SrMnO}_3)_{2m}$ for $m=1-3$, respectively.

In the $(\text{LaMnO}_3)_{2n}(\text{SrMnO}_3)_n$ superlattices, we have studied the metal-insulator transition that occurs as a function of increasing n . Using neutron scattering, we have established that the insulating state at low temperatures for $n=5$ is associated with a strongly modulated

ferromagnetic order parameter, with a modulation wave-vector commensurate with the superlattice (with Mike Fitzsimmons, Los Alamos). This suggests a Mott-like transition from a 3-D uniform ferromagnetic metal at low n to a quasi-2D modulated ferromagnetic insulator at high n . Furthermore, exploiting a forbidden peak in the x-ray reflectivity, using resonant Bragg scattering at the O-K edge, we have obtained direct evidence for electronic reconstruction at LMO/SMO interfaces by measuring the evolution of this forbidden peak while cooling through the ferromagnetic transition (with Peter Abbamonte, UIUC).

In the $(\text{LaMnO}_3)_m(\text{SrMnO}_3)_{2m}$ system, we have observed signatures of an increase in the magnetic ordering temperature for $m=1-3$, above the known bulk Neel temperature for the material. This study is ongoing.

Future Plans:

Theme 1: Novel Two-Dimensional Electron Gas systems

The two dimensional electron gas (2-DEG) sets the stage for some of the best known manifestations of strong correlations, ranging from quantum-hall states in high mobility 2-DEGs to high-temperature superconductivity in the two-dimensional cuprates. New methods of realizing 2-DEGs at interfaces of complex oxides in the past few years have opened up a range of new possibilities. In one realization,¹ interfaces between two insulators, LaTiO_3 (a Mott-insulator) and SrTiO_3 (band insulator), were found to be conducting, a result of charge transfer between the two materials. Electrons ‘leak’ from the Ti d^1 in LaTiO_3 into the adjacent Ti d^0 states in SrTiO_3 , where they become mobile.² This in principle analogous to delta-doping in high-mobility quantum wells using conventional semiconductors, where the electron gas is situated in a region removed at a distance from the dopant ions. This method of introducing charge at coherent interfaces allows for the realization of ‘doped’ materials without the disorder that is inherent to chemical doping strategies. The ability to engineer the distribution of charge using a suitable arrangement of digital layers within a heterostructure will allow the exploration of phases that may emerge in many binary pairs of materials such as $\text{LaMnO}_3/\text{SrMnO}_3$, $\text{LaCuO}_4/\text{SrCuO}_4$, without the disorder that results in the usual chemical doping methods.

Using a different strategy, polar insulators (eg. LaAlO_3) and non-polar insulators (eg. SrTiO_3) may be brought together to create charged interfaces, and the consequent electric field can cause mobile charge to be induced in order to screen the interfacial potential.³ This idea has been tried with $\text{LaAlO}_3/\text{SrTiO}_3$, and a high mobility electron gas was observed at low temperatures.⁴ However, at this time it is believed that the observations are clouded by extrinsic effects such as oxygen vacancies in the SrTiO_3 .⁵ Furthermore it has been found that the effect is quite sensitive to the exact sequence of atomic layers between the two materials – for example $\text{AlO}_2/\text{LaO}/\text{TiO}_2/\text{SrO}$ is found to behave quite differently from $\text{LaO}/\text{AlO}_2/\text{SrO}/\text{TiO}_2$, as might be expected from considerations of polar discontinuities at the interfaces.

If the past is any indicator, creating cleaner materials with better control may lead to interesting new phenomena, and the paradigms listed above give us a roadmap to explore possibilities with different combinations of materials. We intend to address some of the key materials issues with our state-of-the-art deposition system. Firstly, we shall be using ozone as the oxidizing gas, which is known to be six orders of magnitude more effective than oxygen. We anticipate that this

will go a long way in addressing the problem of oxygen vacancies that tends to inadvertently dope materials with carriers. Furthermore, using MBE we can deposit an arbitrary sequence of oxide layers and are not constrained by the stoichiometry of a target, as is the case in sputtering or Pulsed Laser Deposition. This gives us an additional degree of control over the exact configuration of the interface, and allows greater flexibility in engineering their properties.

Having a two dimensional electron gas in a perovskite heterostructure that can be readily integrated with other perovskite materials opens up very interesting possibilities. Just to name a few, integrating these structures with gate dielectrics would open up the path to a new class of field-effect transistors, using half metallic ferromagnetic electrodes would allow the exploration of spin transport within these 2-DEGs, and superconducting electrodes could possibly lead to laterally coupled Josephson devices.

Theme 2: Tuning Magnetism with Electric Fields

In this section, we propose two different ways that electric fields may be used to influence the coupling between magnetic atoms.

In the first instance, we introduce a simple modification of the idea mentioned in a previous section of using digital layers to create carrier doping at coherent interfaces. We shall extend these ideas to the magnetic doping of semiconducting perovskites.⁶ As is done routinely in conventional semiconductors, we will adapt these strategies to create modulation-doped structures of the system $\text{La}_{0.5}\text{Sr}_{0.5}\text{Ti}_{1-y}\text{M}_y\text{O}_3$, ($\text{M} = \text{Co}, \text{Mn}..$) where the functionalities of magnetism and charge doping are separated. Here, the carriers that mediate the exchange interaction between the magnetic atoms are obtained at the $\text{LaTiO}_3/\text{SrTiO}_3$ interface, while the magnetic dopants are placed in a ‘delta’ layer of $\text{SrTi}_{1-y}\text{M}_y\text{O}_3$ in the vicinity of this interface. In the dilute limit ($y \ll 1$), this allows us to fabricate material with very low magnetic dopant density, bypassing the issues of clustering observed in systems where higher levels of magnetic doping had to be used to introduce sufficient charge carriers. By varying the proximity of the magnetic dopant atoms from the LTO/STO interface in unit-cell steps, we should be able to tune the exchange coupling between them mediated by the electron gas. Theoretical calculation indicate that the itinerant charge density falls off with distance from the interface, from more than 0.6 carriers per unit cell at the interface, to about half that value one unit cell away, rapidly declining at distances beyond two unit cells away. Depending upon the ratio of this carrier density to the density of magnetic dopants, and the effective overlap of the itinerant Ti-band with the magnetic dopants’ levels, this would give rise to exchange couplings that range from ferromagnetic to oscillatory RKKY-like, giving rise to different magnetic phases as a function of the carrier induced coupling.

The second idea in using electric fields has to do with engineering broken inversion symmetries in superlattices. The idea is best illustrated with a cartoon. The layers are sequenced as $(\text{LaMnO}_3)_{2n} (\text{SrMnO}_3)_n (\text{SrTiO}_3)_p$. This structure breaks inversion symmetry (as would any sequence ABCABC). It has an internal electric field E_{int} due to the fact that the holes from the SrMnO_3 layer diffuse into the LaMnO_3 in order to establish a uniform chemical potential (as in a p-n junction). We anticipate that this superlattice will be ferromagnetic⁷ for $n \leq 5$ (as we have also measured in our own samples). The system is inherently multiferroic, and measurements that reveal the interplay between electric fields and magnetic order will yield fundamental insight

into the connections between charge and spin degrees of freedom in the mixed valence manganites. Application of an external electric field that opposes E_{int} will reverse the diffusion of holes from SrMnO₃ to LaMnO₃ and presumably change the magnetic properties.

References:

1. “Artificial charge-modulation in atomic-scale perovskite titanate superlattices”, A. Ohtomo, D. A. Muller, J. L. Grazul and H. Y. Hwang, *Nature* **419**, 378 (2002).
2. “Electronic reconstruction at the interface between a Mott insulator and a band insulator”, S. Okamoto and A. J. Millis, *Nature* **428** (2004).
3. “Polar Heterojunction Interfaces”, W. A. Harrison, E. A. Kraut, J. R. Waldrop and R. W. Grant, *Phys. Rev. B* **18**, 4402 (1978).
4. “High mobility electron gas at the LaAlO₃/SrTiO₃ heterointerface”, A. Ohtomo and H. Y. Hwang, *Nature* **427**, 423 (2004).
5. “Origin of charge density at LaAlO₃ on SrTiO₃ heterointerfaces: possibility of intrinsic doping”, W. Siemons, G. Koster, H. Yamamoto, W. A. Harrison, G. Lucovsky, T. H. Geballe, D.H.A. Blank and M. R. Beasley, *cond-mat* 0612223.
6. “Ferromagnetic Semiconductors: moving beyond (Ga,Mn)As”, A. H. MacDonald, P. Schiffer and N. Samarth, *Nature Materials* **4**, 195 (2005).
7. “Growth and magnetoresistive properties of (LaMnO₃)_m(SrMnO₃)_n superlattices”, P. A. Salvador, A.-M. Haghiri-Gosnet, B. Mercey, M. Hervieu and B. Raveau, *Appl. Phys. Lett.* **75**, 2638 (1999); “SrTiO₃(100)/(LaMnO₃)_m(SrMnO₃)_n layered heterostructures: A combined EELS and TEM study”, J. Veerbeck, O.I. Lebedev, G. Van Tendeloo and B. Mercey, *Phys. Rev. B* **66**, 184426 (2002).

DOE Sponsored Publications:

1. “Electrostatic modification of novel materials”, C. H. Ahn, A. Bhattacharya, M. di Ventura, J. N. Eckstein, C. Daniel Frisbie, M. E. Gershenson, A. M. Goldman, I. H. Inoue, J. Mannhart, A. J. Millis, A. F. Morpurgo, D. Natelson, J-M. Triscone, *Reviews of Modern Physics* **78**, 1185 (2006).

Polymer-Assisted Formation of Nanostructured Transition Metal Clusters and Crystals

B. Chu, C. Krishnan, C. Burger and R. Muñoz-Espí
Department of Chemistry, Stony Brook University, NY 11794-3400

(i) Program Scope Potential applications in various fields of technology related to transition metal clusters and crystals have prompted us to carry out investigations on the mechanism and the development of such nano-structured materials using small and wide-angle X-ray scattering, Raman spectroscopy, thermal analysis (DSC, TGA), and electrochemistry. Among the many possible synthetic pathways, we have been particularly interested in how polymeric systems can affect nanofabrication [1]. Macromolecules may specifically control the nucleation-growth processes or may act as templates or structure directing agents. In some cases, polymers can stabilize phases that otherwise are metastable. The organic component can, at times, be incorporated into an inorganic matrix and then be easily removed by dissolution or calcination.

We have synthesized nano-structured porous molybdenum oxide clusters from an aqueous solution of peroxy-molybdate in the presence of long-chain poly(ethylene oxide) (PEO) homopolymers or commercial PEO-containing triblock copolymers (Pluronic) [2]. The highly ordered structure of the nanoporous oxide cluster resembles that of zeolite, albeit on a much larger length scale, as sketched in Figure 1 (cubic lattice constant of about 5 nm instead of a 1 nm typical for a Linde type A zeolite). A smaller icosahedral polyoxomolybdate cluster ("Keplerate") with a diameter of 2.5 nm and having 132 Mo (60 Mo^{V} and $72 \text{ Mo}^{\text{VI}}$) atoms has been synthesized (Figure 2) from solutions of ammonium molybdate, ammonium acetate, acetic acid and hydrazine sulfate [3]. These studies clearly demonstrate the dominant role of the mixed valence of molybdenum in forming nanostructures and/or supramolecular assemblies.

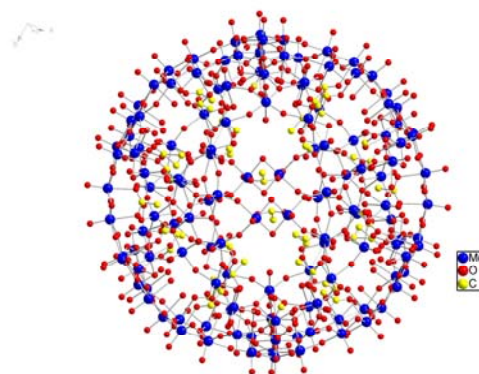
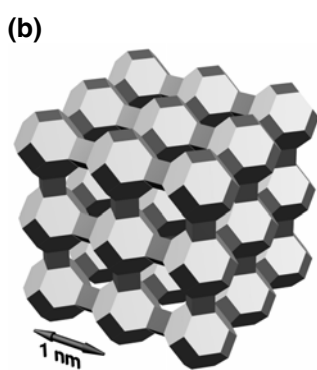
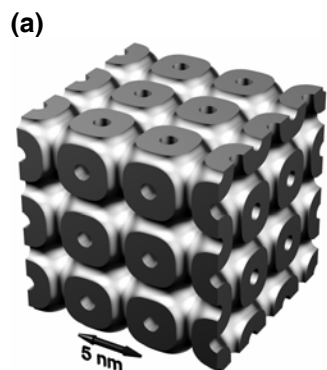


Figure 1 Schematic structure models for (a) the primitive cubic nanostructured porous molybdenum oxide and (b) the Linde Type A zeolite. They show similar scattering patterns, but on a different length scale [2].

Figure 2 Polyoxomolybdate Keplerate cluster $(\text{NH}_4)_{42}[\text{Mo}^{\text{VI}}_{72}\text{Mo}^{\text{V}}_{60}\text{O}_{372}(\text{CH}_3\text{COO})_{30}^-(\text{H}_2\text{O})_{72}] \cdot \text{ca. } 300\text{H}_2\text{O}$

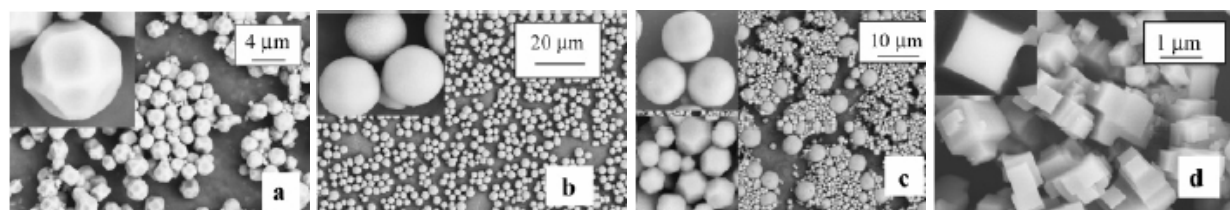


Figure 3 SEM images of mesostructured molybdenum oxides prepared from peroxy-molybdate precursor and polyethylene oxide with different molar masses ($[\text{Mo}]:[\text{ethylene oxide}] = 1:5$): (a) 400, (b) 4600, (c) 10,000, and 100,000 g/mol. Insets show high magnification images

(ii) Recent Progress We have developed a convenient sonochemical procedure at temperatures of 25–70 °C using aqueous solutions of peroxy-molybdate and polymers for the morphogenesis of highly ordered mixed-valent molybdenum oxide mesostructures with well-defined shapes. Depending on the ratio of Mo/polymer, the morphology can be controlled (Figures 3 and 4) [4,5]. Ultrasound irradiation

reduces the time needed for the growth of the oxide from weeks to a few hours. The low complexity of the sonochemical set-up also compares favorably to conventional hydrothermal/solvothermal processes. The surface area of the calcified molybdenum oxide whiskers ($55.4 \text{ m}^2/\text{g}$) was found to be much higher than typical data for molybdenum oxide nanorods or nanofibers reported in the literature ($13\text{--}35 \text{ m}^2/\text{g}$) [5,6].

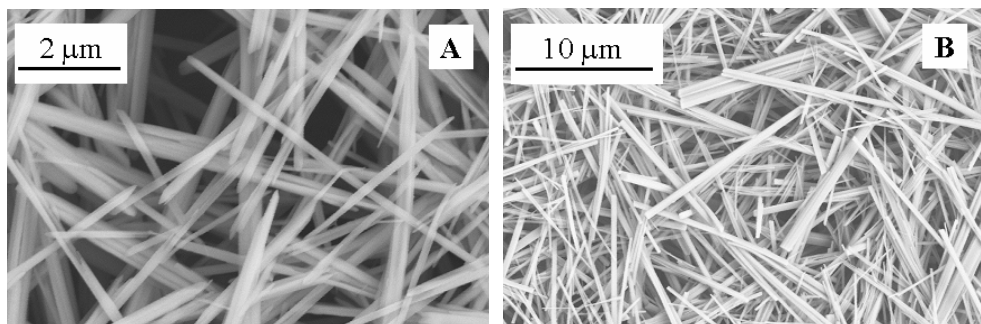


Figure 4 SEM images of molybdenum oxide whiskers grown from a 0.5 M peroxy-molybdate precursor solution in the presence of PEG, $M_w = 10,000 \text{ g}\cdot\text{mol}^{-1}$, at different [Mo]:[EO] ratios: (a) 100:1, (b) 2:1.

The growth rate of various crystal faces seems to be controlled by a coordination of the Mo atom in peroxy-molybdate ions to pseudocrown ether cavities formed by PEG. The proposed mechanism based on the experimental evidence is presented in Figure 5.

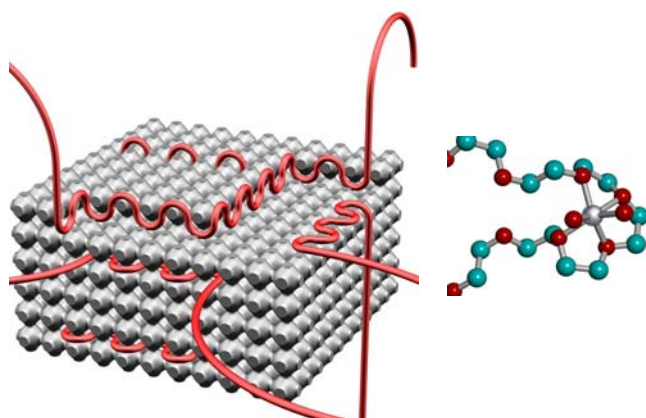


Figure 5 Schematic representation of the interaction of ethylene-oxide-containing polymers with the molybdenum oxide surfaces, influencing the crystal growth. The crystal growth proceeds by incorporating building units at steps on the crystal faces. PEO reversibly adsorbs onto these steps, blocking and freeing them, and thereby controlling the growth of the crystal.

Typically, MoO_3 and WO_3 films can be synthesized using various techniques, such as chemical vapor deposition, vacuum evaporation, radiofrequency sputtering, electron beam evaporation, sol-gel and spin coating [6]. There is less hydration in the oxides prepared by non-electrochemical methods and, consequently, less proton transport and poor charge transfer kinetics.

The quantity of metal oxide grown by anodic oxidation using a metal substrate is difficult to control. Cathodic electrodeposition to different substrates from peroxomolybdates and pure molybdates has also been reported [7]. Low temperature and soft processing capabilities make electrodeposition attractive. The products obtained at various potentials [8,9], viz., $\text{Mo}_2\text{O}_5\cdot 3\text{H}_2\text{O}$ at +0.18 to +0.02V, $2[\text{Mo}_3\text{O}_8\cdot\text{H}_2\text{O}]$ at +0.02 to -0.01V, $\text{Mo}_3\text{O}_8\cdot\text{H}_2\text{O}$ at -0.01 to -0.4V, and $\text{Mo}_3\text{O}_{8-x}(\text{OH})_x\cdot x\text{H}_2\text{O}$ at -0.4 to -0.6V, indicate the richness of the electrodeposition method. It offers the possibility to control the stoichiometry, water content, and oxidation state by control of applied potentials. In order to focus our attempt on this technique, we had to characterize the substrate, peroxomolybdate, first at various potentials. Some preliminary results are discussed below.

We have observed complex impedance behavior for the adsorbed species (Figure 6a) at slight anodic potentials. We have also observed oscillations in impedance as well as in color [10] at high frequencies (Figure 6b) at high cathodic potentials. Oscillations in capacitance were also seen at a fixed frequency (Figure 6c) when the potential was varied. These results suggested the richness of information that can be obtained by controlling the frequency as well as potential.

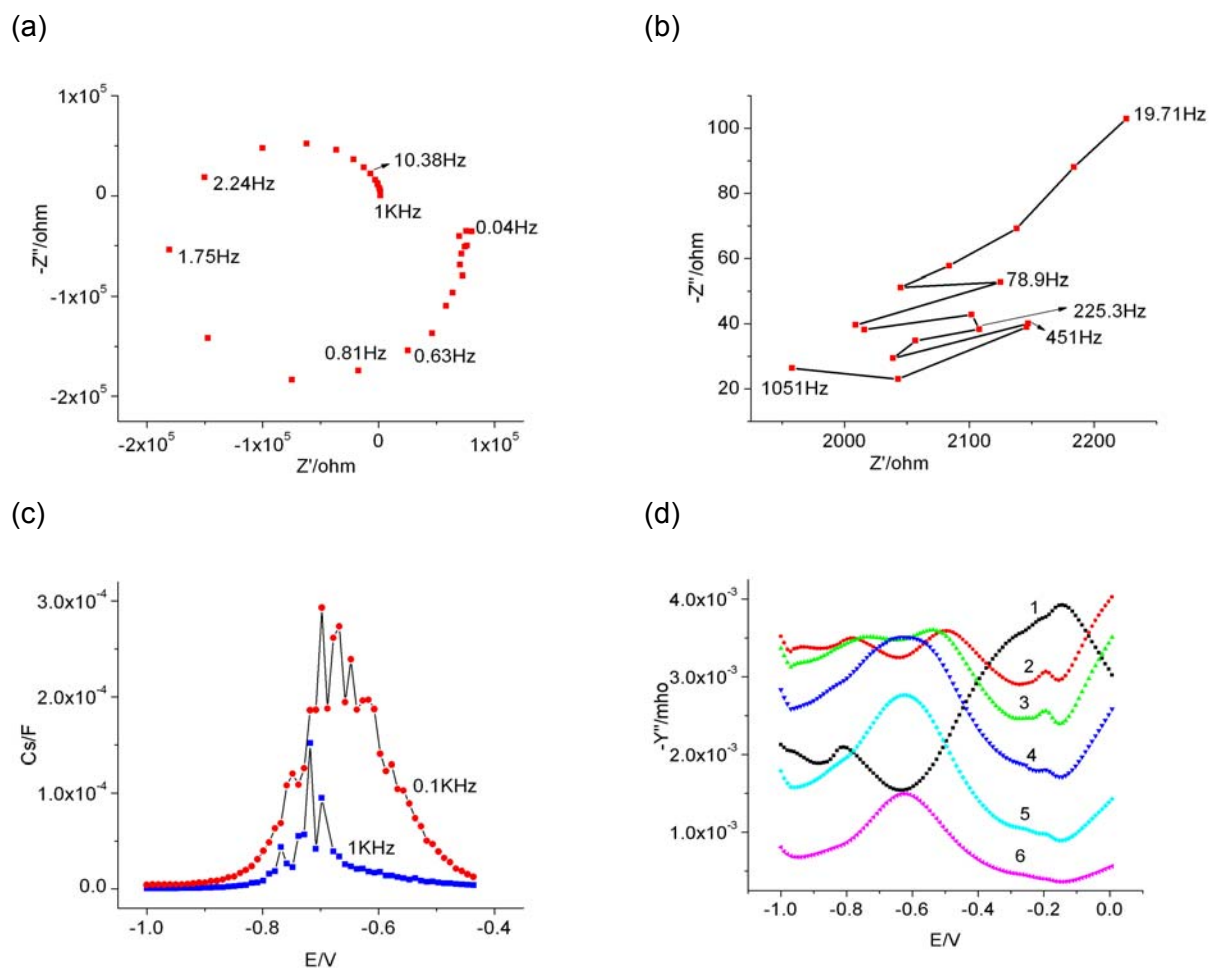


Figure 6 (a) Impedance of 0.005M $\text{H}_2\text{Mo}_2\text{O}_3(\text{O}-\text{O})_4(\text{H}_2\text{O})_2$, pH 1.87, after 1 day of preparation, 0.1V. (b) Impedance of 0.005M $\text{H}_2\text{Mo}_2\text{O}_3(\text{O}-\text{O})_4(\text{H}_2\text{O})_2$, pH 1.72 after 1 day of preparation, -0.8V . (c) pH 1.72 after 1 day of preparation, -0.8V , pH 1.90, after 3 days of preparation. (d) Admittance of 0.095 M $(\text{NH}_4)_6\text{Mo}_7\text{O}_{24}$, 0.47 M $\text{CH}_3\text{COONH}_4$ and 2.08 M CH_3COOH solution without reducing agent at different frequencies. pH = 3.84. 1: 5000 Hz; 2: 1000 Hz; 3: 750 Hz; 4: 500 Hz; 5: 250 Hz; 6: 100 Hz.

The electrochemical admittance behavior of the substrate needed to synthesize the complex polyoxomolybdate shown in Figure 2 is illustrated in Figure 6d. Its anion has a beautiful hollow spherical structure, with an icosahedral symmetry, composed of 12 $\{\text{Mo}_6^{\text{VI}}\}$ fragments and 30 $\{\text{Mo}_2^{\text{V}}\}$ fragments. In this molecular ion, there are 132 oxygen atoms of the type $\text{M}=\text{O}$ outside and pointing away from the sphere, 72 oxygen atoms from acetate ions bonded to the Mo inside the sphere and pointing towards the center of the sphere, and the rest of the oxygen atoms on the surface of the sphere, with an overall charge of -42 for the ion. To understand the admittance behavior, one has to consider cooperation as well as competition arising from the orientation changes of water molecules inside the spherical polyoxomolybdate ion along with the water orientation between the negatively charged mercury electrode and the ion. It is possible to have a cooperative interaction with one hydrogen of the water oriented towards the negatively charged mercury and the other one towards the oxygen of the $\text{M}=\text{O}$ or the surface oxygen. During admittance measurements, when the voltage of the electrode changed from negative to less negative and finally to zero, the orientation of the water molecules should also change correspondingly in all the environments mentioned above, whether it was free water molecules near the double layer or bound water molecules of hydration around the ion or inside the spherical molecule.

The above observations warrant several future studies to find out whether the ratio of mixed valent oxides with different water contents deposited can be controlled by studying (1) the characteristics of the

electrodeposited species at different frequencies and (2) the characteristics of the electrodeposited species at different potentials and fixed frequencies.

(iii) Future Plans

1. In order to understand the nature of WO_3 , we have to first completely characterize the nature of the substrate, Na_2WO_4 similar to the extensive electrochemical measurements we had carried out with Na_2MoO_4 , the substrate for MoO_3 .
2. The substrates extensively used for synthesizing MoO_3 and WO_3 are the respective peroxo complexes obtained by the dissolution of the metals in concentrated H_2O_2 . We have characterized the electrochemical nature of the peroxo-molybdate species, but the characterization of the peroxo-tungstate remains to be done.
3. A comparison of the different techniques used to prepare a particular kind of MoO_3 or WO_3 , the usefulness of the technique for producing large quantities, and the cost analysis of producing the material by a particular technique remain open challenges.
4. The metastable β - MoO_3 transforms into the thermodynamically stable α - MoO_3 above 350 °C. It remains a challenge to control the synthesis of their mixtures with definite ratios in order to control their catalytic and electronic properties. At present, a suitable technique needed to synthesize these mixtures is not obvious.
5. MoO_3 and WO_3 have different structures and their mixtures can be considered similar to mixtures of α - and β - MoO_3 with respect to structure. These mixtures also offer additional special electronic properties because of enhanced electron transfer possibilities between the different metals and their different valence states.
6. Electrochemistry seems very promising to prepare these oxides with controlled water of hydration, controlled ratios of mixed-valences, and controlled electrochromic properties. The studies done so far by us and others are only in their infancy. This cost effective technique offers the possibility to control potential and thus to control redox properties. By combining this technique with quartz crystal microbalance one can also poke into the mechanism of formation of these oxides.
7. Functionalization of polyoxomolybdate superstructures (inside, outside or both) with specific groups or chains providing special properties may offer potential applications in drug delivery and catalysis.
8. We have discovered that corrosion processes of metals can be understood better by studying the passivation phenomena with a fresh surface of the metal, rather than studying the passivated film. It also provides better opportunities to study corrosion protection with electrolytes such as molybdates.

(iv) References

- [1] T. Liu, C. Burger, and B. Chu, *Prog. Polym. Sci.* **2003**, *28*, 5
- [2] T. Liu, Q. Wan, Y. Xie, C. Burger, C.; L. Z. Liu, and B. Chu, *J. Am. Chem. Soc.* **2001**, *123*, 10966
- [3] A. Müller, E. Krickemeyer, H. Bögge, M. Schmidtman, and F. Peters, *Angew. Chem., Int. Ed.* **1998**, *37*, 3359
- [4] J. Chen, C. Burger, C. V. Krishnan, and B. Chu, *J. Am. Chem. Soc.* **2005**, *127*, 14140
- [5] C. V. Krishnan, J. Chen, C. Burger, and B. Chu, *J. Phys. Chem. B* **2006**, *10*, 20182
- [6] T. Xia, Q. Li, X. Liu, J. Meng, and X. Cao, *J. Phys. Chem. B* **2006**, *110*, 2006, and references therein
- [7] L. Kondrachova, B.P. Hahn, G. Vijayaraghavan, R.D. Williams, K.J. Stevenson, *Langmuir*, **2006**, *22*, 10490, and references therein
- [8] T.M. McEvoy, K.J. Stevenson, *J. Mater. Res.* **2004**, *19*, 429
- [9] T.M. McEvoy, K.J. Stevenson, *Anal. Chim. Acta* **2003**, *496*, 39
- [10] C.V. Krishnan, M. Garnett, B. Hsiao, and B. Chu, *Int. J. Electrochem. Sci.* **2007**, *2*, 29

(v) Recent DOE-Supported Publications

1. J. Chen, C. Burger, C. V. Krishnan, and B. Chu, *J. Am. Chem. Soc.* **2005**, *127*, 14140
2. C. V. Krishnan, J. Chen, C. Burger, and B. Chu, *J. Phys. Chem. B* **2006**, *110*, 20182
3. C. V. Krishnan, M. Garnett, B. Hsiao and B. Chu, *Int. J. Electrochem. Sci.* **2007**, *2*, 29

Bulk Materials Synthesis and Characterization

Cedomir. Petrovic and Rongwei Hu

Condensed Matter Physics and Materials, Science, Brookhaven National Laboratory, Upton NY 11973, USA

i) Program Scope

The focus of the program is design, discovery and characterization of new materials of current interest in fundamental areas of condensed matter physics. New model materials are created for test of various theoretical approaches. New and innovative synthetic techniques are developed in order to boost exploratory efforts. Automated physical and structural characterization equipment is the essential component of this program. Quite often the same methods are used to probe and perturb crystal structure, transport, thermodynamic and magnetic properties of new materials at low temperatures, high magnetic fields and pressures. This program also includes training of next generation of scientists. Extensive collaborations exist with many universities and national labs at the Northeast and throughout the US. Students from Johns Hopkins (where PI has adjunct professor appointment starting 2007), Brown University and Columbia University are being educated in arts and crafts of crystal growth, materials synthesis and characterization.

ii) Recent progress

1. Development of new tools and synthesis/crystal growth methods

Newly built laboratory for bulk materials synthesis and characterization combines diverse crystal growth and materials synthesis methods with fast structural and physical properties feedback. The former includes furnaces for crystal growth from solvents at both high and low temperatures (intermetallic, oxide, chalcogenide and halide), crystal growth and deposition from vapors, furnaces for solid state and gas reactions as well as intermetallic alloy and crucible sealing arc melting/welding system. The latter includes measurement of electrical and thermal transport, heat capacity and magnetization as well as powder X-ray analysis.

▪ New Synthesis Methods (1): In – Situ Decanting High Temperature Flux (ISDHTF) method

Crystal growth from high temperature metallic solutions has been successfully employed over the past few decades. Solution methods lowers melting point of the solute and is well suited for both congruently and incongruently melting crystals. The crystals however, have to be etched or mechanically removed from the solidified flux after going through peritectic. This exposes them to stress due to flux solidification and enhances possibility for creation of second phases. Fisk and Remeika pioneered decanting outside the furnace using the centrifuge at room temperature, encapsulating crucibles in quartz tubes to prevent oxidation and using quartz wool for filtration [1]. Consequently decanting was possible for temperatures below quartz melting point (1200°C). However, removing samples above 1000°C led to temperature gradients since samples would cool by the time flux is decanted, thus crystals could not be grown very close to peritectic. ISDHTF method developed in Petrovic lab at BNL enables inside the furnace decanting below 1700°C. New crucible sets are designed with built-in filter; therefore there is less possibility for contamination from quartz wool. It is possible to decant crystals very close to eutectic or peritectic since there is no need to remove samples from the furnace.



Fig. 1: In-situ decanting high T flux furnace

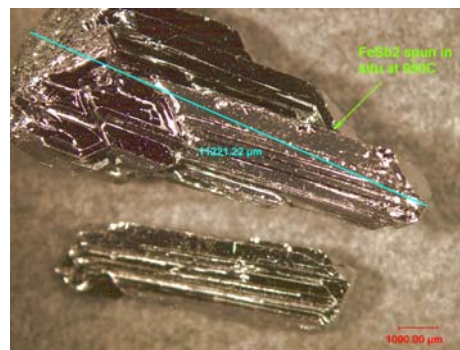


Fig. 2: Crystals grown by in-situ decanting

This enables crystal growth of phases that have very narrow range of coexistence with the liquid. The method reduces possibility of oxidation and crystallization of impurity phases. More materials (pure elements as well as compounds) can be used as a flux thus the vast unexplored synthesis space will open, particularly in phase diagrams containing B, C, Si, Ti and other elements with high melting points, paving way not only for new correlated electron materials in basic science but also for applications, for example high temperature and lightweight alloys. It was successfully tested for in-situ decanting both below (650°C) and above quartz melting point (1250°C) in Petrovic lab at BNL(Figs. 1 and 2)

- New Synthesis methods (2): Decanting from large crucible volumes

Creation and decanting of crystals from large crucible volumes (50ml) enables crystal growth from solvents in very narrow solubility ranges and small concentrations of solute. It also enables creation of crystals previously unavailable for any or some physical property measurements. In some cases supercooling is possible over limited temperature range ($T_m - T_d$), where T_m is melting point of the crystal and T_d is the decanting temperature. The existence of competing phases with lower chemical potential could result in energetically unfavorable difference $\Delta\mu = \mu(\text{melt}) - \mu(\text{crystal})$ and other crystal phases may exclusively or partially form. Assuming that previous factors do not inhibit crystal growth, the crystal volume is: $V = [n_0 - n_e(T)]V/\rho$ where n_0 is the initial solubility at time $t=0$, n_e is the solubility at temperature T , V is volume of the solution and ρ is the density of the solution. Density of solution can be influenced by increasing the quantity of solute and the cooling rate could be adjusted in order to maximize $n_0 - n_e(T)$. Larger crucible volumes directly influence crystal size, in addition to above mentioned factors. Increased crucible volume decreases the ratio of wetted crucible surface to the volume of solution, thus decreasing possibility of incorporation of crucible material in crystals. In addition, smaller wetted ratio decreases number of possible nucleation sites, favoring larger crystals on average. Advanced synthesis and decanting of crystals from melts at high temperatures in 50 ml crucibles can often enhance crystal size. This is 10 times the volume currently used in the equivalent laboratories in the US and the world (5ml). A new centrifuge was developed (Fig. 3) in Petrovic lab at BNL that enables stable rotation up to 1000 rpm of 50 ml crucibles sealed in quartz tubes. That crucible volume often yields intermetallic crystals of the size necessary for inelastic neutron scattering (INS) measurement (Fig. 4). Crystals grown using molten metallic fluxes usually reveal their natural growth habit, as opposed to floating zone crystals. Therefore there is usually no need for crystal orientation. Arranging several crystals in mosaic is quite easy when many nucleation sites exist (more smaller crystals) rather than one or a few (large 1 cm³ size of individual crystals).



Fig. 3: Centrifuge system for 50 ml crucibles



Fig. 4: YbRh₂Si₂ single crystals for INS measurements

2. Exploratory synthesis and characterization of novel materials

- Development of large c-axis and low residual resistivity ($\rho_0 = 0.037 \mu\Omega\text{cm}$) crystals of quasi 2D heavy fermion superconductors. This work enabled observation of field induced quantum critical point, uncondensed electrons coexisting with nodal quasiparticles in extreme multiband (multigap) scenario, field dependent coherence length and square vortex lattice for the first time in any non-BCS type superconductor. Recently, a breakdown of Landau Fermi liquid and a new type of violation of Wiedeman-Franz (WF) law has been established in CeCoIn₅. (Science, in press 2007). WF law is one of the oldest laws of condensed matter physics and a corner stone of the standard theory of metals. Discovery of multiple superconducting and magnetic phases in single crystal alloys of Nd_{1-x}Ce_xCoIn₅
- Classification of FeSb₂ as a new nearly magnetic (Kondo) insulator. Results were subsequently confirmed by both theoretical and experimental analysis. Discovery of colossal magnetoresistance in Fe_{1-x}Co_xSb₂ and giant mobility of carriers in doped FeSb₂ semiconductor alloy crystals of marcasite structure.

- Discovery of anisotropic superconductivity in metallic chains of quasi-1D Nb₂Se₃.
- Synthesized crystals of a canonical field induced quantum critical point material YbRh₂Si₂ using several different solvents, thus enabling investigation of potential role of disorder on non-Fermi liquid properties
- Synthesized oxide pyrochlores, many halide and chalcogenide crystals, wide gap semiconductor crystals (CdTe), crystals of fluorides and low dimensional oxides using innovative solvents. Many crystals were made to support efforts in materials science and chemistry (various thermoelectrics oxides and antimonides, oxides for catalysis) and at Johns Hopkins (materials for spin injection)
- Extensive collaboration in progress with many research groups at BNL and elsewhere (Princeton, Columbia, Rutgers, Brown, Johns Hopkins, CCNY, Northwestern, UCSD, Ameslab, LANL, Toronto, Sherbrooke, ETH Zürich, ISIS, Yonsei University (Korea)).

III). Future Plan

1. Development of new tools and synthesis/crystal growth methods

▪ **High temperature solution methods**

For continuous operation above 1250°C, it would be necessary to upgrade to more robust internal parts. Extension of in-situ decanting system for crystal growth from rarely used metallic solvents (silicon), high temperature oxide and fluoride solvents. Target materials are layered oxide structures, and various frustrated spin liquid materials where control over synthesis process would enable tuning of properties by substitution and intercalation. New crucibles that do not utilize quartz wool in large volumes and new crucibles (besides alumina) will be developed.

▪ **Vapor transport and deposition in extremely large (1000°C) gradients**

The large gradient multi-zone vapor transport furnace has been custom designed for Petrovic lab at BNL in order to extend available parameter space and number of transported materials in the standard vapor-liquid-solid (VLS) technique. In the future period we will concentrate on its multi – element version (MEVLS) where we would seek to transport many elements in single eutectics in order to grow correlated electron nanowires. Since many metals form halide vapors and eutectics at different temperatures, it is desirable to work in large gradient space.

2. Exploratory synthesis and characterization of novel materials

- Increased power of ab-initio computational methods has stimulated predictions for novel phonon based superconducting structures [2-3]. Vast majority are intermetallic compounds containing light elements, such as B and C. In order to synthesize materials, test and help develop theory, very high temperatures are often necessary. Using ISDHTF method and new structures will be explored, materials with 2D boron networks, B-C compounds, graphite intercalate compounds with 3d and 4d high melting point metals, metal doped icosahedral B₁₂ and various forms of cage – like carbon clusters (C₂₀, C₂₈, C₃₆) with large electron – phonon coupling in bands with σ -character (MgB₂-like). Bonding in boride compounds depends on metal/boron ratio. When it exceeds 12, boron forms icosahedral clusters. Innovative high T flux methods offer clear advantage since it will be possible to dissolve compounds with high boron content. Besides superconductivity, cage and clathrate-like clusters are promising thermoelectric materials (Phonon Glass Electron Crystal concept) and may be important as superhard and materials for high temperature applications. For example, it is proposed that carbon-analogue of silicon clathrate Na₂Ba₆Si₄₆ could have bulk modulus 15% larger than diamond [4].
- Extension of the study of the k-space inhomogeneity to two-layer quasi-2D heavy fermion superconductors Ce₂MIn₈ (M=Co,Rh,Ir). Intermetallic materials with high spin fluctuation temperature will be explored in the effort to find new host crystal structures at quantum critical point where one could tune the nature magnetic interactions by moving from AFM to FM quantum criticality by chemical substitution
- In parallel, insertion of carriers into low dimensional and frustrated magnetic materials will be performed, with a goal of obtaining model materials with conductive electronic states in the background of a quantum spin liquid. Synthesis of bulk crystals of doped layered 2D wide gap semiconductor, exploratory crystal growth and characterization of wide gap semiconductors (including solar cell materials).

iv). References

- [1] Z. Fisk, J. P. Remeika in K.A. Gschneider, Jr. L. Eyring (Eds), Handbook on the Physical Chemistry of rare earths, Vol. 12, 1989, Elsevier Amsterdam
[2] S. Gunji et al in Phys. Rev. B 54, 13665 (1996)
[3] J. K. Dewhurst et al in Phys. Rev. B 68, 020504 (2003)
[4] G. Benedek, E. Galvani and S. Sanguinetti in Nuovo Cimento D 17, 97 (1995)

v). Publications FY 05-07

1. J. Paglione, M. A. Tanatar, D. G. Hawthorn, E. Boaknin, R. W. Hill, F. Ronning, M. Sutherland, L. Taillefer, C. Petrovic and P. C. Canfield "Heat Transport as a Probe of Electron Scattering by Spin Fluctuations: the Case of Antiferromagnetic CeRhIn₅" **Phys. Rev. Lett.** **94**, 216602 (2005)
2. P. M. C. Rourke, M. A. Tanatar, C. S. Tyrel, J. Berderklis, J. Y. T. Wei and C. Petrovic "Spectroscopic Evidence for Multiple Order Parameters in the Heavy Fermion Superconductor CeCoIn₅" **Phys. Rev. Lett.** **94**, 107005 (2005)
3. C. Petrovic, Y. Lee, T. Vogt, N. Dj. Lazarov, S. L. Bud'ko and P. C. Canfield "Kondo Insulator description of the spin state transition in FeSb₂" **Phys. Rev. B** **72** (4), 045103 (2005)
4. F. Simon, A. Jánossy, T. Fehér, F. Murányi, S. Garaj, L. Forró, C. Petrovic, S. Bud'ko, R. A. Ribeiro, and P. C. Canfield "Magnetic-field-induced density of states in MgB₂: Spin susceptibility measured by conduction-electron spin resonance" **Phys. Rev. B** **72**, 012511 (2005)
5. M. A. Tanatar, J. Paglione, D. G. Hawthorn, E. Boaknin, R. W. Hill, F. Ronning, M. Sutherland, L. Taillefer, C. Petrovic and P. C. Canfield "Unpaired electrons in the superconducting state of heavy fermion CeCoIn₅" **Phys. Rev. Lett.** **95**, 067002 (2005)
6. J. Hudis, R. Hu, C. L. Broholm, V. Mitrovic and C. Petrovic, Magnetic and Transport properties of RCoIn₅ (R=Pr,Nd) and RCoGa₅ (R=Tb-Tm) **Journal of Magnetism and Magnetic Materials** **307**, 301-307 (2006).
7. C. C. Agosta, C. Martin, H. A. Radovan, E. Palm, T. P. Murphy, S. W. Tozer, J. C. Cooley, J. A. Schlueter and C. Petrovic, Penetration depth studies of organic and heavy fermion superconductors in the Pauli paramagnetic limit, **J. Phys. Chem. Solids** **67**, 586 (2006).
8. J. Paglione, M. A. Tanatar, D. G. Hawthorn, F. Ronning, R. W. Hill, M. Sutherland, L. Taillefer and C. Petrovic, Non-vanishing energy scales at the quantum critical point of CeCoIn₅, **Phys. Rev. Lett.** **97**, 106606 (2006).
9. L. DeBeer-Schmitt, C. D. Dewhurst, B. W. Hoogenboom, C. Petrovic and M. R. Eskildsen, "Field Dependent Coherence Length in the High-kappa Superconductor CeCoIn₅", **Phys. Rev. Lett.** **97**, 127001 (2006).
10. A. Perucchi, L. Degiorgi, R. Hu, C. Petrovic and V. Mitrovic, "Optical investigation of the metal-insulator transition in FeSb₂", **European Physical Journal B** **54**, 175 (2006)
11. Rongwei. Hu, V. F. Mitrovic and C. Petrovic, "Anisotropy in magnetic and transport properties of Fe_{1-x}Co_xSb₂", **Phys. Rev. B** **74**, 195130 (2006).
12. Rongwei Hu, K. Lauritch-Kullas, J. O'Brian, V. F. Mitrovic and C. Petrovic, "Anisotropy of electrical transport and superconductivity in quasi one dimensional chains of Nb₂Se₃", **Phys Rev. B** **75**, 064517 (2007)
13. Rongwei. Hu, J. Hudis, C. L. Broholm and C. Petrovic, "Single crystal growth of YbRh₂Si₂ using Zn flux", **Journal of Crystal Growth in press** (2007).
14. M.A. Tanatar, J. Paglione, L. Taillefer and C. Petrovic, "Violation of a universal law at a quantum critical point", **Science in press** 2007
15. H. Shakeripour, M. A. Tanatar, S. Y. Li, L. Taillefer and C. Petrovic, "Hybrid gap structure in the heavy-fermion superconductor CeIrIn₅", **Submitted to Phys. Rev. Lett** (2006), **cond-mat/0610052**.
16. Y. Onose, N. P. Ong and C. Petrovic "Thermal Hall Conductivity and long lived quasiparticles in CeCoIn₅", **Submitted to Phys. Rev. Lett** (2006). **cond-mat/0610713**

17. Rongwei. Hu, K. J. Thomas, Y. Lee, T. Vogt, E. S. Choi, V. F. Mitrovic, R. P. Hermann, F. Grandjean, P. C. Canfield, J. W. Kim, A. I. Goldman and C. Petrovic, "Colossal Magnetoresistance in a Doped Nearly Magnetic Semiconductor", **Submitted to Phys. Rev. Lett (2006)**.
18. C. Stock, C. L. Broholm, J. Hudis, H. J. Kang and C. Petrovic "Antiferromagnetic spin fluctuations and superconductivity in CeCoIn₅" **Submitted to Phys. Rev. Lett. (2007)**
19. F. Simon, F. Muranyi, T. Feher, A. Janossy, L. Forro, C. Petrovic, S. L. Bud'ko and P C. Canfield "Conduction electron spin lattice relaxation rate in MgB₂ superconductor" **Submitted to Phys. Rev. B (2007)**
20. Rongwei Hu, V. F. Mitrovic and C. Petrovic "Magnetic and electrical properties of Fe_{1-x}Cr_xSb₂" **Submitted to Phys. Rev. B (2007)**

This page is intentionally blank

Growth and study of mercury-based high-temperature superconductors

Martin Greven^{1,2,*}, Xudong Zhao^{2,3}, Guichuan Yu⁴, Yong-Chan Cho², Guillaume Chabot-Couture¹, Neven Barisic², Philippe Bourges⁵, Nobuhisa Kaneko², Yuan Li⁴, Li Lu¹, Eugene Motoyama⁴, Owen P. Vajk⁶

1. Department of Applied Physics, Stanford University, Stanford, California 94305, USA
2. Stanford Synchrotron Radiation Laboratory, Stanford, California 94309, USA
3. State Key Laboratory of Inorganic Synthesis and Preparative Chemistry, College of Chemistry, Jiling University, Changchun 130023, P.R.China
4. Department of Physics, Stanford University, Stanford, California 94305, USA
5. Laboratoire Léon Brillouin, CEA-Saclay, 91191 Gif-sur-Yvette Cedex, France
6. NIST Center for Neutron Research, Gaithersburg, MD 20899, USA

*e-mail: greven@stanford.edu

Program Scope

The discovery of high-temperature superconductivity in the lamellar copper oxide $\text{La}_{2-x}\text{Ba}_x\text{CuO}_4$ radically changed the way we think about the technological potential and the physical properties of transition metal oxides (TMO). These materials provide a wealth of new, applicable properties. Examples include ferroelectricity for electronic applications, colossal magneto-resistance (CMR) for computer memories, and fast oxygen ion conduction at room temperature for fuel cell applications or catalysis. Apart from their technological significance, TMO, and especially the high-temperature superconductors (HTSC), represent a formidable challenge to the development of new theoretical concepts devised to describe their physical properties. Traditional theories were unable to forecast the properties of HTSC, in part because they could not treat properly the electron-electron correlations characteristic of these materials. The development of a profound understanding of the strong electron correlation mechanisms that give rise to the fascinating properties of these materials has already had crucial consequences on the development of condensed matter physics.

The mercury-based family of materials $\text{HgBa}_2\text{Ca}_{n-1}\text{Cu}_n\text{O}_{2n+2+\delta}$ can be viewed as model HTSC due to a) their record superconducting transition temperatures ($T_c = 98$ K for $n = 1$ and $T_c = 134$ K for $n=3$, at ambient pressure), b) their relatively simple crystal structures, and c) their property of confining chemical disorder to the Hg-O layers, relatively far away from the superconducting copper-oxygen sheets. Unfortunately, these materials received relatively little attention because of the lack of sizable single crystals.

Recent Progress

Of particular interest is the compound with one copper-oxygen plane in the unit cell ($n=1$, referred to subsequently as Hg1201), since it is structurally the simplest member of the family. The biggest crystals reported in the literature do not exceed a

volume of 1 mm³, and are hence insufficient for studies by high-resolution experimental techniques, such as neutron scattering and photoemission. Very recently, we reported a major breakthrough in the growth of Hg1201. Our new method¹ yields single crystals larger than 100 mm³, enabling detailed spectroscopic studies for the first time.

One of the difficulties in preparing Hg1201 crystals is the relatively high vapor pressure of mercury oxide required during the growth. This problem must be handled with special care since mercury is very toxic. Therefore, encapsulation of the crucible containing the precursors is needed. This problem was solved by avoiding conventional silica tubes, which react with HgO, and instead using high-quality (no air bubbles) quartz tubes, and by controlling the mercury pressure. The latter was achieved by carefully dosing and mixing HgO with the Ba-Cu-O precursor, and by finding an adequate temperature profile for the crystal growth, thus allowing the kinetics of the chemical reactions to be tuned.

Preparation of an adequate precursor is an essential, yet highly sensitive step in the growth of Hg1201 crystals. The key is to produce a very clean precursor, containing only Ba, Cu and O compounds with the correct overall stoichiometry of 2:1:3. Impurities tend to stop the chemical reactions, leading to small or indeed no crystals. Therefore, any kind of contamination should be eliminated, if possible. The main difficulty is to obtain clean BaO₂, since it easily reacts with CO₂ to form BaCO₃. Thus, we used a method based on a mixture of Ba(NO₃)₂ and CuO which results in the cleanest precursors. The mixture is heated to 920° C in a home-made vertical kettle with pure oxygen flow, which ensures that there is no water or other gas contamination. The Ba(NO₃)₂ decomposes into BaO and NO₂ and forms Ba₂CuO₃ with CuO. After adding HgO to the precursor and mixing the two, the mixture is immediately placed into a zirconia crucible and sealed in a quartz tube. The last step of the crystal growth is a thermal treatment of the quartz tube according to the temperature profile reported in Ref. [1].

After the crystal growth, we used standard characterization tools: Inductively Coupled Plasma Mass Spectrometry to determine the crystal stoichiometry; X-ray powder diffraction to ensure that there are no secondary phases; neutron diffraction at the NIST Center of Neutron Research to determine the crystal mosaic.

As is well known, the physical properties of TMO are very sensitive to disorder², and the HTSC are no exception in this regard³. Therefore, one should be very careful to distinguish effects arising from different types of disorder, e.g., vacancies, doping, substitutions, oxygen disorder, etc. To ensure that the results obtained by advanced spectroscopic methods are of the highest quality, it is necessary to establish a procedure for selecting the highest-quality samples from a large number of synthesised crystals. In this respect, resistivity in the normal state (above T_C) carries important information since it is one of the rare probes that tests the bulk properties. Samples with the very same normal-state temperature dependence of resistivity that does not depend on the contact or the sample geometry are identified as homogeneous and of a high quality. In contrast to

¹ X. Zhao *et al.*, Adv. Materials **18**, 3243 (2006)

² E. Dagotto, Science **309**, 257 (2005)

³ H. Eisaki *et al.*, Phys. Rev. B **69**, 064512 (2004)

the resistivity, which probes the normal state, the zero-field cooled (ZFC) magnetic susceptibility is commonly used for the characterization of the superconducting state. We carefully measured the absolute value of the diamagnetic signal (Meissner effect) and the sharpness of T_C , which are usually taken as criteria for the sample quality. These criteria are disputable since they may be sensitive to the spatial distribution of T_C values (e.g., a sphere and a hollow sphere made from otherwise homogeneous superconducting material will have the same ZFC response). Therefore, to test and truly characterize the superconducting state of the crystal bulk, we have additionally measured the field cooled (FC) susceptibility, conducted etching studies, and revisited the Wohleben effect.^{4,5}

In our Hg1201 crystals, the difference between the ZFC and FC (field perpendicular to the CO₂ sheets), although sample dependent, is surprisingly low in comparison with the other HTSC. For a typical sample, this difference is smaller than 15%, which is much less than the usual 50 to 80%.⁶ This result indicates a very low density of trapped magnetic flux, and it demonstrates that we were able to synthesise and select the Hg1201 samples of superior quality (i.e., with a very few pinning centers). Since the flux trapping is also closely related to the strength and the temperature dependence of the Wohleben effect, we have used this effect as a unique and very simple bulk probe of the superconducting state. A convincing way to check if there is a gradient of the T_C as a function of the distance from the surface is to etch the crystal and consequentially measure its susceptibility as a function of the etched volume. The etching is done by dipping the crystal in diluted bromic acid, dissolving the external part of the crystal. We have established that, for the long-term annealed samples (350⁰ C in air for a month), the temperature susceptibility profile does not change across the sample indicating a homogeneous oxygen distribution. This important information can be used subsequently when annealing large Hg1201 crystals.

In the HTSC, annealing is a complex problem since the created oxygen vacancies (and other heat-induced disorder) are mobile at elevated temperatures. Therefore, upon cooling, defects may self-organize and create new structures, which in turn create difficulties in distinguishing between the intrinsic and extrinsic properties of the system. Annealing of Hg1201 crystals turned out to be even more subtle than this. Although several groups have tried to resolve this problem, the results have been unsatisfactory thus far. Additional difficulties arise due to the decomposition of the sample, surface problems, and the different time scales involved in the annealing process. Nevertheless, we have managed, for the most part, to master the annealing process and thus obtain optimally- and under-doped samples. This success opens numerous possibilities for further experimental work, such as advanced spectroscopic methods including neutron scattering, ARPES, STM, Raman, Kerr effect, etc. Due to the technical demands of those methods, there are some additional requirements concerning sample size and surfaces, which should be satisfied. During the last few years, we have achieved important progress in meeting these conditions.

⁴ A.K. Geim, Nature **396**, 144 (1998)

⁵ W. Braunisch *et al.*, Phys. Rev. Lett. **68**, 1908 (1992)

⁶ R. Liang *et al.*, Physica C **383**, 1 (2002)

Future Plans

Due to the proximity of antiferromagnetism and superconductivity in the phase diagram of the cuprates, it is believed by many that antiferromagnetic interactions play a crucial role in the mechanism of high-temperature superconductivity. While the long-range Néel order of the insulating parent compounds is suppressed when a small density of holes is doped into the Cu-O sheets, dynamic spin correlations nevertheless persist in the superconducting phase. The most prominent feature in the magnetic excitation spectrum of the cuprates is the so-called magnetic resonance,^{7,8,9} a sharp magnetic excitation located at the antiferromagnetic zone center (π,π), which can be observed by inelastic neutron scattering. To take advantage of the momentum resolution of this technique, a large volume of material is required. By co-mounting about a dozen crystals with total volume of about 0.5 cm³, we overcame this problem, thus enabling the first inelastic neutron measurements on a Hg-based HTSC. We performed energy and momentum scans as a function of temperature which provide the first evidence of the existence of magnetic resonance in Hg1201. Interestingly, the resonance energy of ~ 57 meV is remarkably high for our as-grown, underdoped ($T_C \sim 80$ K) sample. In the near future, we plan to determine the full magnetic excitation spectrum and to extend these measurements to optimal doping. We will furthermore use polarized neutron diffraction to search for “hidden” magnetic order in the pseudogap state above T_C .

Although it was believed for a long time that Hg1201 crystals do not cleave naturally, we have found a rather simple method with which to obtain uncontaminated, atomically flat, surfaces parallel to the Cu-O sheets by *in situ* cleaving. This step is crucial for future ARPES and STM studies, which require uncontaminated, atomically flat, surfaces. In addition to ARPES and STM, our collaborative work will include optical spectroscopy, NMR, μ SR, and other complementary measurements in order to arrive at a comprehensive understanding of the physical properties of Hg1201. The combination of synchrotron-based X-ray diffraction and EXAFS will allow us to determine the subtle structural properties of the Hg-O layers.

Finally, we will begin to extend our crystal growth work to the double (Hg1212) and triple-layer (Hg1223) members of the Hg-based family of HTSC.

Related DOE sponsored publications (2005-2007)

1. Optical and thermodynamic properties of the high-temperature superconductor HgBa₂CuO_{4+ δ} . E. van Heumen *et al.*, Phys. Rev. B **75**, 054522 (2007)
2. Crystal growth and characterization of the model high-temperature superconductor HgBa₂CuO_{4+ δ} . X. Zhao *et al.*, Adv. Materials **18**, 3243 (2006)
3. Charge-Transfer Excitations in the Model Superconductor HgBa₂CuO_{4+ δ} . L. Lu *et al.*, Phys. Rev. Lett. **95**, 217003 (2005)

⁷ H.F. Fong *et al.*, Phys. Rev. Lett. **75**, 316 (1995)

⁸ H. He *et al.*, Science **295**, 1045 (2002)

⁹ P. Bourges *et al.*, Phys. Rev. B **53**, 876 (1996)

DE-FG02-03ER46053

Thermochemistry of Anion Defect and Charge Coupled Substitutions in Fluorite and Perovskite Based Materials

Alexandra Navrotsky

Peter A. Rock Thermochemistry Laboratory and NEAT ORU
University of California at Davis
Davis CA 95616

Program Scope

Using the unique calorimetric capabilities of the Peter A. Rock Thermochemistry Laboratory at UC Davis, this project investigates the thermodynamic properties of a variety of oxide systems relevant to energy production and distribution. Emphasis is on materials based on the fluorite structure and its ordered variants such as pyrochlore and C-type rare earth oxides. Ultra-high-temperature thermal analysis (to 2400 °C) is used to investigate phase transitions in rare earth oxides. The relations among energetics of amorphous, fluorite, and pyrochlore structures in rare earth doped tetravalent oxides of Ti, Zr, Hf, and other elements is studied by scanning calorimetry and oxide melt solution calorimetry. Solution calorimetry of nanoparticles of rare earth doped tetravalent oxides will elucidate both surface energies and differences in the energetics of defect formation and the energetics of mixing of different cations and of anions and vacancies in bulk and nanomaterials. Calorimetric methodology for thin films is being developed and applied to these oxides.

The outcome of this research will be strong fundamental understanding of an important family of materials applicable to solid oxide fuel cells, catalysts, thermal barrier coatings, nuclear power, and other technologies. Linking macroscopic thermodynamics to structure and properties provides guidance for developing new optimized materials for energy applications and for overcoming materials compatibility issues in these emerging technologies. Direct comparison of bulk, nanophase, and thin film thermodynamics for the same chemical compositions is essential to understand the behavior of systems such as nanophase catalysts, thin film solid oxide fuel cells, and gate dielectrics. Such information is also essential for understanding the environmental degradation, transport, and pollution potentially encountered by such materials. The thermodynamic data offer direct comparison and benchmarking of theoretical calculations.

Recent Progress

Here two specific findings of papers in press are highlighted: (a) systematic trends in mixing properties in rare-earth doped zirconia and hafnia, and (b) preliminary studies on doped urania. Energetics of rare earth, yttrium and scandium stabilized zirconia and hafnia have been systematically investigated by oxide melt solution calorimetry. The enthalpies of formation with respect to the oxide end members were simultaneously fit to a quadratic function to extract interaction parameters and enthalpies of transition of the oxide end members to the fluorite structure. ZrO_2 - and HfO_2 - $SmO_{1.5}$ show the most exothermic enthalpies of formation and interaction parameters, whereas ZrO_2 - $ScO_{1.5}$ has the least exothermic enthalpy of formation and interaction parameter. This suggests that the ZrO_2 - $ScO_{1.5}$ system shows the least short range order among all investigated systems, consistent with its high ionic conductivity. The extrapolated enthalpy of transition of the rare earth oxide end members to the cubic fluorite structure increases to more endothermic values with decreasing cation size. The γ - cubic phase transition in ZrO_2 - $ScO_{1.5}$ was investigated by differential scanning calorimetry (DSC). The phase transition is reversible, occurs at 1000-1200 °C and shows hysteresis (~ 100 °C). The enthalpy of transition is endothermic on heating and increases from 1.7 ± 0.1 kJ/mol (22 mol% $ScO_{1.5}$) to 2.9 ± 0.2 kJ/mol (30 mol% $ScO_{1.5}$). Trends are summarized in Figure 1.

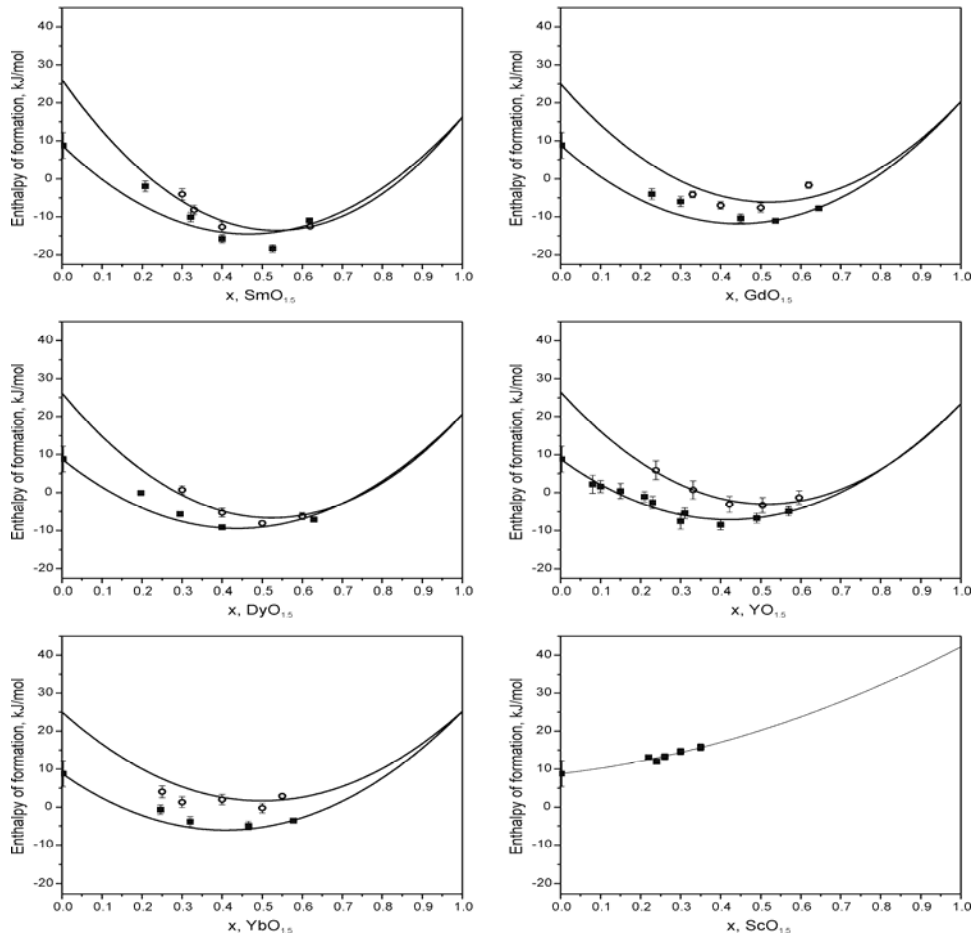


Figure 1: Enthalpies of formation from monoclinic zirconia or hafnia and C-type rare earth oxide of $ZrO_2-REO_{1.5}$ and $HfO_2-REO_{1.5}$ solid solutions.

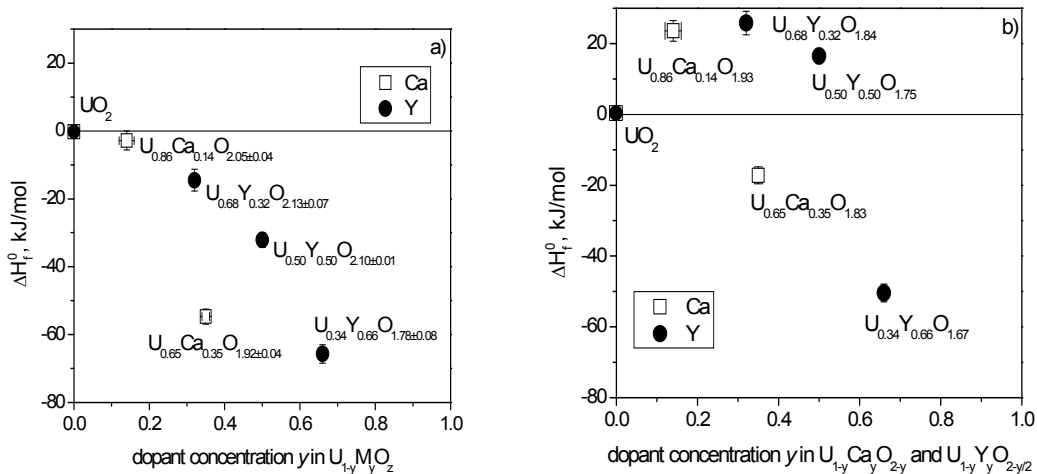


Figure 2. (a) Enthalpies of formation from oxides (UO_2 , UO_3 and CaO or $YO_{1.5}$) of samples with as-synthesized oxygen contents (shown on figure). (b) Enthalpies of formation of modeled fully reduced (all uranium tetravalent) UO_2-CaO and $UO_2-YO_{1.5}$ solid solutions relative to UO_2 and CaO or $YO_{1.5}$. The correction for the effect of oxidation was made assuming that oxidation of U^{4+} to U^{6+} in the solid solution matrix has the same enthalpy as oxidation of UO_2 to UO_3

Quantitative study of thermodynamic properties of solid solutions of UO_{2+x} with divalent and trivalent oxides is important for predicting the behavior of oxide fuel. Although early work measured vapor pressure in some of these solid solutions, direct calorimetric measurements of enthalpies of formation have been hampered by the refractory nature of such oxides. First measurements of the enthalpies of formation in the systems $\text{UO}_{2+x}\text{-CaO}$ and $\text{UO}_{2+x}\text{-YO}_{1.5}$, obtained by high temperature oxide melt solution calorimetry, are reported. Both systems show significantly negative heats of formation from binary oxides (UO_2 , plus O_2 and CaO or $\text{YO}_{1.5}$, as well as from UO_2 plus UO_3 and CaO or $\text{YO}_{1.5}$), consistent with earlier free energy measurements in the urania - yttria system. The energetic contributions of oxygen content (oxidation of U^{4+}) and of charge balanced ionic substitution as well as defect clustering are evaluated, see Figure 2. . The substantial additional stability in the solid solutions compared to pure UO_{2+x} may retard, in both thermodynamic and kinetic sense, the oxidation and leaching of spent fuel to form aqueous U^{6+} and uranyl phases.

Future Work

Work in the next year will focus on nanophase YSZ. The goal is to determine the surface energy of nanopowders and seek thermodynamic and structural evidence for or against differences in clustering and/or surface segregation in nanophase versus bulk materials. Some nanocomposite materials may also be studied. Exploratory work on thin films has begun. In terms of bulk materials, we are studying a series of transition metal doped perovskites with complex defect chemistry and both ionic and electronic conductivity. The goal is to relate thermochemistry and models of defect structures and their dependence of stoichiometry on oxygen partial pressure.

Publications in Last Two Years

“Thermochemistry of $\text{La}_{1-x}\text{Sr}_x\text{FeO}_{3-\delta}$ Solid Solutions ($0.0 \leq x \leq 1.0$, $0.0 \leq \delta \leq 0.5$)”, J. Cheng, A. Navrotsky, X.D. Zhou, and H.U. Anderson, *Chem. Mater.* 17(8), 2197-2207 (2005).

“Enthalpy of Formation of Li_xCoO_2 ($0.5 \leq x \leq 1.0$)”, M. Wang, A. Navrotsky, S. Venkatraman, A. Manthiram, *J. Electrochemical Society*, 152(7), J82-J84 (2005).

“Thermochemistry of a New Class of Materials Containing Dinitrogen Pairs in an Oxide Matrix”, F. Tessier, L. Le Gendre, F. Chevre, R. Marchand, and A. Navrotsky, *Chemistry of Materials*, 17(13), 3570-3574 (2005).

“Direct Calorimetric Measurement of Enthalpies of Phase Transitions at 2000 – 2400 °C in Yttria and Zirconia”, A. Navrotsky, L. Benoist, and H. Lefebvre, *Journal of the American Ceramic Society*, 88(10), 2942-2944 (2005).

“Direct Measurement of Water Adsorption Enthalpy on Hafnia and Zirconia”, S. V. Ushakov and A. Navrotsky, *Applied Physics Letters* 87(16) 164103 (2005).

“Energetics of Cubic Si_3N_4 ”, Y. Zhang, A. Navrotsky, and T. Sekine, *Journal of Materials Research* 21 (1), 41-44 (2006).

“Effect of Structure and Thermodynamic Stability on the Response of Lanthanide Stannate Pyrochlores to Ion-Beam Irradiation”, J. Lian, K.B. Helean, B.J. Kennedy, L.M. Wang, A. Navrotsky, and R.C. Ewing, *J. Phys. Chem. B.* 110, 2343-2350 (2006).

“High-temperature Calorimetry of Zirconia: Heat Capacity and Thermodynamics of Monoclinic-tetragonal Phase Transition”, Y. Moriya and A. Navrotsky, *Journal of Chemical Thermodynamics* 38, 211-223 (2006).

"Energetics of LiFePO_4 and Polymorphs of its Delithiated Form, FePO_4 ", R.G. Iyer, C. Delacourt, C. Masquelier, J.-M. Tarascon, A. Navrotsky, *Electrochemical and Solid State Letters* 9(2), A46-A48 (2006).

"Thermochemical Study of Trivalent-doped Ceria Systems: $\text{CeO}_2\text{-MO}_{1.5}$ (M = La, Gd, and Y)", W. Chen and A. Navrotsky, *Journal of Materials Research*, 21, 3242-3251 (2006).

"Energetics of Defect Fluorite and Pyrochlore Phases in Lanthanum and Gadolinium Hafnates", S. V. Ushakov, A. Navrotsky, J. A. Tangeman, and K. B. Helean, *Journal of the American Ceramic Society*, 90, 1171-1176 (2007).

"Calorimetric Measurements of Energetics of Defect Interactions in Fluorite Oxides", A. Navrotsky, P. Simoncic, H. Yokokawa, W.Q. Chen, and T. Lee, *Faraday Discussions*, 134 (2007).

"Energetics of Cerium-Zirconium Substitution in the $x\text{Ce}_{0.8}\text{Y}_{0.2}\text{O}_{1.9}\text{-(1-x)}\text{Zr}_{0.8}\text{Y}_{0.2}\text{O}_{1.9}$ System", W. Chen, A. Navrotsky, Y. P. Xiong, and H. Yokokawa, *Journal of the American Ceramic Society*, 90, 584-589 (2007).

"Calorimetric Measurements of Energetics of Defect Interactions in Fluorite Oxides", A. Navrotsky, P. Simoncic, H. Yokokawa, W.Q. Chen, and T. Lee, *Faraday Discussions*, 134 (2007).

Synthesis of atomically smooth films of cuprate superconductors and related oxides

I. Bozovic, G. Logvenov, A. Gozar, A. Bollinger and V. Butko

Department of Condensed Matter Physics and Materials, Science, Brookhaven National Laboratory, Upton NY 11973, USA

i) Program Scope

Understanding the mechanism of high-temperature superconductivity (HTS) is considered by many as the most important open problem in Condensed Matter Physics; many basic questions are indeed still open. In many cases, the large scatter in experimental results can be traced back to the materials science problems. HTS compounds have rich phase diagrams with many stable phases; for this and other reasons the samples tend to be chemically inhomogeneous. This is in particular true for HTS thin films, which typically contain many secondary-phase precipitates.

This research project engages an advanced atomic-layer molecular beam epitaxy (MBE) synthesis technique (see Fig. 1) for deposition of complex oxides, to fabricate state-of-the-art HTS thin films, multilayers, and superlattices.¹⁻⁵

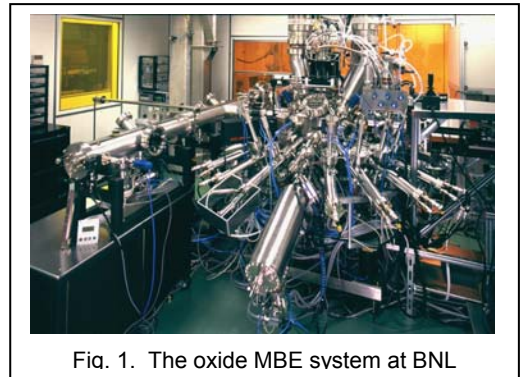


Fig. 1. The oxide MBE system at BNL

This allows us to perform a series of experiments that were not previously possible; we expect that these will provide conclusive answers to some of the key questions about the mechanism of HTS and significantly impact research on HTS and other strongly-correlated electron materials.

ii) Recent Progress

1. We have synthesized a number of atomically smooth and secondary phase defect-free thin films of stable BiSrCaCuO phases (2201, 2212, 2223). The highest T_c in as grown-film was 91 K; this surpasses all films grown by MBE in the past (Varian, Oxxel, etc.). We have also synthesized a number of superlattices such as nx2201:mx2212; these were studied in detail by both hard and soft X-ray diffraction⁴ (the latter by S. Smadici and P. Abbamonte at NSLS). A number of BSCCO films were delivered to S. Cybart and R. Dynes (U. California, Berkeley) for fabrication of ion-implanted planar Josephson junctions. We have grown films of Bi-2234, a metastable phase that does not exist in the bulk form, and observed $T_c = 75$ K – an example of artificial HTS compound synthesized by atomic-layer engineering. [Previously only semiconducting films of these phase were grown.]
2. We have also synthesized atomically smooth BaBiO₃ (BBO) films on SrTiO₃ substrates – a surprise given the large mismatch of the lattice constants. We have studied the surface of BBO films by angle-resolved time-of-flight ion scattering and recoil spectroscopy (TOF-SARS) and demonstrated that the technique has a potential for determination of crystallographic structure of the surface layer with high resolution.
3. We have mastered growth of atomically smooth films of La_{2-x}Sr_xCuO₄ over a broad range of doping, $x = 0$ to $x = 0.50$, to the extent that the yield is essentially 100%, unprecedented anywhere. Over a hundred such films have been made, many of them in the form of multilayers and superlattices. They were characterized by Reflection High-Energy Electron Diffraction (RHEED) in real time, see Fig. 2, and by XRD, trans-

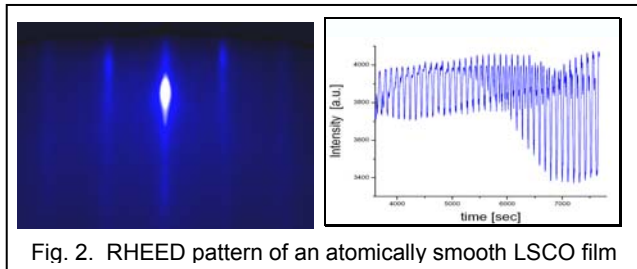


Fig. 2. RHEED pattern of an atomically smooth LSCO film

port (resistivity and magnetic susceptibility as a function of temperature) and Atomic Force Microscopy (AFM), see Fig. 3, ex-situ.

4. We have studied a number of bilayers formed of two non-superconducting materials, undoped insulator La_2CuO_4 and overdoped metallic $\text{La}_{1.55}\text{Sr}_{0.45}\text{CuO}_4$, and discovered interface superconductivity with $T_c = 30$ K. Upon ozone annealing, such samples routinely show $T_c \approx 50$ K. We are studying intensely both phenomena, and expect to report these soon in a high-profile journal.
5. In collaboration with J. Demsar (Konstanz, Germany), we have discovered and studied long-lived photo-induced excitations in LaSrAlO_4 . We have identified the physical cause as electron states trapped on defects (oxygen vacancy sites). The results have been written up and the paper has been submitted for publication in the *Phys. Rev. Letters*.
6. J. He and Y. Zhu studied some La_2CuO_4 and $\text{La}_{2-x}\text{Sr}_x\text{CuO}_4$ films by TEM and the findings have been published⁷ in *Journal of Applied Physics*, see Fig. 4. More studies are underway, including LSCO films grown on bicrystal SrTiO_3 substrates as a part of new project in collaboration that also involves Praveen Chaudhari.
7. N. Gedik and A. Zewail studied our LCO films by ultrafast optical pump-electron diffraction probe and discovered photo-induced phase transitions and colossal expansion, see Fig. 5. The findings are reported in a paper⁶ accepted for publication in *Science* magazine. With Z. Radovic (theory) and N. Bozovic (numerical simulations) we have already sorted out the physics of the effect. The effect is not thermal, but involves large-amplitude, coherent lattice oscillations.⁸ It originates from strong coupling of in-plane charge excitations to out-of-plane lattice vibrations, notably including c -axis longitudinal acoustic phonons. This strong coupling has not been noticed so far, and chances are it has important bearings on the physics of cuprates. The corrugation of the La-O plane has been identified as the soft coordinate that responds the most to charge-transfer excitation and to uniaxial pressure. This is unusual, and so is the fact that La_2CuO_4 can be perceived as consisting of rigid layers (in which all the atoms are in ‘hard contact’, i.e., the chemical bonds are equal to the sum of the ionic radii) that ‘levitate’ on the Madelung potential, without hard contact with one another.
8. A large sample set (7 sets of 4 identical 1 cm^2 films each) has been synthesized for low-energy muon spin resonance (μSR) experiments done at the Paul Scherrer Institute, Zurich, Switzerland by E. Morenzoni and A. Suter. The focus was on underdoped $\text{La}_{2-x}\text{Sr}_x\text{CuO}_4$. The experiments are still in progress; so far, we can say that the samples look very homogeneous (in contrast to other samples studied so far) and show no signs of spin glass behavior, seen by other groups in polycrystalline samples and postulated to be universal feature of cuprates.
9. Several $\text{La}_{2-x}\text{Sr}_x\text{CuO}_4$ samples were studied by R. Pindak (BNL) and Y. Yacobi (Technion) at the ALS in Argonne, using their unique surface-crystallography technique, COBRA. The experimental data already taken showed several unexpected features, and the experiment continues with good promise.
10. Surface XRD is being studied on our $\text{La}_{2-x}\text{Sr}_x\text{CuO}_4$ films by S. Wilkins and J. Hill (BNL) at NSLS and interesting surface reconstruction features have been detected.

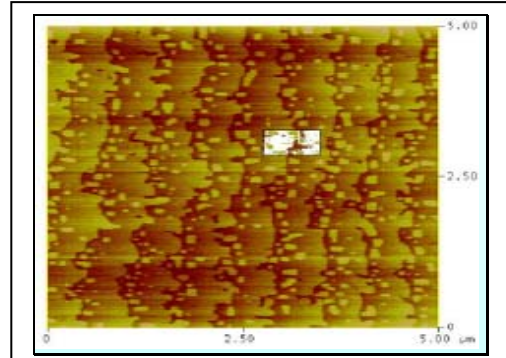


Fig. 3. AFM image of an LSCO film. The steps are one-half unit cell tall and originate from substrate miscut. The terraces are atomically flat.

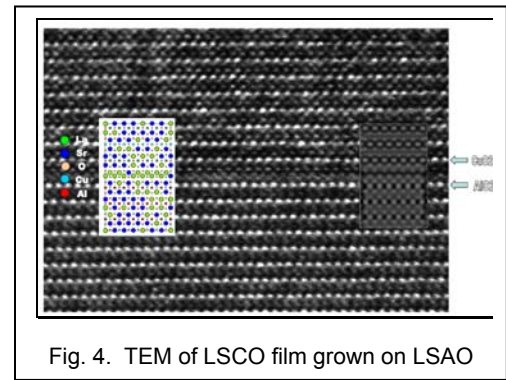


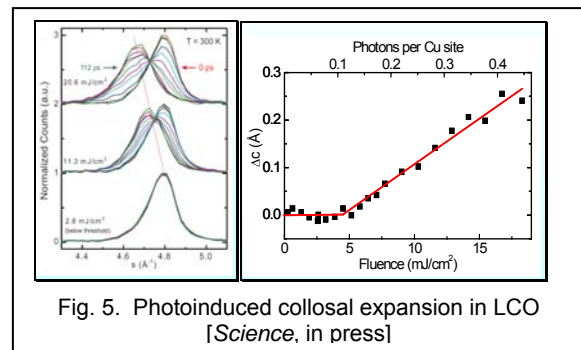
Fig. 4. TEM of LSCO film grown on LSAO

- Several other collaborations (optics, ultrafast pump-probe, transport in high magnetic fields, COMBI measurements of transport properties in search of Quantum Critical Points) are ongoing and more experimental results are expected before long.

iii) Future Plans

Some experiments that we are planning in near future are as follows.

- Combinatorial study of transport (resistivity and Hall Effect) in overdoped $\text{La}_{2-x}\text{Sr}_x\text{CuO}_4$;
- Bicrystal Josephson Junctions (with H. Shim and P. Chaudhari, BNL)
- Optics (transmittance) in underdoped $\text{La}_{2-x}\text{Sr}_x\text{CuO}_4$ in high magnetic field (with L. Mihaly, Stony Brook);
- High-field magnetoresistance in overdoped $\text{La}_{1.55}\text{Sr}_{0.45}\text{CuO}_4$ – undoped La_2CuO_4 bilayers (with S. Riggs and G. Boebinger, NHFML, and F. Balakirev, LANL);
- A new study of Giant Proximity Effect (which we have discovered earlier⁹) in optimally doped $\text{La}_{1.85}\text{Sr}_{0.15}\text{CuO}_4$ - underdoped $\text{La}_{1.92}\text{Sr}_{0.08}\text{CuO}_4$ - $\text{La}_{1.85}\text{Sr}_{0.15}\text{CuO}_4$ trilayers using low-energy μSR (with E. Morenzoni and A. Suter, PSI, Zurich, Switzerland);
- Search for photo-induced midgap states in La_2CuO_4 films by ultrafast pump-probe spectroscopy (with J. Demsar, Konstanz, Germany).
- EXAFS in $\text{La}_{2-x}\text{Sr}_x\text{CuO}_4$ films doped to different levels (with S. Konradson, LANL)
- X-Ray Raman spectroscopy and VUV ellipsometry in $\text{La}_{2-x}\text{Sr}_x\text{CuO}_4$ films doped to different levels (with A. Rusidy, Hamburg, Germany).
- Ion-implanted Josephson junctions and arrays (with S. Cybart and R. Dynes, Berkeley).



iv) References

- I. Bozovic, J. Eckstein and G. Virshup, *Physica C* 235, 178 (1994).
- I. Bozovic, *IEEE Trans. Appl. Superconduct.* 11, 2686 (2001).
- I. Bozovic et al., *Phys. Rev. Lett.* 89, 107001 (2002);
- P. Abbamonte, et al., *Science* 297, 581 (2002).
- I. Bozovic et al., *Nature* 422, 873 (2003).
- N. Gedik et al., *Science* (2007) in press.
- J. He et al., *Journal of Applied Physics* (2006) in press.
- I. Bozovic et al., *Phys. Rev. B* 69, 132503 (2004).
- I. Bozovic et al., *Phys. Rev. Lett.* 93, 157002 (2004).

v) *Publications in 2006-2007*

1. G. Logvenov, A. Gozar and I. Bozovic, "Interface Superconductivity with $T_c \sim 30$ K in La_2CuO_4 / metallic non-SC $\text{La}_{2-x}\text{Sr}_x\text{CuO}_4$ Bilayers", to be sent to *Nature*.
2. J. Demsar, V. Thorsmolle, A. Taylor, A. Gozar and I. Bozovic, "Photo-induced midgap states in LaSrAlO_4 ", submitted to *Phys. Rev. Lett.* (2007)
3. A. Gozar, G. Logvenov, V. Y. Butko, and I. Bozovic, Surface Structure of Atomically Smooth BaBiO_3 Films, submitted to *Phys. Rev. B.* (2007)
4. G. Logvenov, V. Butko, C. Deville-Cavellin, J. Seo, A. Gozar and I. Bozovic, Engineering Interfaces in Cuprate Superconductors, *Physica B* (2007) in press.
5. N. Gedik, D.-S. Yang, G. Logvenov, I. Bozovic and A. Zewail, "Non-equilibrium Phase Transitions in Cuprates Observed by Ultrafast Electron Crystallography", *Science* (2007) in press.
6. I. Bozovic, "Possible Jahn-Teller effect and strong electron-phonon coupling in beryllium hydride", in Festschrift for K. A. Mueller, ed. by A. Bussman-Holder (Springer, Berlin, 2007) in press.
7. G. Logvenov, I. Sveklo, and I. Bozovic, "Combinatorial Molecular Beam Epitaxy of $\text{La}_{2-x}\text{Sr}_x\text{CuO}_{4+\delta}$ " *Physica C* (2006) in press.
8. G. Logvenov and I. Bozovic, "Molecular Beam Epitaxy of Complex Oxides", Proc. 2nd International conference "On problems of High Temperature Superconductivity" ed. by I. Mitsin, Zvenigorod, Russia (2006).
9. J. He, R. F. Klie, G. Logvenov, I. Bozovic and Y. Zhu, "Microstructure and possible strain relaxation mechanisms of $\text{La}_2\text{CuO}_{4+\delta}$ thin films grown on LaSrAlO_4 and SrTiO_3 substrates", *Journal of Applied Physics* (2006) in press.
10. A. Bollinger, G. Logvenov and I. Bozovic, "Atomic-Scale Engineering of Thin Films of Complex Oxides Using ALL-MBE", Proc. ICCE-14, ed. by D. Hui, 2006.
11. I. Bozovic, "About Physics, Myself, and Ginzburgs", *Journal of Superconductivity* **19**, 469 (2006).
12. G. Logvenov and I. Bozovic, "Artificial superlattices grown by MBE: can we design novel superconductors?", *Proc. Workshop on Room Temperature Superconductivity*, ed. by B. Janko, University of Notre Dame, 2006.
13. M. Reehuis, C. Ulrich, K. Prokes, A. Gozar, G. Blumberg, S. Komiyama, Y. Ando, P. Pattison and B. Keimer, "Crystal structure and high field magnetism in La_2CuO_4 ", *Phys. Rev. B* **73**, 144513 (2006).
14. L. Benfatto, M. Silva-Neto, A. Gozar, B. Dennis, G. Blumberg, L. Miller, S. Komiyama and Y. Ando, "Field dependence of the magnetic spectrum in anisotropic and Dzyaloshinskii-Moriya antiferromagnets. II. Raman spectroscopy", *Phys. Rev. B* **74**, 024416 (2006).
15. A. Rogachev, T. -C. Wei, D. Pekker, A. T. Bollinger, P. M. Goldbart and A. Bezryadin, "Magnetic-Field Enhancement of Superconductivity in Ultranarrow Wires", *Phys. Rev. Lett.* **97**, 137001 (2006).
16. A. T. Bollinger, A. Rogachev, and A. Bezryadin, "Dichotomy in short superconducting nanowires: Thermal phase slippage vs. Coulomb blockade", *Europhys. Lett.*, published online September 27, 2006.
17. V. Y. Butko, H. Wang and D. Reagor, "A Metallic State in a Crystalline Insulator due to the Normal Electron Proximity Effect", submitted to *Physical Review Letters* (2006).
18. W. So, D. V. Lang, V. Y. Butko, X. Chi, J. C. Lashley and A. P. Ramirez, "Relationship between Mobility and Localized Gap States in Single-Crystal Organic Field-Effect-Transistors", submitted to *Physical Review Letters* (2006).

Rational Growth, Control and Manipulation of Novel Materials

T. A. Lograsso, R. W. McCallum and P. C. Canfield
Materials and Engineering Physics, Ames Laboratory, Ames IA 50010

Program Scope

The design, synthesis and characterization of new materials that lead to important discoveries, both expected and unexpected, as well as new knowledge and techniques, within and across traditional disciplinary boundaries, are critical components of the DOE, Basic Energy Sciences' mission. In support of this mission, the *Rational Growth, Control and Modification of Novel Materials* effort will advance Ames Laboratory's capabilities to synthesize and characterize high purity, high quality materials, primarily in single crystal form, spanning a range of sizes. This will involve research focused on quantifying and controlling the processing-structure-property relationship of responsive materials as well as examining promising phase spaces (either physical or chemical) that we identify as compelling based upon advances in synthesis and / or control of novel materials.

During the next three years, this effort will advance both the Bridgman and solution growth techniques by implementing greater control over the nucleation and growth processes so as to improve overall homogeneity and volume. In addition, we will augment our suite of growth capabilities and develop a wide range of new fluxes, primarily for light, reactive and/or volatile elements. These advances in synthesis will allow us to develop model systems which exhibit a high degree of sensitivity to controllable chemical and structural imperfection. These model systems will allow for the systematic study of the dominant mechanisms that lead to or affect responsive behaviors. In specific, we will focus on behaviors controlled by twin boundary motion, clustering in solid solutions, defect density and fine-scale phase heterogeneity.

Recent Progress

An example of early synergy between our research groups was joint efforts on the physics, metallurgy and surface science of quasicrystalline materials. Each group utilized their individual growth and characterization methods to produce a wide range of large single grain quasicrystalline compounds, e.g., Al-Pd-Mn, R-Zn-Mg Al-Cu-Fe, Al-Ni-Co and, most recently, binary Cd-Yb quasicrystals and their approximant phases. The availability of these materials as single grains from the Ames Laboratory has had significant impact on the scientific understanding of this new class of materials. For instance, our large, highly perfected, single grains challenged the idea that these materials were inherently disordered due to their aperiodic structure. High resolution TEM studies (Figure 1) of solution grown R-Zn-Mg found that these quasicrystals had the lowest density of phason strain (gross equivalent of defect density) of any known quasicrystals [1].

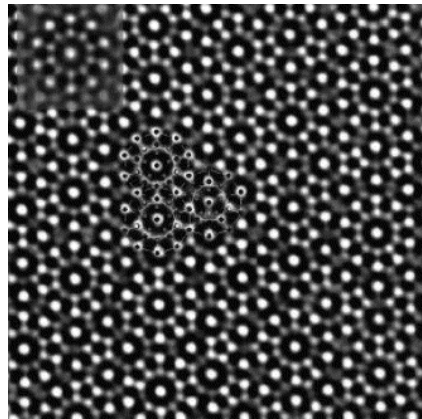


Figure 1 HRTEM image taken along the 5f (10×10 nm) for the Y-Mg-Zn face centered icosahedral and model structure (near center) with small inset showing the multi-slice calculation for a single cluster.

Although being able to grow “lots of really big” crystals is a fine accomplishment, it is vital to keep in mind that issues of purity, stoichiometry, and structural perfection are ubiquitous problems in new materials physics. The *Rational Growth* group has been, and will continue to be, active in clarifying such issues on a wide range of new materials that are either of direct interest to the group, or are of particular interest to other groups within the Ames Laboratory and elsewhere. Recent examples include preparation of Ni-Mn-Ga ferromagnetic shape memory alloys with low enough defect densities to allow for the high

mobility of twin boundaries. These highly mobile twin boundaries are necessary for achieving the full theoretical value (6%) of magnetic field induced strain [2]. Other examples of this are the relationship between transport properties and boron purity in MgB_2 (the intermetallic superconductor with the current highest T_c) [3] and the establishment of an extreme sensitivity of the temperature dependent resistivity of single crystalline $\text{YbNi}_2\text{B}_2\text{C}$ (a model heavy fermion compound) to the dislocation line density [4]. In this latter case, we were able to control the dislocation density via judicious post growth annealing and we were able to quantify the dislocation density using TEM. In these examples, the establishment of clear and controllable relations between the sample preparation, growth and processing, and the physical properties allowed for a clearer understanding of the underlying physics.

As part of our effort to define and manipulate the tuning and requisite control parameters, we have also found it necessary to push the frontiers of new materials growth and design. This has taken the form of modifying existing growth techniques to allow for better control of growth and processing conditions; creating new growth techniques to allow for new combinations of control parameters; devising new types of solutions for the growth of samples, and new types of crucibles for their containment and manipulation. In order to improve phase purity and reduce physical cracking in $\text{R}_5(\text{Si}_{1-x}\text{Ge}_x)_4$ compounds, we implemented tri-arc crystal pulling methods [5] to avoid crucible interactions encountered in the Bridgman methods. In order to produce single crystals of complex Pr-Ni-Si compounds with very narrow exposed liquid solidus surfaces we devised a solution growth / Bridgman hybrid growth technique [6]. In order to grow single grain of R-Mg-Zn quasicrystals, we developed sealed Ta crucibles with a fully enclosed filter that allowed for the use and decanting of volatile Mg-rich solutions [7].

Future Plans

The goals of the *Rational Growth, Control and Modification of Novel Materials* group are to:

- Advance the ability to synthesize and characterize high purity, high quality materials, primarily in single crystal form, spanning a range of sizes;
- Quantify and control processing-structure-property relationships: the basic science of how chemical inhomogeneities and structural defects affect the properties of highly responsive materials;
- Explore promising phase spaces (either physical or chemical) that we identify as compelling based upon advances in synthesis and / or control of novel materials.

We will address these goals through work on a number of activities. In the area of growth capabilities, we will advance both Bridgman and solution growth techniques by implementing greater control over the nucleation and growth processes so as to improve overall sample homogeneity and volume. In addition, we propose to augment our suite of growth capabilities by implementing vapor transport methods. Quantification and control of twin boundaries, clustering in solid solutions and defect density will be systematically studied in a number of model systems that have become accessible to us through our wide range of growth techniques. Finally, we will explore promising phase spaces by (i) developing a wide range of new fluxes, primarily for light, reactive and/or volatile elements and (ii) studying the effects of chemical and phase inhomogeneities on the wide range of groundstates existing in the Heusler/half-Heusler structural families.

For this meeting, we will discuss our ongoing research on clusters in solid solutions. Recently, Fe-Ga alloys were discovered to possess the highest single crystalline magnetostrictive strain (~13x that of pure Fe) of binary alloys. Our ability to prepare single crystals via several growth methods with controlled compositions over a large composition range ($0 < x < 35$) and through several different, but similar phase fields, has directly allowed for extensive property measurements and structural studies to be conducted. Based on these single crystal investigations, there is growing theoretical and experimental evidence suggesting non-random distributions or clustering of Ga atoms within the Fe lattice plays an important role in enhancing the magnetoelasticity. Specifically, the nature of non-random Ga clusters and how they

affect the strain, elasticity and magnetic moment distributions within the Fe Lattice are open questions. How does Ga substitution and clustering affect the band structure of Fe? What is the nature of Ga short range order? What lattice distortions are created by the short range order (type, crystallographic nature, magnitude of strains) and do these and/or other types of distortions or chemical ordering lead to enhanced magnetoelasticity?

We will continue to investigate Fe-X alloys to understand the role of clustering (random and non-random) of solute atoms on the magnetoelastic coupling of Fe and, more broadly, on the magnetic and transport properties in solid solutions. In the course of this investigation we will directly address the question of how non-random clustering can be analyzed and controlled through physical property measurement and structural characterization. We will extend these studies to other binary Fe-X systems where clustering of solute is reported to occur (e.g. Al, Si, Ti, Mn, Mo) to examine the effect of atomic size and electronic structure on the effectiveness of the clusters to control magnetoelastic interactions. We will utilize X-ray diffraction during in-situ heating/cooling with applied magnetic fields to examine the structural evolution and distortions arising from magnetically induced strains, evolution of two-phase mixtures during thermal processing and quantification of the phase distributions. Phase identification will also be confirmed by TEM investigations and time resolved single crystal diffraction at the Advanced Photon Source. Detailed TEM convergent beam studies will examine localized lattice distortions and symmetry associated with short range order. When coupled with unique *in-situ* heating, we will link microstructural evolution associated with phase distribution, domain and defect structure, and crystallography with magnetic properties and processing. This detailed characterization of clusters and their influence on properties will lead to the ability to tailor the synthesis routes and chemistry to optimize the magnetoelastic response of existing alloys and to provide intelligent search criteria for discovering new compounds or alloys.

References

1. M. J. Kramer, S. T. Hong, P. C. Canfield, I.R. Fisher, J. D. Corbett, Y. Zhu, and A. I. Goldman, *J. Alloys and Comp.*, **342**, 82 (2002).
2. S. J. Murray, M. Marioni, S. M. Allen, R. C. O'Handley and T. A. Lograsso, *Appl. Phys. Lett.*, **77**, 886 (2000).
3. R. A. Ribeiro, S. L. Bud'ko, C. Petrovic, and P. C. Canfield, *Physica C*, **382**, 194 (2002).
4. M. A. Avila, Y.Q. Wu, C. L. Condron, S. L. Bud'ko, M. Kramer, G. J. Miller and P. C. Canfield, *Phys. Rev. B*, **69**, 205107 (2004).
5. T. A. Lograsso, D. L. Schlagel and A. O. Pecharsky, *J. Alloy Comp.*, **393**, 141 (2005).
6. D. Wu, R. W. McCallum and T. A. Lograsso, Unpublished Research (2004).
7. I. R. Fischer, M. J. Kramer, Z. Islam, T. A. Wiener, A. Kracher, A. R. Ross, T. A. Lograsso, A. I. Goldman and P. C. Canfield, *Mat Sci. Eng. A*, **294-296**, 10 (2000).

Publications (last 2 years)

- T. A. Lograsso, D. L. Schlagel and A. O. Pecharsky, "**Synthesis and Characterization of Single Crystalline $Gd_5(Si_xGe_{1-x})_4$ by the Bridgman Method**", *J. Alloy Comp.*, **393**, 141 (2005).
- H. Wende, A. Scherz, C. Sorg, Z. Li, P. Pouloupoulos, K. Baberschke, A. Ankudinov, J. J. Rehr, F. Wilhelm, N. Jaouen, A. Rogalev, D. L. Schlagel and T. A. Lograsso, "**Temperature Dependence of Magnetic EXAFS for Rare Earth Elements**", *Physica Scripta*, **T115**, 600 (2005).
- M. Huang and T. A. Lograsso, "**Experimental Investigation and Thermodynamic Modeling of the Ni-Pr System**", *J. Alloy Comp.*, **395**, 75 (2005).

- A. E. Clark, J. B. Restorff, M. Wun-Fogle, K. W. Dennis, T. A. Lograsso, and R. W. McCallum, **“Temperature Dependence of the Magnetic Anisotropy Constants of Fe_{100-x}Ga_x, x=8.6, 16.6, 28.5”**, J. Appl. Phys., **97**, 10M316 (2005).
- M. Huang, R. W. McCallum and T. A. Lograsso, **“Experimental Investigation and Thermodynamic Modeling of the Nd-Ni System”**, J. Alloy Comp., **398**, 127 (2005).
- M. Huang, D. Wu, K. W. Dennis, R. W. McCallum and T. A. Lograsso, **“Revised Phase Diagram for the Ni-Pr System in Pr-rich Region”**, J. Phase Equil. Diff., **26**, 209 (2005).
- L. Tan, A. Kreyssig, J. W. Kim, A. I. Goldman, R. J. McQueeney, D. Wermeille, B. Sieve, T. A. Lograsso, D. L. Schlagel, S. L. Budko, V. K. Pecharsky and K. A. Gschneidner, Jr., **“The Magnetic Structure of Gd₅Ge₄”**, Phys. Rev. B, **71**, 214408 (2005).
- A. L. Lima, A. O. Tsokol, K. A. Gschneidner, Jr., V. K. Pecharsky, T. A. Lograsso, and D. L. Schlagel, **“The Magnetic Properties of Single Crystal DyAl₂”**, Phys. Rev. B, **71**, 024403 (2005).
- M. J. Kramer, D. J. Sordelet and T. A. Lograsso, **“Solid and Liquid Thermal Expansion and Structural Observations in the Quasicrystalline Cd₈₄Yb₁₆ Compound”**, Phil Mag. Lett., **85**, 151 (2005).
- M. Pasquale, C. P. Sasso, L. H. Lewis, L. Giudici, T. Lograsso and D. Schlagel, **“Magneto-structural Transition and Magnetocaloric Effect in Ni₅₅Mn₂₀Ga₂₅ Single Crystals”**, Phys. Rev. B., **72**, 094435 (2005).
- J. L. Zarestky, V. O. Garlea, T. A. Lograsso, D. L. Schlagel and C. Stassis, **“Compositional Variation of the Phonon Dispersion Curves of bcc Fe-Ga Alloys”**, Phys. Rev. B, **72**, 180408 (2005).
- Y. Janssen, M. Angst, K. W. Dennis, P. C. Canfield and R. W. McCallum, **“Differential Thermal Analysis and Solution Growth of Intermetallic Compounds.”**, J. Crystal Growth, **285**, 670 (2005).
- D. Wu, O. Ugurlu, L. S. Chumbley, M. J. Kramer and T. A. Lograsso, **“Synthesis and Characterization of Hexagonal Cd₅₁Yb₁₄ Single Crystals”**, Phil. Mag., **86**, 381 (2006).
- O. Ugurlu, L. S. Chumbley, D. L. Schlagel and T. A. Lograsso, **“Orientation and Formation of Atypical Widmanstätten Plates in the Gd₅(Si_xGe_{1-x})₄ System”**, Acta Mat., **54**, 1211 (2006).
- X. Moya, L. Manosa, A. Planes, T. Krenke, M. Acet, O. Garlea, T. Lograsso and J. Zarestky, **“Lattice Dynamics of Ni-Mn-Al Shape Memory Alloys”**, Phys. Rev. B, **73**, 064401 (2006).
- Y. Janssen, S. Chang, B. K. Cho, A. Llobet, K. W. Dennis, R. W. McCallum, R. J. McQueeney, and P. C. Canfield, **“YbGaGe: Normal Thermal Expansion”**, J. Alloys Comp., **389**, 10 (2005).
- Z. Islam, D. Haskel, J. C. Lang, G. Srajer, Y. Lee, B. N. Harmon, A. I. Goldman, D. L. Schlagel and T. A. Lograsso, **“An X-Ray Study of Non-Zero Nickel Moment in a Ferromagnetic Shape-Memory Alloy”**, J. Mag. Magn. Mat., **303**, 20 (2006).
- X. Moya, L. Mañosa, A. Planes, T. Krenke, M. Acet, M. Morin, J. L. Zarestky, and T. A. Lograsso, **“Temperature and Magnetic-field Dependence of the Elastic Constants of Ni-Mn-Al Magnetic Heusler Alloys”**, Phys. Rev. B, 024109 (2006).
- Y. Janssen, M. Angst, K. W. Dennis, P. C. Canfield and R. W. McCallum, **“Small Sealed Ta Crucible for Thermal Analysis of Volatile Metallic Samples”**, Rev. Sci. Instr., **77**, 056104 (2006).
- J. L. Zarestky, O. Moze, J. W. Lynn, Y. Chen, T. A. Lograsso and D. L. Schlagel, **“Spin Wave Dispersion in Magnetostrictive Fe-Ga Alloys”**, Phys. Rev. B, **75**, 052406 (2007).

Neutron Scattering: Growth of Large Single-Crystal Samples

John M. Tranquada, Genda Gu, Markus Hückler, and the Neutron Scattering Group
jtran@bnl.gov, ggu@bnl.gov, huecker@bnl.gov, <http://neutrons.phy.bnl.gov/>

Condensed Matter Physics & Materials Science Department,
Brookhaven National Laboratory, Upton, NY 11973-5000

Program Scope

The main scope of the program is the study of cooperative phenomena in complex solids using neutron scattering techniques. We are especially interested in correlated-electron phenomena in transition-metal oxide compounds such as the cuprate high-temperature superconductors. Experiments use neutron and X-ray diffraction to study static spin and charge ordering, and inelastic neutron scattering to study spin and lattice dynamics. The neutron experiments are performed at the best facilities in the U.S. and the world, including the NIST Center for Neutron Research, and the High Flux Isotope Reactor at Oak Ridge; we look forward to using the Spallation Neutron Source in the future. Many of the experiments would not be practical without the availability of very large ($> 1 \text{ cm}^3$) single-crystal samples. We grow many of these crystals at BNL using two infrared image furnaces. The crystals are also shared with collaborators in other groups at BNL and outside, especially for studies with infrared reflectivity, angle-resolved photoemission spectroscopy, and soft X-ray resonant diffraction.

Recent Progress

A wide variety of crystals have been grown successfully over the last few years, including: $\text{La}_{2-x}(\text{Sr,Ca})_x\text{CaCu}_2\text{O}_6$, $\text{La}_{2-x}\text{Sr}_x\text{CuO}_4$, $\text{La}_{2-x}\text{Ba}_x\text{CuO}_4$, $\text{Bi}_2\text{Sr}_2\text{CaCu}_2\text{O}_{8+d}$, $\text{Nd}_{1.67}\text{Sr}_{0.33}\text{NiO}_4$, LuFe_2O_4 , SrCu_2O_3 , and Cu_2O . Four large co-aligned crystals of $\text{La}_{2-x}\text{Ba}_x\text{CuO}_4$ with $x = 1/8$ were used to map out the dispersion of magnetic excitations in the stripe ordered phase. We have now extended those measurements to higher temperatures and shown that the spectrum is not very sensitive to static ordering. Measurements of the bond-stretching phonon mode reveal evidence for a strong electron-phonon coupling at a special wave vector; the effect is strongest in a sample with stripe order, but is also present in samples without static order. Transport measurements on the same material have revealed evidence for two-dimensional superconducting correlations below the spin-ordering temperature, suggesting that the stripes are good for electronic pairing but stripe ordering is bad for superconducting phase coherence. Optimally-doped crystals of $\text{Bi}_2\text{Sr}_2\text{CaCu}_2\text{O}_{8+d}$ have been studied with both polarized and unpolarized inelastic neutron scattering to reveal the magnetic excitations. The results are presently being analyzed.

Future Plans

The phase diagram of $\text{La}_{2-x}\text{Ba}_x\text{CuO}_4$ will be investigated for $x \neq 1/8$. This will involve neutron, x-ray, infrared, photoemission, and transport studies of the stripe order, electronic response, and superconductivity. Efforts will also be directed towards preparing large crystals of $\text{Bi}_2\text{Sr}_2\text{CaCu}_2\text{O}_{8+d}$ in the underdoped regime for studies of the

magnetic excitations. In terms of facilities, we are interested in expanding our crystal growth capabilities. In particular, we would like to be able to grow crystals in high oxygen partial pressure (our present limit is 11 bar). As a first step, we are working to acquire a hot isostatic press capable of greater than one thousand bar oxygen partial pressure. We are also monitoring the development of image furnaces capable of pressures up to 100 bar.

Selected DOE-Sponsored Publications, 2005-2007

Behr, G., Löser, W., Apostu, M.-O., Gruner, W., Hücker, M., Schramm, L., Souptel, D., and Werner, J. Floating zone growth of CuO under elevated oxygen pressure and its relevance for the crystal growth of cuprates. *Cryst. Res. Technol.* **40**, 21 (2005).

Hücker, M., Kim, Young-June, Gu, G.D., Tranquada, J.M., Gaulin, B.D., and Lynn, J.W. Neutron scattering study on $\text{La}_{1.9}\text{Ca}_{1.1}\text{Cu}_2\text{O}_{6+\delta}$ and $\text{La}_{1.85}\text{Sr}_{0.15}\text{CaCu}_2\text{O}_{6+\delta}$. *Phys. Rev. B* **71**, 094510 (2005).

Hücker, M., Gu, G.D., and Tranquada, J.M. Spin Susceptibility and Magnetization of a Stripe-Ordered Cuprate. cond-mat/0503417.

Kim, Y.-J., Hill, J.P., Gu, G., Chou, F., Wakimoto, S., Birgeneau, R., Komiya, S., Ando, Y., Motoyama, N., Kojima, K., Uchida, S., Casa, D., and Gog, T. Molecular orbital excitations in cuprates. *Phys. Rev. B* **70**, 205128 (2004).

Abbamonte, P., Rusydi, A., Smadici, S., Gu, G.D., Sawatzky, G.A., and Feng, D.L. Spatially Modulated "Mottness" in $\text{La}_{2-x}\text{Ba}_x\text{CuO}_4$. *Nature Phys.* **1**, 155-158 (2006)

Castellan, J. P., Gaulin, B. D., Dabkowska, H. A., Nabialek, A., Gu, G., Liu, X., and Islam, Z. Two- and three-dimensional incommensurate modulation in optimally-doped $\text{Bi}_2\text{Sr}_2\text{CaCu}_2\text{O}_{8+\delta}$. *Phys. Rev. B* **73**, 174505 (2006).

Dordevic, S.V., Homes, C.C., Gu, G.D., Si, W., and Wang, Y.J. Effect of a magnetic field on the electron-boson spectral function of cuprate superconductors. *Phys. Rev. B* **73**, 132501 (2006).

Fischer, D., Moodenbaugh, A., Li, Q., Gu, G., Zhu, Y., Davenport, J., and Welch, D. Soft X-ray Absorption Spectroscopy of the MgB_2 Boron K Edge in an MgB_2/Mg Composite. *Mod. Phys. Lett. B* **20**, 1207-16 (2006).

Gu, G.D., Hücker, M., Kim, Y.-J., Tranquada, J.M., Dabkowska, H., Luke, G.M., Timusk, T., Gaulin, B.D., Li, Q., Moodenbaugh, A.R. Crystal growth and superconductivity of $(\text{La}_{1-x}\text{Ca}_x)_2\text{CaCu}_2\text{O}_{6+\delta}$. *J. Phys. Chem. Solids* **67**, 431-4 (2006)

Gu, G.D., Hücker, M., Kim, Y.-J., Tranquada, J.M., Li, Q., and Moodenbaugh, A.R. Single-crystal growth and superconductivity of $(\text{La}_{1-x}\text{Sr}_x)_2\text{CaCu}_2\text{O}_{6+\delta}$. *J. Crystal Growth* **287**, 318-22 (2006).

Homes, C.C., Dordevic, S.V., Gu, G.D., Li, Q., Valla, T., and Tranquada, J.M. Charge order, metallic behavior, and superconductivity in $\text{La}_{2-x}\text{Ba}_x\text{CuO}_4$ with $x=1/8$. *Phys. Rev. Lett.* **96**, 257002 (2006).

Hücker, M., Gu, G.D., Tranquada, J.M., Zimmermann, M.v., Klauss, H. -H., Curro, N.J., Braden, M., Büchner, B. Coupling of stripes to lattice distortions in cuprates and nickelates. *Physica C* (accepted).

Izquierdo, M., Avila, J., Roca, L., Gu, G.D., and Asensio, M.C. Polarization Effects in Photoemission Disentangle the Origin of the Shadow Bands in Bi-based Superconductors. *Phys. Rev. B* **72**, 174517(2005).

Izquierdo, M., Megtert, S., Albouy, J.P., Avila, J., Valbuena, M.A., Gu, G.D., Abell, J.S., Yang, G., Asensio, M.C., and Comes, R. X-ray diffuse scattering experiments from bismuth based high T_c superconductors. *Phys. Rev. B* **74**, 054512 (2006).

Reznik, D., Pintschovius, L., Ito, M., Iikubo, S., Sato, M., Goka, H., Fujita, E., Yamada, K., Gu, G.D., and Tranquada, J.M. Electron-Phonon Coupling Reflecting Dynamic Charge Inhomogeneity in Copper-oxide Superconductors. *Nature* **440**, 1170-1173 (2006).

Reznik, D., Pintschovius, L., Fujita, M., Yamada, K., Gu, G.D., and Tranquada, J.M. Electron-Phonon Anomaly Related to Charge Stripes: Static Stripe Phase Versus Optimally-doped Superconducting $\text{La}_{1.85}\text{Sr}_{0.15}\text{CuO}_4$. *J. Low Temp. Phys.* (accepted); cond-mat/0611079.

Richard, P., Pan, Z. -H., Neupane, M., Fedorov, A.V., Valla, T., Johnson, P.D., Gu, G.D., Ku, W., Wang, Z., and Ding, H. Nature of oxygen dopant-induced states in high-temperature $\text{Bi}_2\text{Sr}_2\text{CaCu}_2\text{O}_{8+x}$ superconductors: A photoemission investigation. *Phys. Rev. B* **74**, 094512 (2006).

Savici, A.T., Fukaya, A., Gat-Malureanu, I.M., Ito, T., Russo, P.L., Uemura, Y.J., Wiebe, C.R., Kyriakou, P.P., MacDougall, G.J., Rovers, M.T., Luke, G.M., Kojima, K.M., Goto, M., Uchida, S., Kadono, R., Yamada, K., Tajima, S., Masui, T., Eisaki, H., Kaneko, N., Greven, M., and Gu, G.D. Muon Spin Relaxation Studies of Magnetic-Field-Induced Effects in High- T_c Superconductors. *Phys. Rev. Lett.* **95**, 157001 (2005).

Savici, A.T., Zaliznyak, I.A., Gu, G.D., and Erwin, R. Stripeless Incommensurate Magnetism in a Doped Strongly Correlated Oxide. *Phys. Rev. B* (submitted); cond-mat/0608575

Shapiro, S.M., Xu, G., Gu, G.D., Gardner, J., and Fong, R.W. Lattice dynamics of the high temperature shape memory alloy Nb-Ru. *Phys. Rev. B* **73**, 214114 (2006).

Tranquada, J.M., Woo, H., Perring, T.G., Goka, H., Gu, G.D., Xu, G., Fujita, M., and Yamada, K. Universal magnetic excitation spectrum in cuprates. *J. Phys. Chem. Solids* **67**, 511-15 (2006).

Valla, T., Kidd, T.E., Rameau, J.D., Noh, H.-J., Gu, G.D., Johnson, P.D., Yang, H.-B., Ding, H. Fine details of the nodal electronic excitations in $\text{Bi}_2\text{Sr}_2\text{CaCu}_2\text{O}_{8+\delta}$. *Phys. Rev. B* **73**, 184518 (2006).

Wakimoto, S., Kimura, H., Fujita, M., Yamada, K., Noda, Y., Shirane, G., Gu, G.D., Kim, H.K. and Birgeneau, R.J. Incommensurate Lattice Distortion in the High Temperature Tetragonal Phase of $\text{La}_{2-x}(\text{Sr},\text{Ba})_x\text{CuO}_4$. *J. Phys. Soc. Jpn.* **75**, 074714 (2006).

Wang, Y., Li, L., Naughton, M.J., Gu, G.D., Uchida, S., and Ong, N.P. Field-enhanced diamagnetism in the pseudogap state of the cuprate $\text{Bi}_2\text{Sr}_2\text{CaCu}_2\text{O}_{8+\delta}$ superconductor in an intense magnetic field. *Phys. Rev. Lett.* **95**, 247002 (2005).

T. Valla, A. V. Fedorov, Jinho Lee, J.C. Davis, and G. D. Gu. The Ground State of the Pseudogap in Cuprate Superconductors. *Science* **314**, 1914 (2006)

T. Valla, T. E. Kidd, W.-G. Yin, G. D. Gu, P. D. Johnson, Z.-H. Pan, and A. V. Fedorov. High-Energy Kink Observed in the Electron Dispersion of High-Temperature Cuprate Superconductors. *Phys. Rev. Lett.* **98**, 167003 (2007).

D. C. Schmadel, G. S. Jenkins, J. J. Tu, G. D. Gu, Hiroshi Kontani, and H. D. Drew. Infrared Hall conductivity in optimally doped $\text{Bi}_2\text{Sr}_2\text{CaCu}_2\text{O}_{8+d}$: Drude behavior examined by experiment and fluctuation-exchange-model calculations. *Phys. Rev. B* **75**, 140506 (2007).

M. Hücker, M. v. Zimmermann, and G. D. Gu. Robust charge stripe order under high electric fields in $\text{Nd}_{1.67}\text{Sr}_{0.33}\text{NiO}_4$. *Phys. Rev. B* **75**, 041103 (2007).

Guangyong Xu, J. M. Tranquada, T. G. Perring, G. D. Gu, M. Fujita, and K. Yamada. High-energy magnetic excitations from dynamic stripes in LBCO ($x=1/8$). [cond-mat/0702027](#).

Q. Li, M. Huecker, G. D. Gu, A. M. Tsvelik, and J. M. Tranquada. Two-Dimensional Superconducting Fluctuations in Stripe-Ordered $\text{La}_{1.875}\text{Ba}_{0.125}\text{CuO}_4$. [cond-mat/0703357](#).

Poster Session

- I. Structural and Chemical Complexity**
- II. Defect-Controlled Synthesis**

This page is intentionally blank

Odd-parity, spin-triplet superconductivity in Sr_2RuO_4 and the physics of ruthenates in $\text{Sr}_{n+1}\text{Ru}_n\text{O}_{3n+1}$ series: Single crystals, eutectic systems, and thin films

Ying Liu

Department of Physics, Pennsylvania State University, University Park, PA 16802. liu@phys.psu.edu.

1. PROGRAM SCOPE

Almost all known superconducting materials, ranging from elemental superconductors to exotic high- T_c cuprates, feature an even-parity, spin-singlet (s - or d -wave) pairing symmetry. Odd-parity, spin-triplet (p - or f -wave) superconductivity, a spectacular manifestation of electron correlations, is rare. Sr_2RuO_4 , the only Cu-free layered perovskite superconductor with a T_c of 1.5 K, is considered the first experimentally established odd-parity, spin-triplet superconductor. In this research program, we have pursued work on Sr_2RuO_4 and other closely related compounds in Ruddeldsen-Popper series of $\text{Sr}_{n+1}\text{Ru}_n\text{O}_{3n+1}$, including the preparation and characterization of bulk single crystals, thin films, and eutectic systems of these complex transition metal oxides. Specifically, we have been working on 1) phase-sensitive measurements on $\text{Au}_{0.5}\text{In}_{0.5}\text{-Sr}_2\text{RuO}_4$ superconducting quantum interference devices (SQUIDs) and single junctions on high quality single crystal of Sr_2RuO_4 , which showed unambiguously for the *first* time that Sr_2RuO_4 is indeed an odd-parity, spin-triplet superconductorⁱ; 2) single-particle tunneling measurements on several eutectic systems of Sr_2RuO_4 , including $\text{Ru/Sr}_2\text{RuO}_4$, $\text{Sr}_2\text{RuO}_4/\text{Sr}_3\text{Ru}_2\text{O}_7$, and $\text{SrRuO}_3/\text{Sr}_2\text{RuO}_4$, revealing fascinating physical phenomena such as a possible mixed pairing state; 3) low-temperature scanning SQUID studies of Sr_2RuO_4 to seek for direct evidence for the presence of exotic topological defects including domain walls, d -vector solitons, and half-flux vortex quanta; 4) magnetic, electrical transport, and thermopower measurements on the $n = 3$ member of the $\text{Sr}_{n+1}\text{Ru}_n\text{O}_{3n+1}$ series, $\text{Sr}_4\text{Ru}_3\text{O}_{10}$, which sits at the boundary between superconductivity (in Sr_2RuO_4) and ferromagnetism (in SrRuO_3) within this series; and finally, 5) the preparation of thin films of Sr_2RuO_4 by pulsed-laser deposition (PLD), molecular beam epitaxy (MBE), and a novel mechanical exfoliation approach, and their characterization. We have been collaborating with a number of leading groups specializing on single crystal and epitaxial thin film synthesis and on low-temperature scanning SQUID measurements in these efforts.

2. RESEARCH PROGRESS

2.1. Single-crystal-based Sr_2RuO_4 SQUIDs and single junctions: Pairing symmetry of Sr_2RuO_4

While the original motivation for studying Sr_2RuO_4 was to obtain insight into the high- T_c problem, it soon became clear that the most interesting aspect of superconductivity in Sr_2RuO_4 was that Sr_2RuO_4 might be a p -wave superconductor. A phase-sensitive experiment, the most stringent test of the pairing symmetry as demonstrated in the high- T_c work, was needed to fully establish the pairing symmetry of a superconductor. Since superconducting thin films of Sr_2RuO_4 are yet to be grownⁱⁱ, we pursued experiments on single-crystal-based $\text{Au}_{0.5}\text{In}_{0.5}\text{-Sr}_2\text{RuO}_4$ SQUIDs and single junctions. Over the years we have been working with our collaborators to grow high-quality single crystals suitable for preparing the SQUID, and more recently single junctions that require a finely controlled stoichiometry and with a ultralow impurity level – 100 ppm non-magnetic impurities of Al would completely destroy superconductivity in Sr_2RuO_4 . Our measurements show that Sr_2RuO_4 is a chiral p -wave superconductorⁱ, most likely with horizontal line nodesⁱⁱⁱ, a conclusion that is to be universally accepted.

2.2. Eutectic system of $\text{Sr}_2\text{RuO}_4/\text{Sr}_3\text{Ru}_2\text{O}_7$ – Magnitude of the superconducting energy gap of Sr_2RuO_4

In addition to the symmetry, the magnitude of the superconducting order parameter of Sr_2RuO_4 is also important for the understanding of superconductivity in Sr_2RuO_4 . Single-particle tunneling measurements on Sr_2RuO_4 in various junction configurations showed that the superconducting gap on the ab face of a superconducting Sr_2RuO_4 single crystal is essentially zero, most likely due to the rotation of the RuO_6 octahedra on the surface (by 14°), found originally in a scanning tunneling microscope (STM) study.

We recently performed tunneling measurements on $\text{Sr}_2\text{RuO}_4\text{-Sr}_3\text{Ru}_2\text{O}_7$ eutectic single crystals^{iv}, a rather unusual phase grown by floating zone method by our collaborators, and found superconducting gap was not suppressed on its surface. Fitting the spectrum yielded a gap of 0.20meV at 0.3K, almost exactly the weak-coupling BCS value ($\Delta/k_B T_c = 1.76$) for an experimental T_c of 1.3K. Gap values were reported for Sr_2RuO_4 previously in point contact (1meV) and STM (0.5meV) measurements, inconsistent with our results. The Sr_2RuO_4 phase in the eutectic crystal appears to grow epitaxially with the $\text{Sr}_3\text{Ru}_2\text{O}_7$ majority phase that features a 7° RuO_6 octahedra rotation. It is likely that the Sr_2RuO_4 in the eutectic phase does not rotate even at its surface, leaving superconductivity intact.

2.3. Eutectic system of Ru/Sr₂RuO₄: Existence of a mixed pairing state

Another fascinating eutectic system is Ru/Sr₂RuO₄ – pure Ru microdomains embedded in single crystalline of Sr₂RuO₄. Even though the intrinsic T_c of Ru is 0.5 K, and that for Sr₂RuO₄ is 1.5 K, T_c of the interface region between the two can be as high as 3 K (thus referred to as the 3K phase of Sr₂RuO₄). Since the occurrence of superconductivity in bulk Sr₂RuO₄ is known to be extremely sensitive to disorder, and the interface region between Ru and Sr₂RuO₄ is not particularly ordered, it is surprising that the T_c at the interface can actually be larger than those on both sides of the interface – Ru and Sr₂RuO₄. Therefore the study of the 3K phase may provide insight into the mechanism of superconductivity in Sr₂RuO₄.

We performed single-particle tunneling measurements on Ru/Sr₂RuO₄. The tunnel spectrum as a function of temperature shows two prominent features. First, a gap edge opens up below 0.5 K (the bulk T_c of Ru). The zero-temperature limit of the gap, 0.1 meV, is larger than that expected in BCS theory, 0.07 meV, estimated from the value of T_c as the gap value of Ru has never been measured. The second feature is the zero-bias conductance peak (ZBCP), which is due to the presence of Andreev surface bound states originating from the p -wave pairing. It appears that we observed both s - and p -wave pairings in the same spatial region. Even though the presence of inversion symmetry in the crystalline symmetry does not allow the coexistence of the s - and p -wave pairings, a mixed pairing state is not prohibited when the size of the superconductor is reduced, as in the case of Ru microdomain. The occurrence of a mixed pairing state may be driven by the interplay between the condensation and kinetic energies. While the presence of the p -wave pairing in Ru will cost certain condensation energy as the p -wave pairs cannot take advantage of the net attractive energy as effectively as the s -wave pairs, the kinetic energy caused by the order parameter gradient from having to match the order parameter of the s -wave Ru microdomain and that of the surrounding p -wave superconductor of Sr₂RuO₄ is actually reduced. The magnetic field dependences of the tunneling spectrum further suggests that s - and p -wave pairings coexisting in the central part of the Ru microdomain form a chiral mixed pairing state of the form $s + ip$, which is totally unexpected.

2.4. Single crystalline Sr₄Ru₃O₁₀: Towards understanding the mechanism of superconductivity in Sr₂RuO₄

The evolution from ferromagnetism in SrRuO₃ to superconductivity in Sr₂RuO₄ among compounds in Sr_{*n*+1}Ru_{*n*}O_{3*n*+1} series as the effective dimensionality, quantified by the number of layers, n , is reduced points to the important role played by ferromagnetic fluctuations in the occurrence of superconductivity in Sr₂RuO₄. The triple-layer ($n = 3$) member of the Sr_{*n*+1}Ru_{*n*}O_{3*n*+1} series, Sr₄Ru₃O₁₀, is the most two-dimensional ferromagnetic compound in the series. We recently performed a series of measurements on single-crystal Sr₄Ru₃O₁₀ grown by our collaborators using again a floating zone method. We found, surprisingly, that the ferromagnetism is highly orbital dependent, which may provide a context for the orbital-dependent superconductivity in Sr₂RuO₄. Furthermore, we observed an unexpected strong magnetoelastic coupling in this compound, which led to, among other things, a highly unusual increase in thermal power as the applied magnetic field is increased, a unique phenomenon that have not been reported for other oxides and is contributed to the strong magnetoelastic coupling in Sr₄Ru₃O₁₀.

2.5. PLD and MBE grown thin films of Sr₂RuO₄: Suppression of superconductivity by structural disorder

In collaboration with Darrell Schlom, we have over the years grown epitaxial thin films of Sr₂RuO₄ by pulsed-laser deposition (PLD) from high-purity (99.98%) targets and by molecular beam epitaxy (MBE) on (001) LaAlO₃, SrTiO₃, and other substrates and found that these films were not superconducting. The highest room-temperature to residual resistivity (RRR) ratio, about 10, and lowest residual resistivity, 32 $\mu\Omega$ cm, for our films are respectively 16 and 32 times worse than the corresponding numbers for bulk superconducting Sr₂RuO₄ single crystals. Structural disorder, rather than chemical impurities, is believed to be responsible for the suppression of superconductivity. We observed a correlation between higher RRR ratios in electrical transport measurements and narrower x-ray diffraction rocking curve widths of the Sr₂RuO₄ films. High-resolution transmission electron microscopy (HRTEM) revealed that the dominant structural defects in the films are {011} planar defects, with their spacing comparable to the in-plane zero-temperature superconducting coherence length of Sr₂RuO₄, which may be responsible for the size of the rocking curve, and the loss of superconductivity in the films.

We also synthesized the $n = 1 - 5$ and ∞ members of the layered Sr_{*n*+1}Ru_{*n*}O_{3*n*+1} series by MBE. X-ray and HRTEM studies showed that these epitaxial thin films possessed excellent layering (Fig. 1a) and were >98% phase-pure. The magnetic and electrical measurements on these films showed a systematic evolution of their properties with the effective dimensionality in this oxide system. We find that Sr₂RuO₄ films with the high level of layering showing in Fig. 1a and phase purity are still not superconducting. Furthermore, a minimum of three perovskite RuO₂

layers ($n > 2$) are necessary to support ferromagnetism, and the tendency towards Mott insulating behavior is enhanced systematically as n decreases.

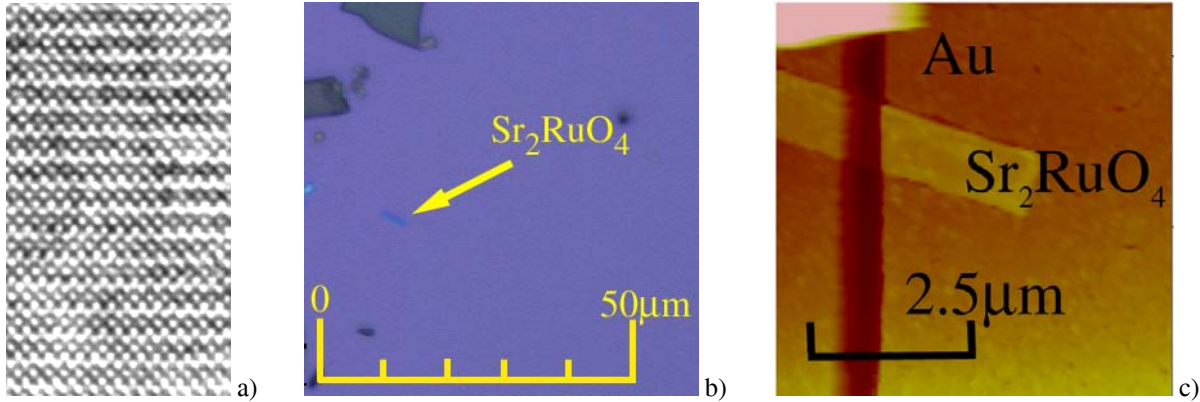


Figure 1. a) Cross-sectional HRTEM image of an epitaxial thin film of Sr_2RuO_4 grown by MBE. The two adjacent white rows in the images correspond to the [100] projections of the rock-salt SrO layers. The [100] projection of the SrRuO_3 perovskite sheet lies between the double SrO layers; b) Single-crystalline flakes of Sr_2RuO_4 prepared by mechanical exfoliation. The scale bar and an atomically thin flake of Sr_2RuO_4 are indicated; c) A Sr_2RuO_4 flake sample with Au electrodes for electrical transport measurements.

2.6. Preparation of single-crystalline thin films of Sr_2RuO_4 by mechanical exfoliation

Recently 1-layer graphene (1LG) featuring a Dirac cone band structure and massless charge carriers, which provides intriguing possibilities for future electronics applications, has been prepared and characterized. Atomically thin films of n -layer graphene (nLG), with $n = 1, 2, 3$ and possibly higher, have also been prepared. We have developed a unique lithography-free, all-dry process for fabricating devices on nLG flakes prepared by mechanical exfoliation. This technique, which is free of the possible contamination of the graphene during lithographic process, is simple to implement, versatile, and has potential of achieving a high mobility. Our work on nLG was motivated in part by the desire of developing an alternative approach to the preparation of superconducting thin films of Sr_2RuO_4 . Given that minimizing structural disorder is the key towards this goal, we applied the mechanical exfoliation technique we developed in the graphene work to prepare atomically thin, single-crystalline thin films of Sr_2RuO_4 from a superconducting parent single crystal. We have so far prepared atomically thin flakes of Sr_2RuO_4 (Figs. 1b and c), and are performing electrical transport measurements on these flakes.

3. FUTURE PLANES

3.1. Orbital and k dependences of the order parameter and mechanism of superconductivity in Sr_2RuO_4

The determination of the precise form of the superconducting order parameter will provide a constraint as well as a test of theories of superconductivity mechanism for Sr_2RuO_4 . The precise k dependence of the order parameter for Sr_2RuO_4 has not been settled. The Fermi surface for Sr_2RuO_4 consists of three cylindrical sheets. The power-law behaviors that have been observed experimentally suggest that Sr_2RuO_4 either possesses a k dependent order parameter that features nodes on the Fermi surface (horizontal or vertical) or is in fact an example of orbital-dependent superconductivity (ODS) in which scenario the gaps on α and β bands are tiny in comparison with that on the γ band. We will perform single-particle tunneling measurements to help resolve this issue.

3.2. Mechanism of superconductivity in Ru microdomain embedded in single crystalline Sr_2RuO_4

We plan to pursue further tunneling measurements on a single Ru microdomain to better characterize superconductivity within the Ru microdomain and in the 3K phase of Sr_2RuO_4 . Working with our collaborators we will also pursue low-temperature scanning SQUID measurements to detect the existence of chiral current expected in the mixed pairing state of the form $s + ip$.

3.3. Domain walls and other topological defects in single crystals of Sr_2RuO_4

Experimental results available so far suggest that the order parameter in Sr_2RuO_4 is that of the Γ_5^- state with $\mathbf{d} = z(k_x \pm ik_y)$. This chiral p -wave state features a relative phase between the two components of the order parameter, γ , either $\pi/2$ or $-\pi/2$, leading to the formation of domains, domain walls, and other topological defects. We will

continue to pursue the phase-sensitive measurements to detect the domain walls, and work with our collaborators on detecting the domain walls and other topological defects using a scanning SQUID microscope.

3.4. Preparation of atomically thin, superconducting films of Sr_2RuO_4 by mechanical exfoliation

Building on our initial success of preparing single crystalline thin films of Sr_2RuO_4 by mechanical exfoliation, we would like to demonstrate p -wave superconductivity in atomically thin films, which will allow the exploration of novel properties of a two-dimensional p -wave superconductor that has never been available previously. We will work with our collaborators to grow suitable single crystals of Sr_2RuO_4 – those that are easy to cleave, yet possess sufficient mechanical strength to facilitate exfoliation. We will also extend the technique to other superconductors.

3.5. Possible applications of Sr_2RuO_4 in quantum computing

Theoretical studies suggest that chiral p -wave superconductors will be useful for novel applications, such as spintronics devices, or quantum computing. These applications will require the use of thin films. We will use Sr_2RuO_4 to pursue two possible spin-triplet superconductor qubits. In the first approach, we will make use the two possible orientations of the d vector in the in-plane and the c -axis directions. In such a qubit the d vector will function as a giant spin. The second possibility is to use the chiral current of a single domain – the so-called l vector, to build a qubit. In both configurations we will use magnetic field to switch the qubit. However, other means, such as an electrical field from a gate that will tune the spin-orbital coupling, will also be explored.

4. PUBLICATIONS RELATED TO THE PROPOSED WORK IN PAST TWO YEARS

- 1) V. O. Dolocan, C. Veauvy, F. Servant, P. Lejay, K. Hasselbach, Y. Liu, and D. Mailly, “Observation of Vortex Coalescence in the Anisotropic Spin-Triplet Superconductor Sr_2RuO_4 ,” **Phys. Rev. Lett.** 95, 097004 (2005).
- 2) W. Tian, J. H. Haeni, E. Hutchinson, B. L. Sheu, M. A. Zurbuchen, M. M. Rosario, P. Schiffer, X. Q. Pan, Y. Liu, and D. G. Schlom, “Effect of dimensionality on magnetism in the layered $\text{Sr}_{n+1}\text{Ru}_n\text{O}_{3n+1}$ oxide series,” **Appl. Phys. Lett.** 90, 022507 (2007).
- 3) N. Staley, H. Wang, C. Puls, J. Forster, T.N. Jackson, K. McCarthy, B. Clouser, Y. Liu, “Lithography-Free Fabrication of Graphene Devices,” **Appl. Phys. Lett.** 90, 143518 (2007).
- 4) K.D. Nelson, Z.Q. Mao, Y. Liu, and Y. Maeno, “Josephson effect as a probe of spin-orbit coupling in Sr_2RuO_4 ,” submitted to Phys. Rev. B (2006).
- 5) Zhuan Xu, Xiangfan Xu, Rafael S. Freitas, Zhenyi Long, Meng Zhou, David Fobes, Minghu Fang, Peter Schiffer, Zhiqing Mao, and Ying Liu, “Existence of two electronic states in $\text{Sr}_4\text{Ru}_3\text{O}_{10}$ at low temperatures,” submitted to Phys. Rev. B (2007).
- 6) Wei Bao, Z.Q. Mao, M. Zhou, J. Hooper, J.W. Lynn, R.S. Freitas, P. Schiffer, Y. Liu, H.Q. Yuan, and M. Salamon, “Magnetic transition and magnetic structure of $\text{Sr}_4\text{Ru}_3\text{O}_{10}$,” submitted to Phys. Rev. Lett. (2006). Posted online: cond-mat/0607428.
- 7) Z. Long, C. Andreou, Z.Q. Mao, H. Yaguchi, Y. Maeno, Y. Liu, “Observation of a mixed pairing state in Ru microdomains embedded in Sr_2RuO_4 ,” submitted to Phys. Rev. Lett. Posted online: cond-mat/0608066 (2006).

5. REFERENCES

-
- i. K.D. Nelson, Z.Q. Mao, Y. Maeno, and Y. Liu, “Odd-parity superconductivity in Sr_2RuO_4 ,” **Science** 306, 1151 (2004).
 - ii. M.A. Zurbuchen, Y. Jia, S. Knapp, A.H. Carim, D.G. Schlom, L-N. Zou, and Y. Liu, “Suppression of Superconductivity by Crystallographic Defects in Epitaxial Sr_2RuO_4 Films,” **Appl. Phys. Lett.** 78, 2351 (2001).
 - iii. K.D Nelson, Z.Q. Mao, Y. Maeno, and Y. Liu, “Phase-sensitive Josephson and single-particle tunneling measurements on the gap structure of Sr_2RuO_4 ,” to be submitted to Physical Review Letters (2007).
 - iv. Y. Liu, H. Wang, K.D Nelson, Z.Q. Mao, M. K. Haas and R. J. Cava, “Eutectic phase of $\text{Sr}_2\text{RuO}_4/\text{Sr}_3\text{Ru}_2\text{O}_7$ and the superconducting energy gap of Sr_2RuO_4 ” to be submitted to Nature Physics (2007).

MATERIALS PREPARATION CENTER

Principal Investigator
L. L. Jones, Director

Contributing Principal Investigators:
I. E. Anderson, T. A. Lograsso, D. J. Sordelet

Program Scope

Established in 1981, the Materials Preparation Center (MPC) is one of the DOE's designated "BES Scientific User Facilities;" specifically, a *Specialized Single-Purpose User Facility*. The Materials Preparation Center, as its name implies, is focused on establishing and maintaining materials and processing capabilities crucial for the discovery and development of new materials. The primary motivation for the formation of the MPC was to provide the materials science community, particularly associated DOE Laboratories, effective access to the unique materials processing and expertise developed during the first 35 years of DOE sponsored basic energy research at Ames Laboratory. Most notably, the MPC is regarded as the premier source of high purity rare earth metals, alloys and compounds and continues to synthesize and prepare rare earth metals according to processes originally developed by Ames Laboratory. Currently, ***the primary mission of the MPC is to enable fundamental research by providing otherwise unavailable materials that are critical for scientific investigation and to synthesis or process them with well controlled purity into specified physical form and with desired microstructure.***

To that end, the MPC maintains an extensive suite of materials processing equipment and a deep knowledge base in the utilization of said equipment. This includes both commercial and unique research equipment that enabled new processes to be designed and developed by researchers in the Ames Laboratory. MPC consists of four functional sections: (1) high purity rare earth metals and alloys; (2) general alloy preparation; (3) single crystal synthesis; and (4) metallic powder atomization. A Principal Investigator whose individual expertise is aligned with the function of each section provides scientific and technical guidance for each area. Additionally, the MPC supports electron-beam characterization and quantitative metallography services as well as interstitial gases analysis.

MPC supports the BES sponsored research efforts of the Ames Laboratory's Materials and Engineering Physics (MEP) Program by providing synthesis and processing efforts specific to the MEP Program's research portfolio. The relationship between the MPC and research efforts in the MEP program as well in the other programs in the Ames Laboratory are crucial to the vitality of the MPC and are a significant factor in maintaining the MPC as a world class facility. This relationship results in a synergy that strengthens both the development of processing and material synthesis capabilities and the scientific understanding that is achieved in the research efforts at Ames Laboratory. MPC's materials synthesis and processing capabilities are also available to all DOE program laboratories as well as other government, academic, and industrial laboratories, both nationally and internationally.

Recent Progress

During FY2006, the MPC provided materials and services to internal and external users. Approximately 2/3 of MPC's efforts support the research activities of Principal Investigators and Scientists within the Ames Laboratory. The MPC also completed 144 external materials requests

during FY2006 for the following entities, which include 97 different clients at 82 academic, national and industrial laboratories worldwide:

MPC maintains and operates a wide range of equipment for the preparation and processing of a variety of metallic materials. Facilities included are: melting and casting systems; a variety of vacuum and inert gas atmosphere furnaces; mechanical processing equipment for forming and consolidation; rapid solidification systems for atomization and melt spinning; and crystal growth systems for preparation of single crystalline metallic alloys and intermetallic compounds. This breadth of process allows the MPC to select appropriate methods and develop protocols for synthesis of a wide range of scientifically interesting materials, examples include:

The MEP's research effort on amorphous and aperiodic materials, which established the range of oxygen content necessary for glass formation in melt-spun $Zr_{80}Pt_{20}$ ribbons by utilizing MPC's high purity metals processing expertise and equipment to handle this air-sensitive material. Melt spinning was used to obtain $Zr_{80}Pt_{20}$ ribbons with controlled levels of oxygen. Utilizing real time in-situ high temperature x-ray diffraction coupled with thermal analysis, the role of oxygen in stabilizing a particular atomic coordination (e.g., icosahedral) that promotes glass formation was elucidated [1,2].

A close collaborative relationship with the *Extraordinary Responsive Magnetic Rare Earth Materials* research to develop synthesis of the magnetocaloric $Gd_5Si_2Ge_2$ family of compounds spanning a range of sizes. For these high melting ($>1800^{\circ}C$), highly reactive compounds, MPC acquired tri-arc crystal growing capabilities to overcome crucible reactions and thermal cracking, thereby producing single crystals of excellent quality for a wide variety of physical properties determination and of sufficient size for both x-ray and neutron determination of the magnetic and crystallographic structures [3-6].

The availability of high purity rare earth metals, provided to the Ames' Condensed Matter Physics' *Novel Materials & Ground States* effort, has made significant contributions to metallic spin-glass systems: compounds such as RNi_2B_2C , RNi_2Ge_2 and $R_3Mg_{51}Zn_{46}$ (R = Rare Earth element) which are candidate model systems for testing spin-glass theories have been prepared. Discovery of new rare earth quasicrystals have been realized with R-Mg-Zn (R = Rare Earth element) systems [7-10].

Thermal barrier coatings (TBC) shown to significantly improve reliability and durability of turbine blades, thus enabling higher operating efficiencies and extending engine life. Research at Ames has determined that the addition of platinum significantly improves the oxidation resistance of nickel-rich bulk alloys having the same type of structure as the turbine alloy. MPC's ability to carefully prepare controlled chemical composition alloys for this study has been critical to the success of this effort. Researchers at Ames Laboratory received a 2005 R&D 100 Award for their development of these TBC alloys.

Processing techniques that have been recently added to the MPC include: a state-of-the-art melt spinner with extensive diagnostic capabilities, a plasma-arc melting furnace for the preparation of highly reactive alloys, and an expansion of single-crystal preparation capabilities. The installation of an injection caster for melting and injection casting of aperiodic and amorphous alloys in support of the BES-sponsored research was installed in mid 2006 and a laser welding system was very recently installed to support MEP research efforts.

MPC's effort to provide aluminum-rare earth based amorphous metal alloy powders for DARPA's Structural Amorphous Materials Program continued in FY2006, beginning a two year Phase II Structural Amorphous Materials effort in cooperation with Pratt & Whitney. An additional Bulk Amorphous Materials project was continued in FY2006 with Kennametal Inc., funded by the U.S. Army's Aberdeen Proving Grounds. MPC's unique high-pressure gas atomization system plays a critical role in our involvement in these programs.

Aluminum based metallic glass alloys offering a significant increase in specific strength and ductility over current aluminum alloys are being developed for application in aircraft engines. Development of these alloys has been enabled by MPC's atomization capability. Al-Y-Ni-Co alloy powder with low oxygen content in fine atomized powders has resulted in strength levels of 110 ksi and unparalleled 10% elongation. Funding is provided by DARPA's Structural Amorphous Metals (SAM) Program.

Critical composition and impurity control that can be achieved by the MPC is illustrated by our effort to prepare kilogram quantities of $\text{LaNi}_{5-x}\text{Sn}_x$ alloy for sorption cryocoolers for the joint ESA-NASA Planck Surveyor mission vehicle. MPC's ability to produce high purity base metal and stoichiometrically precise and homogeneous alloy with low oxygen impurity levels was critical in achieving high hydrogen loading at low partial pressures to satisfy JPL/ESA materials performance requirements. MPC previously prepared $\text{LaNi}_{5-x}\text{Sn}_x$ for the University of California, Santa Barbara (UCSB) Long Duration Balloon (LDB) Cosmic Microwave Background Radiation experiment in Antarctica in December 1997.

Future Plans

The availability of MPC rare earth metals and alloys is a key underpinning element to many of the experimental research efforts at the Ames Laboratory as well as throughout the DOE materials science and condensed matter physics community. MPC has benefited from large historical inventories of the 16 rare earth metals; these inventories have been consumed due to the growing scientific and technological importance of the rare earth metals. With their rapid consumption, our production capacity is not meeting current research demand; newly created metal inventory is quickly consumed. In order to maintain our international leadership role in materials science and physics of rare earth metals and compounds the MPC plans to increase rare earth element production efforts to ensure an adequate supply of high purity metals for research.

It is vital to continually strive to improve rare earth element purity to ensure that research performed on rare earth materials provided by the MPC meets the stringent requirements of the science drivers and provides a true identification of intrinsic properties. The demand for higher purity, lower oxygen, rare earth elements by research scientists supports the need to return to high-temperature hydrofluorination processing (melting of a rare earth fluoride under a flow of anhydrous hydrogen fluoride gas), which further reduces the interstitial oxygen, nitrogen, and hydrogen content as well as reducing the fluorine content in the final metal by promoting a more complete reduction reaction.

MPC's unique experience in the preparation of reactive rare earth and alkaline earth elements provides a core competency in the preparation and handling of air sensitive materials. Future effort would extend this core competency to other alloy systems and build on the existing inert atmosphere handling capabilities. Expansion of inert processing to incorporate preparation capabilities (arc and resistance melting), structure characterization (XRD, microscopy), and thermal property measurement (DTA, DSC) are future goals. These capabilities will support current and proposed efforts to synthesize light metal (Li and Ca) aluminides, efforts to evaluate hydrogen storage capacity, and investigate the kinetics of the absorption/desorption of hydrogen from surface of single crystals. These Ca-based compounds, first discovered at the Ames Laboratory in 1998, have been identified as potential candidates for hydrogen storage materials. Additionally, this type of facility will be central to a new effort to evaluate low melting reactive metals for extension of solution growth methods to broader classes of compounds.

Publication

1. I.M. H.Lee, X. Yang, M. J. Kramer, and D. J. Sordelet, *Phil. Mag.*, **86**, 443 (2006).
2. M. J. Kramer and D. J. Sordelet, *J. Non-Crystalline Solids*, **351**, 1586 (2005).
3. D. L. Schlagel, T. A. Lograsso, A. O. Pecharsky, J. A. Sampaio, *Light Metals 2005*, Ed. H. Kvande, TMS (The Minerals, Metals & Materials Society), Warrendale, PA, 1177 (2005).
4. V. O. Garlea, J. L. Zarestky, C. Y. Jones, L. L. Lin, D. L. Schlagel, T. A. Lograsso, A. O. Pecharsky, V. K. Pecharsky, K. A. Gschneidner Jr., and C. Stassis, *Phys. Rev. B*, **72**, 104431 (2005).
5. T. A. Lograsso, D. L. Schlagel and A. O. Pecharsky, *J. Alloy Comp.*, **393**, 141 (2005).
6. S. L. Bud'ko and P. C. Canfield, *Comptes Rendus Physique*, **7**, 56 (2006).
7. F. Venturini, J. C. Cezar, C. De Nadaï, P. C. Canfield and N. B. Brookes, *J. Phys.: Condens. Matter*, **18**, 9221 (2006).
8. E. Morosan, S. L. Bud'ko and P. C. Canfield, *Phys. Rev. B*, **71**, 014445 (2005).
9. J. L. Zarestky, V. O. Garlea, T. A. Lograsso, D. L. Schlagel and C. Stassis, *Phys. Rev. B*, **72**, 180408 (2005).
10. X. Moya, L. Manosa, A. Planes, T. Krenke, M. Acet, O. Garlea, T. Lograsso and J. Zarestky, *Phys. Rev. B*, **73**, 064401 (2006).

The Molecular Design Basis for Hydrogen Storage in Clathrate Hydrates

Principal Investigator: Vijay T. John, Tulane University

Co-Principal Investigators: Henry L. Ashbaugh, Tulane University, Gary L. McPherson, Tulane University, Camille Y. Jones, Hamilton College.

Program Scope

Our research objective is to develop new clathrate hydrates as inclusion compounds for hydrogen storage at moderate pressure (<100 bar), and at ambient or near-ambient temperatures. Specifically, we seek to determine if semi-clathrate materials are capable of encapsulating hydrogen for storage. In semi-clathrate materials, a portion of the guest chemically binds to the host framework, effectively replacing a water molecule in the lattice.¹ The remainder of the guest is then free to interact with the lattice through either van der Waals forces or hydrogen bonding. The strong hydrogen bonding lattice-guest interactions act as an “anchor” to rigidly hold the guest and reduced the translational and rotational degrees of freedom thus increasing the bulk material thermodynamic stability. There are several examples in the literature of semi-clathrate guest interactions with host lattices containing alcohols, phosphine oxides, phosphine sulfides, amines, amides, carbonyls, and aldehyde functional groups. There are also examples of ion pairs acting as host-guest stabilizers.

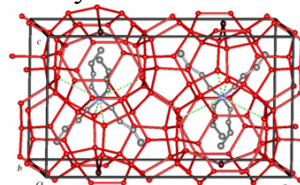
The research involves a collaboration between the investigators on this project, and a team at Los Alamos National Laboratory (R. Currier and S. Obrey) who are developing novel hydrotrope additives that dramatically reduce the pressure requirements for clathrate formation. The theoretical aspects of the research are complemented by computational studies which is lead by H. Ashbaugh. The research is strongly enhanced by collaboration from C. Jones (Hamilton College) whose expertise is the use of neutron scattering and computational methods for the study of the structure and dynamics of lattice inclusion compounds and molecular solids.

Recent Progress

Research has progressed along several complementary directions both at Tulane and at Hamilton College. The following summarize the directions and observations.

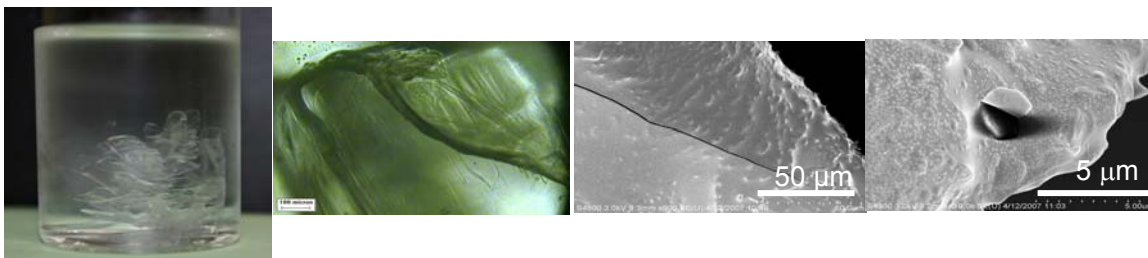
Research into the formation of semiclathrates containing hydrogen.

We are using a commercial high pressure view cell (Thar Instruments) to understand the formation of hydrogen hydrates in semiclathrates formed by quaternary ammonium salts (tetrabutylammonium bromide(TBAB) and tetrabutyl ammonium fluoride (TBAF)). Semiclathrates are different from the normal gas hydrates, since the organic species actually occupies some of the lattice sites. The structure of TBAF hydrates are shown in the accompanying figure (from Shimada et al.²).





The sequence of images above show elongated hydrate crystals of tetrabutylammonium fluoride forming under a hydrogen pressure of 130 bar at ambient temperature (panels 1-3). Panels 4-6 illustrate the depressurization and bubble formation indicating hydrogen release from the clathrate structure. We are also carrying out studies to understand the formation of semiclathrates to studies of crystal growth.



The figure above illustrates TBAF hydrates allowed to nucleate at ambient conditions (left panel). The second panel from the left is the optical micrograph of such hydrates while the two panels on the right illustrate cryo scanning electron micrographs of the crystals. Our current work relates to understanding hydrogen content and x-ray/neutron diffraction and spectroscopic characterization of such hydrates.

Molecular Modeling to design guest molecules in hydrates

M. Flanders '09 (supported by a NSF/Dreyfus research grant and the Dean of Faculty) at Hamilton, used molecular modeling techniques to characterize known and potential guest molecules, establishing trends correlating guest shape, size, dipole moment, etc. with ease of hydrate formation. On the basis of its shape and dipole moment, 4,4-dimethyltetrahydropyran (44DMTHP) was identified as a promising sH hydrate former. In order to test its clathrate-forming ability, 44DMTHP (unavailable commercially) was synthesized by Thomas Nevers '10 (participation supported by a STEP/Dreyfus Summer Fellowship, chemicals funded by DOE). An initial attempt to synthesize a sH hydrate with 44DMTHP and H₂S was completed, and a solid formed. The next experiments to be performed will be the synthesis of additional 44DMTHP and a second sH hydrate synthesis, to confirm the formation of hydrate and determine whether this molecular modeling approach to guest molecule design is a useful strategy.

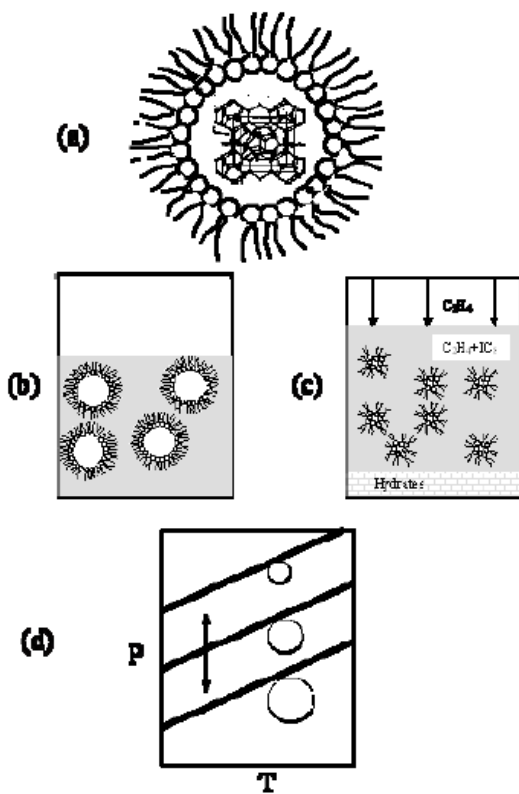
Studies on the effect of additives on the formation of semiclathrates (Hamilton)

Research at Hamilton investigated the effect of tetrahydrofuran and trimethylene oxide (TMO) on the stability of four quaternary ammonium salts: tetra-n-butyl ammonium hydroxide (TBAH), fluoride (TBAF), chloride (TBAC), and bromide (TBAB). THF and TMO were chosen as additives because they are both structure II hydrate-forming molecules that differ slightly in their size. TBAF with THF added displays different behavior at concentrations above and below a THF:water molar ratio of 0.01. Above 0.01, there is a dramatic lowering of the melting point that varies linearly with

concentration. Below 0.01, THF does not affect the melting point of TBAF. For TBAB and TBAC, THF lowers the melting point at all concentrations. Different behavior is observed for TMO, which lowers the melting point of TBAC in a similar fashion as THF, but hardly affects the melting point of TBAF at any concentration. We suspect that the doped TBAF is stable because it can accommodate some THF and TMO within empty cavities, TMO moreso than THF because of its small size. Our next step is to prove this with crystal structure determinations. The major challenge regarding the X-ray diffraction of clathrate hydrate is that hydrates look and behave very similar to ice. Therefore, in order to use an X-ray diffractometer to measure a semiclathrate or clathrate hydrate, the specimen needs to be cooled. To do this, we have designed a miniature thermoelectric cooler permitting the X-ray diffraction without risk of the melting of the specimen.

Continuing and Future Work

We are carrying out research on the formation of hydrogen containing clathrates in confined geometries. Three directions have been identified.



1. The use of reverse micelles (water-in-oil microemulsions) as confined nanoenvironments for hydrate formation. Reversed micelles are microdroplets of water suspended in a bulk organic solvent (e.g. isooctane) and stabilized by a surfactant, typically the double-tailed anionic bis(2-ethyl) sodium sulfosuccinate (AOT). These systems have enormous interfacial areas for gas contact, of the order of the order $3.6 \times 10^4 \text{ m}^2/\text{liter}$ of solution. The figure on the left illustrates concepts of hydrate formation in the water pools of reverse micelles as shown in our earlier work on hydrates from hydrocarbon gas species^{3,4,5}. These systems present novel and relevant environments for hydrate formation. They are especially interesting as they impose a tremendous interfacial area for gas water contact, and thus serve to dramatically enhance hydrate formation kinetics aided by the increase in partial pressure of

hydrogen in localized regions. Current work both at Tulane and Hamilton seeks to use these systems to form hydrates with hydrogen. To this extent, C. Jones at Hamilton is designing a high pressure neutron scattering cells to understand modifications of micelle structure and the initial steps in hydrate nucleation.

2. The use of templated nanocarbons as environments for hydrate formation. Here we will focus on the carbon inverse templates of zeolites that have been proposed by Yang et al.⁶ as high surface area adsorbents for hydrogen.
3. The use of metal organic frameworks in inverse micelles as hosts for hydrate formation. Metal organic frameworks (MOFs) are of great interest as media for hydrogen storage, and recent work has demonstrated the formation of water clusters within these frameworks.⁷ Our work seeks to determine if hydrate formation can occur in such systems with enhancement of hydrogen storage capacities.

Additionally, three proposals for beam time have been submitted to the NIST Center for Neutron Research. Three proposals have been submitted, two for diffraction experiments and a third for a small-angle neutron scattering experiment. The original proposal for a SANS study, submitted two years ago, was resubmitted due to the time elapsed during the recovery efforts at Tulane after Hurricane Katrina. This study will investigate reversed-micellar solutions containing dissolved hydrate-forming gases to understand their effects on the nanoscale micellar structure. The same reversed-micellar solutions will be studied by means of neutron powder diffraction, at concentrations where crystallization of hydrates will occur. These studies will examine the crystallinity of the hydrates formed under various conditions. The third study will endeavor to determine the structures of semiclathrates containing additives. Work performed at Hamilton over the last year has provided the means for the synthesis of the hydrate materials to be studied in the planned neutron scattering experiments.

Publications

No publications have resulted from this project to date. Facilities at Tulane have been fully restored, and research personnel (1 Ph.D. student and a post-doctoral scholar) have joined the program. We expect research to proceed at a rapid pace over the next year.

-
1. Jeffrey, G.A. *Accounts of Chemical Research* **1969**, *2*, 344. Franks, F. (ed.), *Water in crystalline hydrates; aqueous solutions of simple non-electrolytes*, Plenum Press, New York, 1973.
 - 2 Shimada, W.; Shiro, M.; Kondo, H.; Takeya, S.; Oyama, H.; Ebinuma, T.; Narita, H. "Tetra-n-butylammonium bromide-water", *Acta Crystallographica Section C.*, **2005**, *C61*, o65-o66.
 3. Nguyen, H., Phillips, J.B., John, V.T., "Clathrate Hydrate Formation from Reversed Micelles", *J. Phys. Chem.* **1989**, *93*, 8123. Nguyen, H., Reed, W., John, V.T., "Characteristics of Protein-Containing Reversed Micelles when subjected to Hydrate Formation Conditions", *J. Phys. Chem.*, **1991**, *95*(3), 1467.
 4. Nguyen, H., Kommareddi, N., John, V.T., "A Thermodynamic Model to Predict Clathrate Hydrate Formation in Reversed Micellar Systems", *Journal of Colloid and Interface Science*, **1993**, *155*(2), 482.
 5. John, V.T., Rao, A.M., Kommareddi, N., Karayigitoglu, C., Tata, M., McPherson, G.L., "New Directions in Hydrate Technology - Applications to Biotechnology and Advanced Materials", *Annals of the New York Acad. Sci* **1994**, *715*, 468.
 - 6 Yang, Z.; Xia, Y.; Mokaya, R. "Enhanced hydrogen storage capacity of high surface area zeolite-like carbon materials" *J. Am. Chem. Soc.*, **2007**, *129*, 1673.
 - 7 Wei, M.; He, C.; Hua, W.; Duan, C.; Li, S.; Qingjin, M.; "A large protonated water cluster in a 3D Metal-Organic Framework", *J. Am. Chem. Soc.*, **2006**, *128*, 13318.

A Fundamental Study of Type II Clathrate Materials

G.S. Nolas (PI), S. Witanachchi & P. Mukherjee, University of South Florida, Tampa, FL, 33620

i) Project Scope

The class of materials known as type II clathrates has a rich variety of compositions. The crystal structure is constructed from face sharing polyhedra large enough to hold atoms or molecules.[1] In type II clathrates the concentration of the inclusion species can be varied from empty, to partially filled, to fully filled. In addition, substitution on the group-IV atoms comprising the framework results in a large number of possible new compounds. These materials thus offer a unique opportunity to investigate fundamental properties of group-IV elements in novel crystal structures. The intellectual merit of investigating these clathrate materials is tied very closely with the novel structure that these materials exhibit and the corresponding electrical, thermal and optical properties. The goal in this Department of Energy Basic Energy Sciences Program is to develop a fundamental understanding of the structure-property relationships in these materials with an interest in exploiting the knowledge base for power conversion applications.

The thrust is thus two fold:

- (1) Develop a fundamental understanding and investigate the fundamental processes operative in the synthesis of these materials, and
- (2) Fully characterize their structural, electrical, thermal and optical properties.

ii) Recent Progress

Temperature dependent electrical resistivity, ρ , and thermal conductivity, κ , measurements for representative type II silicon clathrates are shown in Figure 1. Room temperature values for ρ span seven orders of magnitude between $\text{Cs}_8\text{Na}_{16}\text{Si}_{136}$ (metallic) and $\text{Na}_1\text{Si}_{136}$ (insulating), with ρ decreasing with increased alkali content. The polyhedra in $\text{Cs}_8\text{Na}_{16}\text{Si}_{136}$ are ‘fully filled’; alkali atoms occupy the positions inside each polyhedra in the unit cell. $\text{Na}_1\text{Si}_{136}$ and $\text{Na}_8\text{Si}_{136}$ contain Na ‘partially filling’ the polyhedra and indicate activated temperature dependences. The data shows that the Na concentration directly influences the electrical properties. The κ of these compounds is also strongly influenced by the Na filling fraction with a lower κ resulting from an increased Na content in non-metallic compositions due to the added phonon scattering centers the Na atoms provide. These data represent the first time thermal transport in these material has been investigated.

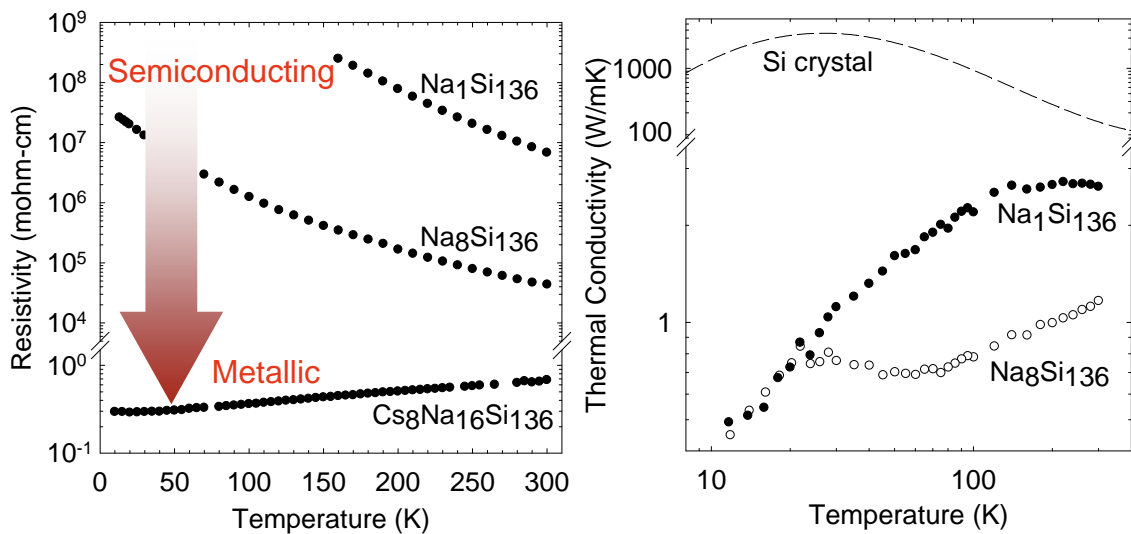


Figure 1. Temperature dependent ρ and κ measurements on ‘partially filled’ type II silicon clathrates. ρ data on $\text{Cs}_8\text{Na}_{16}\text{Si}_{136}$ and κ data on diamond-structured silicon is also shown.

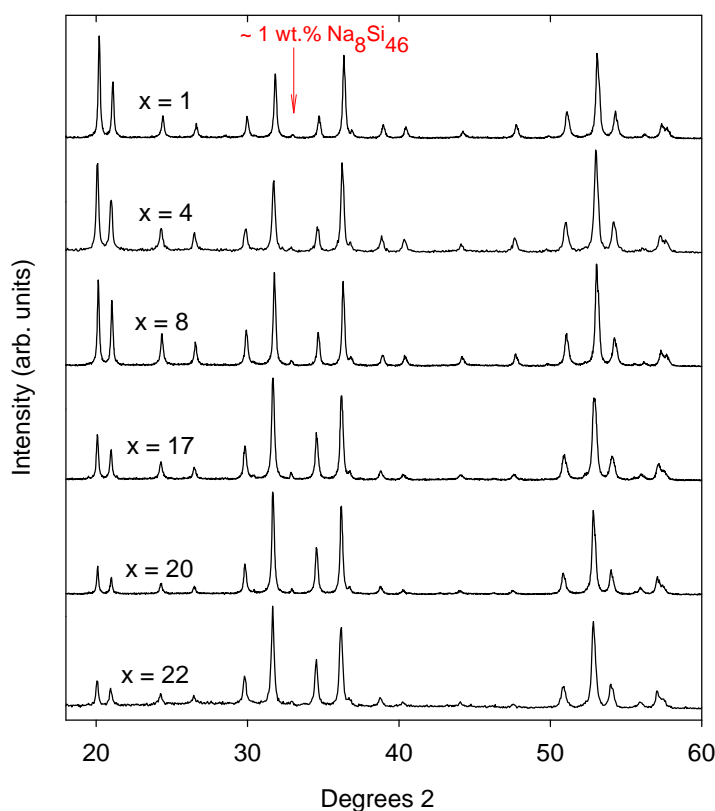


Figure 2. XRD spectra for $\text{Na}_x\text{Si}_{136}$.

We have also optimized our bulk synthesis techniques so that we can now synthesize, reproducibly, $\text{Na}_x\text{Si}_{136}$ with impurity ($\text{Na}_8\text{Si}_{46}$) fractions less than 1 wt% in large enough single batch amounts for transport measurements. Previously it had been necessary to combine specimens from several batches synthesized under the same conditions. Figure 2 shows X-ray diffraction (XRD) patterns for representative $\text{Na}_x\text{Si}_{136}$ specimens synthesized using our optimized procedure. The arrow indicates the most intense reflection due to $\text{Na}_8\text{Si}_{46}$. The Na content in these specimens has been determined by Rietveld refinement, and will be confirmed by electron microprobe data. All specimens shown contain ~ 1 wt% $\text{Na}_8\text{Si}_{46}$ or less.

To date very little has been reported on the stability of type II clathrates under substitution of the framework atoms by other species and no previous work on this topic in Ge-clathrates exists, to our knowledge. We have therefore begun an investigation on new framework substituted type II germanium clathrates. Three specimens ($\text{Cs}_8\text{Na}_{16}\text{Ag}_x\text{Ge}_{136-x}$ with $x = 0, 5.9,$ and 6.7) were prepared employing a direct synthesis approach optimized in our laboratories resulting in small single crystals.[2] All three specimens crystallized in the cubic type II clathrate structure (space group $Fd\bar{3}m$). The XRD spectra are shown in Figure 3. The refined atomic positions, occupancies, and thermal parameters are given in Ref. 2. The Na atoms were found to exclusively occupy the smaller Ge_{20} dodecahedra, while the Cs atoms occupy the larger Ge_{28} hexacaidecahedra. The Ag atoms show a clear preference for substitution on one of the framework crystallographic sites (the $96g$ site). Preferential occupation of substituting species has also been observed in type I clathrates, and several structural studies revealed a preference for the $6c$ site in those materials.[3, 4, 5] The refined atomic displacement parameters (U_{iso}) for the Cs and Na atoms in the $\text{Cs}_8\text{Na}_{16}\text{Ag}_x\text{Ge}_{136}$ specimens are both significantly larger than those for the framework Ge/Ag atoms, in agreement with those previously reported for $\text{Cs}_8\text{Na}_{16}\text{Ge}_{136}$. [1, 6, 7] The larger U_{iso} for Cs and Na can be attributed to the weaker bonding between guest and framework, allowing for relatively large thermal motion of the guest atoms inside their framework cages.[7] The presence of such loosely bound guest atoms in type I clathrate materials results in the very low lattice thermal conductivities certain clathrates possess.[7] This low lattice thermal conductivity can be attributed to the scattering of the heat carrying acoustic phonons by the localized, incoherent guest vibration modes. Previous results suggest a similar effect may occur in type II clathrates.[8, 9] From the large U_{iso} values we expect the lattice thermal conductivity of $\text{Cs}_8\text{Na}_{16}\text{Ag}_x\text{Ge}_{136-x}$ to be low.

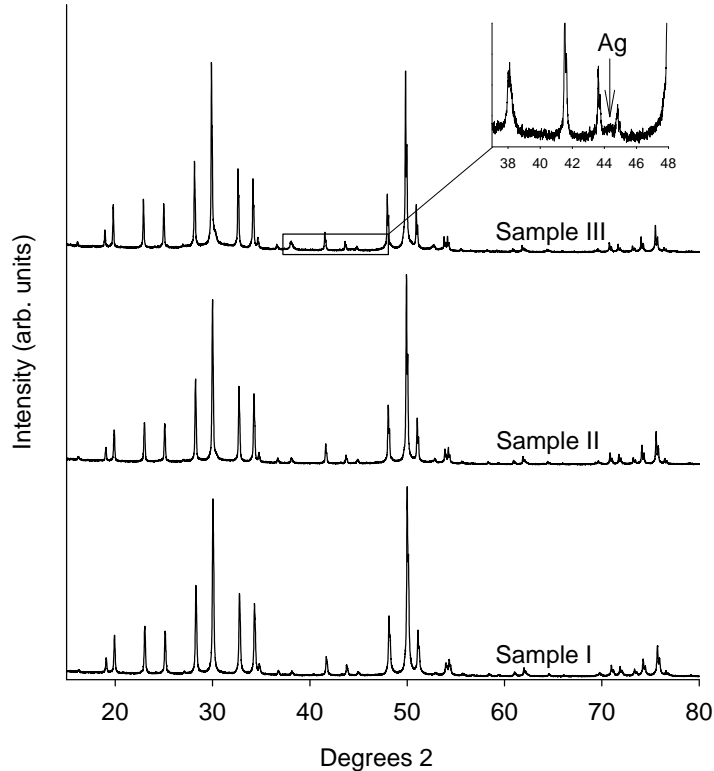


Figure 3. Powder XRD patterns for the three $\text{Cs}_8\text{Na}_{16}\text{Ag}_x\text{Ge}_{136-x}$ specimens. The inset is a magnification showing the trace amount of elemental Ag present in one of the specimens.

iii) Future Plans

Future plans include the synthesis of Si-Ge alloys with the type II clathrate crystal structure. Research towards this task has already begun with the synthesis of $\text{Na}_8\text{Si}_{128}\text{Ge}_8$ employing similar techniques as was used to prepare the materials described above. Increasing the Ge content will require new synthesis approaches. Solution phase techniques have recently been identified in producing high yields of type II clathrates.[10] We will also develop an understanding of the thermodynamic parameters involved in the synthesis of clathrate alloys, followed by a complete structural characterization before preparing specimens for transport and optical studies. The role of ordering on the framework site by substitutional doping or alloying will also be investigated. Infrared and Raman scattering spectroscopy will be employed to investigate the vibrational modes of the framework in further understanding the bonding in these materials. The synthesis of thin film type II clathrates by the laser-ablation will also be investigated. To grow clathrates a new synthesis method that involves film deposition in a high sodium flux will be employed. Optical diagnostic techniques such as emission spectroscopy and Intensified Charge-Coupled Device imaging will be used to study the dynamics of the growth process. An investigation of the structural, spectroscopic, morphological, optical and electronic transport measurements of thin films will be accomplished as part of our research plan.

iv) References

1. G.S. Nolas, G.A. Slack and S.B. Schujman in *Semiconductors and Semimetals*, Vol. 69, ed. T.M. Tritt, Academic Press, 2001, p 255.
2. M. Beekman, W. Wong-Ng, J.A. Kaduk, A. Shipario, and G.S. Nolas, *J. Solid State Chem* **180**, 1076 (2007).

3. G. Cordier and P. Woll, *J. Less-Common Metals* **169**, 291 (1991).
4. B. Eisenmann, H. Schäfer, and R. Zagler, *J. Less-Common Metals* **118**, 42 (1986).
5. A.P. Wilkinson, C. Lind, R.A. Young, S.D. Sharstri, P.L. Lee, and G.S. Nolas, *Chem. Mater.* **14**, 1300 (2002).
6. G.S. Nolas, D.G. Vanderneer, A.P. Wilkinson, and J.L. Cohn, *J. Appl. Phys.* **91**, 8970 (2002).
7. S. Bobev and S.C. Sevov, *J. Solid State Chem.* **153**, 92 (2000).
8. C.W. Myles, J. Dong, O.F. Sankey, *Phys. Stat. Sol. (b)* **239**, 26 (2003).
9. M. Beekman and G.S. Nolas, *Physica B*, **383**, 111 (2006).
10. A. M. Guloy, R. Ramlau, Z. Tang, W. Schnelle, M. Baitinger and Y. Grin, *Nature* **443**, 320 (2006).

v) Publications

Journal Articles

- M. Beekman, W. Wong-Ng, J.A. Kaduk, A. Shipario, and G.S. Nolas, ‘Synthesis and single-crystal X-ray diffraction studies of new framework substituted type II clathrates, $C_8Na_{16}Ag_xGe_{136x}$ ($x < 7$)’, *J. Solid State Chem* **180**, 1076 (2007).
- C.L. Condrón, J. Martin, G.S. Nolas, P.M.B. Piccoli, A.J. Schultz, and S.M. Kauzlarich, ‘Structure and Thermoelectric Characterization of $Ba_8Al_{14}Si_{31}$ ’, *Inorg. Chem.* **45**, 9381 (2006).
- M. Beekman and G.S. Nolas, ‘Synthesis and thermal conductivity of type II silicon clathrates’, *Physica B* **383**, 111 (2006).
- C.L. Condrón, S.M. Kauzlarich and G. S. Nolas, ‘Structure and Thermoelectric Characterization of $A_xBa_{8-x}Al_{14}Si_{31}$ ($A = Sr, Eu$) Single Crystals’, *Inorganic Chem*, in press.

Conference Proceedings

- M. Beekman, R.H. Hyde, D. Mukherjee, S. Witanachchi, P. Mukherjee, and G. S. Nolas, ‘Preparation and Physical Properties of Group IV Clathrates’, to appear in the Proceedings of Ceramic Engineering and Science, 2007.
- R.H. Hyde, M. Beekman, D. Mukherjee, G.S. Nolas, P. Mukherjee and S. Witanachchi, ‘Growth and characterization of germanium-based type I clathrate thin films deposited by pulsed laser ablation’, to appear in the Proceedings of Ceramic Engineering and Science, 2007.
- M. Beekman, J. Gryko, and G.S. Nolas, ‘Transport Properties of Type II Sodium-Silicon Clathrates,’ *Mat. Res. Soc. Symp. Proc.* **886**, 395 (2006).
- S. Witanachchi, R. Hyde, H.S. Nagaraja, M. Beekman, G.S. Nolas, and P. Mukherjee, ‘Growth and Characterization of Germanium-based Type I Clathrate Thin Films Deposited by Pulsed Laser Deposition,’ *Mat. Res. Soc. Symp. Proc.*, **886**, 401 (2006).
- S. Witanachchi, R. Hyde, V. Vithianathan, M. Beekman, P. Mukherjee and G.S. Nolas, ‘Synthesis and characterization of bulk and thin film type I and type II clathrate materials for thermoelectric and optoelectronic application’, *Proc. of the Twenty Fifth International Conference on Thermoelectrics (IEEE catalog # 06TH8931, Piscataway, NJ, 2006)*, p. 44.
- M. Beekman, J. Gryko, H.F. Rubin, J.A. Kaduk, W. Wong-Ng, and G.S. Nolas, ‘Synthesis and Transport Properties of Type II Clathrates,’ *Proc. of the Twenty Fourth International Conference on Thermoelectrics (IEEE catalog # 05TH8854, Piscataway, NJ, 2005)*, p. 219.

Effect of Polyethers on the Structure of Polyoxometalates and Derived Oxides

Rafael Muñoz-Espí, Chirakkal V. Krishnan, Christian Burger, and Benjamin Chu
Department of Chemistry, Stony Brook University, Stony Brook, NY 11794-3400

Nature shows many examples in which the formation of inorganic structures is controlled by the presence of biogenic macromolecules. Hydroxyapatites in bone or teeth and calcium carbonate in corals or shells of sea creatures are the best known examples. However, the study of this phenomenon is not only important in biology, but also of interest for technological applications. Imitating nature, synthetic polymers have been applied to assist inorganic crystallization.^[1] Macromolecules can specifically control the nucleation and/or growth processes or act as templates or structure-directing agents. In some cases, polymers can stabilize phases that otherwise are metastable. In typical polymer-fabricated materials, the organic component becomes incorporated into the inorganic matrix, and it can be conserved, generating polymer–inorganic hybrids that have often improved toughness, or removed, either by dissolution or by calcination.

Polyoxometalates are metal-oxide cluster anions of transition metals mostly of groups 5 and 6, in particular molybdenum, tungsten or vanadium, although uranium clusters have also been reported. A wide range of sizes and geometries is known for these materials, depending on composition and synthesis parameters. Their versatility allows applications to different fields, such as optics, catalysis or medicine.

Here we focus on the so-called Keplerate polyoxomolybdate cluster synthesized for first time by Müller et al.^[2] This compound, with formula $(\text{NH}_4)_{42}[\text{Mo}^{\text{VI}}_{72}\text{Mo}^{\text{V}}_{60}\text{O}_{372}(\text{CH}_3\text{COO})_{30}(\text{H}_2\text{O})_{72}] \cdot \text{ca. } 300\text{H}_2\text{O}$, is highly hydrophilic and contains 30 acetate ligands bridging the Mo_2^{V} groups. In our approach we aim to replace the acetate ligands with compatible groups containing larger hydrophobic sections. In this sense, the peroxomolybdate structure could be functionalized or “decorated” depending on the specific needs. So far, different candidates, such as propionate, butyrate, haloacetates and small amino acids, have been screened, and the results show that the size of the ligands is a critical parameter. In the conventional Keplerate cluster, the ligands are inside the sphere, but it remains a challenge to investigate whether the increase of hydrophobicity will place them pointing to the outer part, making the final compound more soluble in apolar solvents. This concept is schematically illustrated in Figure 1.

In the second part of the work it is shown how the presence of polymers containing poly(ethylene oxide) (PEO) influences the morphology and the structure of products obtained from peroxomolybdate aqueous solutions. Homopolymeric PEO and commercial PEO–poly(propylene oxide)–PEO triblock copolymers (Pluronic) were used. Precipitates appear spontaneously after several weeks, but the crystallization time can be reduced to hours by ultrasound irradiation.^[3] In the presence of polymer, the original yellow solution turned blue, indicating a partial reduction of Mo(VI) species to Mo(V). The exact nature of the long-known mixed-valent “molybdenum blues” remains a matter of active research. The poly(ethylene oxide)

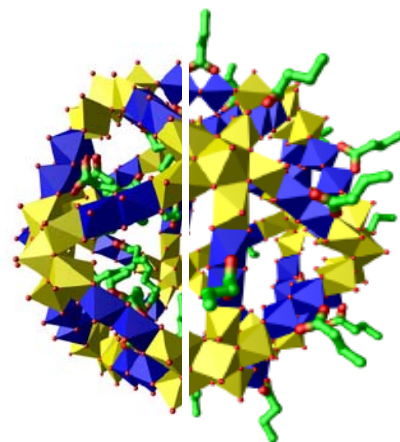


Figure 1. Schematic illustration of a Keplerate cluster with organic ligands (represented in green) inside (left hand side) and outside (right hand side) the polyoxomolybdate cage (in yellow: $\text{Mo}^{\text{VI}}\text{Mo}_5^{\text{VI}}$ pentagons, in blue: Mo_2^{V} bridges, and in red: oxygen).

chains might be assumed to act as a mild reducing agent. In addition, the polymer strongly affects the shape of the obtained crystals, ranging from nanowires over regular polyhedrons to microspheres, as shown in the micrographs of Figure 2. The control on the crystal growth may be explained in terms of the interaction of the EO groups with the molybdenum ions, causing a reversible adsorption of the polymer chains to kink sites at which the crystal grows. Of special interest are the nanometric fibers obtained in the presence of a small concentration of polymer, showing a very monodisperse size distribution and large surface area (Figure 2b). From the X-ray diffraction patterns, the products obtained in the absence of polymer were identified as the monohydrate phase $\text{MoO}_3 \cdot \text{H}_2\text{O}$, whereas in the presence of polymer the hemihydrate $\text{MoO}_3 \cdot 0.5 \text{H}_2\text{O}$ was systematically obtained, regardless of the type of PEO-containing polymer or concentration. The hydrate water content was confirmed by the results from thermogravimetric analysis. It has been reported that the hemihydrate phase has a higher Li^+ diffusion and shows a much better performance than the anhydrous MoO_3 as a cathode of rechargeable lithium batteries.^[4] Accordingly, our materials could have potential uses in electrochemistry and energy storage.

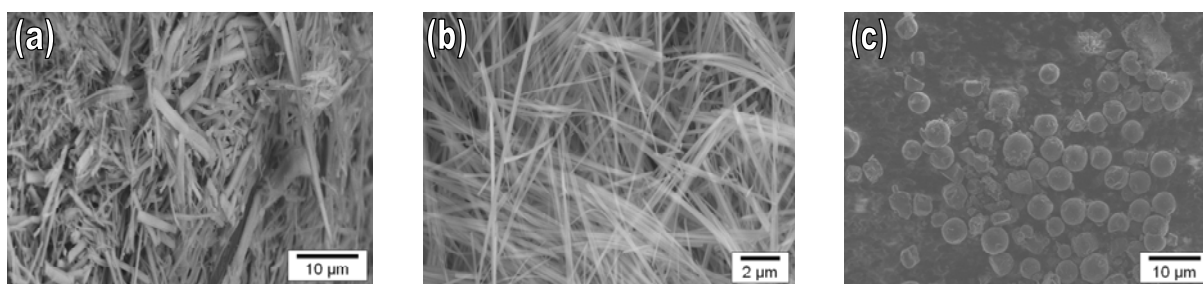


Figure 2. Scanning electron micrographs of molybdenum oxide samples prepared from peroxomolybdate solutions via a sonochemical process (a) in the absence of any polymer, and in the presence of (b) $1 \text{ g}\cdot\text{L}^{-1}$ and (c) $100 \text{ g}\cdot\text{L}^{-1}$ of PEO, $M_r = 35\,000$.

Small- and wide-angle X-ray scattering showed that the presence of the polymer resulted in an increase in the structural organization. Patterns for samples prepared at high concentrations of PEO homopolymer or PEO-PPO-PEO triblock copolymers show a large number of diffraction peaks at low scattering angles that do not appear without the polymer. Previous results suggest the formation of a zeolite-resembling highly porous structure, albeit at considerably larger length scale,^[5] which might be suitable for catalytic applications.

The extension of the synthetic pathway using peroxotungstate precursor solutions and the generation of molybdenum–tungsten double oxides are being currently investigated.

[1] K. Gorna, R. Muñoz-Espí, F. Gröhn, G. Wegner, *Macromol. Biosci.* **2007**, *7*, 163.

[2] A. Müller, E. Krickemeyer, H. Bögge, M. Schmidtman, F. Peters, *Angew. Chem. Int. Ed.* **1998**, *37*, 3360.

[3] C. V. Krishnan, J. Chen, C. Burger, B. Chu, *J. Phys. Chem. B* **2006**, *10*, 20182.

[4] G. Guzman, B. Yebka, L. Livage, C. Julien, *Solid State Ion.* **1996**, *86*, 407; B. Yebka, C. Julien, G. A. Nazri, *Ionics* **1999**, *5*, 236.

[5] T. Liu, Q. Wan, Y. Xie, C. Burger, L. Z. Liu, B. Chu, *J. Am. Chem. Soc.* **2001**, *123*, 10966.

Science of Nanowire Epitaxy
(DE-FG02-06ER46345, start date 15-Aug-06)

Jeff Drucker, Department of Physics and School of Materials, Arizona State University

PhD students: Prashanth Madras, SoM
Eric Dailey, SoM
Collaborators: Tom Picraux, CINT-LANL/ASU
Dave Smith, ASU
Teresa Clement, ASU

i) Program Scope

Vapor-liquid-solid (VLS) growth is a convenient and flexible method for synthesizing 1-D nanowires (NWs). These structures are a fundamental building block of nanoscale architectures that exhibit many novel and exciting properties but the fundamental material science of their formation is not completely understood. In VLS, a gas-phase precursor (*e.g.*, (di)silane, (di)germane) transports the material of interest to a seed particle where it dissolves, forming a liquid metal eutectic. The size of this eutectic seed fixes the NW diameter, which can be as small as 3nm. As the NW crystallizes at the liquid/solid interface, the seed particle 'floats' at its tip. VLS growth produces high quality, single crystal NWs and heterostructures that are electrically contacted to the substrate. Simply by tuning the growth parameters, precursor pressure/chemistry and/or substrate temperature, we are able to grow a variety of NW heterostructures including axial heterowires and core/shell structures. The reduced lateral constraint afforded by the nanoscale diameter allows formation of perfect epitaxial interfaces at lattice mismatches inaccessible to 2D planar geometries. This capability offers unprecedented flexibility for heterostructure design to optimize electronic and thermal transport properties.

This project seeks to define the fundamental materials science of 1-D nanowire heteroepitaxy using the vapor-liquid-solid (VLS) growth technique. A unique combination of *in situ* growth monitoring techniques are being employed to investigate nanowire growth using Ge and Si nanowires and nanowire heterostructures as a model system. These monitoring techniques include real-time, atomic resolution imaging in an environmental transmission electron microscope during nanowire growth and an optical reflectometry technique that allows real-time monitoring during growth in our UHV CVD reactor. Since similar growth behavior and nanowire morphologies are observed across several semiconductor nanowire systems, we expect that these results will be broadly applicable. By defining the fundamental material science of nanowire heteroepitaxy, we expect to

- define the limits for 1-D, defect-free epitaxial heterostructure growth enabling novel strain-induced electronic properties,
- enable increased control over crystallographic orientation and nanowire morphology
- extend the principles of VLS growth to vapor-solid-solid growth using patterned silicide seeds to fabricate an entirely new class of epitaxial nanostructures.

ii) Recent Progress

Recent progress includes our development of a process that significantly increases the fraction of Si nanowires that grow normal to the substrate. This result will facilitate incorporation of epitaxial nanowires into functional architectures. Typically, we form seed particles by thermal deposition of Au onto Si(111) surfaces held at 250°C. Subsequent NW growth from silane at a pressure of 45 mtorr and a temperature of 600°C results in a forest of ~30 nm diameter NWs that grow along all four of the <111> directions in approximately equal

proportions, as shown in figs 1(a) and (c). In contrast, we find that annealing the Au seeds at $T \geq 500^\circ\text{C}$ for times longer than 5 min prior to NW growth dramatically increases the fraction of NWs that grow normal to the surface. Figs. 1(b) and (d) display the results of VLS growth using the same conditions that resulted in the NWs displayed in figs 1(a) and (c), but with a 5 min anneal of the Au seed particles at $T=600^\circ\text{C}$ prior to NW growth.

During the pre-VLS anneal, the Au seed particles capture diffusing Si adatoms that have been thermally excited from low-coordination sites at surface steps [1]. This results in the formation of a pedestal below the Au seed particle, as shown in fig. 2. Tromp [2] has shown that there is a significant population of thermally excited Si adatoms on the Si(100) surface at temperatures comparable to those we employ for annealing the Au seed particles. These diffusing adatoms are captured by the Au seeds that then become supersaturated driving crystallization of the pedestal at their base. By analyzing large-area micrographs from which the image displayed in fig. 2 was extracted, we find that each Au seed particle captures the equivalent of several Si monolayers from the area for which it collects Si. This capture area is inversely proportional to the density of Au seed particles on the surface. Pedestals with heights of several nm can be produced during the anneal.

We believe that this pedestal is key to the stabilization of vertical NW growth. In the absence of a pedestal, the Au seed particle consumes sub-surface Si during heating to the VLS growth temperature, potentially forming a faceted etch pit. Inclined $\{111\}$ facets may be

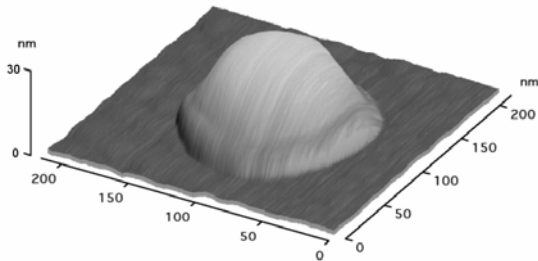


Fig. 2 AFM image of Au seed deposited at 250°C and annealed for 10 min at 500°C . The dome-shaped Au seed particle sits atop a Si pedestal, evident as the 'skirt' surrounding the base of the seed, formed during the anneal. Subsequent Si NW growth results in an increased fraction of NWs that grow normal to the substrate.

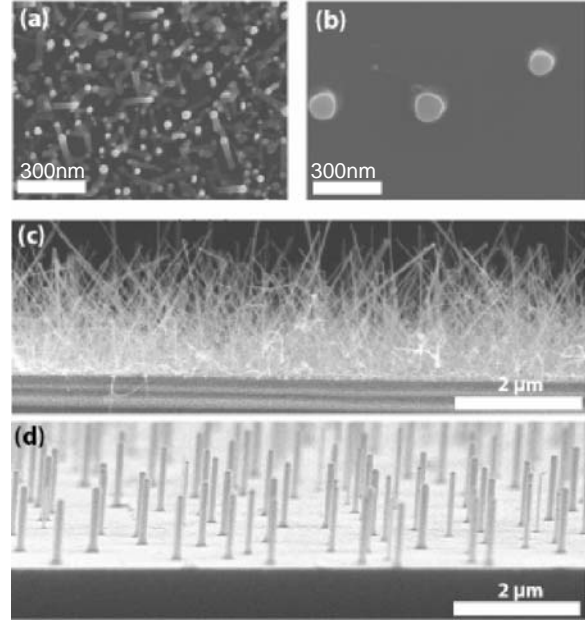


Fig. 1 (a) and (b) are plan-view and (c) and (d) are cross-sectional SEM images of Si NWs grown from disilane at a substrate temperature of 600°C . All Au seeds were deposited at 250°C using a deposition rate of $0.2 \text{ \AA}/\text{min}$. (b) and (d) were annealed at $T=600^\circ\text{C}$ prior to NW growth. Note that the NWs grow normal to the Si(111) surface if the Au seeds are annealed, but grow along all four $\langle 111 \rangle$ directions without the anneal.

responsible for the inclined NW growth observed in figs. 1(a) and (c). While further work is necessary, we believe that the pedestal alters the Si consumption process below the Au seed. In this case, Si is consumed from the pedestal during heating to the growth temperature so that no inclined $\{111\}$ facets are formed. This may be related to an altered force balance resulting from the different contact angles between the AuSi droplet atop the pedestal as compared to the planar Si $\{111\}$ surface. The existence of such a mechanism may explain our observation that there is a correlation between the mean pedestal height and the fraction of vertical NWs. That is, if the

pedestal is not large enough to completely saturate the Au seed at its eutectic composition, subsurface Si is consumed, potentially forming a faceted etch pit, and some inclined NWs grow.

iii) Future Plans

Future work will include formulating a more complete mechanistic understanding of the role that Au seed annealing to form Si pedestals plays in stabilizing NW growth normal to the substrate surface. Additional topics include investigating formation mechanisms and limits on the formation and stability of coherent interfaces in highly strained NW heterostructures. Recent theoretical work [3,4] has predicted that there are limiting dimensions for the formation of coherent (defect-free) axial and core/shell NW heterostructures analogous to the critical thickness for misfit dislocation introduction into planar epitaxial heterostructures. We are currently nearing completion of a second generation growth system that will allow completely automated growth. This capability will enable precise control of heterostructure growth conditions to ensure run-to-run repeatability that will allow systematic investigation of the diameter, length and misfit dependence for the growth of coherent NW heterostructures. This understanding will allow the use of strain to engineer the electronic properties of NW heterostructures. The benefits of this approach are already becoming apparent through the formation of 'transparent' ohmic contacts to core/shell NW heterostructures [5]. This strategy relies on a strain-related shift in the valence band position of the core, causing it to favorably align with the contact metal Fermi level.

We will also employ *in situ* high spatial resolution electron microscopy to characterize the VLS process. Recent dramatic results obtained by the IBM group have demonstrated the power of this approach [6,7]. However, their investigations are limited by the maximum pressure attainable in their microscope so that they are constrained to work in a pressure-temperature regime that is not normally employed for VLS growth. Our environmental transmission electron microscope at ASU is capable of atomic resolution imaging at temperatures of up to 1000°C in pressures of 10 torr. Thus, we will be able to span the entire range of pressures and temperatures necessary for growth of the full range of NWs and NW heterostructures. Our initial investigations will focus on determining the relationship between NW growth rate and diameter. There are conflicting reports in the literature that propose various kinetic or thermodynamic mechanism for observed variations in NW growth rates. However, in the absence of *in situ* observation, it is not clear whether these observations report actual growth rate differences, or different times required to initiate NW growth. A more challenging *in situ* investigation will be to characterize the initial stages of NW growth using reflection electron microscopy. This so-called 'nucleation event' is completely uncharacterized. We have recently developed a sample holder to enable this investigation that is the final stages of testing.

iv) References

1. B. Ressel, K. C. Prince, S. Heun and Y. Homma, *J. Appl. Phys.*, **93**, 3886 (2003).
2. R.M. Tromp and J.B. Hannon, *Surf. Rev. Lett.* **9**, 1565 (2002).
3. F. Glas, *Phys. Rev. B*, **74**, 121302 (2006).
4. S. Raychaudhuri and E.T. Yu, *J. Vac. Sci. Technol. B*, **24**, 2053 (2006).
5. W. Lu, J. Xiang, B. P. Timko, Y. Wu and C. M. Lieber, *Proc. Nat. Acad. Sci.* **102** (2005) 10046.
6. S. Kodambaka, J. Tersoff, M.C. Reuter and F.M Ross, *Phys. Rev. Lett.*, **96**, 096105 (2006).
7. F.M Ross, J. Tersoff and M.C. Reuter, *Phys. Rev. Lett.*, **95**, 146104 (2005).

v) Publications in Last 2 Years

Supported by NSF Grant DMR 0413523, Heteroepitaxy of 1-D Nanostructures

In situ studies of semiconductor nanowire growth using optical reflectometry, T. Clement, S. Ingole, S. Ketharanathan, Jeff Drucker and S.T. Picraux, Appl. Phys. Lett., **89**, 163125 (2006).

Ion Beam Analysis of VLS Grown Ge Nanostructures on Si, J. L. Taraci, T. Clement, J. W. Dailey, J. Drucker and S. T. Picraux, Nuclear Instruments and Methods B, **242**, 205 (2006).

Strain mapping in nanowires, J.L. Taraci, M.J. Hytch, T. Clement, P. Peralta, M.R. McCartney, Jeff Drucker and S.T. Picraux, Nanotechnology, **16**, 2365 (2005).

Supported by NSF grant DMR 0304743, Epitaxial Ge/Si(100) Quantum Dots and Mn-Based Ferromagnetic Group IV Semiconductors

Real-time coarsening dynamics of Ge/Si(100) nanostructures, Michael R. McKay, John Shumway and Jeff Drucker, J. Appl. Phys., **99**, 094305 (2006).

Kinetic control of Ge(Si)/Si(100) dome cluster composition, E.P. McDaniel, Qian Jiang, P.A. Crozier, Jeff Drucker and David J. Smith, Appl. Phys. Lett., **87**, 223101 (2005).

Growth and Characterization of Si_{1-x}Mn_x Alloys on Si(100), Yangting Zhang, Qian Jiang, David J. Smith and Jeff Drucker, J. Appl. Phys., **98**, 033512 (2005).

Supported by NSF grant ECS-0103061, Direct Electron Beam Writing for Fabrication of Functional Nanoscale Architectures

Electron beam induced deposition of pure, nanoscale Ge, Sutharsan Ketharanathan, R. Sharma, P.A. Crozier and Jeff Drucker, J. Vac. Sci. Technol. B, **24**, 678 (2006).

Nanoscale electron stimulated chemical vapor deposition of Au in an environmental transmission electron, Sutharsan Ketharanathan, R. Sharma and Jeff Drucker, J. Vac. Sci. Technol. B, **23**, 2403 (2005).

Properties of surfaces and films over large length and time scales

Hongbo Zeng, Jacob N. Israelachvili*, Matthew Tirrell

Chemical Engineering Department, Materials Department, Materials Research Laboratory, University of California, Santa Barbara, CA 93106

*Email: jacob@engineering.ucsb.edu

Classical contact mechanics theories or models that describe the adhesion and deformations of two elastic solid surfaces, are static (equilibrium) models, which can not describe the *dynamics* of surface contact and adhesion, especially for soft materials. The transitions and transients associated with the adhesion and/or coalescence of surfaces ranging from elastic solids to viscous liquids are not clear. Recent experimental results have shown how surface energy, surface texture (roughness, etc.), and the bulk properties of materials affect their adhesion, adhesion hysteresis and friction, and in turn, determine some of the fundamental differences between the modes of adhesion and failure of materials. This talk will review some recent results from our group to correlate the nano- and micro-scale properties of various thin film and surface phenomena (adhesion, adhesion hysteresis, friction, surface deformations and wear), identifying the fundamental physical mechanisms at the molecular and micro-scales aimed at providing equations and scaling relations in terms of the characteristic lengths and relaxation times of the materials.

The talk will describe recent progress in the following areas:

- Surfaces deformations at the nano- and micro-scales during adhesion (coalescence), spreading, and separation (detachment, rupture, fracture and failure) processes (figures 1-3).
- The differences and transitions between liquid-like and solid-like behavior of material adhesion, friction and fracture, i.e., the transition from liquid to viscoelastic to ductile/plastic to brittle behavior. Complex transient or dynamic shape changes occurring in these transitions involve sub-micron ripples, waves, rounded Saffman-Taylor fingers and sharp cracks (figures 1-3).
- The (scaling) effects of length and time on the adhesion and friction of rough and patterned surfaces, ranging from the atomic (angstrom) to the large asperity (micron) regime (figures 4-5).
- New techniques to study electric field effects on the rheology of nano- and micro- or colloidal particle suspensions, and patterns induced by an electric field in thin films.

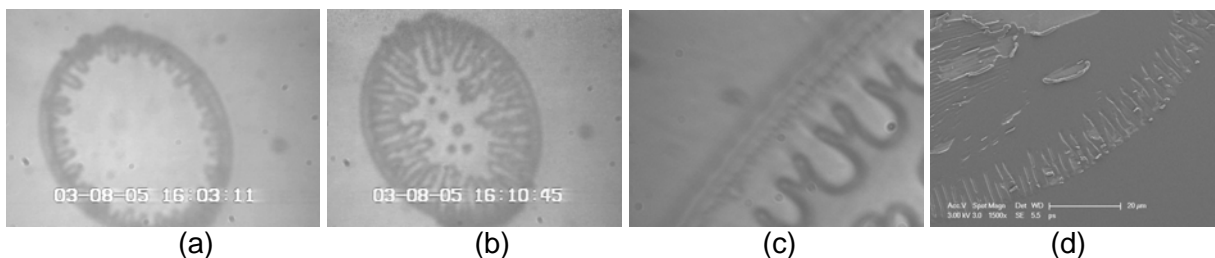


Fig. 1. Normal optical microscope images through thinning junctions during the tensing and ultimate rupture of two polymer (a, b, d) and sugar (c) surfaces in the viscoelastic and glassy

states. Sugar was chosen to mimic small metallic and other molecules, in contrast to polymers: the viscosity of sugar varies by many orders of magnitude over a narrow temperature range.

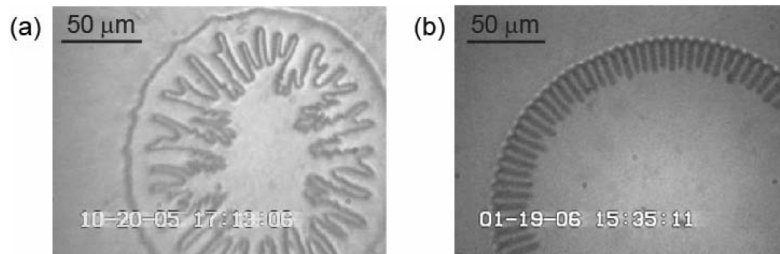


Figure 2. (a) Irregular Saffman-Taylor-like instability observed during the rupture of a polymer neck. (b) Typical highly ordered transient fingers developed during the adhesion and coalescence of two viscous or viscoelastic polymer films.

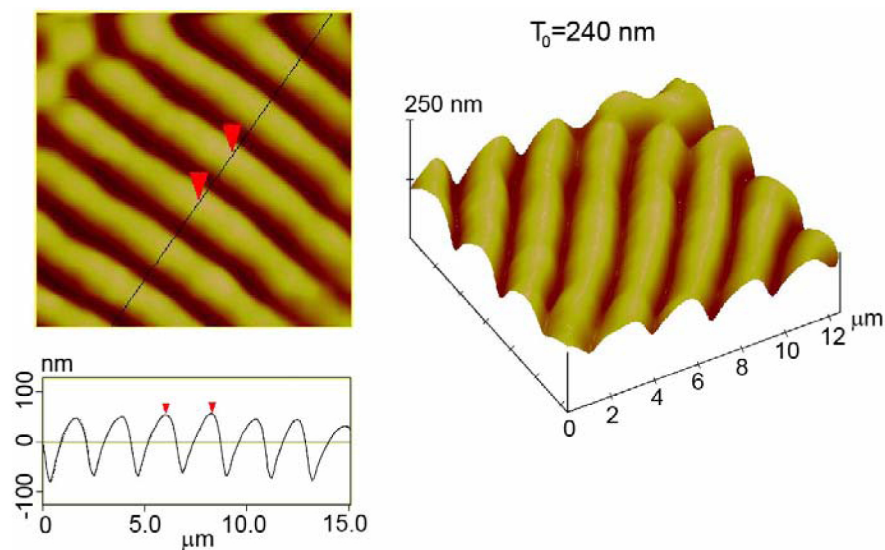


Figure 3. AFM images of the fractured surface through the center of the adhesive junction or neck showing highly ordered transient fingers.

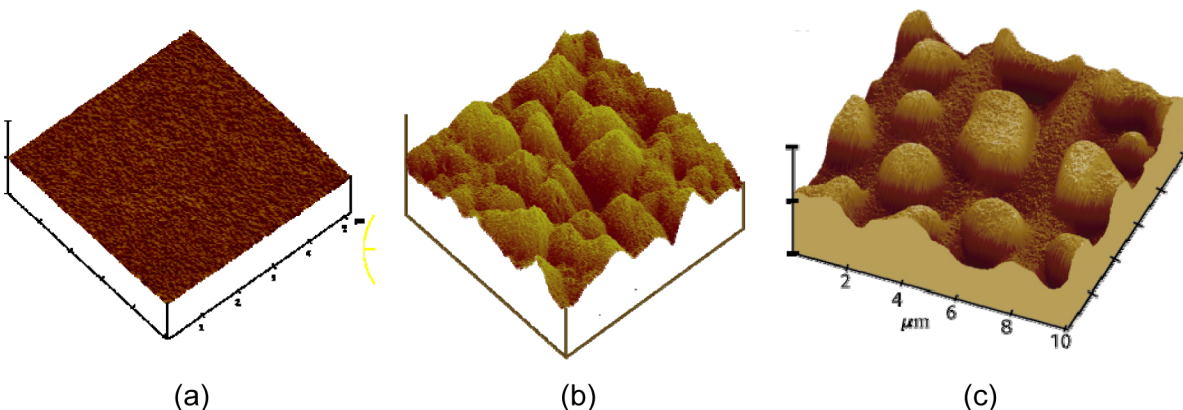


Fig. 4. AFM images of some of the surfaces prepared for adhesion and friction measurements whose rms height roughness varied from 0.5 to 200 nm. (a) and (b): Randomly rough surfaces

of RMS = 0.5 and 45 nm, respectively. (c) Patterned (semi-ordered) surfaces with an RMS roughness of 6 nm.

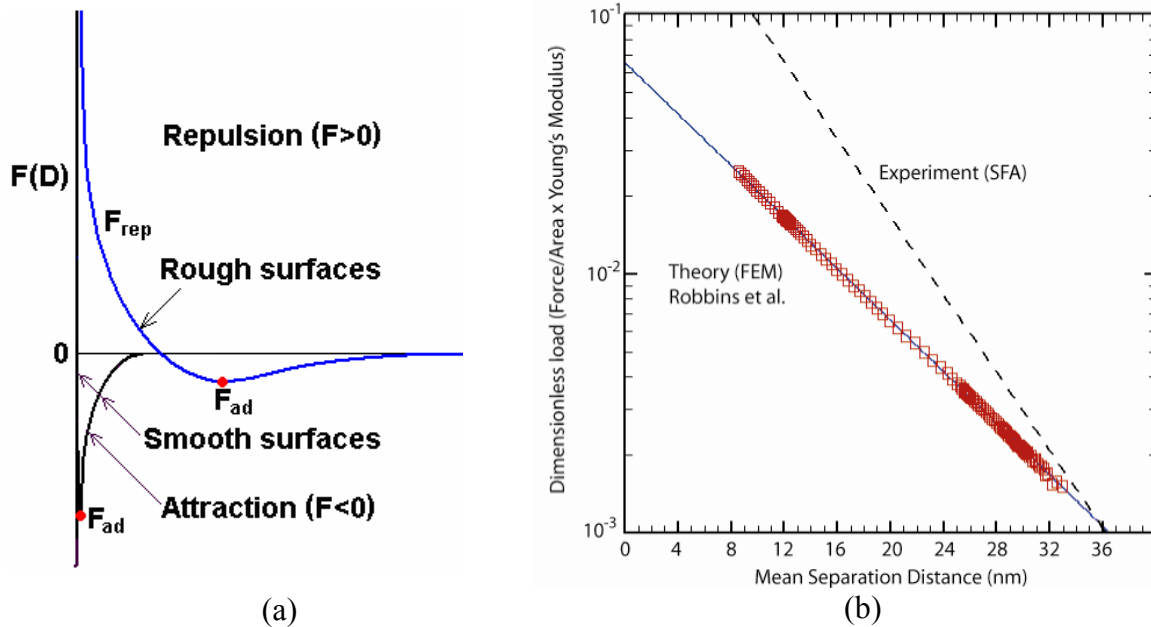


Fig. 5. (a) Generic net force-distance or energy-distance profiles between two smooth and rough surfaces. (b) Finite Element analysis applied to digitized surface images, as in Fig. 4, to obtain the theoretical repulsive force-distance curve for surfaces of RMS = 15 nm. The measured repulsion is shown by the dashed line.

As shown schematically in Fig. 5a, in general, with increasing roughness the force profile moves ‘outward’: the adhesive minimum moves out as the adhesion force decreases, and the repulsion becomes longer ranged, i.e., ‘softer’ (due to the elastic or plastic compression of the asperities). The repulsion is generally exponential. Figure 5b shows a theoretical Finite Element Analysis of the repulsive part of the force curve for two patterned surfaces with a RMS roughness of 15 nm. The measured repulsion is shown by the dashed line, showing very good agreement between theory and experiment

Acknowledgement

We thank the Department of Energy for supporting this research under grant No. DE-FG02-87ER45331.

Reference:

1. Zeng, H. B.; Maeda, N.; Chen, N. H.; Tirrell, M.; Israelachvili, J., Adhesion and friction of polystyrene surfaces around Tg. *Macromolecules* **2006**, *39*, 2350-2363.
2. Zeng, H. B.; Tirrell, M.; Israelachvili, J., Limit cycles in dynamic adhesion and friction processes: A discussion. *Journal of Adhesion* **2006**, *82*, 933-943.
3. Zeng, H. B.; Zhao, B. X.; Tian, Y.; Tirrell, M.; Leal, L. G.; Israelachvili, J., Transient surface patterns during adhesion and coalescence of thin liquid films. *Soft Matter* **2007**, *3*, 88 - 93.

4. Zeng, H. B.; Zhao, B. X.; Tian, Y.; Tirrell, M.; Israelachvili, J., Transient Interfacial Patterns and Instabilities Associated with Liquid Film Adhesion and Spreading. *Langmuir* **2007** (in press).
5. Zeng, H. B.; Tian, Y.; Anderson, T. H.; Tirrell, M.; Israelachvili, J. N., New SFA techniques for studying surface forces and thin film patterns induced by electric fields. *Langmuir* **2007**, submitted.
6. Zhao, B. X.; Zeng, H. B.; Tian, Y.; Israelachvili, J., Adhesion and detachment mechanisms of sugar surfaces from the solid (glassy) to liquid (viscous) states. *PNAS* **2006**, 103, 19624-19629.
7. Benz, M.; Rosenberg, K. J.; Kramer, E. J.; Israelachvili, J. N., The deformation and adhesion of randomly rough and patterned surfaces. *Journal of Physical Chemistry B* **2006**, 110, 11884-11893.
8. Zeng, H. B.; Tian, Y.; Tirrell, M.; Israelachvili, J., Transient Surface Patterns and Instabilities at Adhesive Junctions of Viscoelastic Films. **2007** (to be submitted).
9. Tian, Y.; Zeng, H. B.; Anderson, T. H.; Zhao, B. X.; McGuiggan, P.; Israelachvili, J., Transient filamentous network structure of a colloidal suspension excited by stepwise electric fields. *Physical Review E* **2007**, 75, 011409:1-6.
10. Zappone, B., Rosenberg, K. J., Israelachvili, J., Role of nanometer roughness on the adhesion and friction of a rough polymer surface and a molecularly smooth mica surface, *Tribology Letters*, **2007** (in press, available on line, DOI: 10.1007/s11249-006-9172-y).

Ion Enhanced Synthesis of Materials

Michael Nastasi (nasty@lanl.gov), Greg Swadener (swadener@lanl.gov), Jung-Kun Lee(jklee@lanl.gov), Zengfeng Di (zengfeng@lanl.gov) Yongqiang Wang (yqwang@lanl.gov), Los Alamos National Laboratory;
Lin Shao (lshao@tamu.edu) Texas A & M University

Program Scope

This program aims to develop a fundamental understanding of how energetic ions can be used to enhance the synthesis of novel materials. Through the combined use of experiment and modeling, we study how ion-solid interactions influence the microstructures, properties and functionalities of ion synthesized materials. Our intent is to use this fundamental knowledge to produce new and enhanced materials or develop more efficient synthesis methods. One area of emphasis is to evaluate the role of ion irradiation on the development of intrinsic stress in ion-synthesized materials and use said stress to manipulate materials properties and/or enhance materials synthesis. A specific example involves the study of how the defects generated in silicon during ion implantation contribute to the build up of compressive stress and how the combination of stress and defects can be manipulated to enhance the evolution of hydrogen extended defects that allow for the controlled cleavage, delaminating, and transfer of nanolayers of single crystalline material. Our research team includes personnel with expertise in ion-solid interactions, thin film science, defects and diffusion, materials characterization, materials science, modeling and molecular dynamic simulations.

Recent Progress

We have studied the ion beam based synthesis of several different classes of materials over the course of this project, including metallic thin films, functional oxides and semiconductors. In the area of functional oxides, for example, we have used ion implantation to study the origin of n-type conductivity via shallow donors in ZnO. The interesting nature of ZnO, such as very stable excitons and effective radiative electron-hole combination, are traced to its unique electronic structure. Therefore, a huge research effort has been placed on the science of carriers in ZnO. In spite of intensive research, the origin of n-type conductivity is still debated. Our work in this area was motivated by previous theory and experiment that suggested that hydrogen acting as a shallow donor in ZnO yields its intrinsic n-type conductivity [1,2]. If this is true, we could potentially increase the carrier concentration in ZnO and thereby enhance its photonic and electronic functionality by doping ZnO with hydrogen. In our approach we studied the optical, electrical, and structural properties of H or He implanted ZnO using low temperature photoluminescence (PL), Hall measurement, and infrared spectroscopy (IR). We found that H implantation influenced the relative luminescence intensities of the donor bound excitons, enhancing the 3.361 eV peak. Hall measurements showed that the introduction of H by ion implantation produced a nearly order of magnitude increase in the carrier concentration. Control experiments with He implantation showed these changes were not due to implantation damage. Furthermore, the increase in the relative intensity of the 3.361 eV peak and carrier concentration was observed to coincide with an appearance of H vibrational modes in the IR spectra of ZnO. From these findings we

concluded that the implanted H forms O-H bonds at Zn vacancies, and that it is these defect complexes which give rise to the shallow donors participating in the observed bound-exciton luminescence at 3.361 eV. These results on the role of H are currently being used to explore the possibility to enhance the properties of various ZnO nanostructures formed by a variety of methods such as the ion implantation of Zn and O in SiO₂ or the solution based self assembly [3]. We are also exploring the advantages of using hydrothermal methods, i.e. high pressure and low temperature reaction, to super saturate H into ion-beam synthesized ZnO nanocrystals.

We have also used ion beam processing to tailor the defect and stress distributions in Si and to study their role on the evolution of H-extended defects. Our motivation for this was based on the observation that implanted H in Si and other semiconductors can lead to cleavage and the transfer of layers of single crystalline material to other substrates. However, the basic mechanisms responsible for this phenomenon were never fully understood. Furthermore, if the basic materials science was understood new opportunities to freely integrate thin layers with different electronic, magnetic and optical properties would become possible, thereby providing the basis for the production new microelectronics, three-dimensional electronics, and the integration of nanostructured systems with a wide variety of functionalities.

Through a combination of experiment, modeling, and molecular dynamic simulations our research in this area showed for the first time that planer-hydrogen-defects (platelets) in H ion implanted Si nucleate and grow in response to the lattice defects and stress that are a natural bi-product of the implantation process[4,5]. Specifically, we have shown that H-platelet formation is controlled by the depth of the peak in radiation-induced damage and developed a model that considers the influence of stress to correctly predict platelet orientation and the depth at which platelet nucleation density is a maximum. Hydrogen platelet formation is the critical first step in the process that allows controlled cleavage of Si along the plane of the platelets and subsequent transfer and integration of thin sliced Si with other substrates.

Our stress stimulated cleavage model was recently confirmed when we showed that hydrogen induced cleavage in Si can occur with out ion implantation if a controlled stress can be introduce in the wafer during its synthesis. This was accomplished by growing in a strain center consisting of a 3 nm thick SiGe layer into single crystal Si during molecular beam epitaxy growth [6]. A strain analysis of the sample using high resolution X-ray diffraction showed the SiGe layer to be in a state of in plane compressive stress and the Si-SiGe interface to be in shear. Following the introduction of H in to the sample by plasma hydrogenation, elastic recoil detection showed the preferential accumulation of H at the Si-SiGe interface and an analysis with transmission electron microscopy showed a nearly atomically sharp layer cleavage along the interface. At present, this method has been usefully used to cleave a 15 nm thick layer of single crystalline Si. Work is currently in progress to understand the role of the strain layer on H diffusion and H-defect formation prior to cleavage.

Future Plans

Future work will progress in several directions. In the area of ion enhanced synthesis of nanostructures we will continue to explore the role of H ion implantation on the optical and electrical properties of ZnO nanostructures. One goal is to understand how the large fraction of surface area in nano-crystalline ZnO influences the properties arising from the

H associated donor bound excitons. In the area of stress stimulated H-defect formation in Si, we will continue to extend our work to studies of plasma hydrogenation in materials that have had strain layers grown in or introduced by ion irradiation damage. In this work our goal will be to understand the role of strain on H diffusion and accumulation in the strain region, and the defect evolution that brings about material separation.

References

1. Chris G. Van de Walle and J. Neugebauer, *Nature* **423** (2003) 626.
2. D. M. Hofmann, A. Hofstaetter, F. Leiter, H. Zhou, F. Henecker, B. K. Meyer, S. B. Orlinskii, J. Schmidt, and P. G. Baranov, *Phys. Rev. Lett.* **88** (2002) 045504.
3. Z.R. Tian, J.A. Voigt, J. Liu, B. Mchenzie, M.J. Mcdermott, M.A. Rodriguez, H. Konishi, and H. Xu, *Nature Materials* **2** (2003) 821.
4. M. Nastasi, *et. al*, *Appl. Phys. Lett.*, **86** (2005) 154102
5. J.G. Swadener, M.I. Baskes, and M. Nastasi, *Phys. Rev. B* **72** (2005) 201202
6. L. Shao, *et. al*, *Appl. Phys. Lett.* **87** (2005) 91902.
7. L. Shao, *et. al.*, *Appl. Phys. Lett.*, **87** (2005) 251907.

Publications (2005-2006)

1. Optical observation of donor-bound excitons in hydrogen-implanted ZnO, J. K. Lee, D. W. Hamby, D. A. Lucca, and M. Nastasi, *Appl. Phys. Lett.* **86** (2005) 171102.
2. Synthesis of ZnO Nanocrystals by sequential implantation of Zn and O species, J. K. Lee, C. R. Tewell, R. K. Schulze, M. Nastasi, D. W. Hamby, D. A. Lucca, H. S. Jung, and K. S. Hong, *Appl. Phys. Lett.* **86** (2005) 183111.
3. Ion Implantation, M. Nastasi, J.W. Mayer, and K.C. Walter, in *Kirk-Othmer Encyclopedia of Chemical Technology*, 5th Edition (John Wiley & Sons, Inc, 2005)
4. The effects of ion irradiation on porous silicon photoluminescence, L.G. Jacobsohn, B.L. Bennett, D.W. Cooke, R.E. Muenchausen and M. Nastasi, *J. Appl. Phys.* **97** (2005) 33528.
5. Investigation of plasma hydrogenation and trapping mechanism for layer transfer, P. Chen, P.K. Chu, T. Hochbauer, J.K. Lee, M. Nastasi, D. Buca, S. Mantl, R. Loo, M. Caymax, T. Alford, J.W. Mayer, N.D. Theodore, M. Cai, B. Schmidt, S.S. Lau, *Appl. Phys. Lett.*, **86** (2005) 31904.
6. Stress-induced platelet formation in silicon: A molecular dynamics study, J.G. Swadener, M.I. Baskes, and M. Nastasi, *Phys. Rev. B* **72** (2005) 201202
7. Optimized energy window of He beams for accurate determination of depth in channeling Rutherford backscattering spectrometry, Lin Shao, Y.Q. Wang, C.J. Wetteland, M. Nastasi, P.E. Thompson, and J.W. Mayer, *Appl. Phys. Lett.* **86** (2005) 221913
8. Nucleation and growth of platelets in hydrogen-ion-implanted silicon, M. Nastasi, T. Hochbauer, J.K. Lee, A. Misra, Amit; J.P. Hirth, M. Ridgway, T. Lafford, *Appl. Phys. Lett.*, **86** (2005) 154102.
9. The role of the chemical nature of implanted species on quenching and recovery of photoluminescence in ion irradiated porous silicon, L.G. Jacobsohn, D.W. Cooke, B.L. Bennett, R.E. Muenchausen and M. Nastasi, *J. Appl. Phys.* **98** (2005) 76108.
10. Methods for the accurate analysis of channeling Rutherford backscattering spectrometry, Lin Shao and M. Nastasi, *Appl. Phys. Lett.* **87** (2005) 64103.
11. A technique to study the lattice location of light elements in silicon by channeling elastic recoil detection analysis, Lin Shao, Y.Q. Wang, J.K. Lee, M. Nastasi, P.E. Thompson, N.D. Theodore, and J.W. Mayer, *Appl. Phys. Lett.* **87** (2005) 131901

12. Strain-facilitated Process for the Lift-off of a Si Layer of Less Than 20 nm Thickness, L. Shao, Y. Lin, J. G. Swadener, J.K. Lee, Q. X. Jia, Y.Q. Wang, M. Nastasi, P.E. Thompson, N.D. Theodore, T.L. Alford, J.W. Mayer, P.Chen, and S.S. Lau, *Appl. Phys. Lett.*, **87** (2005) 251907.
13. Plasma hydrogenation of strained Si/SiGe/Si heterostructure for layer transfer without ion implantation, Lin Shao, Yuan Lin, J.K. Lee, Q.X. Jia, Yongqiang Wang, M. Nastasi, Phillip E. Thompson, N. David Theodore, Paul K. Chu, T. L. Alford, J. W. Mayer, P. Chen, and S.S. Lau, *Appl. Phys. Lett.* **87** (2005) 91902.
14. Si Layer transfer using plasma hydrogenation, Peng Chen, S. S. Lau, Paul K. Chu, Kimmo Henttinen, Tommi Suni, I. Suni, N. David Theodore, T. Alford, J. W. Mayer, Lin Shao, and M. Nastasi, *Appl. Phys. Lett.* **87** (2005) 111910.
15. Microwave-cut silicon layer transfer, D. C. Thompson, T. L. Alford, and J. W. Mayer, T. Hochbauer and M. Nastasi, S. S. Lau. N. David Theodore, K. Henttinen, Ilkka Suni, and P. K. Chu, *Appl. Phys. Lett.*, **28** (2005) 224103.
16. Application of high energy ion beam for the control of boron diffusion, L. Shao, M. Nastasi, P.E. Thompson, J.Liu and Wei-Kan Chu, *Nucl. Instrum. Method.* **B242** (2006) 670..
17. The Energy Dependence of Excessive Vacancies Created by High Energy Si⁺ Ion Implantation in Si, L. Shao, M. Nastasi, P.E. Thompson, I. Rusakova, J. Liu and Wei-Kan Chu, *Nucl. Instr. Meth.* **B 242** (2006) 506.
18. Ion-cut of Si facilitated by interfacial defects of Si substrate/epitaxial layer grown by molecular beam epitaxy, L. Shao, M. Nastasi, J.K. Lee, T. Hochbauer, P.E. Thompson, I. Rusokova, J.Liu and Wei-Kan Chu, *Nucl. Instr. Method.* **B 242** (2006) 509.
19. Ion irradiation of porous silicon: the role of surface states, L.G. Jacobsohn, B.L. Bennett, D.W. Cooke, R.E. Muenchausen and M. Nastasi, *Nucl. Instrum. Method.* **B242** (2006) 164
20. A new iterative process for accurate analysis of displaced atoms from channeling Rutherford backscattering spectrometry, Lin Shao, Y.Q. Wang, and M. Nastasi, *Nucl. Instrum. Method.* **B249** (2006) 250.
21. Effects of hydrogen implantation on the photoluminescence and carrier mobility of ZnO films, D.W. Hamby, D.A. Lucca, J.K. Lee, M. Nastasi, H.S. Kang, S.Y. Lee, *Nucl. Instrum. Method.* **B249** (2006) 196
22. Photoluminescence of He implanted ZnO, D. W. Hamby, D. A. Lucca, J. K. Lee, and M. Nastasi, *Nucl. Instrum. Method.*, **B 242** (2006) 663.
23. Formation of hydrogen complexes in proton implanted silicon and their influence on the crystal damage, T. Hochbauer, A. Misra, M. Nastasi, J.W. Mayer, W. Ensinger, *Nucl. Instr. Meth.* **B 242** (2006) 623.
24. H-induced platelet and crack formation in hydrogenated epitaxial Si/Si_{0.98}B_{0.02}/Si structures, L. Shao, Y. Lin, J. G. Swadener, J.K. Lee, Q. X. Jia, Y.Q. Wang, M. Nastasi, P.E. Thompson, N.D. Theodore, T.L. Alford, J.W. Mayer, P.Chen, and S.S. Lau, *Appl. Phys. Lett.* **88** (2006) 21901
25. Effect of substrate growth temperatures on H diffusion in hydrogenated Si/Si homoepitaxial structures grown by molecular beam epitaxy, L. Shao, J.K. Lee, Y.Q. Wang, M. Nastasi, P.E. Thompson, N.D. Theodore, T.L. Alford, J.W. Mayer, P. Chen, S.S. Lau, *J Appl. Phys. Lett.* **99** (2006) 126105.
26. Structure and optical properties of plasma immersion ion processed boron-alloyed diamondlike carbon films, X-M. He, K.C. Walter and M. Nastasi, *J. Mater. Res.* **21** (2006) 1451.
27. *Ion Implantation and Synthesis of Materials*, M Nastasi and J.W. Mayer (Springer-Verlag, Berlin, 2006)

Determining and Controlling the Fundamental Mechanisms of Sputter Ripple Formation

Eric Chason

Brown University, Division of Engineering, Providence, RI
DOE Award number: DE-FG02-01ER45913

I. Program Scope

Bombarding solid surfaces with collimated beams of low energy ions can create well-ordered patterns known as sputter ripples. An example of such a sputter ripple pattern is shown in figure 1 for a Cu(001) surface bombarded with Ar ions. The observed pattern develops by a spontaneous self-organization process that originates from the fundamental surface kinetic processes occurring during ion bombardment. Understanding the pattern formation is therefore a way to study the kinetics and energetics of defect-mediated surface evolution under non-equilibrium sputtering conditions. These processes are critical for understanding how surfaces evolve on the nanoscale and for controlling the stability of nanostructures. Since the patterns form without masks or focused beams, they also represent a promising route for low-cost generation of patterned features on surfaces.

Our sputter ripple research consists of an integrated program of experiments, analytical model development and computer simulation designed to understand the kinetic mechanisms controlling ion-induced pattern formation and non-equilibrium surface evolution in general. The experiments focus on quantifying the wide variety of patterning behavior that emerges under different processing conditions. The analytical models relate the underlying atomic-level processes to features that develop on much larger length and time scales. Kinetic Monte Carlo (KMC) simulations enable different kinetic processes to be modeled on an atomic level in order to study how their interactions control surface evolution.

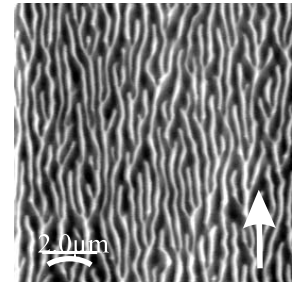


Fig. 1. Sputter ripple pattern on Cu(001) surface.

II. Recent Progress

1. Experiments on Cu surfaces

Our experimental work has been done primarily on Cu(001) surfaces because of the rich variety of patterning behavior found under different conditions. To measure the evolution of the ripple wavelength and amplitude, we use a light scattering spectroscopy technique (LiSSP) that we developed [1] that enables the surface morphology to be monitored in real-time. AFM is also used to measure the pattern in real space. In one series of studies, we focused on a type of patterning that has features of an instability model proposed by Bradley and Harper (BH) [2]. These ripples are characterized by a wavelength that remains essentially constant, an amplitude that increases exponentially before saturating and a pattern orientation that is determined by the ion beam direction and not the surface crystallography. BH ripples have been seen previously on semiconductor and amorphous surfaces, but we have shown they can be formed on metal surfaces under appropriate conditions.

We measured the temperature dependence of the wavelength (see fig. 2a) and found that it does not have a simple Arrhenius form, indicating that multiple activated kinetics processes are playing a role. We also found that the flux dependence of the wavelength changes with temperature. At high temperature (481 K, fig. 2b), the wavelength decreases with increasing flux while at low temperature (409 K, fig. 2c) the wavelength is independent of the flux. We have explained these results in terms of the instability theory coupled with a model for the temperature-dependent defect concentration, as described below.

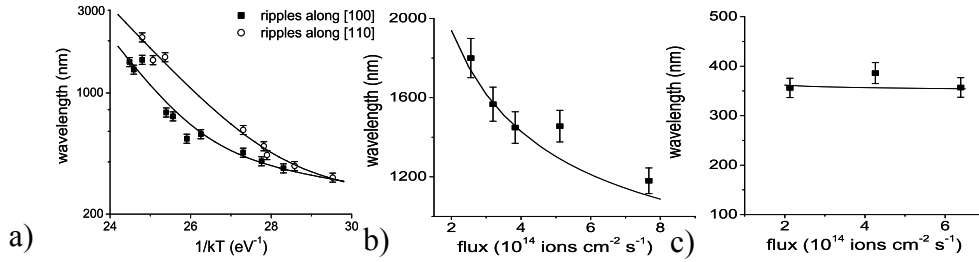


Fig. 2. a) Dependence of ripple wavelength on temperature. Flux dependence of ripple wavelength at b) $T=481$ K and c) $T=409$ K.

2. Continuum model of ripple formation

To quantitatively understand the mechanisms of pattern formation, we analyze our experimental results in terms of an extended version of the BH instability model [3,4]. This model relates the evolution of the surface height to different surface kinetic processes, e.g., sputtering with a yield that depends on the local surface curvature [5] or defect diffusion driven by surface energy minimization [6]. In the linear regime, these processes act independently on each Fourier component of the surface roughness, so the amplitude grows exponentially with a rate that depends on the wavevector and the processing conditions. The amplitude of the wavevector with the largest growth rate increases faster than all the others, which results in a characteristic periodicity on the surface (i.e., the ripple wavelength).

From this continuum theory, the ripple wavelength and growth rate can be related to the processing parameters (flux, f and temperature, T) and fundamental surface processes such as the diffusivity (D_s) and concentration (C) of mobile surface defects. To compare the experiments with the model, we developed a model for the dependence of the defect concentration on flux and temperature due to ion-induced and thermally-generated defects. The results of the continuum theory using this defect model are shown as the solid lines in fig. 2. The instability theory coupled with our model of defect generation and annihilation, is able to explain the complex temperature dependence of the ripple wavelength and the change in flux dependence with temperature.

3. Kinetic Monte Carlo simulation of ripple formation

As an alternative to the continuum theory, we have developed a KMC computer simulation that implements on an atomistic level [7] the same processes of ion sputtering and surface diffusion included in the extended BH model. The resulting simulated ripples (as shown in fig. 3a) have features characteristic of BH pattern formation (constant wavelength, exponential

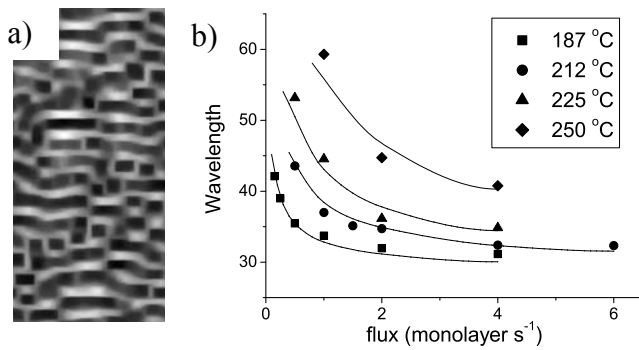


Fig. 3. a) Ripple pattern from kinetic Monte Carlo simulations. b) Flux and temperature dependence of simulated ripples. Solid lines are calculations from continuum theory.

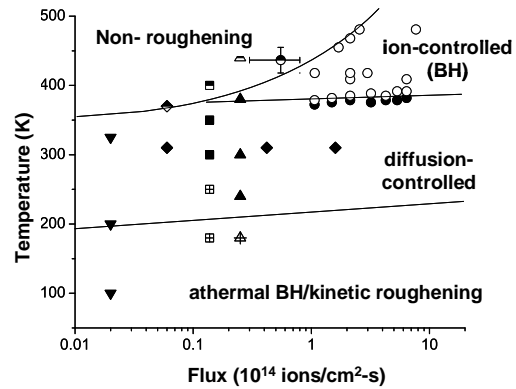


Fig. 4 Kinetic phase diagram showing different regimes of patterning behavior on Cu(001).

growth, ion-induced orientation). In addition, we have compared the f and T dependence of the simulated ripple wavelength (solid symbols on fig. 3b) with the predictions of the continuum model (solid lines on fig. 3b). We find excellent agreement between them, indicating that the BH instability mechanism is an adequate model for pattern formation due to the curvature-dependent Sigmund sputtering mechanism. This further indicates that observed discrepancies between the model and experiments are likely due to additional physical roughening mechanisms not included in the model.

4. Kinetic phase diagram

To develop a broader understanding of the relationship between the patterning behavior and the processing conditions, we have organized our measurement and those of others on Cu(001) surfaces into a kinetic phase diagram (fig. 4) that shows the regions of flux and temperature over which different types of patterning are seen. We have also measured the transitions between non-roughening and BH behavior and between high temperature BH and diffusion-controlled and analyzed them in terms of different competing kinetic mechanisms to explain why different behavior dominates in different regimes. The full range of behavior is described in an invited review article recently submitted to Applied Physics Reviews.

III. Future plans

Differences between our experimental studies and the predictions of the continuum and computer models suggest the areas where future work is needed. The most significant difference occurs between the experimentally determined ripple growth rate on Cu(001) and the value calculated from the instability theory using simulated values of the ion-solid interaction. The deviation suggests that we should consider other roughening mechanisms not included in the model. We are currently exploring the effects of ion-induced surface stress and diffusive barriers at step edges on increasing the roughening rate relative to the standard model.

In another area of research we are exploring patterning effects on alloy surfaces due to differential sputtering and surface diffusion. Our theoretical model indicates this mechanism

may enable ion-induced compositional modulations on surfaces. To assist future work on nanoscale evolution and fabrication, we are developing a new system with an integrated scanning electron microscope to allow us to monitor surface evolution in real-time during sputtering and deposition.

References

1. E. Chason, M.B. Sinclair, J.A. Floro, J.A. Hunter and R.Q. Hwang, “Spectroscopic light scattering measurements for real-time measurements of thin film and surface evolution”, *Appl. Phys. Lett.* **72**, (1998).
2. R. M. Bradley, J. M. E. Harper, “Theory of ripple topography induced by ion bombardment”, *J. Vac. Sci. Technol. A* **6**, 2390 (1988).
3. M. A. Makeev, R. Cuerno and A.-L. Barabasi, “Morphology of ion-sputtered surfaces”, *Nucl. Instr. Meth.* **B197**, 185 (2002).
4. W. L. Chan and E. Chason, “Sputter ripples and radiation-enhanced surface kinetics on Cu(001)”, *Phys. Rev. B* **72**, 165418 (2005).
5. P. Sigmund, “A mechanism of surface microroughening by ion bombardment”, *J. Mater. Sci.* **8**, 1545 (1973)
6. W. W. Mullins, “Flattening of a nearly plane solid surface due to capillarity”, *J. Appl. Phys.* **30**, 77 (1959).
7. E. Chason, W.L. Chan, M.S. Bharathi, “Kinetic Monte Carlo simulations of ion-induced ripple formation: dependence on flux, temperature and defect concentration in the linear regime”, *Phys. Rev. B* **74**, 224103 (2006)

Publications in the last two years

1. Wai Lun Chan, Eric Chason, “Temperature and flux dependence of ion-induced ripples: a way to study defect and relaxation kinetics during ion bombardment”, *MRS Symp Proc.* **849**, 97 (2005).
2. Ari-David Brown, Wai Lun Chan, Eric Chason, Jonah Erlebacher, “Transient topographies of ion patterned Si(111)”, *Phys. Rev. Lett.* **95**, 056101 (2005).
3. W.L. Chan, E. Chason, “Sputter ripples and radiation-enhanced surface kinetics on Cu(001)”, *Phys. Rev. B.* **72**, 165418 (2005).
4. KINETICS DRIVEN NANOPATTERNING AT SURFACES, eds. E. Chason, H. Huang, G. Gilmer, E. Wang, Materials Research Society Symposium Vol **849**, 2005.
5. E. Chason, W.L. Chan, “Kinetic mechanisms in ion-induced ripple formation on Cu(001) surfaces”, *Nucl. Instr. Meth. B* **242**, 232 (2006).
6. Wai Lun Chan, Eric Chason, “Morphology of ion sputtered Cu(001) surfaces: transition from unidirectional to bidirectional roughening”, *Nucl. Instr. Meth. B* **242**, 228 (2006).
7. E. Chason, W.L. Chan, M.S. Bharathi, “Kinetic Monte Carlo simulations of ion-induced ripple formation: dependence on flux, temperature and defect concentration in the linear regime”, *Phys. Rev. B* **74**, 224103 (2006)
8. Eric Chason and Wai Lun Chan, “Low energy ion bombardment and surface topography: continuum theories and kinetic Monte Carlo simulations” in Ion Beam Science: Solved and Unsolved Problems, *Mat. Fys. Medd. Dan. Vid. Selsk.* pp. 207 (2007)
9. Eric Chason and Wai Lun Chan, “Kinetic phase diagram for morphological evolution on Cu(001) surfaces during ion bombardment”, *Nucl. Instr. Meth. B* **256**, 305 (2007).
10. Wai Lun Chan, Eric Chason, C. Iamsuang, “Surface stress induced in Cu foils during and after low energy ion bombardment”, *Nucl. Instr. Meth. B* (2007).
11. Wai Lun Chan and Eric Chason, “Making waves: kinetic processes controlling surface evolution during low energy ion sputtering”, *Applied Physics Reviews*, in press.
12. Y. Maekawa, K. Sato, E. Chason and T. Mizoguchi, “Orientation of nano-grains in hard-disk media on ion beam textured substrates”, *IEEE Trans. Man.*, in press.
13. V. B. Shenoy, W. L. Chan, and E. Chason, “Compositionally modulated ripples induced by sputtering of alloy surfaces”, *Phys. Rev. Lett.*, submitted.

Strain engineered Si-based nanomembranes: ultra-thin, transferable, and flexible single-crystal Si

S. A. Scott and M. G. Lagally

University of Wisconsin-Madison

We have shown in the last several years the vast potential for novel science and new technology that strain-engineered Si-Ge nanomembranes provide¹. Here we discuss some very recent work and potential ideas for future work.

1: *Elastic strain-sharing in heterostructure membranes*

High-quality tensilely strained Si is generated in membrane form, via the release and consequent strain sharing between the layers of an epitaxial Si:SiGe:Si heterostructure, where silicon on insulator (SOI) is the starting substrate². The general membrane release and transfer process is depicted in Fig 1, although many variants are possible depending on the final desired use.

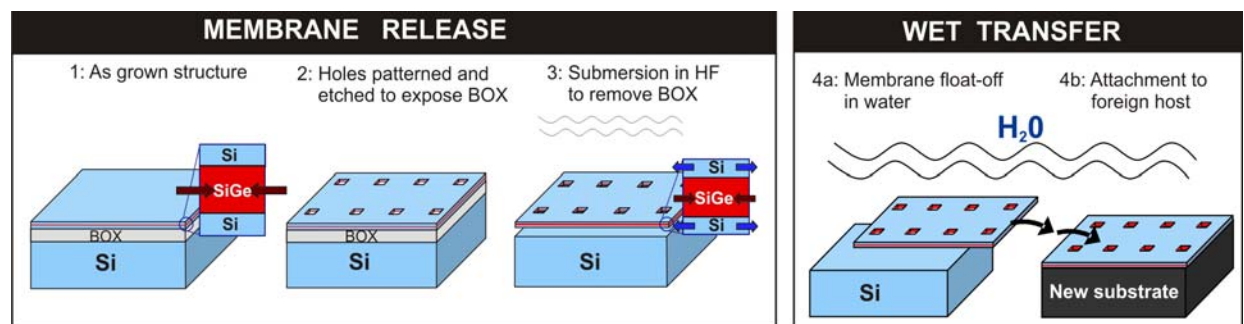


Fig.1 Schematic illustration of the nanomembrane fabrication process.

For the technologically important Si(001) orientation, tensile strain provides a dramatic enhancement in electron mobility even at low levels of strain, however the hole mobility is initially degraded, requiring significantly higher levels of strain to produce improvements in p-type carrier mobility³. An appealing alternative for high-mobility p-type devices is the use of Si(110), as the hole mobility is known to be significantly higher than in Si(001), but is still less than the Si(001) electron mobility. Recently it has been shown that straining Si(110) improves the hole mobility even further, and also offers enhancements in electron mobility over unstrained Si(110)⁴. Straining Si(110) over large areas via the use of SiGe(110) buffer layers is more problematic than for the case of the (001) orientation: for a given Ge concentration, the critical thickness for relaxation via dislocation generation is less than in the (001) orientation⁵, and results in a threading dislocation density that is more than an order of magnitude higher. Consequently, the nanomembranes approach, which avoids dislocations altogether, is particularly desirable for the Si(110) orientation. This offers the potential to increase performance in p-type FETs substantially and also in advanced CMOS applications, where high mobility of both electrons and holes is highly sought after.

We present recent results of strain sharing between the layers of a (110) oriented nanomembrane with composition 12nm Si(110) / 80nm Si_{0.91}Ge_{0.09} / 10nm Si, which produces a strain in the Si layers of 0.23%. In this case a SOI(110) substrate is used, which consists of a

Si(110) template layer with a Si(001) handle. Fig. 2 shows optical microscope images of released (110) membranes.

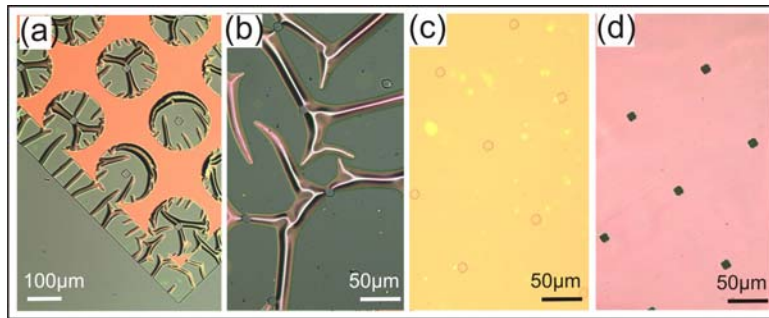


Fig. 2. Optical microscope images of (110) nanomembranes. (a) Snapshot of the release process. Etchant access to the buried oxide layer is enhanced by patterning and etching an array of holes through the tri-layer membrane. This image shows the etch front, where the rippled morphology results from the lateral expansion of the membrane as it elastically relaxes in place. (b) Membrane released in place on its original handle substrate. (c) Wet transfer to new Si host. (d) Alternative dry transfer to paper.

While the nanomembrane route to tensilely strained Si(001) is appealing because of the lack of dislocations, the growth of (110) membranes by chemical vapor deposition (CVD) suffers from a rough growth front. We show that molecular beam epitaxy (MBE) produces an order of magnitude improvement in growth front roughness, rendering this technique applicable for the growth of higher-Ge-composition membranes in order to maximize the strain transfer to the Si layers. A comparison of the two growth techniques will be presented. We will also discuss the direction of future work with flexible strained Si(110) membranes, including carrier mobility measurements to determine applicability for high-performance CMOS (on any substrate), and X-ray absorption total-electron-yield measurements to correlate the electron mobility changes with the strain induced conduction-band valley splitting.

2: *Ultra-thin membranes: When surface properties dominate*

Ultra-thin Si membranes provide the ultimate means for investigating when surfaces completely dominate the properties of a material. With the current availability of high-quality ultra-thin SOI wafers, and the development of our own various releasing and cleaning procedures, we can release and transfer membranes as thin as 8 nm.

A particularly interesting aspect of reducing the membrane thickness is the impact on conductivity. In ultra-thin membranes the number of dopants is reduced compared to the bulk; ultra-thin membranes should become nonconductive due to full charge depletion via interface trapping. On the contrary, under UHV membranes conduct just as well as bulk Si. We have previously proposed that this conduction arises from the interaction of the bulk and band-like surface states⁶.

The clean Si(001) surface is terminated by a (2×1) reconstruction, which leads to localized surface bands. These surface bands are positioned in energy such that interaction between the bulk band structure and surface bands becomes possible, generating high-mobility holes in the bulk valence band, and conduction becomes possible in Si nanomembranes irrespective of doping.

An intriguing question is what happens to the conductivity as the Si dimers are *gradually* eliminated by the likes of hydrogen. Dimers that are hydrogen filled have an influence over non-

filled dimers some distance from the hydrogen site, and can delocalize the dimers from their surroundings- how does this affect the surface/bulk interaction? UHV van der Pauw measurements in conjunction with STM and modeling are proposed to investigate the influence of hydrogen adsorption on the conduction mechanism.

The bulk/surface conduction mechanism, given the name surface transfer doping, should be generalizable to other nanoscale systems with appropriately positioned surface bands. We are investigating using organic molecules and inorganic oxides with appropriate HOMO and LUMO bands that may allow this same conduction mechanism to exist outside of vacuum.

Si(110) is rapidly becoming a technologically important orientation because of the enhanced hole mobility in this orientation compared to Si(001). Yet comparatively little is known about its surface structure and electronic properties. Well prepared Si(110) has a (16×2) surface reconstruction, the precise electronic nature of which is unknown. We are currently investigating Si(110) nanomembranes with the aim of determining whether suitably positioned surface state bands exist to enable conduction in ultra-thin Si(110) membranes. If such bands are identified, 2-photon photoemission will be used to probe their structure and density of states.

Electronic transport in nanomembranes is just one aspect of their novelty; their structural properties on an atomic scale are equally captivating. The topic of mixed crystal facets is becoming increasingly important with, for example, the accelerating interest in nanowires, which in single-crystal form are terminated by different crystal planes, and will be susceptible to surface effects as the wire dimensions are shrunk. Also, mixed Si orientations for electronic applications are gaining popularity. For example, hybrid orientation technology (HOT) involves fabricating mixed regions of Si(110) (for p-channel devices) and Si(001) (for n-channel devices) on a single wafer. With these considerations, fundamental questions about the nature of Si surfaces and the interaction between different crystal orientations becomes increasingly relevant. Membranes provide a convenient way to investigate these questions, as the use of SOI(110) allows release of a (110) template layer from a (001) handle substrate. The holes that are used to enhance etchant access (shown in Fig. 2) reveal the Si(001) substrate which is surrounded by the (110) membrane. Subsequent rebonding of the membrane to host allows epitaxial overgrowth, with mixed (001) and (110) regions, and because growth of (001) regions is faster than (110), a degree of planarization of the etch holes is possible. It then becomes possible to investigate, with STM, what happens on an atomic scale when a 2×1 (001) reconstruction meets with a 16×2 (110) reconstruction in the same plane.

As mentioned earlier, much interest in nanomembranes stems from dominance of surface properties over the bulk. What happens to the atomic structure of a membrane in the limit where it is so thin that the bottom membrane surface is capable of “communicating” with the top surface? In this limit, we expect that the nature of the interface bonding will affect the entire membrane, and influence the structure of the top (vacuum) surface. We are using UHV-STM to study this question.

3: *Self-assembled quantum dots on membranes: Ordering mechanisms and applications*

Organized self-assembly of quantum dots has been a topic of immense interest for several decades. Certainly a reasonable degree of ordering can be obtained from multilayer superlattice systems in which the strain promotes increased ordering with each successive layer. However, the use of multiple stacks is cumbersome and the long-range ordering is not sufficient to meet the demands required for technological integration.

Ultra-thin membranes provide a unique stage for assembling nanostructures because they are mechanically compliant. Consequently the membrane has an unusual degree of influence over the assembly of structures during growth. Using CVD, we simultaneously grow Ge on *both* sides of a Si nanomembrane. A strong anticorrelation is observed between islands grown on the top and bottom of the membrane, as well as ordering of islands into rows along narrow free-standing wire-like membranes (Fig. 3), producing a highly ordered array of self assembled quantum dots (QD) in a single layer. The local strain in the membrane under each island, coupled with the remarkable ordering, leads to a highly periodic strain field in the membrane, and the opportunity to take advantage of the periodic band structure modification along the length of the wire for the development of optical, electronic, and thermal devices.

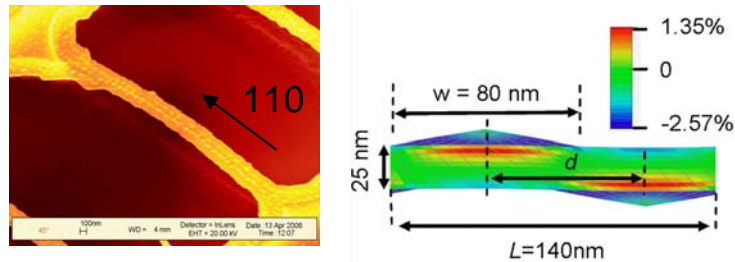


Fig. 3: Left: Self-organized QDs on a membrane wire. Right: The strain field surrounding QDs on a membrane, and demonstrating the anti-correlation. The maximum tensile strain is directly under the apex of each dot.

Certainly one of the unique features of these membrane wires with their electronic lattice resulting from the periodic band structure modulation, is that the need for laborious manipulation of wire positioning into circuits (the traditional bottle neck for self-organized nanostructures such as carbon nanotubes) is entirely eliminated. The wire is patterned in position on an SOI substrate prior to CVD growth, allowing complete control of its position and the opportunity to continue with conventional device processing after growth.

This approach to producing self-organized periodic strain fields is not limited to the Si/Ge system. We anticipate that similar structural and electronic effects can be obtained using self-organized stressors in a variety of materials systems where a sacrificial layer is available to selectively release the membrane. For example, QDs in the GaAs/InAs system, thermoelectric materials based on QDs in the PbSeTe/PbTe system and nanomagnets formed from SrRuO₃/LaAlO₃.

Acknowledgements:

The work described here is contributed to by M. M. Roberts, P. P. Zhang, C. S. Ritz, A. C. Opatowsky, C. Euaruksakul, and D. E. Savage,

References:

- 1 S. A. Scott and M. G. Lagally, *J. Phys. D.* **40**, R75 (2007).
- 2 M. M. Roberts, L. J. Klein, D. E. Savage et al., *Nature Materials* **5**, 388 (2006).
- 3 K. Rim, K. Chan, L. Shi et al., *IEDM Tech. Digest* 3.1.1 (2003).
- 4 T. Mizuno, N. Sugiyama, T. Tezuka et al., *Mater. Sci. Semicond. Process.* **8**, 327 (2005).
- 5 R. Hull, J. C. Bean, L. Peticolas et al., *Appl. Phys. Lett.* **59**, 964 (1991).
- 6 P. P. Zhang, E. Tevaarwerk, B-N. Park et al., *Nature* **439**, 703 (2006).

Session II

Defect-Controlled Synthesis

Session Chair: Jeff Drucker, Arizona State University

This page is intentionally blank

USE OF NANO-ISLANDS (WITH DOPANT AND “CODOPANT”) FOR IMPROVED DOPING IN WIDE-BANDGAP SEMICONDUCTORS

Maria C. Tamargo,¹ Gertrude F. Neumark,² Yinyan Gong,² Igor Kuskovsky³ and Aidong Shen⁴
¹City College of New York, Department of Chemistry, ² Columbia University, Department of Applied Physics and Applied Mathematics ³ Queens College, Department of Physics, ⁴ The City College of New York, Grove School of Engineering

I. Program Scope

There have been continuous efforts to achieve good bipolar doping in wide bandgap semiconductors. We have recently developed a new doping technique, involving the use of a standard dopant together with a "co-dopant" used to facilitate the incorporation of the dopant (the "co-dopant" does not need to be strictly a dopant as generally used for semiconductors). Specifically, we have applied this approach to ZnSe and obtained about an order-of-magnitude improvement in net acceptor concentration over bulk doping [1]. This research is to continue to explore this novel doping technique, with emphasis on the understanding of the basics about the formation of the nano-islands, how the growth procedure may affect the nano-island formation, and how the optical and electrical properties may change with the island manipulation.

II. Recent Progress

MBE Growth

Several series of samples have been grown by molecular beam epitaxy (MBE) in order to study the (Te+N) co-doping in ZnSe. In all cases, the “triple” δ^3 -doping (δ^3) technique previously developed by our group [1] was used. Five sets of experiments were done: (1) We have grown a series of “standard” samples as described in Ref. [1]. Both δ^3 -ZnSe:Te and δ^3 -ZnSe:(Te+N) samples have been grown. The same shutter sequence was used, which involves 5 seconds of growth interruption (GI) after each material deposition. (2) Samples in which the ZnSe spacer layers were doped with N have been grown. The purpose of the study is to lower the potential barrier between ZnTe:N islands and ZnSe spacer so that holes in the ZnTe:N islands can be more easily delocalized throughout the layer. (3) To study the impact of having the N atoms fully surrounded by ZnTe, we have grown samples with (N+Te) doping in the center of the δ^3 region, but only Te doping in the outer two layers. We call the structure “center N-doped δ^3 structure”. (4) Combining (2) and (3), we have grown “center N-doped δ^3 structure” samples with the ZnSe spacer also doped with N. (5) To manipulate the island size, we have begun to grow samples with modified shutter sequences. Samples with reduced or no growth interruptions after (Te+N) deposition have been grown. We expect that by changing the waiting time after (Te+N) deposition, we can alter the adatom migration and therefore change the island size of ZnTe:N.

Material Characterization

A. X-Ray Diffraction

We have performed High Resolution X-ray diffraction measurements (in the Synchrotron light source of Brookhaven laboratories) on the δ^3 -doped ZnSe:(Te,N) samples, which allows us to extract average Te concentrations in the layer. The incorporation of δ -doped Te produces a

strain marker in the ZnSe layers, therefore satellite peaks arising from the periodic doping can be observed. From the separation of the satellite peaks, the thickness of the ZnSe spacer layer can be determined. Fig. 1 shows the x-ray diffraction curves for a set of samples in series (5) described in the growth section. The time (0-5 sec) is the growth interruption (GI) after Te shutter is opened for 5 seconds. It is apparent that a slight change in growth sequence (in this case, the GI time) significantly changes the layer structures. The satellite peak intensity increases with the decrease of GI time, which is probably an indication of the buildup of more strain due to the fact that less Te is desorbed from the surface with reduced GI. This is further supported by the fact that the periodicity also increases (satellite peak spacing decreases) with the decrease of GI time. It is interesting to note the existence of a set of sub-satellite peaks in the samples. Although not understood at present, the intensity of the sub-satellite peaks also increases with the decrease of GI time. Further analysis, such as by doing the dynamical simulation of the x-ray data, may help us to better understand the structure.

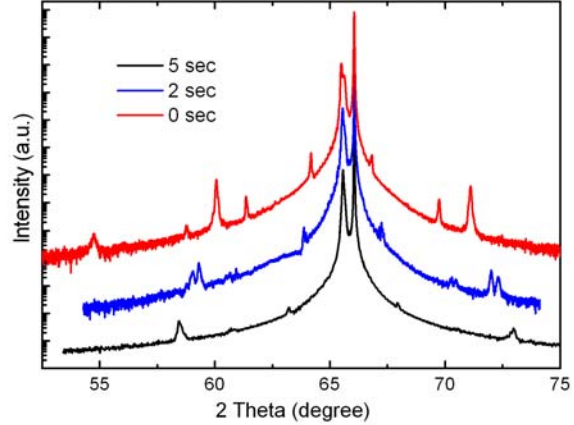


Fig. 1 X-ray diffraction curves for set set of samples with different time of growth interruption.

B. Photoluminescence

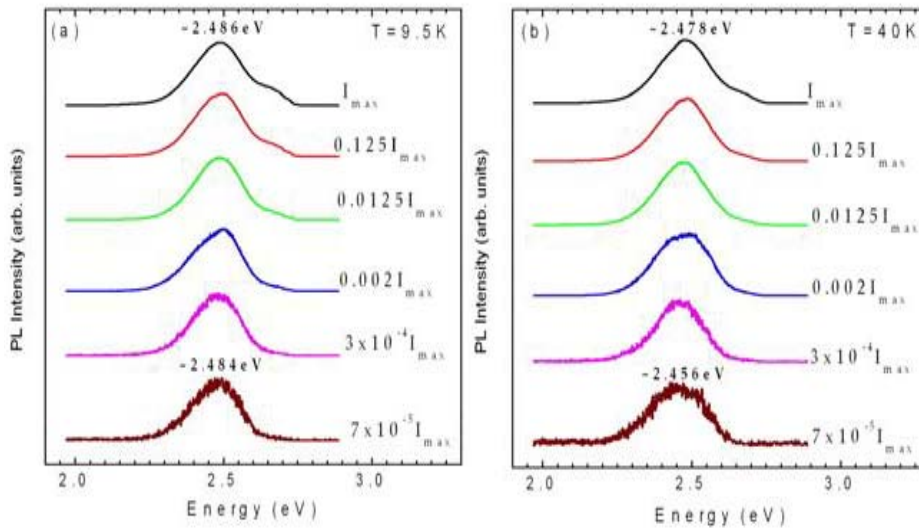


Figure 2. PL spectra of a δ^3 -doped ZnSe:Te under various excitation intensities: (a) T=9.5K; (b) T=40K.

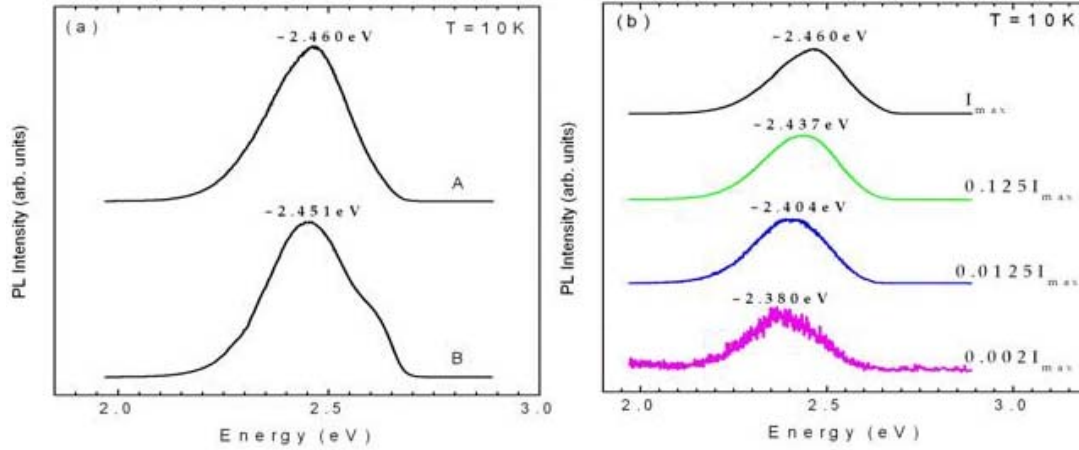


Figure 3. (a) PL spectra of the new type of δ^3 -doped ZnSe:(Te,N) sample with N-doped spacer regions (curve A) and a standard δ^3 -doped ZnSe:(Te,N) sample (curve B); (b) PL spectra of the new type sample at various excitation intensity.

The samples have also been characterized by temperature and intensity dependent photoluminescence (PL). We found that the sample without nitrogen co-doping does not exhibit an intensity shift at very low temperatures, indicating that isoelectronic centers dominate the defect structure [2]. After heating the sample up to 40 K, we indeed observed the shift, demonstrating the fact that ZnTe-rich nano-islands are still present in the system (see Figs. 2-(a) and (b)).

We performed PL measurements on a new type of sample with N-doped spacer regions. The recorded PL spectrum under maximum excitation intensity is plotted in Fig. 3-(a), and the PL spectrum of a standard δ^3 -doped ZnSe:(Te,N) sample is shown as a reference. A broad peak centered at a comparable spectral region dominates the PL spectra of both samples. Fig. 3-(b) shows the PL spectra of the new sample under various excitation intensities. A clear shift of peak position with excitation intensity is observed where the intensity is reduced by three orders of magnitude. Such behavior is typical for δ^3 -doped ZnSe:(Te,N) samples.

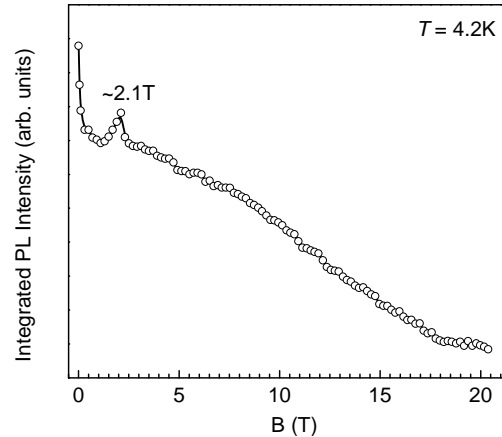


Figure 4 Integrated PL intensity of a δ -ZnSe:Te sample as a function of magnetic field.

C. Magneto-optical measurement results

We have also performed magneto-optical measurements on δ -ZnSe:Te sample. Figure 4 show the integrated PL intensity of the sample as a function of magnetic field B along the growth

direction. The major feature here is the presence of a strong oscillation in the integrated intensity at $B_0 \approx 2.1$ T. The oscillatory behavior of overall PL intensity is consistent with the predicted optical Aharonov-Bohm (AB) effect for type-II QDs of cylindrical symmetry [3, 4]). A similar phenomenon has also been observed for the δ^3 -ZnSe:Te sample [5]. These results confirmed the formation of type-II quantum dots in the samples.

III. Future Plans

In summary, we have performed systematic studies on the growth and characterization of δ -doped and co-doped ZnSe:Te layers. Several series of samples were grown by MBE in which either the doping position or the growth sequence were altered. The X-ray diffraction measurement showed that a slight change of the doping sequence can significantly change the sample structures. PL studies showed that the isoelectronic centers dominate the defect structure in samples without N co-doping. Magneto-optical measurements confirmed the formation of type-II quantum dots in the structures.

We plan to continue to pursue our work in the ZnSeTe system. We will explore ways to modify the growth sequence in order to obtain smaller islands, which will increase the probability of hole activation. We will also explore the possibility of using other dopants, such as As, which may have a smaller binding energy in ZnTe. We will continue to systematically study the properties of the structures by various techniques such as high-resolution x-ray diffraction, PL, magneto-PL, and AC Hall measurements.

IV. REFERENCES

1. W. Lin, S. P. Guo, M. C. Tamargo, I. Kuskovsky, C. Tian, G. F. Neumark, Enhancement of p-type Doping of ZnSe Using a Modified (N + Te) δ -doping Technique, *Appl. Phys. Letters*, **76**, 2205 (2000).
2. Y. Gu, Igor L. Kuskovsky, M. van der Voort, G.F. Neumark, X. Zhou, and M.C. Tamargo, *Zn-Se-Te Multilayers With Sub-monolayer Quantities of Te: Type-II Quantum Structures and Isoelectronic Centers*, *Phys. Rev. B*, **71**, 045340 (2005).
3. A. O. Govorov, A. V. Kalameitsev, R. Warburton, K. Karrai, S.E. Ulloa, *Physica E*: **13**, 297 (2002).
4. K.L. Janssens, Partoens, B., Peeters, *Phys. Rev. B* **66**, 075314 (2002)
5. I. L. Kuskovsky, W. MacDonald, A.O. Govorov, L. Mourokh, X. Wei, M. C. Tamargo, M. Tadic, and F. M. Peeters, *Optical Aharonov-Bohm effect in stacked type-II quantum dots*, *Phys. Rev. B* (2007) accepted for publication.

V. PUBLICATIONS & PRESENTATIONS

1. I. L. Kuskovsky, W. MacDonald, A.O. Govorov, L. Mourokh, X. Wei, M. C. Tamargo, M. Tadic, and F. M. Peeters, *Optical Aharonov-Bohm effect in stacked type-II quantum dots*, *Phys. Rev. B* (2007) accepted for publication.
2. Y. Gong, Hanfei F. Yan, I. L. Kuskovsky, Y. Gu, I. C. Noyan, and G. F. Neumark, and M. C. Tamargo, *Structure of Zn-Se-Te system with sub-monolayer insertion of ZnTe grown by migration enhanced epitaxy*, *J. Appl. Phys.* **99**, 064913 (2006).
3. Y. Gong, Hanfei F. Yan, I. L. Kuskovsky, Y. Gu, I. C. Noyan, and G. F. Neumark, and M. C. Tamargo, *Structure of Zn-Se-Te System with Sub-monolayer Insertion of ZnTe Grown by Migration Enhanced Epitaxy*, Fall MRS Meeting, Boston, 2005.

Silicon-Based Nanomembranes, Nanoribbons, and Quantum Dots

Max G. Lagally, University of Wisconsin-Madison, lagally@engr.wisc.edu

Program Scope: We have been performing research that is setting the stage for what is essentially a new materials nanotechnology platform, strain engineered Si-based nanomembranes (SiNMs). The novelty of SiNMs (and by extension other materials that can be grown heteroepitaxially and released from a bulk substrate, including other compound semiconductors, functional oxides such as piezoelectrics and ferroelectrics, and even metals) is several-fold: they are highly strained, they are flexible, they are transferable to many other hosts and bond easily to most, and they can be made to take on a large range of shapes by engineering the strain and the geometry. Properly prepared, they retain the perfect-single-crystal, dislocation-free nature of the original Si substrate, even though now all the layers are significantly strained. They additionally have a very high interface-to-volume ratio, with surfaces or interfaces potentially very important contributors to unique membrane electrical conduction and surface chemical properties. In the form of nanowires (SiNWs) or nanoribbons (easily made by selective patterning before etching to release them) they may have a modified band structure and density of states if sufficiently small, and, combined with the strong dependence of the conductivity on the surface condition, significant potential as nanowire sensors or devices.

Nanomembrane systems offer the choice of nano-size in one, two, or three dimensions, as well as the integration of structures with different dimensions in novel ways. We use top-down fabrication methods that allow us to make hundreds of identical structures, and combine these with bottom-up self-assembly techniques to create unique new structures. Although our work has so far been in strain engineered Si-based nanomembranes (SiNMs), the paradigm is extendable to other materials and a range of structures and functions, using the approaches we have developed.

In addition to the potential for elegant new processing science this system presents us, the technological potential is clear-cut. We have filed several patents during the last four years, with the likelihood of transfer of at least some of the technology to the commercial sector within 2-3 years.

The members of the research team are:

- Max G. Lagally, E.W. Mueller Professor of Materials Science and Engineering and Physics. Primary responsibility for the experimental effort in film growth, membrane fabrication, structural characterization and surface modification, and new materials combinations.
- Mark Eriksson, Associate Professor of Physics. Electronic transport, low-temperature transport, and fabrication of single-electron transistor structures.
- Feng Liu, Associate Professor of Materials Science, University of Utah, will lead the theoretical effort.

The goals of our research are:

- Develop new Si nanomembrane materials, including research on structures, processing, and materials combinations
- Develop Si nanomembrane release, transfer, and bonding science
- Create nanowires and nanoribbons from Si nanomembranes and explore their properties
- Explore quantum dots on membranes or ribbons, a double-nano system, via heteroepitaxial growth and strain organized self-assembly

- Characterize electronic transport in membranes and ribbons, exploiting unique effects related to surface transfer doping; explore potential for sensor technology
- Explore periodic strain modulation in QD nanoribbons, and resultant band structure and electron transport modulation
- Explore adsorption, impurities, and defects, and relation to conduction in SiNMs
- Perform a variety of theoretical studies both in support of the experiments and to drive new experiments.

Recent Progress:

- *Free-standing, elastically strain sharing Si nanomembrane fabrication:* we developed the processes required to grow, release, and transfer to new hosts very thin Si-based strained membranes (Fig.1).

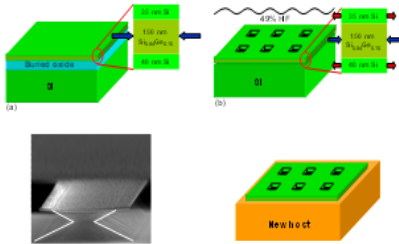


Figure 1. Schematic diagram of membrane fabrication processing, plus image of oxide undercutting

- *Growth of QDs on free-standing membranes:* we made samples that were used to determine the stress and bending created by individual quantum dots, using high-spatial resolution x-ray diffraction.
- *High-surface sensitivity strain measurements in nanomembranes:* using soft-x-ray absorption spectroscopy with synchrotron radiation, we determined the near-surface sub-band splitting as a function of strain in thin elastically strain sharing Si nanomembranes for a range of strains. This is a new application of the technique – such data could not be obtained in other ways.

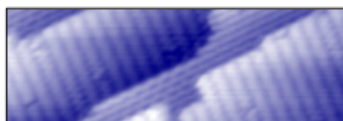
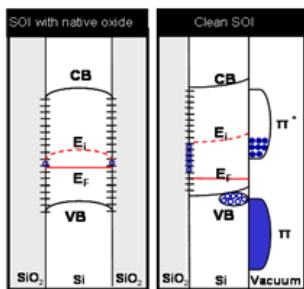


Figure 2. STM image of 10nm-thick membrane. Such measurements are possible because of surface transfer doping, as illustrated in the band diagram above.

- *Electronic transport in very thin semiconductor membranes:* we identified surface transfer doping in SiNMs using the surface bands as “parking lots” for charges. Without these states, the SiNM would be intrinsic because it is so thin. This work has major implications for sensors and semiconductor devices (Fig. 2).
- *Low-temperature magnetotransport measurements:* using such membranes, we showed that we could strain engineer the band offsets. The measurement showed we could get a single bound state into a Si quantum well by elastically relaxing the membrane (Fig. 3).
- *Quantum dot growth on both sides of a membrane: enhanced self-organization via strain communication:*

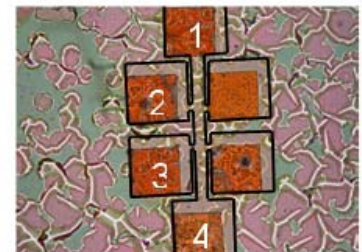


Figure 3. Contact layout on a released membrane for magnetotransport measurement.

We have discovered a novel effect. Growing Ge QDs on both sides of a thin Si membrane allows dots growing on opposite surfaces of the membrane to interact with each other via the strain fields they induce in the Si, leading to much higher order

and an effective strain superlattice. This strain superlattice in turn produces an electronic superlattice, which we believe will have novel phononic and electronic properties that may be useful in nanothermoelectrics.

Future Work: In a continuation of this research, we will focus on the following areas

1. **Nanomembrane materials: structures, processing, and materials combinations.** Essentially we will explore all aspects of the precursor materials to forming membranes
2. **Nanomembranes.** Topics include release of membranes, transfer techniques, bonding to new hosts, stacking/bonding, contacts to membranes, and membrane stability
3. **Wires and ribbons.** These can be single-component ribbons or multilayer membrane ribbons. Issues in the fabrication of free-standing or attached ribbons or wires will be different from those for membranes. In addition, we introduce a measure of directionality (which will affect electronic properties, strain, and possibly chemistry). We also introduce a shape variable: wires can be in the form of flat ribbons, square boxes, or even with rounded edges via preferential oxidation. See Fig. 4.
4. **Quantum dots on membranes or ribbons - a double-nano system.** We will investigate an entirely new regime of nanoscience, namely the self-assembly of nanostructures on Si nanomembranes.
5. **Membrane characterization – electronic transport, structure, defects, and chemical bonding.** We will characterize a range of very novel properties of membranes in all the above areas, also phononic structures.
6. **Surface chemical modification.** Because of the sensitivity of the electronic conductivity to the surface, we will investigate the chemical modification of membrane and ribbon surfaces to functionalize them for chemical specificity.
7. **Theory.** Theoretical studies will be carried out in close interaction with the experiments, to address a broad range of topics from electronic structure, transport, atomic structure, and quantum dot (QD) self-assembly to nanoarchitecture in the context of Si nanomembranes. These will be done by using combinations of different theoretical and computational approaches.

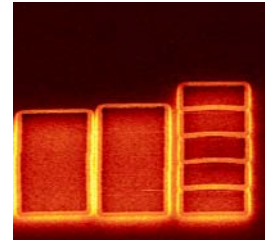


Figure 4. Si nanowires defined in SOI with e-beam lithography and released by etching underneath them.

References

1. V.Ya. Prinz, V.A. Seleznev, A.K. Gutakovskiy, A.V. Chehovskiy, V.V. Preobrazhenskii, M.A. Putyato, and T.A. Gavrilova, *Physica E* **6** 828 (2000)
2. P. P. Zhang, E. Tevaarwerk, B. N. Park, D. E. Savage, G. K. Celler, I. Knezevic, P. G. Evans, M. A. Eriksson, and M. G. Lagally, *Nature* **439** 703 (2006)
3. A. Cho, *Science (Focus)* **313** 165 (2006)
4. O. G. Schmidt and K. Eberl, *Nature* **410** 168 (2001)
5. E. Menard, K. J. Lee, D.-Y. Khang, R. G. Nuzzo, and J. A. Rogers, *Appl. Phys. Lett.* **84** 5398 (2004)
6. R. Service, *Science (Focus)* **312** 1593 (2006)
7. M. M. Roberts, L. J. Klein, D. E. Savage, K. A. Slinker, M. Friesen, G. Celler, M. A. Eriksson, and M. G. Lagally, *Nature Materials* **5** 388 (2006)
8. H.-C. Yuan, Z. Q. Ma, M. M. Roberts, D. E. Savage, and M. G. Lagally, *J. Appl. Physics* **100** 013708 (2006)
9. D. Dunn, <http://informationweek.com/news/showArticle.jhtml?articleID=192202083>
10. Zhenqiang Ma and M. G. Lagally, "PIN Diodes for Photodetection and High-Speed, High-Resolution Image Sensing", # P04389US, patent application, June 2006
11. M. H. Huang, C. Boone, M. M. Roberts, D. E. Savage, M. G. Lagally, N. Shaji, H. Qin, R. Blick, J. A. Nairn and F. Liu, *Adv. Mater.* **17** 2860 (2005)

12. C. Ritz, P.E. Evans, and M.G. Lagally, "Silicon nanomembrane thermoelectric materials and devices", patent application in progress
13. Z. Yuan, B. E. Kardynal, R. M. Stevenson, A. J. Shields, C. J. Lobo, K. Cooper, N. S. Beattie, D. A. Ritchie, and M. Pepper, *Science* **295** 102 (2002)
14. T. Lundstrom, W. Schoenfeld, H. Lee, and P. M. Petroff, *Science* **286** 2312 (1999)
15. S. Tiwari, F. Rana, H. Hanafi, A. Hartstein, E. F. Crabbé, and K. Chan, *Appl. Phys. Letters* **68** 1377 (1995)
16. M. Bayer, P. Hawrylak, K. Hinzer, S. Fafard, M. Korkusinski, Z. R. Wasilewski, O. Stern, and A. Forchel, *Science* **291** 451 (2001)
17. F. M. Ross, R. M. Tromp, and M. C. Reuter, *Science* **286** 1931 (1999)
18. G. Springholz, V. Holy, M. Pinczolits, and G. Bauer, *Science* **282** 734 (1998)
19. P. Sutter and M. G. Lagally, *Phys. Rev. Letters* **84** 4637 (2000)

Publication List:

- "*Electronic Transport in Nanometre-Scale Silicon-on-Insulator Membranes*", P. P. Zhang, Emma Tevaarwerk, B.-N. Park, D. E. Savage, G. Celler, I. Knezevic, P.G. Evans, M. A. Eriksson, and M. G. Lagally, *Nature*, **439**, 703 (2006).
- "*High-Speed Strained-Single-Crystal-Silicon Thin-Film Transistors on Flexible Polymers*", Hao-Chih Yuan, M. M. Roberts, D. E. Savage, ZQ Ma, M. G. Lagally, *J. Appl. Phys.* **100**, 013708 (2006).
- "*Elastically Relaxed Free-Standing Strained-Si Nanomembranes*", M.M. Roberts, L.J. Klein, D.E. Savage, M. Friesen, G. Celler*, M.A. Eriksson, M.G. Lagally, *Nature Materials*, **5**, 388 (2006).
- "*Formation of Micro Tubes from Strained SiGe/Si Heterostructures*", H. Qin, N. Shaji, N. E. Merrill, Hyun S. Kim, R. C. Toonen, R. H. Blick, M.M. Roberts, D. E. Savage, M. G. Lagally, and G. Celler, *New J. of Physics* **7**, 241 (2005).
- "*Electrical Conductivity in Silicon Nanomembranes*", P.P. Zhang, E. P. Nordberg, B.-N. Park, G. K. Celler, I. Knezevic, P.G. Evans, M. A. Eriksson, and M. G. Lagally, *New Journal of Physics* **8**, 200 (2006).
- "*Silicon-Based Nanomembrane Materials: The Ultimate in Strain Engineering*", Hao-Chih Yuan, M. M. Roberts, P.P. Zhang, B.-N. Park, L. J. Klein, D. E. Savage, F. S. Flack, Z.Q. Ma, P. G. Evans, M. A. Eriksson, G. K. Celler, and M. G. Lagally, *Digest of Papers, 2006 Topical Meeting on Si Monolithic Integrated Circuits in RF Systems (SiRF06)*, ed. Rhonda Drayton, IEEE, Piscataway, NJ (2006).
- "*Nanomechanical Architecture of Strained Bilayer Thin Films: From Design Principles to Experimental Fabrication*", Minghuang Huang, C. Boone, M. Roberts, D. E. Savage, M. G. Lagally, N. Shaji, H. Qin, R. Blick, J. A. Nairn, and Feng Liu, *Adv. Mater.* **17**, 2860 (2005).
- "Silicon Nanomembranes", M.G. Lagally, *MRS Bulletin*, Jan 07
- "Strain Engineered Silicon Nanomembranes", M.G. Lagally, *Proceedings ICNT* in press
- "Elastically Strain Sharing Nanomembranes: Flexible and Transferable Strained Silicon and Silicon-Germanium Alloys", S. A. Scott and M. G. Lagally, *J. Phys. D.* March 2007
- "Single Crystal and Amorphous Multilayer Heterostructure based on Membrane Transfer," Weina Peng, E. P. Nordberg, M. A. Eriksson, M. M. Roberts, F. S. Flack, M.G. Lagally, and D. E. Savage, R. J. Hamers and P. E. Colavita, *Appl. Phys. Letters*, in press
- "*Germanium Hut Nanostressors on Free-Standing Ultrathin SOI*", M. M. Roberts, Daniel Tinberg, P. G. Evans, M. G. Lagally, C.-H. Lee, Yanan Xiao, Barry Lai, and Zhonghou Cai, *J. Electrochem. Soc.* Submitted, *Proceedings of the Electrochemical Society* (2005).
- "*Strain and Bending in Microfabricated Substrates for SiGe Epitaxial Growth*", P. G. Evans, P. Rugheimer, M. Lagally, C. H. Lee, A. Lal, Y. Xiao, B. Lai, and Z. Cai, *J. Appl. Phys.* submitted.

Fundamental Studies of Doping and Properties Modification in Oxide Semiconductor Epitaxial Films

Scott A. Chambers^a, Timothy C. Droubay^a, Tiffany C. Kaspar^a, Irene Cheung^a,
Chongmin Wang^a, Steven M. Heald^b, V. Shutthanandan^a, P. Nachimuthu^a

^aPacific Northwest National Laboratory, Richland, WA

^bArgonne National Laboratory, Argonne, Ill

I. Program Scope

Compared to Group IV, III-V, and II-VI semiconductors, transition metal (TM) oxide semiconductors are relatively unexplored. Fundamental insight into doping and the associated effect(s) on properties is lacking. To this end, the goals of this program are to use state-of-the-art epitaxial film growth methods (MBE, PLD and MOCVD), in conjunction with definitive materials characterization plus magnetic, electronic transport, optical and photochemical measurements, to prepare very well-defined materials and elucidate structure-function relationships based on atomic-scale properties.

II. Recent Progress

A. TM doping and the exploration of diluted magnetic semiconductor behavior

We have focused on the three wide-gap host oxides TiO₂ anatase, ZnO and α -Fe₂O₃ doped with Co, Cr and Ti. Co(II) and Cr(III) substitute for the host cation in TiO₂ and ZnO, leading to maximum spin moments of 1 and 3 μ_B per dopant for the low- and high-spin states of Co(II) and Cr(III), respectively [1-3]. α -Fe₂O₃ is a canted antiferromagnet. Ti(IV), a d^0 cation, substitutes for Fe(III), a d^5 cation, leading to a localized reduction in moment [4, 5]. The spin orientations in adjacent cation layers of α -Fe₂O₃ are antiparallel. The spin orientation and layer structure along the c axis can be represented schematically as (M ^{α} -M ^{α} -O₃-M ^{β} -M ^{β} -O₃...), where M-M represents a buckled cation layer. If Ti(IV) locates preferentially in one particular spin sublattice (either M ^{α} -M ^{α} or M ^{β} -M ^{β}), the total spin will be nonzero, and should increase with dopant concentration. In contrast, if Ti(IV) is randomly distributed in both spin sublattices, a dilute system with essentially zero net spin is expected to form. These structures are illustrated in Fig. 1.

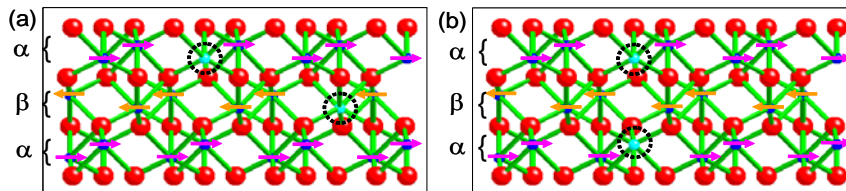


Fig. 1 Structural diagram for Ti-doped Fe₂O₃ in which Ti substitutes for Fe randomly in both spin sublattices (a), and preferentially in one spin sublattice (b).

In the case of MBE-grown Co:TiO₂ and Cr:TiO₂ anatase, we found that the room temperature (RT) saturation moment scales inversely with the crystallographic quality of the films [1-3]. In our early film growth work on these systems, Cr-doped films typically exhibited significant roughening compared to undoped films [6, 7]. Additionally, inclusion of the Co dopant typically resulted in segregation of a Co-rich Co_xTi_{1-x}O₂ phase

(x larger than expected based on fluxes) embedded as nanoparticles within a continuous epitaxial $\text{Co}_x\text{Ti}_{1-x}\text{O}_2$ film phase (x smaller than expected based on fluxes) [8]. Nevertheless, the materials consistently exhibited room-temperature ferromagnetism (RTFM), although the magnetic properties did not scale with dopant and carrier concentrations in any way expected for a magnetic semiconductor. However, as we optimized growth to generate crystallographically superior material, the ferromagnetism essentially disappeared [1-3]. The saturation moment was found to scale inversely with mosaic spread. Our results strongly suggest that defects created at small-angle grain boundaries between crystallites of slightly different orientation activate ferromagnetism. This unanticipated result established that charge compensating O vacancies, introduced when Co(II) or Cr(III) substitutes for Ti(IV) in an otherwise structurally perfect lattice, are not effective at aligning the dopant spins.

We have vigorously pursued the growth and properties of Co-doped ZnO. As-grown films are highly resistive and paramagnetic [9]. However, post-growth n -type doping by vacuum reduction or Zn indiffusion resulted in the simultaneous onset of conductivity and room-temperature ferromagnetism (RTFM), although the carrier concentrations achievable by this means were limited to a small fraction of the Co dopant concentration.. Significantly, the moment per Co was also a small fraction of the value expected for Co(II). Nevertheless, experiments in which Zn-diffused films were annealed in air to draw to the surface and oxidize interstitial Zn (Zn_i) revealed a direct kinetic correlation between Zn_i concentration, conductivity and saturation moment [10]. One interpretation of these results is that exchange coupling between Co spins is activated by shallow bound electrons from Zn_i donors. Significantly, no Co metal was detected in these experiments, which involved thicker films (~ 300 nm). However, experiments on thinner (7 nm) films has revealed that Zn indiffusion results in a reduction of Co(II) to Co(0), presumably by a site exchange redox reaction, suggesting that the observation of RTFM is caused trivially by the presence of Co metal nanoparticles embedded within the film matrix. Experiments to resolve this issue are ongoing. It was found that ZnO could not be doped with Cr because of spontaneous phase separation to form ZnO and Cr_2O_3 .

Finally, $\alpha\text{-Ti}_x\text{Fe}_{2-x}\text{O}_3$ also exhibits RTFM, but not as much as expected if Ti exclusively replaces Fe in one magnetic sublattice (the “non-random” phase) [4, 5]. The hysteresis loops exhibit a dual-lobe structure best interpreted as two microstructurally distinct regions. The dual lobes suggest two magnetic phases, one of high coercivity and one of low coercivity. We conclude that the low-coercivity portion results from coherent rotation with magnetic field while the high-coercivity portion is caused by grain boundary domain wall pinning in the non-random phase. Our combined magnetic and structural results suggest that a minority ($\sim 1/8$) of Ti forms the non-random phase. The resistivity drops with increasing Ti concentration, but not to values expected if all Ti donor electrons are itinerant. This result suggests some degree of carrier localization, and indeed, photoemission shows that localization on Fe sites is detectible at higher Ti concentrations. Ti thus acts as either a deep donor or the source of hopping conductivity through electron localization on Fe sites. Some carriers are also generated by the Ti dopants, but the saturation magnetization is independent of carrier concentration. Thus, we conclude that the ferromagnetism in $\text{Ti}:\alpha\text{-Fe}_2\text{O}_3$ is an intrinsic result of Ti(IV) substituting for Fe(III) in a partially non-random way, and is not coupled to the presence of carriers, which originate with Ti donors.

B. N doped TiO₂ for bandgap reduction

We have investigated the growth and properties of well-defined epitaxial TiO_{2-x}N_x rutile for the first time [11, 12]. This material is of interest because of its potential for photochemical water splitting to make hydrogen. It has been known for years that TiO₂ ($E_g = \sim 3$ eV) can be used to photochemically split water to make hydrogen via UV irradiation. It is of significant current interest to find ways to lower the bandgap so that water splitting can be achieved with visible light absorption. Numerous recent studies of N-doped TiO₂ powders show an enhancement of visible-light photocatalytic activity, but the underlying causes are not apparent. Critically important questions include N speciation, the mechanism by which N is incorporated into the lattice, the maximum achievable dopant concentration, and the effect of dopant concentration on photocatalytic activity. What is lacking in the field is an investigation of well-defined TiO_{2-x}N_x epitaxial films. As a result, little is known about the properties of TiO_{2-x}N_x prepared under highly controlled conditions, and without high defect concentrations. Doing so is the focus of our work. Mixed beams of N and O radicals were prepared in an electron cyclotron resonance plasma source and impinged on various substrates, along with an atomic Ti beam. The associated materials properties were investigated using RHEED, XPS, UPS, XRD, NRA, EPR and UV-visible absorption spectroscopy. We have found that the structural, compositional and electronic properties depend sensitively on the three atomic fluxes, as well as the substrate. In the absence of extensive defect creation, N incorporation is limited to ~ 2 at. %. Interstitial Ti resulting from Ti indiffusion during growth generates shallow donors that fully compensate N acceptors, precluding *p*-type character. Filled Ti-N hybridized states fall deep in the gap and give rise to enhanced optical absorption in the visible above ~ 2.5 eV. However, it is not yet known whether this new state results in itinerant electrons and holes at and above 2.5 eV.

III. Future Plans

Our future thrusts include expanding and refining our understanding of some of the above systems, and investigating new ones. We are currently setting up a variable temperature photoconductivity apparatus to determine if e^-h^+ pair creation at $h\nu \geq \sim 2.5$ eV results in mobile carriers in N:TiO₂. We are also expanding our investigation of this material to include the anatase polymorph. In addition, we are growing (Mn, N, Li):ZnO. Codoping with N and Li shows promise for thermally robust *p*-type doping, and we want to see if we can achieve hole-mediated exchange interaction between Mn spins at and above RT with this mode of electronic doping [13]. Additionally, we are developing a novel preparation methods for doped ZnO. We are collaborating with Professor Daniel Gamelin of the University of Washington to fashion nanoparticles of these materials, grown by direct chemical methods in the Gamelin lab, into PLD targets. At issue is whether or not compositional uniformity on the nanoscale in the target results in superior epitaxial film properties. Initial results are promising.

IV. References

- [1] T. C. Kaspar, S. M. Heald, C. M. Wang, J. D. Bryan, T. C. Droubay, V. Shutthanandan, S. Thevuthasan, D. E. McCready, A. J. Kellock, D. R. Gamelin, S. A. Chambers, Phys. Rev. Lett. **95**, 217203 (2005).
- [2] T. C. Kaspar, T. C. Droubay, V. Shutthanandan, S. M. Heald, C. M. Wang, D. E. McCready, S. Thevuthasan, J. D. Bryan, D. R. Gamelin, A. J. Kellock, M. F. Toney, X. Hong, C. Ahn, S. A. Chambers, Phys. Rev. B **73**, 155327 (2006).

- [3] T. C. Kaspar, T. C. Droubay, V. Shutthanandan, S. M. Heald, C. M. Wang, D. E. McCready, S. Thevuthasan, J. D. Bryan, D. R. Gamelin, A. J. Kellock, M. F. Toney, X. Hong, C. H. Ahn, S. A. Chambers, *Phys. Rev. B: Condens. Matter* **73**, 155327 (2006).
- [4] S. A. Chambers, T. C. Droubay, C. M. Wang, K. M. Rosso, S. M. Heald, D. A. Schwartz, K. R. Kittilstved, D. R. Gamelin, *Mater. Today* **9**, 28 (2006).
- [5] T. C. Droubay, K. M. Rosso, S. M. Heald, D. E. McCready, C. M. Wang, S. A. Chambers, *Phys. Rev. B* **75**, 104412 (2007).
- [6] T. Droubay, S. M. Heald, V. Shutthanandan, S. Thevuthasan, S. A. Chambers, J. Osterwalder, *J. Appl. Phys.* **97**, 046103 (2005).
- [7] J. Osterwalder, T. Droubay, T. C. Kaspar, J. R. Williams, S. A. Chambers, *Thin Solid Films* **484**, 289 (2005).
- [8] S. A. Chambers and R. F. C. Farrow, *MRS Bull.* **28**, 729 (2003).
- [9] A. C. Tuan, J. D. Bryan, A. B. Pakhamov, V. Shutthanandan, S. Thevuthasan, D. E. McCready, D. Gaspar, M. H. Engelhard, J. W. Rogers Jr, K. M. Krishnan, D. R. Gamelin, S. A. Chambers, *Phys. Rev. B* **70**, 054424 (2004).
- [10] K. R. Kittilstved, D. A. Schwartz, A. C. Tuan, S. M. Heald, S. A. Chambers, D. R. Gamelin, *Phys. Rev. Lett.* **97**, 037203 (2006).
- [11] S. A. Chambers, S. H. Cheung, V. Shutthanandan, S. Thevuthasan, M. K. Bowman, A. G. Joly, *Chem. Phys.*, to appear (2007).
- [12] S. H. Cheung, P. Nachimuthu, A. G. Joly, M. H. Engelhard, M. K. Bowman, S. A. Chambers, *Surf. Sci.*, in press (2007).
- [13] J. G. Lu, Y. Z. Zhang, K. K. Ye, L. P. Zhu, L. Wang, B. H. Zhao, *Appl. Phys. Lett.* **88**, 222114 (2006).

V. Selected Sponsored Publications in 2006-2007

T.C. Kaspar *et al.*, “Ferromagnetism and Structure in Epitaxial Cr-doped Anatase TiO₂”, *Phys. Rev.* **B 73**, 155327 (2006).

T.C. Kaspar *et al.*, “Magnetic Properties of Epitaxial Co-doped Anatase TiO₂ Thin Films with Excellent Structural Quality”, *J. Vac. Sci. Technol.* **B24**, 1212 (2006).

K.R. Kittilstved *et al.*, “Direct Kinetic Correlation of Carriers and Ferromagnetism in Co²⁺:ZnO”, *Phys. Rev. Lett.* **97**, 037203 (2006).

Scott A. Chambers, “Ferromagnetism in Thin-Film Oxide and Nitride Semiconductors and Dielectrics” (invited review), *Surf. Sci. Rep.* **61**, 345 (2006).

Scott A. Chambers, “Ferromagnetism in Oxide Semiconductors” (invited review), *Mat Today* **9**, 28 (2006).

L. V. Saraf *et al.*, “Nucleation and Growth of MOCVD-Grown (Cr, Zn)O Films – Uniform Doping vs. Secondary Phase Formation”, *J. Electrochem. Soc.* **154**, D134 (2007).

R. Shao *et al.*, “Growth and Structure of TiO₂ Anatase Films with Rutile Nano-crystallites by MBE”, *Surf. Sci.* **601**, 1852 (2007).

T.C. Droubay *et al.*, “Structure, Magnetism and Conductivity in Epitaxial Ti-doped α -Fe₂O₃ Hematite”, *Phys. Rev.* **B 75**, 104412 (2007).

L.V. Saraf *et al.*, “MOCVD Growth of Carbon-free ZnO Using the Zn(TMHD)₂ MOCVD Precursor”, *J. Mat. Res.*, in press (2007).

Scott A. Chambers *et al.*, “Growth, Electronic and Magnetic Properties of Doped ZnO Epitaxial and Nanocrystalline Films”, *App. Phys. A: Mat. Sci. & Proc.*, in press (2007).

S.H. Cheung *et al.*, “N Incorporation and Electronic Structure in N-doped TiO₂(110) Rutile”, *Surf. Sci.*, in press (2007).

S.A. Chambers *et al.*, “Properties of Structurally Excellent N-doped TiO₂ Rutile”, invited paper in special issue of *Chemical Physics* entitled *Doping and Functionalization of Photoactive Semiconducting Metal Oxides*, ed. C. DiValentin, U. Diebold, A. Selloni, (2007).

S.A. Chambers, “Advances in the Surface Science of TiO₂ – A Global Perspective”, invited review article for *J. Surf. Sci. Jpn.* (2007).

Self-assembled surface patterns in epitaxial thin films

Yaoyu Pang, Sanjay Banerjee, and Rui Huang

Microelectronics Research Center and Department of Aerospace Engineering and Engineering Mechanics, University of Texas, Austin, Texas 78712

I. Program Scope

An epitaxial thin film subjected to a misfit stress can undergo surface instability and break up into discrete islands. The stress field and the interfacial interactions have profound effects on the dynamics of surface evolution, leading to a rich variety of self-assembled patterns at micro-to-nano scales (e.g., self-assembled quantum dots). This project aims to develop a fundamental understanding of the physical mechanisms that control self-assembled surface patterns.

Theoretical modeling, numerical simulations, and experimental methodologies will be developed to probe various material growth conditions and their effects on shape, size, density, uniformity, and spatial organization of self-assembled quantum dots. Of particular interest is the transition from Stranski-Krastanov (SK) to Volmer-Weber (VW) growth mode on non-uniformly strained substrates, on surface-alloyed substrates, and/or on amorphous dielectric substrates. The objectives are: **(1) to explore novel synthesis approaches for improving size uniformity and spatial ordering of SAQDs by strain and surface engineering, and (2) to develop fabrication processes of semiconductor and metal SAQDs on high-k dielectrics for potential applications in high-speed, low-power nonvolatile memory devices.**

II. Recent Progress

A modeling framework for surface evolution and self-assembly of nanoscale quantum dots has been developed, with a physics-based nonlinear evolution equation and a spectral method for numerical simulations. The nonlinear effects of stress and wetting interactions were delineated. By introducing stress and elastic anisotropy, break of symmetry in the evolution process was demonstrated. In addition, a bifurcation in pattern formation was discovered. These results illustrate the rich dynamics of surface self-assembly, suggesting new routes for the making of desirable patterns, and in particular, engineering-directed self-organization of nanoscale quantum dots.

The nonlinear evolution equation takes the form

$$\frac{\partial h}{\partial t} = \Omega^2 M_{\alpha\beta} \frac{\partial^2}{\partial x_\alpha \partial x_\beta} \left[(U_E + U_S + U_W) \sqrt{1 + h_x h_x} \right], \quad (1)$$

where three energetic terms are considered based on a non-equilibrium thermodynamic formulation: U_E for elastic strain energy, U_S for surface energy, and U_W for interfacial wetting potential. The competition of these thermodynamic forces determines the stability and the evolution process of the epitaxial film.

The elastic strain energy is obtained by solving a nonlinear boundary value problem of elasticity with a wavy surface. It is found that the nonlinear stress field has a significant effect on the long-term evolution of surface patterns, although a linear analysis is sufficient for the determination of the critical condition and the short-term evolution at the early stage. Figure 1 shows a circular pit-like pattern from a numerical simulation, resembling the “quantum rings” [1] and “quantum fortresses” [2] patterns observed in experiments.

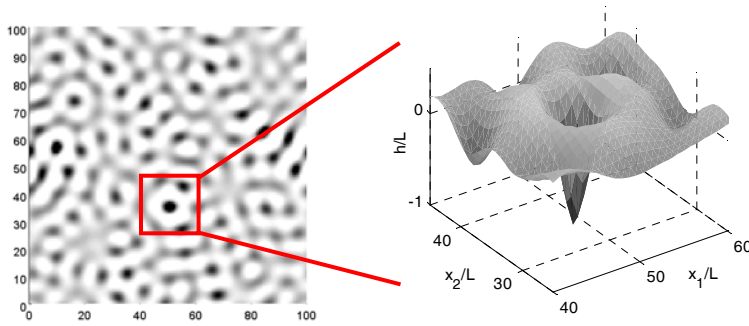


Fig. 1: A circular pit-like pattern from a numerical simulation with the nonlinear stress field.

A nonlinear wetting potential based on a transition-layer model [3] is incorporated in Eq. (1) for the study of interfacial wetting effect. A linear analysis shows that the wetting can stabilize very thin films, which leads to a critical thickness for surface instability. This critical thickness depends on the mismatch stress as well as the thickness of the interfacial transition layer. This is consistent with experimental observations for the Stranski-Krastanov growth of epitaxial thin films. On the other hand, when the surface energy of the film is greater than that of the substrate, the same wetting potential leads to dewetting of the film, characteristic of the Volmer-Weber growth mode.

By combining the nonlinear stress field and the nonlinear wetting potential, our numerical simulations show self-assembly of quantum dots. In the base model, both the film and the substrate are considered to be elastically isotropic. The system is thus fully isotropic when the mismatch stress is equi-biaxial in the plane of the surface. In this case, circular quantum dots (spherical cap in 3D) with random spatial organization are obtained (Fig. 2), which reflects the rotational symmetry of the model system. The symmetry is broken when an anisotropy is introduced, which then leads to different shaped quantum dots (or other patterns) as well as spatial ordering.

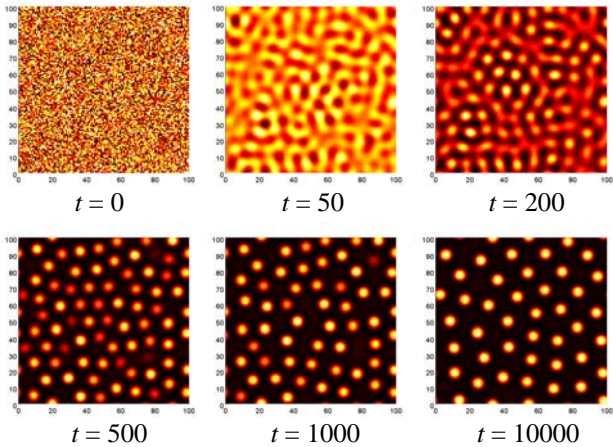


Fig. 2: Numerical simulation of self-assembled quantum dots for an isotropic system.

Various types of anisotropy may be considered for fundamental understanding of their effects, individually and collectively, in the modeling and simulations. In a real material system, the interplay among various origins of anisotropy and ordering forces produces a rich variety of surface patterns. First, we considered the effect of anisotropic mismatch stresses. It is found that, in addition to the generic symmetry breaking, a bifurcation of surface patterns occurs in the range, $-(1-2\nu_s)^{-1} < c < -(1-2\nu_s)$, where $c = \sigma_2/\sigma_1$ is the ratio between the two principal

mismatch stresses and ν_s is the Poisson's ratio of the substrate. Figure 3 shows the simulated long-term pattern evolution for $c = -1$.

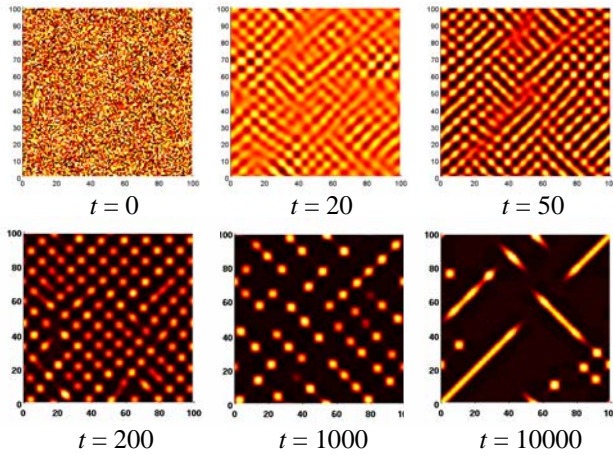


Fig. 3: Numerical simulation of surface pattern evolution under an anisotropic mismatch stress ($c = -1$).

Next, we consider elastically anisotropic films and substrates. The nonlinear stress field for a generally anisotropic epitaxial system is obtained by a Fourier method. To be specific, SiGe films on different Si surfaces are then considered. Figure 4 shows the contours of initial growth rate on Si (001), Si (111), Si (110), and Si (113). The maximum growth rate occurs at different locations (magnitudes and orientations of dominant wave vectors), predicting different patterns at the initial growth. For long-term evolution, numerical simulations show different spatial ordering of self-assembled quantum dots and lines (Fig. 5). It is concluded that the underlying crystal structure of the substrate tends to improve the spatial ordering of the patterns.

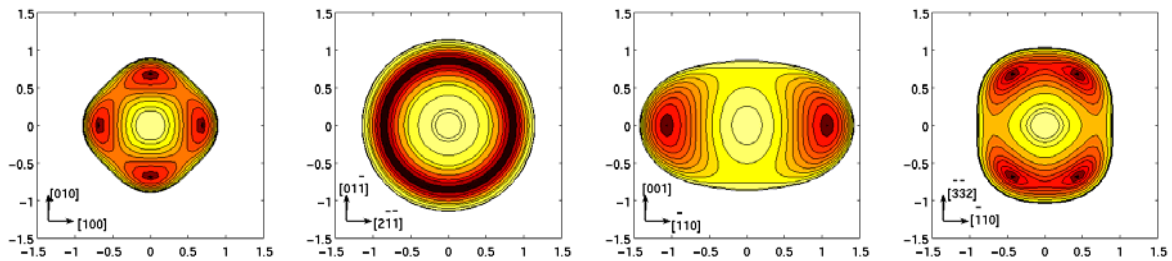


Fig. 4: Contour plots of the initial growth rate on various Si surfaces. From left to right: Si(001), Si(111), Si(110), and Si(113). Dark color indicates high growth rate.

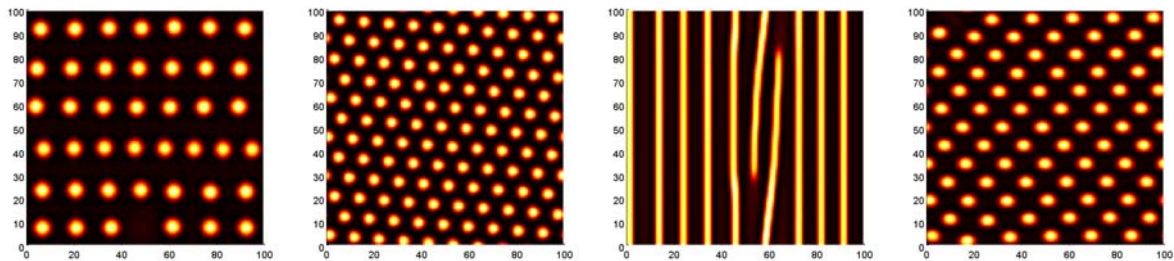


Fig. 5: Self-assembled surface patterns after long-term evolution on various Si surfaces. From left to right: Si(001), Si(111), Si(110), and Si(113).

III. Future Plans

The developed modeling approach will be extended in three directions for the future studies:

- ***Interplay of bulk and surface anisotropy.*** In addition to the elastic anisotropy in the bulk crystal, anisotropic surface energy and surface mobility will be incorporated. This will allow modeling and simulations of more realistic systems, to compare with experimental observations for validation of the model. In addition to the cubic systems (e.g., SiGe and GaAs), we will also investigate surface evolution of hexagonally structured epitaxial films (e.g., Pb and Er silicides), for which some interesting patterns (e.g., nanowires) have been observed experimentally [4,5].
- ***Strain engineering and directed self-assembly.*** Here, we will explore various strategies of strain engineering to achieve directed self-assembly and control the pattern uniformity as well as ordering. Modeling and simulations will be developed for strained substrates, e.g., by embedded stressors or by lithographically patterned surfaces. Furthermore, carbon-alloyed Si surfaces will be investigated as a potential template for nanoscale self-assembly.
- ***Volmer-Weber growth of quantum dots on dielectrics.*** Finally, we will investigate the growth of semiconductor and metal quantum dots on various dielectric substrates for potential applications in solid-state memory devices. Using the same wetting potential but with the surface energy for the film greater than that for the substrate, dewetting of the film will be simulated. Here, due to the lack of mismatch stress, elastic strain energy does not play a role. Instead, quantum confinement and contact potential induced electrostatic interactions may be included as additional energy terms [6,7] competing with surface energy and wetting potential during the evolution process.

IV. References

1. D. Granados and J.M. Garcia, Appl. Phys. Lett. 82, 2401 (2003).
2. J.L. Gray, R. Hull, and J.A. Floro, Appl. Phys. Lett. 81, 2445 (2002).
3. B.J. Spencer, Phys. Rev. B 59, 2011 (1999).
4. Y. Chen, et al., Appl. Phys. A : Mater. Sci. Process. 75, 353 (2002).
5. M. Hupalo and M.C. Tringides, Phys. Rev. B 73, 041405R (2006).
6. Z. Zhang, Q. Niu, C.K. Shih, Phys. Rev. Lett. 80, 5381-5384 (1998).
7. W. Lu and D. Salac, Phys. Rev. B 74, 073304 (2006).

V. Publications in the last two years

- Y. Pang and R. Huang, Nonlinear effect of stress and wetting on surface evolution in epitaxial thin films. Physical Review B 74, 075413 (2006).
- Y. Pang and R. Huang, Pattern evolution of self-assembled quantum dots under biaxial stresses. In: *Nanomanufacturing* (edited by F. Stellacci, J.W. Perry, G.S. Herman, and R.N. Das), Mater. Res. Soc. Symp. Proc., vol. 921E, 0921-T07-08. Warrendale, PA, 2006.
- Y. Pang and R. Huang, Bifurcation of surface pattern in epitaxial thin films under anisotropic stresses. J. Applied Physics 101, 023519 (2007).
- Y. Pang and R. Huang, Surface pattern evolution of epitaxial thin films on cubic crystal substrates. In preparation, April 2007.

Session III

Precision Nanoscale Synthesis

Session Chair: Michael Aziz, Harvard School of Engineering and Applied Sciences

Invited Speaker: Xiaogang Peng, University of Arkansas

This page is intentionally blank

Invited Speaker Presentation

Title: Controlled Synthesis of Colloidal Nanocrystals: From Size, Shape, Bandgap, to Doping

Author: Xiaogang Peng, Department of Chemistry, University of Arkansas

Abstract:

Colloidal nanocrystals are nanometer sized fragments of the corresponding bulk crystals, which can be readily manipulated as solution species. Their properties are often size/shape dependent due to their high surface area and quantum confinement. Synthetic chemistry for these interesting nanomaterials has been developed quite rapidly in the recent years, which makes a few promising applications close to be feasible. This talk will first discuss fundamental principles and synthetic design for size and shape control. Bandgap and composition engineered nanocrystals, as an active and new topic in the field, will also be discussed.

This page is intentionally blank

Synthesis and characterization of novel nanomaterials

S.S.Wong and J.A. Misewich

Department of Condensed Matter Physics and Materials, Science, Brookhaven National Laboratory, Upton NY 11973, USA

i) Program Scope

The potential for significant scientific and technological impact has led to enormous research in nanomaterials. However, most synthesis approaches lead to a diversity of structures and, unfortunately, key nanomaterial properties often sensitively depend on subtle structural differences. This program explores the synthesis and characterization of promising new nanomaterials and also attacks the diversity challenge in two ways: increasing our understanding of synthesis strategies for higher quality synthesis, and high sensitivity techniques to correlate structure and properties of individual nanomaterials (single nanotube or nanowires).

Synthesis research is led by Stanislaus Wong. This work has developed strategies that have allowed for purification, exfoliation, separation, and functionalization of carbon nanotubes. Of note are strategies for the synthesis of 1-d/0-d heterostructured nanotube-nanocrystal materials. This team has developed techniques for attaching quantum dots to nanotubes both through reactions with ligand molecules surrounding the quantum dots, and for directly growing quantum dots in-situ on the sidewalls of nanotubes. In addition, this team has led the development of new synthesis strategies (including solid state analogues) allowing for the production of nanostructured forms of a variety of perovskite oxides, including multiferroic materials.

Experiments in the characterization of nanomaterials are led by James Misewich (one of the PIs). This team has particular expertise in the study of individual nanowires and nanotubes, including transport measurements as well as optical properties. This single nanowire/nanotube approach eliminates the averaging common in ensemble measurements. Our goal is to combine the characterization of the properties of the individual nanowire/nanotube samples with characterization of the structure of the same individual nanowire/nanotube.

In addition to the single nanotube/nanowire approach, BNL is pursuing ensemble characterization techniques that can provide new information as well as feedback to the synthesis team for tuning of their synthesis strategies. One example is BNL's development of NEXAFS studies at the National Synchrotron Light Source (NSLS) for simultaneous studies of the oxygen nature and density in carbon nanotube samples under various conditions used for the removal of impurities.

The experimental work is coordinated with theoretical studies of the behavior of low dimensional materials that are being carried out by Alexei Tselvik. Tselvik has led in the development of the theory of correlation effects in nanomaterials. This includes research into understanding the mechanism of high temperature superconductivity and the role of dimensionality in perovskite oxide superconducting materials. This work also includes theoretical investigations to complement optical studies of carbon nanotubes, including the magnitude of electron-phonon coupling and the role of excitons.

ii) Recent Progress

Synthesis and characterization work continued on generating novel forms of perovskite nanostructures as well as extending our spectroscopic capabilities in studying the electronic structure and chemical composition of carbon nanotubes and one-dimensional, non-carbon nanomaterials.

1. Titanates / Titania Nanostructures

We have used the molten salt synthesis technique to prepare pristine BaTiO₃ nanowires with diameters ranging from 50 to 80 nm and an aspect ratio larger than 25, as well as single-crystalline SrTiO₃ nanocubes with a mean edge length of 80 nm. We found it to be a simple, readily scaleable (in terms of grams) solid-state reaction in the presence of NaCl and a nonionic surfactant. What determines the final shapes of these nanostruc-

tures may be the relative growth rates on the (100) vs. the (111) crystallographic planes, which in turn depends on the relative specific surface energies associated with the facets of the crystal.

Furthermore, this simple molten salt synthetic method recently has been extended to the preparation of a series of single-crystalline $\text{Ca}_{1-x}\text{Sr}_x\text{TiO}_3$ ($0 \leq x \leq 1$) nanoparticles. The composition of the resulting nanoparticles is reproducibly tunable by adjusting the ratio of the reactants. Shapes of the generated $\text{Ca}_{1-x}\text{Sr}_x\text{TiO}_3$ nanoparticles alter from cubes to quasi-spheres with decreasing 'x' values. Typical nanoparticles have sizes ranging between 70 and 110 nm, irrespective of the Sr or Ca content. As an example of the significance of this synthetic capability, the availability of nanosized $\text{Ca}_{0.7}\text{Sr}_{0.3}\text{TiO}_3$ particles may enhance the material's existing usage as an efficient dielectric barrier for the plasma-induced, catalyst-free decomposition of CO_2 .

We have also developed a general synthetic strategy aimed at the preparation of ordered structural motifs of anisotropic titanate and TiO_2 structures at the mesoscopic level through the mediation of an initial, modified template-free hydrothermal reaction followed by an in situ transformation process. These unique structures have been produced using a general redox strategy combined with a hydrothermal reaction involving titanium foil, a NaOH solution, and an oxidizing H_2O_2 solution. Typically, as-prepared 3-D assemblies of titania nanowires have an overall diameters ranging from 0.8 μm to 1.2 μm , while the interior of the aggregates are hollow with a diameter range of 100 to 200 nm, resembling the microscopic variant of a sea urchin with spines. Component anatase TiO_2 nanowires have a diameter range of 7 ± 2 nm and possess lengths of up to several hundred nm. The template-free synthesis of discrete hierarchical structures of nanowires reported is a simple, inexpensive, scalable, and mild synthetic process. We have also demonstrated that the micron scale assemblies of TiO_2 nanowires are active photocatalysts for the degradation of synthetic Procion Red dye under UV light illumination and can be expected to be incorporated as functional components of photonic devices and dye-sensitized solar cells.

As an extension of this study, we analyzed the size and shape dependence of a number of hydrothermally-prepared titanate nanostructure 'reagents' in controllably preparing anatase TiO_2 (titania) products by a reasonably mild hydrothermal process coupled with a dehydration reaction. Conceptually, this approach has implications for nanoscale design as well as for probing of morphology-dependent properties in nanomaterials. Specifically, protonic lepidocrocite titanate nanotubes (prepared at 120°C under hydrothermal conditions) with diameters of ~ 10 nm were transformed into exceptionally high-purity anatase nanoparticles with an average size of 12 nm. Lepidocrocite hydrogen titanate nanowires (prepared under hydrothermal conditions at 180°C) with relatively small diameters (average diameter range of ≤ 200 nm) were converted into single-crystalline anatase nanowires with relatively smooth surfaces. Larger diameter (>200 nm) titanate nanowires (similarly prepared under hydrothermal conditions at 180°C) were transformed into analogous anatase nanowire motifs, resembling clusters of adjoining anatase nanocrystals with perfectly parallel, oriented fringes. All three of these reactions generating anatase TiO_2 products involved an additional hydrothermal processing step involving the initial titanate precursor nanostructures at 170°C . Our results also indicated that our as-synthesized TiO_2 nanostructures possessed noticeably better photocatalytic activity as compared with their commercial counterparts, presumably due to an increase in surface area as well as a rise in anatase mass fraction and crystallinity.

2. *Synthesis, Characterization, and Photocatalytic Properties of Pyrochlore $\text{Bi}_2\text{Ti}_2\text{O}_7$ Nanotubes*

$\text{Bi}_2\text{Ti}_2\text{O}_7$ nanotubes have been synthesized by using a sol-gel technique in the presence of an alumina template. $\text{Bi}_2\text{Ti}_2\text{O}_7$ has attracted considerable attention as a useful component of (a) gate insulators in advanced metal-oxide semiconductor (MOS) transistors, (b) storage capacitors in dynamic random access memory (DRAM) applications, and (c) buffer layers to improve the electrical properties of ferroelectrics such as $\text{Pb}(\text{Zr}_{0.5}\text{Ti}_{0.5})\text{O}_3$ (PZT) and $\text{Bi}_4\text{Ti}_3\text{O}_{12}$. Outer diameters of as-prepared bismuth titanate nanotubes ranged from 180 to 330 nm; the wall thickness was approximately 6 nm. The effects of solvent as well as of precursor ratio were also analyzed, with data suggesting a high degree of parameter control over the dimensions and morphology of bismuth titanate nanotubes. Results confirmed the presence of a phase transformation from $\text{Bi}_2\text{Ti}_2\text{O}_7$ to $\text{Bi}_4\text{Ti}_3\text{O}_{12}$ upon increasing annealing temperature. Kinetic studies on the photocatalytic decolorization of methyl orange confirmed the higher photocatalytic efficiency of 1D nanoscale motifs of bismuth titanate as compared with the bulk sample.

3. Probing alignment in carbon nanotube systems

Probing surface order as well as the degree of structural modification in carbon nanotube systems is of fundamental importance for incorporation of these materials into practical functional devices. The current study pertained to the analysis of the surface order of vertically-aligned single-walled and multi-walled carbon nanotube arrays of varying length and composition by means of NEXAFS. Both NEXAFS and scanning electron microscopy (SEM) studies concluded that the nanotubes in these samples were oriented vertically to the plane of the surface. However, NEXAFS polarization analysis provided for a more quantitative and nuanced description of the surface structure, indicative of far less localized surface order, an observation partially attributed to misalignment and bending of the tubes. In fact, we could obtain quantitative information about order to an overall surface depth of ≈ 5 nm of various vertically aligned single-walled carbon nanotube (SWNT) and multiwalled carbon nanotube (MWNT) array systems using NEXAFS spectroscopy.

Specifically, we could simultaneously determine the comparative extent of surface functionalization and structural integrity across different array samples by monitoring the π^* transitions, measured at the magic angle of 55° . From this study, it was shown that disorder does not necessarily correlate with the extent of chemical functionalization. For instance, the predominantly SWNT array sample showed the lowest degree of surface order, but was the least surface functionalized or oxidized. From the data, it may be implied that the presence of MWNTs in the arrays actually created a more ordered or 'sturdier' array. It is practically necessary to understand both the extent of surface order as well as of chemical functionalization in carbon nanotube arrays so that these nanomaterials can be effectively incorporated and manipulated into future functional devices.

4. Simultaneous spectroscopy and structure of individual carbon nanotubes

The relationship between physical structure and properties lies at the heart of our understanding of materials. This relationship is particularly interesting in nanostructures where the large surface contribution to the total volume produces variations in structure and properties not observed in the bulk. SWNTs exemplify this characteristic of nanostructures. There are, for example, over 200 different structures of diameter less than 2 nm. The corresponding electronic and optical properties of the SWNTs depend sensitively on atomic structure, with distinctive energy-level structures corresponding to both metallic to semiconducting species. Both correct assignments of optical spectra to specific structures and a complete understanding the relationship between the physical and electronic properties of SWNTs are critical to progress in the study and application of these nanostructures. We have recently demonstrated the combination of high-sensitivity optical spectroscopy and electron diffraction to examine individual SWNTs.

Simultaneous application of these experimental techniques has permitted the measurement of *electronic transitions in nanotubes of fully and independently determined structure*. Figure 1 shows the determination of the structure via electron diffraction. Figure 2 shows spectra for nanotubes of characterized chiral vector. These data permit us to test directly the so-called family behavior of the transition energies of semiconducting nanotubes as a function of their precise atomic structure. Our verification of the validity of this prediction is important not only for fundamental understanding of the electronic properties of SWNTs, but because of its critical role in guiding spectroscopic assignments. We also observed, for the first time, splitting of

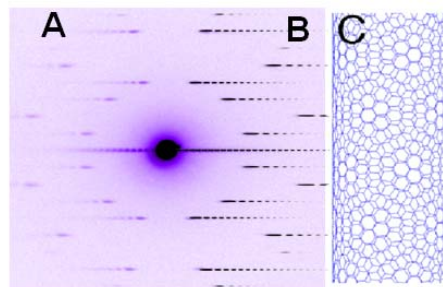


Fig. 1 A: Electron diffraction pattern from a single carbon nanotube B: (black) simulated diffraction pattern for (16,11) nanotube C: model of (16,11) nanotube. This nanotube sample therefore has a diameter of 1.83 nm and a chiral angle of 23.9 degrees.

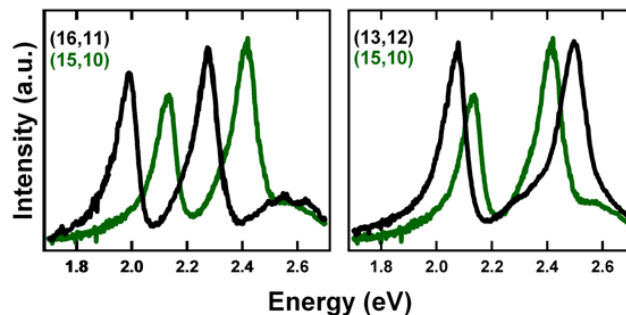


Fig. 2 Left: optical spectra for (16,11) (black) and (15,10) (green) CNTs. This shows the dependence on diameters since these nanotubes have similar chiral angle but differ in diameter by 0.12nm. Right: spectra for (13,12) (black) and (15,10) (green) CNTs. This shows the dependence on chiral angle since these have similar diameter but differ in chiral angle by 5.3 de-

optical transitions in metallic SWNTs. Both this result and family behavior, initially predicted from simple tight-binding zone-folding models, are found to survive in actual SWNTs despite the presence of curvature effects and strong multi-carrier interactions.

iii) Future Plans

We will focus our work on an exploration of the new materials first synthesized in our laboratory in which a quasi 1-d carbon nanotube (CNT) wire structure has been functionalized with semiconductor quantum dots (QD). Specifically we will determine: the efficiency of energy coupling between the localized excitation in the quantum dot and delocalized excitations in the quantum wire, the materials properties that control the energy coupling, optimization of the efficiency of electron hole separation/collection in the quantum wire, and the behavior of nanotube conductivity in the presence of quantum dots. To do this, we will synthesize quantum dots on single wall, double wall, and multiwall carbon nanotubes in order to study energy coupling between the quantum dot and various shells of the quantum wires. We will also develop strategies to control size and shape of quantum dots directly grown in-situ on CNT materials. We also will develop synthesis strategies to control the density of quantum dot functionalization and location of the quantum dot adducts in both classes of CNT-QD materials. We will characterize transport and optical properties of these nanomaterials and correlate these properties with the precise structure via the same combination of techniques that allowed us to simultaneously study the spectroscopy and structure of individual nanotubes.

v) Publications in 2006-2007

M.F. Sfeir, T. Beetz, F. Wang, L. Huang, X.M.H. Huang, M. Huang, J. Hone, S. O'Brien, J.A. Misewich, T.F. Heinz, L. Wu, Y. Zhu, and L.E. Brus, *Science* **312**, 554 (2006).

T. Hemraj-Benny, S. Banerjee, S. Sambasivan, D.A. Fischer, G. Eres, A.A. Puretzky, D.B. Geohegan, D.H. Lowndes, J.A. Misewich, and S.S. Wong, "Imperfect Surface Order and Functionalization in Vertical Carbon Nanotube Arrays Probed by Near Edge X-ray Absorption Fine Structure Spectroscopy (NEXAFS)", invited contribution, *Phys. Chem. Chem. Phys.*, **8(44)**, 5038-5044 (2006).

B.J. Panessa-Warren, J. Warren, S.S. Wong, and J.A. Misewich, "Biological cellular response to carbon nanoparticle toxicity", *J. Phys.: Condens. Matter*, **18**, S2185-S2201 (2006).

Y. Mao, M. Kanungo, T. Hemraj-Benny, and S.S. Wong, "Synthesis and Growth of Titanate and Titania One-Dimensional Nanostructures Self-Assembled into Hollow Micrometer-scale Spherical Aggregates", *J. Phys. Chem. B*, **110(2)**, 702-710 (2006).

T. Hemraj-Benny, S. Banerjee, S. Sambasivan, M. Balasubramanian, D.A. Fischer, G. Eres, A.A. Puretzky, D.B. Geohegan, D.H. Lowndes, W. Han, J.A. Misewich, and S.S. Wong, "Near-edge X-ray Absorption Fine Structure Spectroscopy as a Tool for Investigating Nanomaterials", *Small (Concepts Article)*, **2(1)**, 26-35 (2006).

V. Zorbias, M. Kanungo, S.A. Bains, Y. Mao, T. Hemraj-Benny, J.A. Misewich, and S.S. Wong, "Current-less Photoreactivity Catalyzed by Functionalized AFM Tips", *Chem. Commun.*, (36), 4598-4600 (2005).

S. Banerjee, T. Hemraj-Benny, S. Sambasivan, D.A. Fischer, J.A. Misewich, and S.S. Wong, "NEXAFS Investigations of Order in Carbon Nanotube-Based Systems", invited contribution (George W. Flynn's *Festschrift* issue). *J. Phys. Chem. B*, **109(17)**, 8489-8495 (2005).

T. Hemraj-Benny, S. Banerjee, S. Sambasivan, D.A. Fischer, W. Han, J.A. Misewich, and S.S. Wong, "Investigating the Structure of Boron Nitride Nanotubes by Near-Edge X-ray Absorption Fine Structure (NEXAFS) Spectroscopy", *Phys. Chem. Chem. Phys.*, **7(6)**, 1103-1106 (2005).

SUPERATOMS AND METAL-SEMICONDUCTOR MOTIFS FOR CLUSTER MATERIALS

A. W. Castleman, Jr.
Department of Chemistry, The Pennsylvania State University, University Park,
PA 16802

S. N. Khanna
Department of Physics, Virginia Commonwealth University, Richmond,
VA 23284-2000

Program Scope:

The physical and chemical properties of cluster systems at the sub-nano and nano-scale are often found to differ from those of the bulk and display a unique dependence on size, geometry and composition. Most interesting are systems which display properties that vary dramatically with the number of atoms and composition, rather than linearly scale with the size of the system. This realm of cluster science where “one atom makes a difference” is undergoing an explosive growth in activity, and the Castleman and Khanna groups are recognized as major pioneers in this area in which they have been active for many years. Interest in this field abounds for many reasons, one being the exciting prospects of using clusters as building blocks for tailoring the properties of new materials of nanoscale dimensions. In addition, quantum confinement effects often govern the behavior of matter of this size regime, and studying the reactivity and properties of clusters provides fundamental insights into the interplay of structure, geometry and electronic properties and the chemical behavior that can be manipulated.

One of the major objectives of the research is to identify classes of clusters with motifs that display the stability requisite for implementation as building blocks and the preservation of electronic and magnetic properties upon growth within this motif. Associated with this possibility is the question of the novelty in properties that such nanoscale systems could offer.

Recent Progress:

The past year has been very productive and we have made substantial advances in our focus toward developing a 3-D periodic table using clusters to mimic the properties of individual elements. In past work we demonstrated that in gas phase clusters containing aluminum and iodine atoms, an Al_{13} cluster behaves like a halogen atom while an Al_{14} cluster exhibits properties analogous to an alkaline earth atom. These observations, together with our findings that Al_{13}^- is inert like a rare gas atom, have reinforced the idea that chosen clusters can exhibit chemical behaviors reminiscent of atoms in the periodic table, offering the exciting prospect of a new dimension of the periodic table formed by cluster elements, called superatoms. As the behavior of clusters can be controlled by size and composition, the superatoms offer the potential to create unique compounds with tailored properties. In a paper published in PNAS (November 2006) we provide findings of a new class of superatoms namely Al_7^- , that exhibit multiple valences, like some of the elements in the periodic table, and hence have the potential to form more stable compounds when combined with other atoms. The new findings support the contention that there should be no limitation in finding clusters which mimic virtually all

members of the periodic table. This finding has been of considerable interest to the scientific community and has been the subject of a news article in C&EN (November 27, 2006 page 9) and in Nature Materials (December 15, 2006).

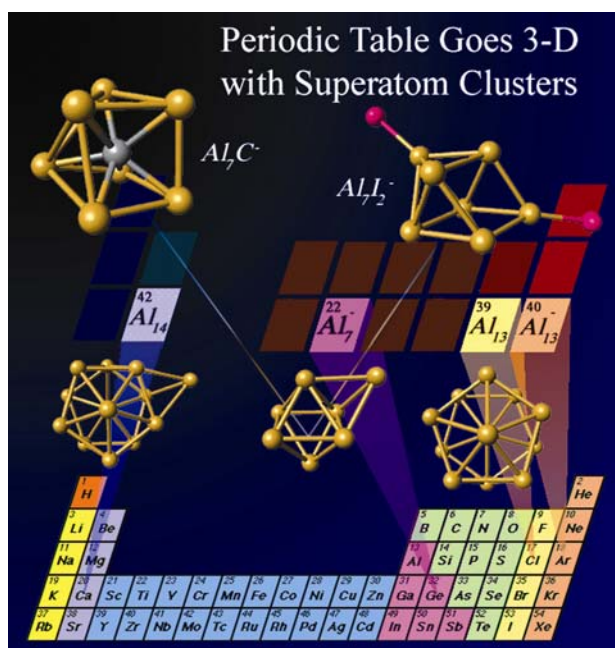


Fig. 1. Al_{13} , Al_{13}^- , Al_{14} and Al_7^- clusters forming a third dimension of the periodic table and resembling the chemical characteristics of the atoms in the conventional periodic chart.

At this point, a key issue is whether such simple electronic counting rules and shell filling can be used to describe the stability of other members of the second row of the periodic table. Because the confined free electron gas exhibits shell closing at 18 and 20 electrons, the above arguments would suggest that Al_7M^- clusters should exhibit enhanced stability for cases where the M atom would require two or four electrons to fill the deep p-bonding orbitals.

Hence it was interesting to inquire as to whether the above considerations could be extended to other elements. In particular, a question arose about whether one could use the above model to understand the bonding of Al_7^- to other elements in the second, third, and fourth row of the periodic table. To this end, we have calculated the binding energy of all of the atoms in the second, third, and fourth rows with and found that the concept holds in all cases. In addition to the binding energy, we examined the variation of the HOMO–LUMO gap. Significantly, the HOMO–LUMO gap follows the stability trend, indicating a chemical inertness.

Work also continued on other element mimic clusters. In particular, the electronic structure, stability, and reactivity of iodized aluminium clusters, which has been investigated via reactivity studies, were examined by first principles gradient corrected density functional calculations. The observed behavior of $Al_{13}I_x^-$ and $Al_{14}I_x^-$ clusters is shown to indicate that for $x \neq 8$, they consist of compact Al_{13}^- and Al_{14}^{++} cores, respectively, demonstrating that they behave as halogen- or alkaline earth-like superatoms. For $x > 8$, the Al cores assume a cage-like structure associated with the charging of the cores. The observed mass spectra of the reacted clusters reveal that $Al_{13}I_x^-$ species are more stable for even x while $Al_{14}I_x^-$ exhibit enhanced stability for odd x ($x \neq 3$). It is shown that these observations are linked to the formation and filling of “active sites”, demonstrating a novel chemistry of superatoms. Experimentally, the reactions with methyl alcohol and methyl iodide show behavior similar to that expected for alkaline earth metals.

In addition to metallic clusters, we have extended our investigations to metal- semiconductor systems to identify the basic rules that govern the stability of these classes of clusters. Through first principles electronic structure calculations we have examined the stability of cationic, neutral, and anionic MSi_{15} , MSi_{16} , and MSi_{17} ($M=Sc, Ti, \text{ and } V$) clusters. $ScSi_{16}^-$, $TiSi_{16}$, and VSi_{16}^+ were found to be particularly stable in agreement with recent experiments. It is shown that the enhanced stability can be reconciled within a model where each Si atom coordinated to the metal contributes one electron to the valence pool. Clusters where the total number of valence electrons obtained by summing one electron from each Si site coordinated to metal atom and the valence electrons of the metal attain 20 are found to be particularly stable. Combined with the earlier reported stability at 18 electrons, it is proposed that such valence pools might be looked upon as a nearly free electron gas inside a silicon cage.

Research Plans for 2007:

As detailed in the original proposal, our continuing program will comprise a combined experimental and theoretical effort to provide a fundamental understanding of the geometrical arrangements, electronic structure, reactivity, and excitation and relaxation dynamics of intermetallic, metal compound, and semiconductor-metal clusters. The next phase of our work will encompass investigating how widely the concept of the Jellium model can be extended. Even though we have seen a number of cases where the simple Jellium model does account for the reactive behavior and stability of various clusters, even we are surprised that it is such a valuable guiding principle for systems comprised of non-metallic component atoms such as carbon and nitrogen. In view of these findings, being supported by first principles electronic structure calculations, we intend to explore a broad range of metal atoms to establish a basis for elucidating those that bond in ways that the Jellium concept provides an appropriate description. In assessing the applicability of these concepts for treating intermetallics, as detailed in our proposal we plan to next devote attention to mixed clusters comprised of selected atoms from several groups of the periodic table such as Mg, Fe, Pd, Pt, V, Ti and Ni, in combination with Al, to further explore our confirming ideas concerning the formation of superatom analogues to elements of the periodic table including those which display mixed valence. We will give particular effort to exploiting the mixed valence concept if it proves to be a general phenomena. Subsequently, efforts will be devoted to combinations with Ag, Au and Cu to determine if these “good metals” can be employed as building blocks in a similar manner to clusters involving aluminum.

In addition, we wish investigate another classes of stable motifs, namely metal clusters passivated by hydrogen atoms. As a first example, we plan to investigate aluminum hydrogen systems because of their applications in hydrogen storage devices. Can one create new metal hydrides, using clusters as the building motifs, that have better hydrogen uptake and release parameters compared to the known alanates? Can these lead to novel high energy materials?

Publications:

“Reactions of Al_nIx^- with methyl iodide: the enhanced stability of Al_7I^- and the chemical significance of active centers”, D. E. Bergeron, P. J. Roach, A. W. Castleman, Jr., N. O. Jones, S. N. Khanna, *J. Am. Chem. Soc.* **127**, 16048-16053 (2005).

“Association of C₃H₆ to Aluminum Cluster Anions”, D. E. Bergeron, A. W. Castleman, Jr., N. O. Jones, S. N. Khanna, *Chemical Physics Letter*, **415**, 230-233, (2005).

“Structural, Electronic, and Chemical Properties of Multiply Iodized Aluminum Clusters”, N. O. Jones, S. N. Khanna, D. E. Bergeron, P. J. Roach, and A. W. Castleman, Jr., *Journal of Chemical Physics*, **124**, 154311 (2006).

“Electronic counting rules for the stability of metal-silicon clusters” J. U. Reveles and S. N. Khanna, *Phys. Rev. B* **74**, 035435 (2006).

“Clusters – A Bridge Across Disciplines”, A. W. Castleman, Jr. and P. Jena, *PNAS* – (Invited perspective on the cluster field)- *PNAS*, **103**, 28, 2006.

“Multiple Valence Superatoms”, J. Ulises Reveles, S. N. Khanna, P. J. Roach, and A. W. Castleman, Jr., *PNAS*, **103**, 2006.

“Silicon Oxide Nanoparticles Reveal the Origin of Silicate Grains in Circumstellar Environments”, A. C. Reber, P. A. Clayborne, J. U. Reveles, S. N. Khanna, A. W. Castleman, Jr., A. Ali, *Nanoletters*, **6**, 1190-1195 (2006).

“Clusters – A Bridge Across Disciplines: Physics and Chemistry”, P. Jena and A. W. Castleman, Jr., *PNAS*, **103**, 28, 2006.

“Clusters – A Bridge Across Disciplines: Environment, Materials Science, and Biology”, A. W. Castleman, Jr. and P. Jena, *PNAS*, **103**, 28, 2006.

“Anion Photoelectron Spectroscopy and Density Functional Investigation of Vanadium Carbide Clusters”, K. L. Knappenberger, Jr., C. E. Jones, Jr., M. A. Sonhy, I. Jordanov, J. Sofo, and A. W. Castleman, Jr., *J. Phys. Chem A*, **110**, 12814-12821 (2006).

“Cobalt doped rings and cages of ZnO clusters: Motifs for magnetic cluster-assembled materials”, A. C. Reber, S. N. Khanna, J. S. Hunjan, and M. Beltran, *Chem. Phys. Lett.* **428**, 376 (2006).

“Influence of Charge State on the Reaction of FeO₃^{+/-} with Carbon Monoxide”, N. M. Reilly, J. U. Reveles, G. E. Johnson, S. N. Khanna, and A. W. Castleman, Jr., *Chemical Physics Letters* (in press).

“Recent Advances in Cluster Science”, A. Welford Castleman, Jr., Proceedings for the Advances in Mass Spectrometry for the 17th IMSC (in press).

“Superatoms: Building Blocks of New Materials”, A. W. Castleman, Jr. and S. N. Khanna, *The Chemical Physics of Solid Surfaces; Volume 12 Atomic Clusters: From Gas Phase to Deposited*, Publishers; Elsevier, Editor: Phil Woodruff (in press).

Publicity

“Beyond the Periodic Table”, C&EN article referencing our research (November 27, 2006, page 9)

“Two-faced superatoms”, *Nature Materials* (December 15, 2006)

Material science and physics at a nanoscale

Judy Wu

University of Kansas

The **scope** of this project is to study one-dimensional nanostructures of semiconductors and superconductors, which have been regarded as promising building blocks for nanoelectronic and nanoelectric devices. The emphasis of this project is on fabrication of the one-dimensional nanostructures, particularly into 3D nano-architectures in self-assembly manner, and investigation of their physical properties as function of various relevant parameters.

Recent progress is summarized in the following. On semiconductor nanostructures, we have developed a two-liquid vapor-liquid-solid process to grow inclined boron nanowire bundles, which led to achievement of fused nanowire junction arrays on Si substrates. On the other hand, we have developed a hydrogen-facilitated rapid solidification process for fabrication of metal/semiconductor coaxial cables directly on semiconductor nanowires. On superconductor nanowires, we have employed electron-beam lithography for generating the high temperature superconducting nanowires. Electric transport characterization of these samples is under way. The details of the recent progress in these two aspects are described in the following.

Semiconductor nanostructures

(1) Fused Nanowire Y-junctions—In this work, we demonstrate that boron nanowire Y-junctions can be synthesized in a self-assembled manner by fusing two individual boron nanowires grown inclined towards each other. We show the presence of a second liquid, in addition to the liquid Au catalyst, is critical to the inclination of the boron nanowire. The structure of the BNYJ arrays that we report here may allow construction of three or multiple-terminal nanowire devices directly on Si-based readout circuits through controlled nanowire growth.

(2) Metal/semiconductor coaxial cables—Metal(core)/semiconductor(shell) coaxial nanocables are promising building blocks for various nanoelectronic devices while *in situ* growth of these nanocables is challenging because of distinctly different synthesis temperature ranges required for metals and semiconductors. To overcome this difficulty, we have developed a hydrogen-facilitated rapid quench process that can be applied to a metal-semiconductor eutectic droplet formed in the standard Vapor-Liquid-Solid (VLS) process to initiate metal/semiconductor nanocable growth. The temperature gradient across the eutectic droplets was found critical in this process. With demonstration of gold/boron nanocables, this method may also be applied to a large variety of metal/semiconductor coaxial nanostructures. In addition, the compatibility of this method with the VLS process allows *in situ* connection of semiconductor nanowires (or nanotubes) with metal/semiconductor nanocables.

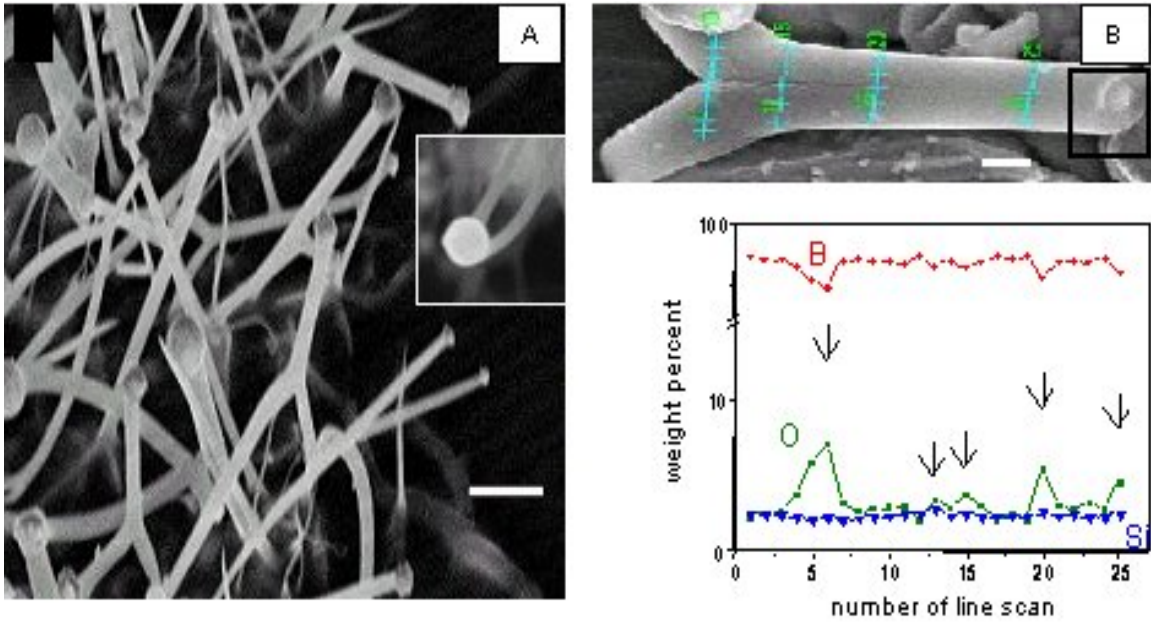


Figure 1 (A) SEM image of BNYJs grown on silicon substrate coated with 10 nm thick gold film. Scale bar: 1 μm . A mixture of pure boron and boron oxide was used as vapor source. Inset: fusing point of two bottom BNW stems. (B) Elemental EDS line scans across a BNYJ removed from the substrate. O peaks were detected on the wall and at the merging point of two bottom stems (Ref. 3). Scale bar: 50 nm.

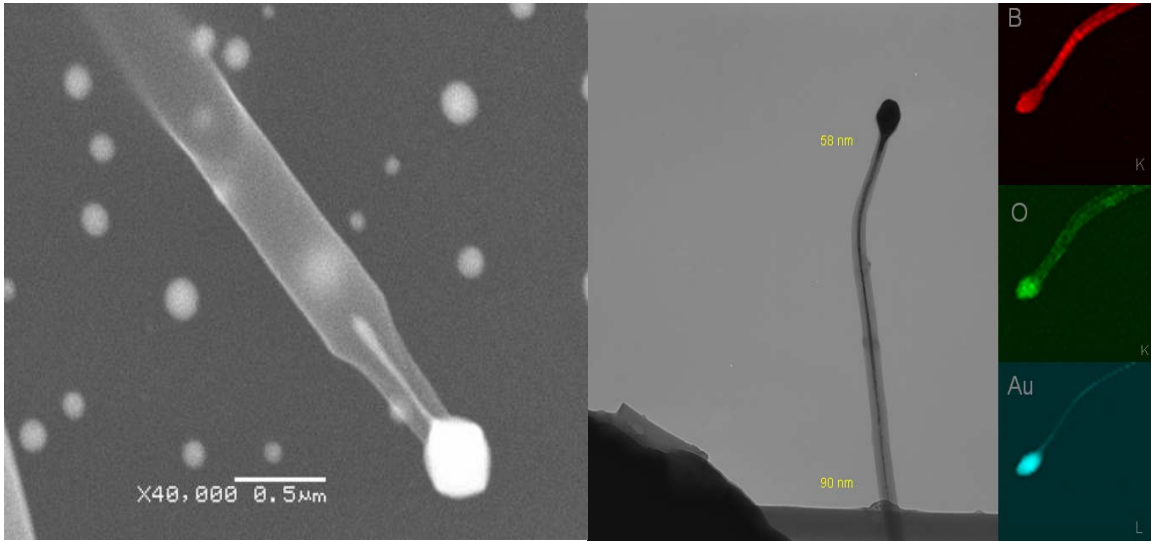


Figure 2. Left panel: SEM image of a gold/boron cable connected to a boron nanowire. Right panel: TEM image of an isolated single gold-boron nanocable and EDS mapping of elements boron, oxygen and gold on it (Ref 1).

Superconducting nanostructures

Superconductivity can be greatly influenced by the dimensionality. For example, magnetic vortices cannot form inside the superconductor when its dimension is smaller than the magnetic penetration depth λ . For $\text{YBa}_2\text{Cu}_3\text{O}_7$, λ is on the order of 300 nm at 77K and decrease to less than 100 nm at 5 K. When magnetic vortices are formed in superconductors, their motion generates dissipation and therefore reduces the super-current. A fundamental issue related to the current carrying capability of high temperature superconductor, which has been commercialized for electric power applications, is that the best critical current density J_c achieved is still an order of magnitude lower than the theoretical depairing J_c . Resolving this issue is of importance not only to basic science, but also to commercialization of superconductor devices. The following figure (Figure 3) shows the images of a four-bridge circuit we have made on a $\text{YBa}_2\text{Cu}_3\text{O}_7$ thin film with bridge width varying from above to much below λ . Electrical transport characterization is ongoing on our superconducting magnet system.

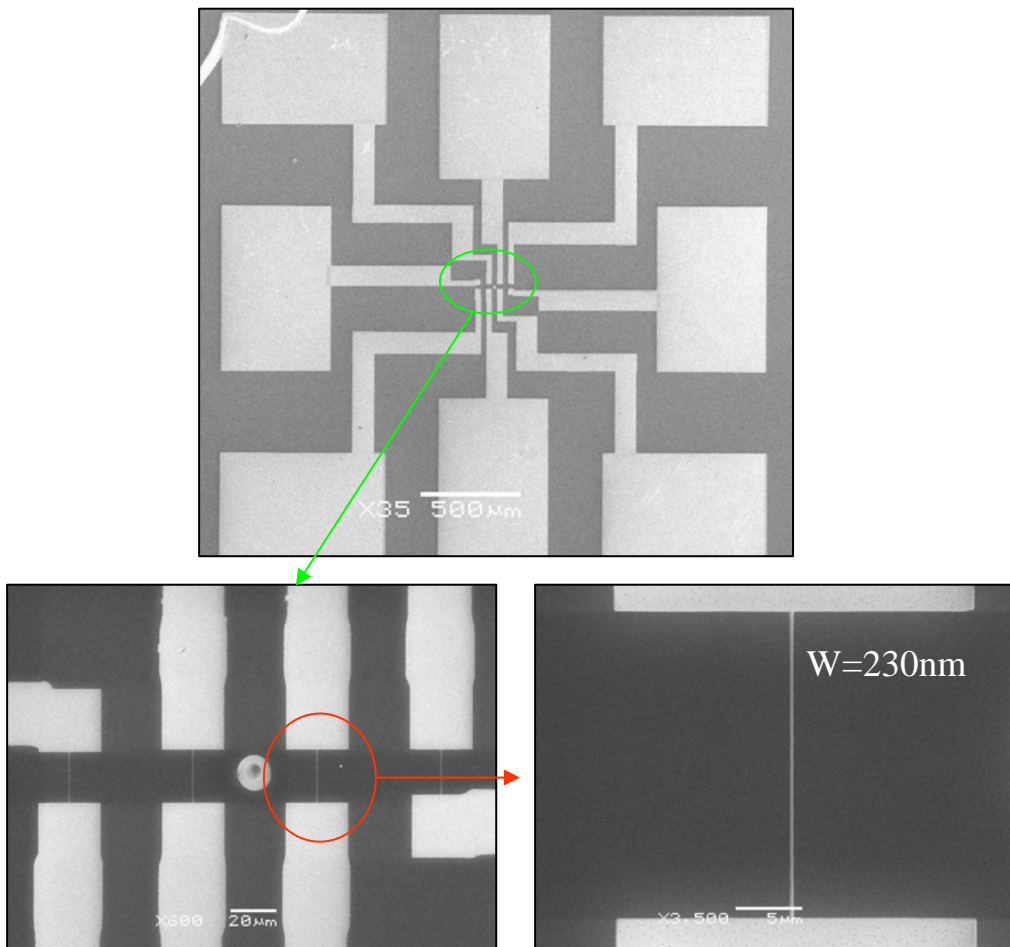


Figure 3. SEM images of a four-bridge circuit on an $\text{YBa}_2\text{Cu}_3\text{O}_7$ film with the bridge width varying from above to much below λ . Top panel: overall circuit on a $3.5 \times 3.5 \text{ mm}^2$ film. Lower left panel: blowup view of the four bridges and lower right panel: a bridge of 230 nm width.

Future plan will mostly continue our current effort. In addition, we will investigate transport properties carbon nanotube networks.

Publications in the last 1.5 years (our project began in August 2005):

1. J.Z. Wu, X. Wang, R. Emergo, and A. Dibos, “Growing nanotubes in superconducting YBCO films”, submitted.
2. Z.Z. Li and J.Z. Wu, “Gold/Boron coaxial nanocables synthesized using rapid quench of eutectic droplets” , submitted.
3. Sang H. Yun, Judy Z. Wu, Alan Dibos, and Xiaodong Zou, “Fused boron nanowire Y-junction arrays”, *Nano Letters* **6**, 385(2006).
4. Z.W. Xing, H. Zhao and J.Z. Wu, “Reversible exchange of Tl and Hg cations on superconducting “1212” lattice”, *Advanced Materials* **96**, 2136 (2006)
5. S.H. Yun, A. Dibos, X. Gao, J.Z. Wu and U.O. Karlsson, “Growth of inclined boron nanowire bundles in an oxide-assisted vapor-liquid-solid process”, *Appl. Phys. Lett.* **87**, 113109 (2005).

From New Kinetic Barrier to Nanorods Design

Hanchen Huang, Rensselaer Polytechnic Institute, Troy, New York

The scope of this program covers the scientific principles of (1) diffusion between surface facets for various crystalline structures, and (2) design and fabrication of nanorods by understanding and controlling the diffusion.

Recent progresses are over the entire scope of this program. The following presentation of progresses, however, will only briefly describe the diffusion investigations and focus on the design and fabrication of nanorods.

In the diffusion investigation, we have examined face-centered-cubic (FCC) Cu and body-centered-cubic (BCC) W, using density-functional-theory based ab initio and embedded-atom-method based molecular mechanics calculations. The ab initio calculations have served as validation and provided additional information on electronic structures surrounding a diffusing

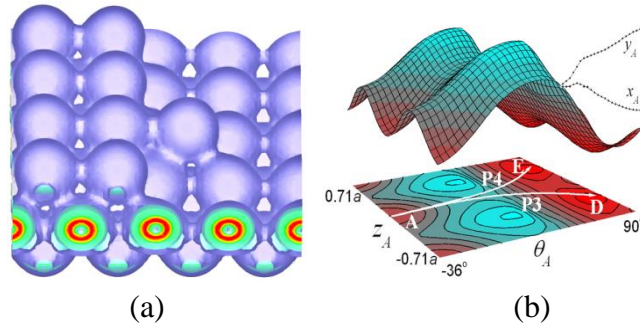


Figure 1: Illustration of simulation methods for diffusion studies: (a) Electronic structure surrounding a diffusing atom, and (b) energy as a function of two diffusion coordinates.

atom. Figure 1a shows the electron re-distribution surrounding a diffusion atom, and Figure 1b a typical energy surface along the diffusion path. Backed up by the validations of ab initio results, molecular mechanics calculations have revealed three new features. First, there is a transition – the three-dimensional Ehrlich-Schwoebel (3D ES) barrier usually increases with step thickness and it can also decrease as step thickness goes up. Second, the 3D ES barrier of individual atoms also dictates the diffusion of clusters on FCC surfaces. Finally, the 3D ES barrier is highly sensitive to the orientation of crystalline steps: it is much smaller over $\langle 112 \rangle$ than over $\langle 110 \rangle$ ridges in FCC crystals, for example.

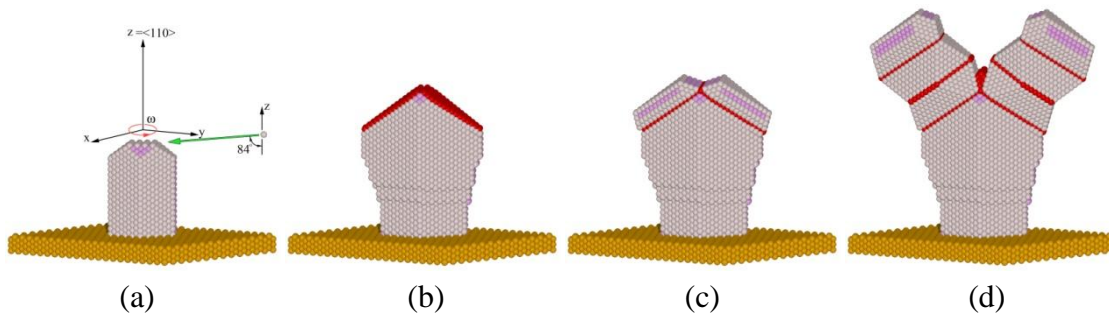


Figure 2: Schematic of a new concept: science-based design of Y-shaped nanorods.

Based on the diffusion investigations, our efforts have led to *science-based design and fabrication* of nanorods. The starting point is a discovery from the diffusion investigation – the large magnitude diffusion barrier separating two neighboring facets, as briefly described in the previous paragraph. The second step is the integration of this discovery with two other pieces of science – geometrical shadowing and twin formation during processing, which have been patented by a Canadian group [1] and documented in standard textbook [2]. It is this integration of new discovery with existing knowledge that has led to the science-based design and fabrication of nanorods. The conceptual integration and design are demonstrated in Figure 2. As shown in Figure 2a, the $\langle 110 \rangle$ nanorods covered with low energy surfaces such as $\{111\}$ are common for FCC metals [3]. Under glancing angle deposition [1] at reasonably low temperatures, atoms deposited on $\{111\}$ are retained because of the large 3D ES barrier. During growth, atoms have finite probabilities, as defined by stacking fault formation energy, to pack according hexagonal-close-packed (HCP) structure, as shown in Figure 2b. This HCP layer becomes a twin boundary if subsequent layers return to FCC packing, which is thermodynamically preferable. When the two twin boundaries meet, their interface is a high-energy $\Sigma 9$ grain boundary, which is thermodynamically non-preferable for deposited atoms and drives them away from it, leading to bifurcation as shown in Figure 3c. Due to the large 3D ES barrier, atoms deposited on top of bifurcated branches stay on top; further enhancing the bifurcation. As deposition proceeds further, a Y-shaped nanorod forms by self-assembly that is controlled by 3D ES barrier, geometrical shadowing, and twin formation.

Based on this conceptual integration and design, we have carried out molecular dynamics simulations. As shown in Figure 3a, the simulations incorporating all details of atomic vibration and diffusion confirm the design in Figure 2. Subsequently, a magnetron sputtering deposition experiment provides the final validation, as shown in Figure 3b.

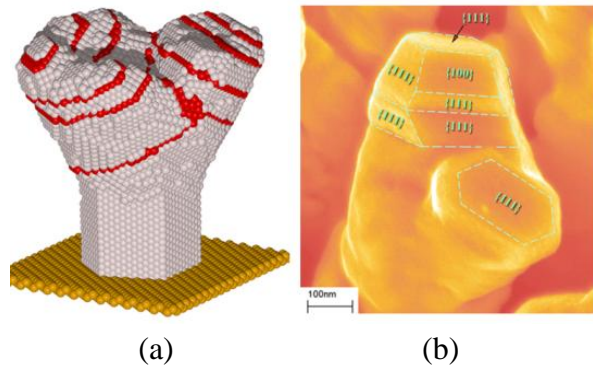


Figure 3: (a) Simulation and (b) experimental results of Y-shaped nanorod.

Future plans of this program, based on the progresses so far and on extra explorations, have two components. The first component is the completion of proposed studies. Specifically, we have studied FCC and BCC structures, and will complete the study of body-centered-tetragonal (BCT) In, in terms of the 3D ES barrier and its impacts on design and fabrication. Our experimental studies have revealed the formation of straight and faceted In nanorods, indicating dominant effects of the 3D ES barrier, and

the proposed atomistic simulations will lead from indication to understanding (and hopefully to science-based design again). The second component is the exploration of diffusion at solid-liquid interfaces; in contrast, our original program focuses on solid-vapor interfaces. This exploration is motivated by the fact that nanowires predominantly grow by vapor-liquid-solid mechanism [4] (while vapor-solid-solid mechanism [5] has also been brought up as an alternative). So far, many exotic nanowires have been fabricated, primarily based on empirical approaches. The controlling kinetics (diffusion and reaction) and thermodynamics at the solid-liquid interfaces remain largely untouched. Our recent explorations, molecular dynamics simulations and fabrication experiments [6], have indicated that the mass transport at solid-liquid interfaces is much easier than that at solid-vapor interfaces. These rewarding explorations will continue while ensuring the successful completion of the original program.

References (excluding those listed as PI's publications)

1. K. Robbie, M. J. Brett, A. Lakhtakia, **Nature** 384 (1996) 616; K. Robbie, and M. J. Brett, **U. S. Patent** No. 5 866 204 (1999).
2. W. D. Callister, Jr., **Materials Science and Engineering: An Introduction**, 5th Edition, John Wiley & Sons, Inc., New York. P80.
3. H. L. Wei, Hanchen Huang, C. H. Woo, R. K. Zheng, G. H. Wen, and X. X. Zhang, **Applied Physics Letters** 80 (2002) 2290-2292.
4. R. S. Wagner and W. C. Ellis, **Applied Physics Letters** 4 (1964) 89.
5. I. Persson, M. W. Larsson, S. Stenstrom, B. J. Ohlsson, L. Samuelson, and L. R. Wallenberg, **Nature Materials** 3 (2004) 677-681.
6. L. G. Zhou and Hanchen Huang, simulation results being prepared for publication; H. W. Shim and Hanchen Huang, experimental results being prepared for publication.

Publications in last two years (early 2005 – early 2007):

- **Journal papers and handbook section (conference papers not included)**
1. Hanchen Huang, *Texture Evolution During Thin Film Deposition*, in **Handbook of Materials Modeling**, Springer Science and Business Media, 2005.
 2. Jian Wang, Hanchen Huang, S. V. Kesapragada, and Daniel Gall, “Growth of Y-shaped Nanorods through Physical Vapor Deposition”, **Nano Letters** 5, 2505-2508 (2005).
 3. A. M. Coronado and Hanchen Huang, “Facet-facet Barrier on Cu{111} Surfaces for Cu Dimers”, **Computer Modeling in Engineering and Science** 10, 39-44 (2005).

4. H. L. Wei, L. Zhang, Z. L. Liu, Hanchen Huang, and X. X. Zhang, "Spontaneous Growth of Indium Nanostructures", **Journal of Crystal Growth** 297, 300-305 (2006).
5. Hanchen Huang, "Fabrication and Mechanics of Nanorods", an invited paper, **Reviews on Advanced Materials Science** 13, 41-46 (2006).
6. L. X. Zhang and Hanchen Huang, "Size-dependent Elastic Moduli of ZnO Nanoplates", **Applied Physics Letters** 89, 183111-1-3 (2006).
7. Z. Xu, L. G. Zhou, Jian Wang, T. S. Cale, and Hanchen Huang, "Three-dimensional Ehrlich-Schwoebel Barriers of W", **Computers, Materials, & Continua** 5, 43-48 (2006).
8. H. W. Shim and Hanchen Huang, "Three-stage Transition during SiC Nanowires Growth", **Applied Physics Letters** 90, 83106-1-3 (2007); *also selected for Virtual Journal of Nanoscale Science & Technology Volume 15, Issue 9*.
9. J. C. Flores, B. H. Aguilar, A. M. Coronado, Hanchen Huang, "Double Rotation Mechanism in Small Cu Clusters Concerted Diffusion over Cu{111} Surfaces", **Surface Science** 601, 931-935 (2007).
10. L. X. Zhang and Hanchen Huang, "Structural Transformation of ZnO Nanostructures", **Applied Physics Letters** 90, 23115-1-3 (2007); *also selected for Virtual Journal of Nanoscale Science & Technology Volume 15, Issue 4*.

Edited volumes

1. **Kinetics-driven Nanopatterning on Surfaces** (MRS, 2004/2005); co-edited (by Hanchen Huang) with Eric Chason of Brown University, George Gilmer of Lawrence Livermore National Lab, and Enge Wang of Chinese Academy of Sciences.
2. **Mechanics of Nanoscale Materials and Devices** (MRS, 2006/2007); co-edited (by Hanchen Huang) with Amit Misra of Los Alamos National Lab, John Sullivan of Sandia National Labs, and Syed Asif of Hystron.
3. *Advances in Computational Study of Nanostructures* as a special issue of **Computer Methods in Applied Mechanics and Engineering** (2006/2007); co-edited (by Hanchen Huang) with Harold Park of Vanderbilt University, Eliot Fang of Sandia National Labs, and Jacob Fish of Rensselaer.

Program Scope

This research is focused on understanding mechanisms that control the synthesis of nanostructured material systems. Specifically, our primary focus is on catalytic synthesis of carbon nanostructures and the synthesis of magnetic alloy nanoparticles encapsulated within these carbon nanostructures. The process of formation and evolution of this carbon-catalyst system involves dynamical reciprocal influences of both components resulting in the intertwined controlled co-synthesis of two nanostructured materials with complementary functions. In this work we investigate (1) the role of the catalyst material composition, crystallographic orientation, and shape on the atomic structure of the resulting carbon nanofibers; (2) links between the macroscopic parameters of plasma enhanced chemical vapor deposition reactor environments and the atomic scale processes at the catalyst nanoparticles; and (3) the influence of the curved graphitic structure on the evolution of the shape and structure of the catalyst nanoparticle. A second connected theme of this research is to gain insight on the magnetic properties of the catalytic nanoparticles and the formation of ordered alloys during and after co-synthesis and after post-synthesis annealing. The magnetic characteristics of nanoparticles can be tuned within this growth process, and the catalyst nanoparticles encapsulated within the carbon nanostructures reside within a unique nanoscale environment for the study of the behavior of confined magnetic alloys. The fundamental understanding of this co-synthesis process makes the precise control of synthesis and assembly of magnetic nanoparticles, carbon nanostructures, and their bi-functional combination possible.

Recent progress

The intimate link between structure and function that is inherent in all materials is even stronger in nanoscale materials, and as a result, the control of synthesis results in the control of function. Toward this goal of

control, we demonstrated that the internal structure of carbon nanofibers (CNFs) is strongly influenced by catalyst preparation and ultimately defined by growth conditions. We have found that when the growth rate is increased by 100-fold, obtained through maximized pressure, plasma power and temperature, the resulting nanofibers have an internal structure approaching that of multi-walled nanotubes. We showed that the deliberate modulation of growth parameters results in the modulation of CNF internal structure, and this property has been used to control the CNF surface along its length for site specific chemistry and electrochemistry (Fig. 1). This work demonstrated the intricate relationship between the growing carbon nanostructure and the malleable, almost fluid nanoparticle (Helveg 2004). The interaction occurs at the interface between a catalyst nanoparticle and a carbon nanofiber (CN-CNF). Thus understanding the physics of this interface is key for controlling nanofiber structure and nanoparticle shape during synthesis.

In our theoretical efforts we developed a phenomenological model that describes the CN-CNF interface. The model is based on fundamental assumptions of anisotropy of the growth rates for a graphitic structure as a function of the curvature and allows prediction of the shape of the CN-CNF interface. We explored the physical solution space of the model both numerically and in asymptotic approximations and discovered an intrinsic instability of a solution for a curved graphite-particle interface near the nanofiber center. In agreement with this prediction, with certain growth conditions we experimentally observed a central cavity in the nanofiber structure. While the model allows prediction of the observed nanofiber structure it relies on some assumptions that need to be confirmed by experimental observations or atomistic level calculations.

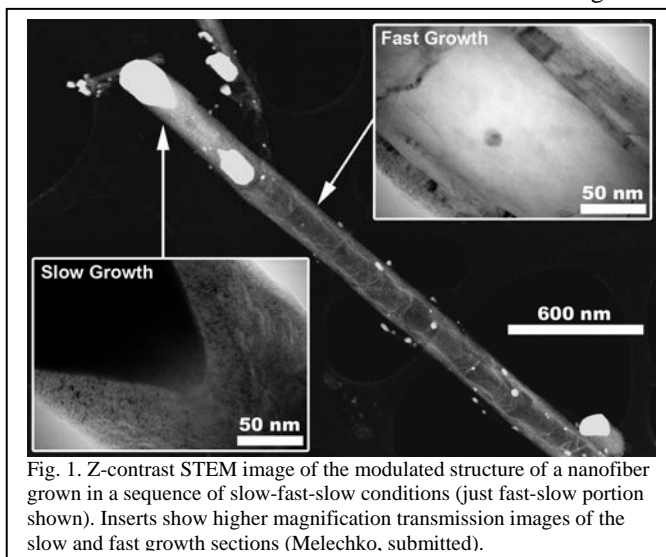
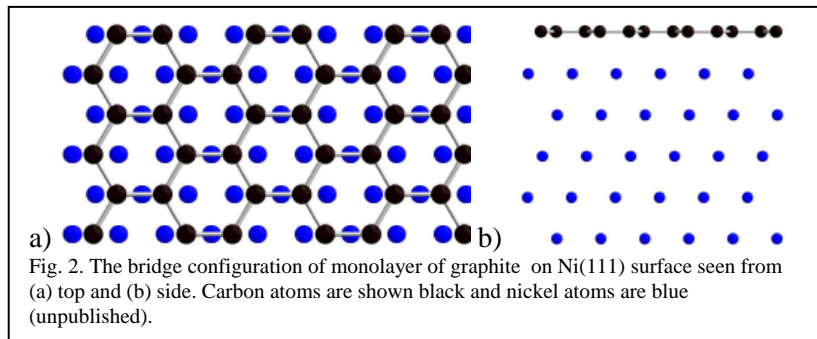
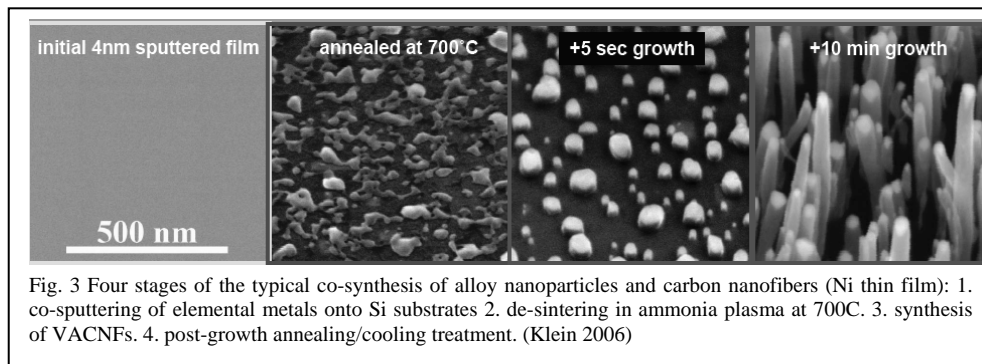


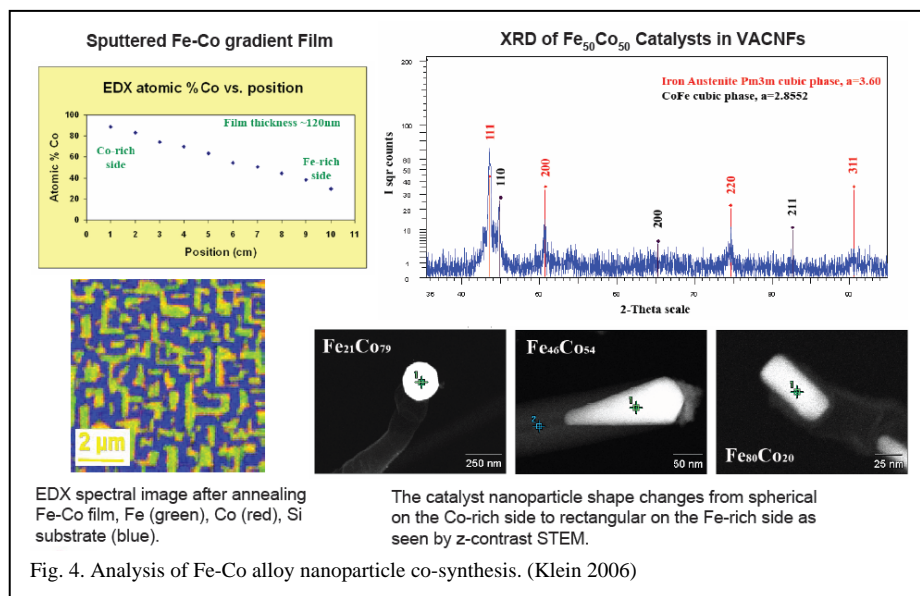
Fig. 1. Z-contrast STEM image of the modulated structure of a nanofiber grown in a sequence of slow-fast-slow conditions (just fast-slow portion shown). Inserts show higher magnification transmission images of the slow and fast growth sections (Melechko, submitted).



configuration of a graphitic overlayer on a clean Ni(111) surface. We found that the DFT results vary significantly depending on the expression chosen to approximate the exchange-correlation potential. However, the most interesting result is the prediction of a new “bridge” structure (Fig. 2) that has not been considered in previous reports on graphene on Ni(111) structure. According to our calculations this structure is the most stable out of four possible (top-fcc, top-hcp, hcp-fcc, bridge), while the structure that has been used in previous investigations to determine energetics of the growth process (hcp-fcc) is the least stable (Helveg 2004). This result, with more careful confirmation, may become an important consideration in understanding the dominant mode (surface diffusion vs. bulk diffusion) of carbon transport to the growth interface.



dimensions these alloys can be locked into phases significantly further from thermodynamic equilibrium. The nanoparticle alloy phase diagrams for these materials is practically uncharted territory. Synthesis of carbon nanostructures with these alloys as nanoparticle catalysts offers a way to confine the nanoparticles within carbon nanostructures. For example, recent studies showed that that gamma-Fe with a face-centered-cubic crystal structure (known to be stable in the temperature range of 912–1394°C for bulk iron) retains its stability at room temperature inside the cavities of CNTs (Kim 2005). Synthesis of vertically aligned carbon nanofibers from alloy thin films deposited with a high degree of control offers a possibility of preparation of confined nanoparticles in a wide range of compositions and sizes. Carbon shell containment gives protection from the environment and from sintering of nanoparticles during heat treatments. We thus create a controlled nanoscale environment for the study of phase transitions. In this work we performed experimental and theoretical investigations directed at various aspects and stages of co-synthesis of the alloy nanoparticle-vertically aligned carbon nanofiber system (AN-VACNF) (Fig.3). The thin alloy films were deposited by co-sputtering of elemental metals onto Si substrates using a RF magnetron system. The films were de-sintered in



Alloys of Fe, Ni, and Co are of high technological importance with their fairly well studied bulk phase diagrams and physical properties that can be tuned to a particular application. However, when confined to a volume of nanoscale

nanoparticles during heat treatments. We thus create a controlled nanoscale environment for the study of phase transitions. In this work we performed experimental and theoretical investigations directed at various aspects and stages of co-synthesis of the alloy nanoparticle-vertically aligned carbon nanofiber system (AN-VACNF) (Fig.3). The thin alloy films were deposited by co-sputtering of elemental metals onto Si substrates using a RF magnetron system. The films were de-sintered in

an ammonia plasma at elevated temperatures (700°C), which was followed by growth of VACNFs in a C₂H₂/NH₃ dc plasma. Following the synthesis, the samples were cooled and analyzed using analytical microscopy, x-ray diffraction, and magnetometry.

In initial studies we used Fe_xCo_{1-x} alloy films to demonstrate this method of nanoparticle preparation and understand its benefits and limitations. Analytical microscopy and XRD was utilized to study compositional and morphological changes during the solid film-to-nanoparticles transition (Fig. 4). SQUID magnetometry showed thermally stable ferromagnetic behavior. These measurements also suggested the loss of magnetic material during synthesis, while the compositional analysis showed preservation of elemental ratio during synthesis. We also observed the variation of final nanoparticle shape depending on the composition.

To study a phase transition in carbon-confined alloy nanoparticles, we chose FeNi₃. In bulk, this alloy undergoes an order-disorder phase transition around 770K (Drijver 1975). We expected to observe size dependent changes in the order-disorder phase transition temperature. Our preliminary electron diffraction studies showed that disordered (i.e. high temperature phase) was stabilized at room temperature.

We are developing a theoretical approach to understanding the structures of the nanoparticles. We used the EAM potentials for Fe-Fe, Co-Co, Fe-Co, and Fe-Ni and performed molecular dynamics simulations in the framework of simulated annealing. Our preliminary results show that the lowest-energy structures for Fe_{0.5}Co_{0.5} (or Fe_{0.5}Ni_{0.5}) nanoparticles smaller than 2nm are partially disordered with notable phase separation between Fe and Co (or Ni) atoms (Fig. 5). The core of the nanoparticle is rich with Co (Ni) atoms and a majority of Fe atoms are distributed in the outer shells of the nanoparticle. We also found that the phase separation becomes more marked at

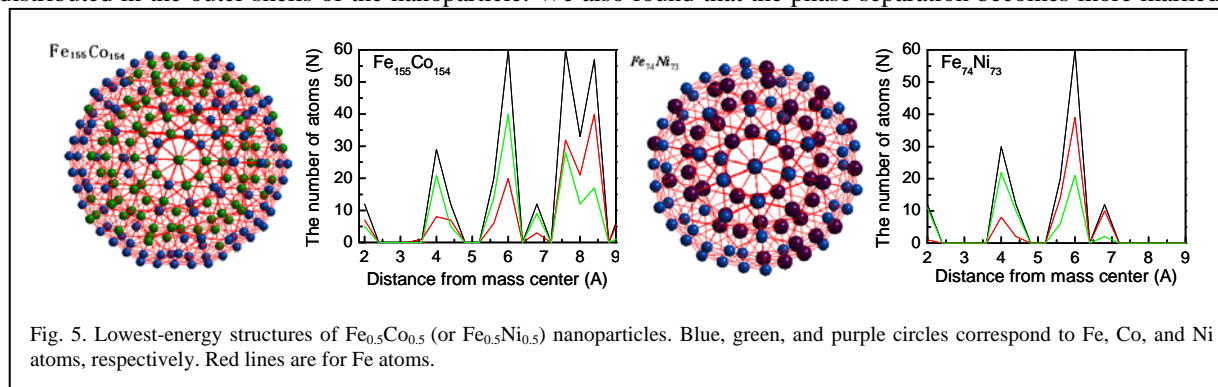


Fig. 5. Lowest-energy structures of Fe_{0.5}Co_{0.5} (or Fe_{0.5}Ni_{0.5}) nanoparticles. Blue, green, and purple circles correspond to Fe, Co, and Ni atoms, respectively. Red lines are for Fe atoms.

higher temperatures around 1000K. We are now studying large nanoparticles (~4nm) with a different composition of Fe to understand the effects of size, temperature and composition on structural properties of the FeCo and FeNi nanoparticles.

Future Plans

Our recent results revealed several fundamental questions important for understanding the mechanisms of co-synthesis and size effects on phase stability. What is the relationship between nanoparticle crystallography and shape and the internal structure of carbon nanofibers? Is it possible to influence the nanoparticle crystallographic orientation during nanofiber synthesis? What is the structure of the catalyst – nanofiber interface? What forces bend the initial flat growth interface to its conical or even cylindrical morphology? How does nanoparticle structure and shape depends on alloy composition and how is that reflected in the internal structure of a carbon nanofiber? How does the phase diagram of a binary alloy change when the alloy is confined within a carbon nanofiber? What are the dynamics of alloy ordering and how do they depend on nanoparticle size? We are conducting experimental and computational investigations that will provide us with the answers to these questions and, concurrently, the underlying fundamental understanding that can bring us to the next level of control of the co-synthesis process of these nanostructures.

References

- Drijver, J. W., F. Vanderwoude and S. Radelaar. **Order-Disorder Transition in Ni₃Fe Studied by Mossbauer-Spectroscopy** *Physical Review Letters* **34**(16): 1026-1029(1975).
- Helveg, S., C. Lopez-Cartes, J. Sehested, P. L. Hansen, B. S. Clausen, J. R. Rostrup-Nielsen, F. Abild-Pedersen and J. K. Nørskov. **Atomic-scale imaging of carbon nanofibre growth** *Nature* **427**(6973): 426-429(2004).
- Kim, H. and W. Sigmund. **Iron nanoparticles in carbon nanotubes at various temperatures** *Journal of Crystal Growth* **276**(3-4): 594-605(2005).

FWP and/or subtask Title under FWP: Design and Synthesis of Nanomaterials **FWP Number:** ERKCM38

Klein, K. L., A.V. Melechko, J.D. Fowlkes, K.D. Sorge, T. Leventouri, R. Rucker, P.D. Rack and M.L. Simpson (2006). Evolution of Fe-Co Magnetic Alloys: from Thin Films to Catalyst Nanoparticles for Carbon Nanofiber Synthesis. Fall MRS Meeting 2006. Boston.

Melechko, A. V., K. L. Klein, J. D. Fowlkes, D. K. Hensley, I. A. Merkulov, T. E. McKnight, P. D. Rack, J. A. Horton, M. L. Simpson. **Control of carbon nanostructure: from nanofiber toward nanotube and back** Submitted to *J. Appl. Phys.*

Publications (2 years)

Submitted:

A. V. Melechko, K. L. Klein, J. D. Fowlkes, D. K. Hensley, I. A. Merkulov, T. E. McKnight, P. D. Rack, J. A. Horton, M. L. Simpson “Control of carbon nanostructure: from nanofiber toward nanotube and back”, Submitted to *J. Appl. Phys.*

I.A. Merkulov, V.I. Merkulov, A.V. Melechko, K. L. Klein, D. H. Lowndes, and M. L. Simpson “Model of carbon nanofiber internal structure formation and instability of catalytic growth interface” Submitted to *Phys. Rev. B*.

In press:

David G.J. Mann, Timothy E. McKnight, Anatoli V. Melechko, Michael L. Simpson, Gary S. Sayler “Quantitative analysis of immobilized DNA on vertically aligned carbon nanofiber gene delivery arrays”

Published:

Dhindsa, M. S., N. R. Smith, J. Heikenfeld, P. D. Rack, J. D. Fowlkes, M. J. Doktycz, A. V. Melechko and M. L. Simpson. Reversible Electrowetting of Vertically Aligned Superhydrophobic Carbon Nanofibers, *Langmuir* 22(21): 9030-9034(2006).

Fletcher, B.L., T.E. McKnight, A.V. Melechko, M.L. Simpson, and M.J. Doktycz, Biochemical functionalization of vertically aligned carbon nanofibres. *Nanotechnology*, 2006. 17(8): p. 2032-2039

Fletcher, B.L., T.E. McKnight, A.V. Melechko, D.K. Hensley, D.K. Thomas, M.N. Ericson, and M.L. Simpson, Transfer of flexible arrays of vertically aligned carbon nanofiber electrodes to temperature-sensitive substrates. *Advanced Materials*, 2006. 18(13): p. 1689+

Fowlkes, J.D., A.V. Melechko, K.L. Klein, P.D. Rack, D.A. Smith, D.K. Hensley, M.J. Doktycz, and M.L. Simpson, Control of catalyst particle crystallographic orientation in vertically aligned carbon nanofiber synthesis. *Carbon*, 2006. 44(8): p. 1503-1510.

Klein, K.L., A.V. Melechko, J.D. Fowlkes, P.A. Rack, D.K. Hensley, H.M. Meyer, L.F. Allard, T.E. McKnight, and M.L. Simpson, Formation of ultrasharp vertically aligned Cu-Si nanocones by a DC plasma process. *Journal of Physical Chemistry B*, 2006. 110(10): p. 4766-4771.

McKnight, T.E., A.V. Melechko, B.L. Fletcher, S.W. Jones, D.K. Hensley, D.B. Peckys, G.D. Griffin, M.L. Simpson, and M.N. Ericson, Resident Neuroelectrochemical Interfacing Using Carbon Nanofiber Arrays. *J. Phys. Chem. B*, 2006. 110(31): p. 15317-15327.

McKnight, T.E., C. Peeraphatdit, S.W. Jones, J.D. Fowlkes, B.L. Fletcher, K.L. Klein, A.V. Melechko, M.J. Doktycz, and M.L. Simpson, Site-specific biochemical functionalization along the height of vertically aligned carbon nanofiber arrays. *Chemistry of Materials*, 2006. 18(14): p. 3203-3211.

Fowlkes, J.D., B.L. Fletcher, E.D. Hullander, K.L. Klein, D.K. Hensley, A.V. Melechko, M.L. Simpson, and M.J. Doktycz, Tailored transport through vertically aligned carbon nanofiber membranes; controlled synthesis, modelling, and passive diffusion experiments. *Nanotechnology*, 2005. 16(12): p. 3101-3109

Cui, H., X. Yang, H. M. Myer, L. R. Baylor, M. L. Simpson, W. L. Gardner, D.H. Lowndes, L. An, and J. Liu, “Growth and Properties of Si-N-C-O Nanocones and Graphitic Nanofibers Synthesized using Three-Nanometer Diameter Iron/Platinum Nanoparticle Catalysts,” *J. Mater. Res.* **20(4)**, 850-855 (2005).

Klein, K. L., A. V. Melechko, P. D. Rack, J. D. Fowlkes, H. M. Meyer, and M. L. Simpson, “Cu-Ni Composition Gradient for the Catalytic Synthesis of Vertically Aligned Carbon Nanofibers,” *Carbon* **43(9)**, 1857-1863 (2005).

Melechko, A. V., V. I. Merkulov, T. E. McKnight, M. A. Guillorn, K. L. Klein, D. H. Lowndes, and M. L. Simpson, “Vertically Aligned Carbon Nanofibers and Related Structures: Controlled Synthesis and Directed Assembly,” *J. Appl. Phys.* **97(4)**, 041301-39 (2005).

Merkulov, I. A., A. V. Melechko, J. C. Wells, H. Cui, V. I. Merkulov, M. L. Simpson, and D. H. Lowndes, “Two Growth Modes of Graphitic Carbon Nanofibers with Herring-Bone Structure,” *Phys. Rev. B* **72**, 045409 (2005).

Books and Book Chapters

McKnight, T. E., A. V. Melechko, M. A. Guillorn, V. I. Merkulov, D. H. Lowndes, and M. L. Simpson, “Synthetic Nanoscale Elements for the Delivery of Materials into Viable Cells,” pp. 191-208 in *BioNanoTech Protocols*, edited by S J. Rosenthal and D. W. Wright, Humana Press (2005).

McKnight, T. E. A. V. Melechko, G. D. Griffin, M. A. Guillorn, V. I. Merkulov, M. J. Doktycz, M. N. Ericson, M. L. Simpson. “Cellular Interfacing with Arrays of Vertically Aligned Carbon Nanofibers and Nanofiber-Templated Materials” in T. Vo-Dinh, Editor, *Nanotechnology in Biology and Medicine*, CRC Press, Boca Raton, Florida (in press 1/23/07).

Abstract for the IWEPNM 2007 INTERNATIONAL WINTERSCHOOL ON
ELECTRONIC PROPERTIES OF NOVEL MATERIALS: MOLECULAR
NANOSTRUCTURE March 10-17, Kirchberg, Austria (Invited Talk)

IN SITU TIME-RESOLVED MEASUREMENTS OF CARBON NANOTUBE AND NANO HORN GROWTH

D. B. Geohegan*, A. A. Puretzky, G. Eres, D. Styers-Barnett, C. M. Rouleau, Z. Liu, I. N. Ivanov, J. Jackson, R. F. Wood, S. Pannala, J. Wells, M.-D. Cheng, H. Cui, H. Hu, B. Zhao, M. Yoon, K. Xiao and M. Garrett

Materials Science and Technology Division and Center for Nanophase Materials
Sciences, Oak Ridge National Laboratory, Oak Ridge, TN 37831

Experiments utilizing time-resolved, in situ imaging and spectroscopic diagnostics are described to investigate the growth mechanisms and kinetics of carbon nanotubes and nanohorns, and the effects of their resulting nanostructure on their properties. Growth conditions for high-yield, laser vaporization production of single-wall carbon nanotubes and nanohorns (SWNHs) using a high-power industrial Nd:YAG laser with tunable, ms-pulse widths has been investigated by high-speed videography and pyrometry. Utilizing laser vaporization with a tunable pulse width laser, growth times for SWNHs and SWNTs were varied to reveal that SWNHs grow at rates comparable to nanotubes without the need for a metal catalyst. The stability of SWNH and SWNT structures at high temperatures were investigated by pulsed laser annealing utilizing fast optical pyrometry, high-resolution TEM, and Raman spectroscopy. Investigations of chemical vapor deposition concentrate upon the growth of vertically-aligned nanotube arrays (VANTAs) with emphasis upon maximizing SWNT content and continuing the growth for multi-millimeter-long arrays. *In situ* optical interferometry and time-resolved imaging are used to directly measure the height of VANTAs during synthesis to understand their nucleation and growth kinetics, and reasons for their coordinated growth and growth termination. In addition, the diameter and number of walls of the nanotubes is often observed to change during VANTA growth to multimillimeter heights, as evidenced by ex situ Raman microscopy and TEM. A kinetic model is proposed to explain the factors determining the changing number of walls for the nanotubes within the array. Thermal properties of VANTA arrays measured utilizing flash diffusivity reveal that they are promising thermal interface materials. Synthesis science supported by the Office of Basic Energy Sciences, Division of Materials Science and Engineering, U. S. Department of Energy with support from characterization capabilities at the Center for Nanophase Materials Sciences, Scientific User Facility Division, DOE-BES.

This page is intentionally blank

From Nanomechanical Science to Nanofabrication Technology: A New Route towards Nanotube Synthesis

Feng Liu (fliu@eng.utah.edu)
Department of Materials Science & Engineering
University of Utah, Salt Lake City, UT 84112

Program Scope

The nanotechnology of the future demands controlled and consistent fabrication of different classes of nanostructures. However, very often the nanostructures are made in an empirical manner lacking a sufficient level of control. Despite the enormous success we have so far enjoyed, such as with carbon nanotubes, nanofabrication and synthesis with most materials are still very difficult. There exists a strong need for the development of nanofabrication techniques with a higher degree of control on size and geometry as well as with a high degree of versatility applicable to different materials. The *objective* of this program is to explore a novel approach of nanofabrication, namely the nanomechanical architecture of thin films (Fig. 1) [1]. The approach

allows fabrication of different types of nanostructures, with a high level of control over their size and shape based on *a priori* theoretical designs. It is extremely versatile, applicable to most materials combinations, including semiconductors, metals, insulators, and polymers. It is also completely compatible with the Si technology, employing the industrial viable thin-film processing of growth, patterning, and lift-off, suitable for

parallel mass production of identical or different nanostructures. By applying multiscale modeling and simulations from first-principles calculation, to molecular dynamics simulation, and to continuum mechanics modeling, we aim to understand how the mechanical bending of nanoscale thin films differs from that of macroscopic thick films and reveal the role played by the atomic nature of the film structure and the intrinsic surface stress, which becomes increasingly prominent at the nanometer scale. We will exploit the unique bending behavior of nanofilms to predict and design the formation of nanostructures, with a special focus on the Si, Ge and C nanotubes. Our studies will significantly further our fundamental understanding of the science of thin-film growth, patterning and nanomechanical architecture, and provide useful guidelines for future experiments. They will have a direct impact on advancing nanostructure processing and synthesis technology for energy applications, to fulfill the mission of the Department of Energy.

Recent Progress

Like a bimetallic strip in a thermostat that bends due to different thermal stress in the two metal strips, a strained bi-layer thin film bends due to lattice-misfit strain in the two layers. In particular, when the film thickness is reduced to the nanometer scale, its bending magnitude can be so large that it can fold into tubular shapes with a characteristic radius of bending curvature also falls into nanometer scale. Remarkably, this simple bending phenomenon has recently been exploited for fabricating a variety of nanostructures [1-3], ranging from nanotubes, nanorings, nanodrills, to nanocoils, as illustrated in Fig. 1. The promising potential shown by this novel and fascinating approach has attracted a lot of recent interests. However, work to date remains largely empirical; most structures are made in a trail-&-error manner. This is due mainly to the lack of good understanding of the underlying physical principles, which hinders a higher degree of experimental control. Therefore, we have made a conscious effort to understand the fundamental

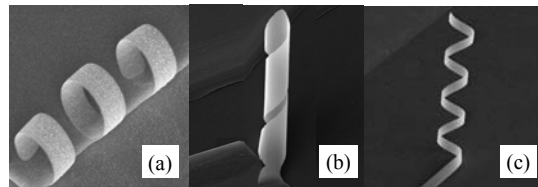


Fig. 1. SEM image of nanoarchitectures fabricated from strained Si/SiGe bi-layer films. (a) Nanoring, (b) nanodrill, and (c) nanocoil.

mechanisms governing the nanomechanical architecture of strained bi-layer thin films. Our long-term goal is to establish certain generic “design principles” that will lead to selective fabrication of different classes of nanostructures and a higher degree of control on their size and shape.

We discover that certain well-defined and universal physical conditions and geometric relationships exist in controlling the size of the same class of nanostructures as well as the formation of different classes of nanostructures. For example, whether a film will fold into a tube or coil is uniquely controlled by some intrinsic relations between the film dimensions and its characteristic bending scales (e.g., $L_0 = 2\pi R_0$, where R_0 is the radius of bending curvature).

There exist two critical geometric conditions for coil formation: $W < L_0$ and $\theta > \theta_c$, as illustrated in Fig. 2. The spiral angle of the coil depends on the folding direction as $\alpha = \tan^{-1}(d/R_0)$ ($d \geq W$), and the minimum allowed spiral angle for any coil is $\theta = \tan^{-1}(W/R_0)$ [1].

We have also realized that the current application of the above approach is fundamentally limited to making nanostructures strictly from bi-layer or multi-layer films [1-3], because misfit strain is employed as the only driving force for bending. The nanostructures, such as nanotubes, so made must have a fixed configuration with the tensile film (such as Si) as the inner layer and the compressive film (such as Ge) as the outer layer, as predefined by the lattice mismatch between the two constituting layer materials. To overcome these limitations, we proposed recently a self-bending mechanism of nanofilms to extend the nanomechanical architecture to single-layer film of one material [4]. Conventionally, a solid film will not bend itself without external load of “surface” stress. This is true, however, only because we have neglected the atomic details of the film structure, especially the surface atomic structure that governs the intrinsic surface stress. Using theoretical analysis of surface stress and direct molecular dynamics simulations, we demonstrate that ultrathin Si and Ge nanofilms may self-bend without external stress load, under its own intrinsic surface stress imbalance arising from surface reconstruction [4]. This leads to self-rolled-up pure Si and Ge nanotubes (Fig. 3a). Under the same mechanism, SiGe bilayer nanofilms may bend toward the Ge side (Fig. 3c), opposite to what defined by misfit strain (Fig. 3b), allowing formation of SiGe nanotubes in an unusual configuration with Ge as the inner layer (Fig. 3c). Such rolled-up nanotubes are found to accommodate very high strains, even beyond the misfit strain defined by lattice mismatch (i.e., larger than $\sim 4\%$ between Si and Ge), which in turn induce large variations of electronic and optoelectronic properties [4].

Another interesting and important recent development is a new method for synthesizing carbon nanotubes (CNTs), which we derived from the nanomechanical architecture of a single-atomic-layer film, the patterned graphene sheet. A US provisional patent has been filed based on our process [5]. CNTs are made so far by three synthetic processes, including arc discharge, laser ablation and chemical vapor deposition. These are all stochastic chemical processes, which render an inherent difficulty in controlling the tube size and chirality. Despite much effort has been put in, synthesizing mass quantity of CNTs with uniform size and chirality remains a great challenge.

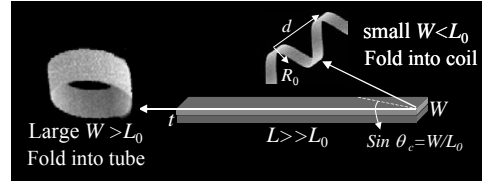


Fig. 2. Illustration of a strained bi-layer film folding into a nanotube when its width W is large, but into a coil when W is small.

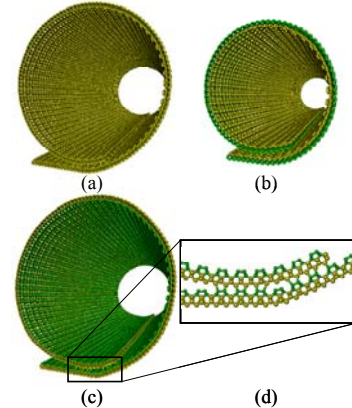


Fig. 3. MD simulated nanotubes. (a) A Si tube. (b) A SiGe tube with Si as the inner layer. (c) A SiGe tube with Ge as the inner layer formed. (d) Atomic structure of folded tube edge.

Post-synthesis separation, purification, and sorting process are often required before putting CNTs in use, which amounts to additional technical difficulties and production cost. Therefore, developing new and alternative methods for synthesizing CNTs with better control of size and chirality is of great interest and economic benefit. We have demonstrated, by first-principles and classical MD simulations, a new method of synthesizing CNTs that practically realizes the imaginative vision of rolling up the graphene sheets (ribbons), based on the physical principle of bending of thin films driven by surface adsorption induced stress. Figure 4 shows the MD simulated CNT formation process for two tubes of different size and chirality. The method consists of three basic steps: (1) patterning of graphene nanoribbons (GNRs) (Fig. 4.a1 and b1), (2) rolling up of GNRs into single-walled nanotubes (SWNTs) by surface adsorption at low temperature (Fig. 4.a2-3 and b2-3), and (3) removing surface adsorbents by high-temperature desorption (Fig. 4.b4-6 and b4-6). In contrast to all the existing CNT synthesis methods that are based on the bottom-up self-assembled growth processes and stochastic in nature, our method, employing a top-down process of patterning combined with a bottom-up process of folding, is deterministic in nature with the tube diameter and chirality predefined by patterning. Furthermore, our method offers a parallel process allowing mass production of SWNTs with uniform size and chirality.

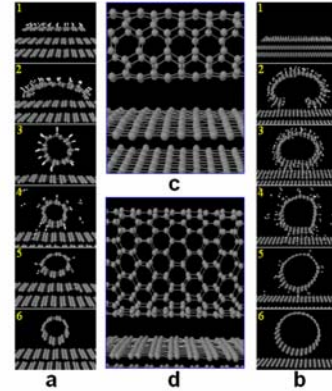


Fig. 4. MD simulations demonstrating the formation process of (a) a 0.5 nm (diameter) armchair and (b) a 0.9 nm zigzag SWNT. (a1-3) and (d1-3) show the tube formation at room temperature upon adsorption of H atoms, (a3-6) and (d3-6) show the desorption of H atoms at 1800K. (c) and (d) show the perspective sideview of the armchair and zigzag SWNT resulting from process (a) and (b), respectively.

Future Plans

- We will continue to expand our current studies as described above in the following areas:
- (1) Continue with more extensive theoretical analyses and computer simulations on the “designing principle and process optimization” of nanomechanical architectures of nanofilms, focusing on the SiGe based nanotube architectures.
 - (2) Extend the study (1) to other forms of SiGe nanoarchitectures, such as nanocoils.
 - (3) Extend the studies (1) and (2) to nanoarchitectures of different materials.
 - (4) Initiate a new study of electronic and electric transport properties of various unique forms of nanoarchitectures as obtained from the studies (1) through (3). A special focus will be on “strain engineering” of electronic structures, as all the nanoarchitectures are inherently strained in novel geometries accommodating high level of strains.
 - (5) Extend the CNT synthesis process to different adsorbates and coverage.

References

1. M. Huang, C. Boone, M. Roberts, D. E. Savage, M. G. Lagally, N. Shaji, H. Qin, R. Blick, J. A. Nairn and Feng Liu, *Adv. Mater.* **17**, 2860 (2005).
2. V.Ya. Prinz et al., *Physica E*, **6**, 828 (2000).
3. O.G. Schmidt and K. Eberl, *Nature*, **410**, 168 (2001).
4. Ji Zang, M. Huang, and Feng Liu, *Phys. Rev. Lett* **98**, 146102 (2007).
5. Feng Liu and D. Yu, “Method of Forming Nanotubes”, US provisional patent, serial no. 60/908,039 (2007).

The DOE funded publications in the last two years

1. “Modeling and Simulation of Strain-Mediated Nanostructure Formation on Surface”, Feng Liu, in “*Handbook of Theoretical and Computational Nanotechnology*”, eds. M. Rieth and W. Schommers, **4**, Chapter 10, 577-625 (2006). **(invited book chapter)**
2. “Quantitative Prediction of Critical Size for the Formation of Semiconductor Quantum Dots”, G.H. Lu and Feng Liu, in “*Physics, J. Chinese Phys. Association*”, **35**, 447 (2006). **(invited review)**
3. “Computational R&D for Industrial Applications”, Feng Liu, News of Center for High-Performance Computing, University of Utah, Fall issue, p. 1 (2005). **(invited article)**
4. “MD simulation of structural and mechanical transformation of single-walled carbon nanotubes under pressure”, J. Zang, O. Aldás-Palacios and Feng Liu, *Commun. in Comput. Phys.* **2**, 451 (2007) **(invited review)**
5. “Directed Self-assembly of Quantum Dots by Local Chemical Potential control via Strain Engineering on Patterned Substrates”, Hangyao Wang, Feng Liu, and M. Lagally, in “*Lateral alignment of epitaxial quantum dots*”, eds. O. Schmidt, Springer, (2007) **(invited book chapter)**.
6. “Mechanism for Nanotube Formation from Self-Bending Nanofilms Driven by Atomic-Scale Surface-Stress Imbalance”, Ji Zang, Minghuang Huang, and Feng Liu, *Phys. Rev. Lett* **98**, 146102 (2007).
7. “Impurity mediated absorption continuum in single-walled carbon nanotubes”, C. Zhang, J.C. Chao, X.G. Guo and Feng Liu, *Appl. Phys. Lett.* **90**, 023106 (2007).
8. “Nucleation-Mediated Lateral Growth on Foreign Substrate”, D.J. Shu, M. Wang, Feng Liu, Z. Zhang, R.W. Peng, R. Zhang, N.B. Ming, *J. Phys. Chem. C*, **111**, 1071 (2007).
9. “Intrinsic current-voltage properties of nanowires with four-probe scanning tunneling microscopy: A conductance transition of ZnO nanowire”, X. Lin, X.B. He, T.Z. Yang, W. Guo, D.X. Shi, H.-J. Gao, D.D.D. Ma, S.T. Lee, Feng Liu, X.C. Xie, and *Appl. Phys. Lett* **89**, 043103(2006).
10. “Surface Mobility Difference between Si and Ge and its Effect on Growth of SiGe Alloy Films and Islands”, Li Huang, Feng Liu, Guang-Hong Lu and X. G. Gong, *Phys. Rev. Lett* **96**, 016103 (2006).
11. “Pressure-Induced Transition in Magnetoresistance of Single-walled Carbon Nanotubes”, J. Z. Cai, L. Lu, H. W. Zhu, C. Zhang, B. Q. Wei, D. H. Wu, and Feng Liu, *Phys. Rev. Lett* **97**, 026402 (2006).
12. “Self-organization of Semiconductor Nanocrystals by Selective Surface Faceting”, B. Yang, P. Zhang, D.E. Savage, M. Lagally, G.H. Lu, M.H. Huang, and Feng Liu, *Phys. Rev. B* **72**, 235413 (2005).
13. “Nanomechanical Architecture of Strained Bilayer Thin Films: from design principles to experimental fabrication”, Minghuang Huang, C. Boone, M. Roberts, D. E. Savage, M. G. Lagally, N. Shaji, H. Qin, R. Blick, J. A. Nairn and Feng Liu, *Adv. Mater.* **17**, 2860 (2005).
14. “Critical Epi-Nucleation on Reconstructed Surfaces and a Model Study of Si(001) Homoepitaxy”, Raj Ganesh S. Pala and Feng Liu, *Phys. Rev. Lett* **95**, 136106 (2005).
15. “First-principles study of strain stabilization of Ge(105) facet on Si(001)”, G.H. Lu, Martin Cuma, and Feng Liu, *Phys. Rev. B* **72**, 125415 (2005).
16. “Bending of Nanoscale Ultrathin Substrates by Growth of Strained Thin Films and Islands”, M.H. Huang, P. Rugheimer, M.G. Lagally, and Feng Liu, *Phys. Rev. B* **72**, 085450 (2005).
17. “Mechanical Stability of Ultra Thin Ge/Si Film on SiO₂: the Effect of Si/SiO₂ Interface”, M.H. Huang, J.A. Nairn, Feng Liu, and M.G. Lagally, *J. Appl. Phys.* **97**, 116108 (2005).
18. “Relative stability of Si surfaces: a first-principles study”, G.H. Lu, M.H. Huang, M. Cuma, and Feng Liu, *Surf. Sci.* **588**, 61 (2005).
19. “Towards Quantitative Understanding of Formation and Stability of Ge Hut Island on Si(001)”, G.H. Lu and Feng Liu, *Phys. Rev. Lett* **94**, 176103 (2005).
20. Pattern Formation on Silicon-on-Insulator”, F. Flack, B. Yang, M. Huang, M. Marcus, J. Simmons, O.M.Castellini1, M.A. Eriksson, Feng Liu and M.G. Lagally, *MRS Proceeding*. Vol. 849, KK1.3.1/JJ1.3.1/U1.3.1 (2005).
21. “Computational Study of Metal Adsorption on TiO₂ (110) Surface”, R. S. Pala, T. N. Truong, and Feng Liu, in “Clusters and Nano-Assemblies”, World Scientific, eds. P. Jena, S.N. Khanna, and B.K. Rao, 135 (2005).

Poster Session

III. Precision Nanoscale Synthesis

IV. Hybrid Materials and Assembly

V. Tools for Synthesis and Novel Approaches

This page is intentionally blank

Low Temperature Synthesis Routes to Intermetallic Superconductors

R.E. Schaak, Texas A&M University

Program Scope

Over the past few years, our group has gained expertise at developing solution-based synthetic pathways to complex nanoscale solids, with particular emphasis on nanocrystalline intermetallic compounds. Our synthetic capabilities are providing tools to reproducibly generate intermetallic nanostructures with simultaneous control over crystal structure, composition, and morphology. This DOE-funded project aims to expand these capabilities to intermetallic superconductors. This could represent an important addition to the tools that are available for the synthesis and processing of intermetallic superconductors, which traditionally utilize high-temperature, high-pressure, or gas-phase vacuum deposition methods. Our current knowledge of intermetallic superconductors suggests that significant improvements could result from the inherent benefits of low-temperature solution synthesis, e.g. metastable phase formation, control over nanoscale morphology to facilitate size-dependent property studies, robust and inexpensive processability, low-temperature annealing and consolidation, and impurity incorporation (for doping, stoichiometry control, flux pinning, and improving the critical fields). Our focus is on understanding the superconducting properties as a function of synthetic route, crystal structure, crystallite size, and morphology, and developing the synthetic tools necessary to accomplish this.

This research program can be divided into two classes of superconducting materials: intermetallics (transition metal/post transition metal) and metal carbides/borides. Both involve the development and exploitation of low-temperature synthesis routes followed by detailed characterization of structures and properties, with the goal of understanding how the synthetic pathways influence key superconducting properties (T_c , H_c , J_c) of selected target materials. Because of the low-temperature methods used to synthesize them and the nanocrystalline morphologies of many of the products, the superconductors and their nanocrystalline precursors are potentially amenable to inexpensive and large-scale solution-based processing into wires, coatings, films, and templated or patterned structures with nanoscale and microscale features. Also, because of the new synthetic variables that play a key role in the low-temperature formation of intermetallics, the possibility exists to discover new superconductors.

Recent Progress

During this first (partial) year of funding, we have focused on ensuring that we can routinely generate superconducting materials using newly developed and modified low-temperature synthetic strategies. This work involved both synthetic development and characterization of the superconducting properties for a selected set of superconducting intermetallics, as proposed. Our initial targets were chosen to ensure that phases which are known to be superconducting as bulk solids synthesized using traditional high-temperature methods are also superconducting when made using low-temperature methods. (This is important, because such “control” studies are often ignored during synthetic development work, yet are critical for ensuring that useful materials can be formed.) Our initial targets were NiBi, Bi₂Pd, and BiIn₂, and all were found to

be superconducting with T_c s matching those reported previously¹ (Figure 1). Of these, only NiBi has been previously reported to form by low-temperature methods.²

NiBi is a strategic first target for this project, because it is a known superconductor that can be made by multiple low-temperature and high-temperature techniques, including arc melting, powder metallurgy, solvothermal methods, polyol synthesis, and other methods for comparison purposes. Our lowest-temperature protocol involves the synthesis of NiBi directly in solution at 260 °C for 3 h using a modified polyol process (Figure 1a). Upon annealing at 550 °C for 3 h, it becomes superconducting with $T_c = 4.2$ K (Figure 1a). The degree of crystallinity can be systematically modified using a range of solution and powder annealing protocols (Figure 1a).

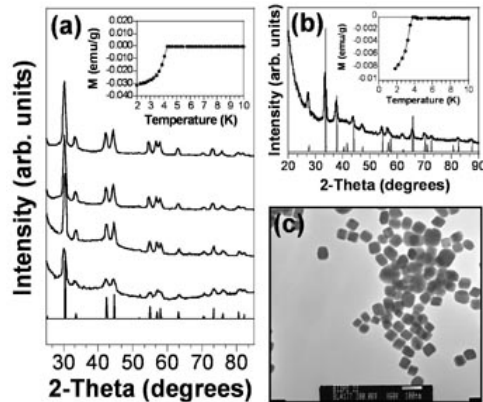


Figure 1. (a) XRD (bottom to top: simulated, 260 °C for 1, 3, 5, and 7 h) and magnetization data for NiBi; (b) XRD, magnetization, and (c) TEM data for Bi₂Pd.

Superconducting Bi₂Pd can also be synthesized as uniform nanocubes using a modified polyol process (Figure 1b,c). Bi₂Pd is a bulk superconductor as-synthesized in solution at 280 °C for 3 h with no additional annealing necessary. Interestingly, the published phase diagram for the Bi-Pd system shows two Bi₂Pd polymorphs. Both have been reported to be superconducting, but the 4.2-K superconductor is the high-temperature polymorph, stable only above 380 °C. We are able to access this polymorph below 280 °C. This provides evidence that we can access metastable intermetallic superconductors as bulk solids using our low-temperature strategies, one of the hypotheses of our original proposal.

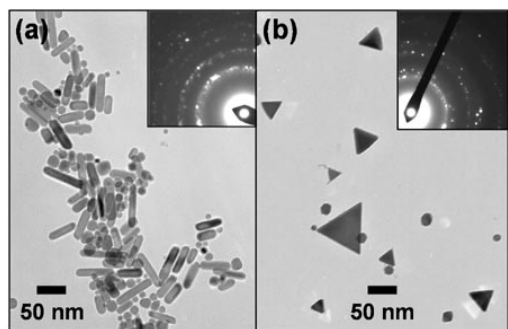


Figure 2. TEM and SAED data for (a) β -Sn nanorods and (b) In nano-triangles.

intermetallics (including new and metastable structures),³ and this provides another potential low-temperature pathway to intermetallic superconductors. Thus, we spent some time preparing nanocrystalline elemental superconductors using similar protocols. Figure 2 shows TEM images of superconducting β -Sn nanorods and In nanotriangles, which can be used as templates for the formation of shape-controlled Sn- and In-based intermetallic superconductors.

As an alternative low-temperature strategy for synthesizing intermetallic superconductors, we have developed a new approach that combines our solution chemistry methods with more traditional metallurgical ideas. To do this, we utilize a polyalcohol solvent (e.g. tetraethylene glycol with a boiling point of ~ 300 °C), and add to it bulk metal powders in stoichiometric ratios. One of the components must be a metal having a melting point close to or below that of the boiling point of the solvent (e.g. Sn, Ga, In, Bi). Since the solvent is weakly reducing, oxidation is minimized, so the reactions do not need to occur in a sealed system (e.g. in sealed

evacuated silica tubes). Also, bulk-scale samples are accessible, and the product morphologies often mimic those obtainable via arc-melting, e.g. ingots that can be crushed into smaller crystallites (Figure 3). So far we have succeeded at accessing Ni_3Sn_4 , NiGa_4 , BiIn , BiIn_2 , CoGa_3 , FeGa_3 , CoSn_3 , Cu_6Sn_5 , FeSn_2 , NiBi , and InSb at temperatures below 300 °C and with no additional annealing (Figure 3). Of these, BiIn_2 is a known superconductor, and we find it to be superconducting as-made (Figure 3). The formation of NiBi using this method is also very important, because it allows us to make comparisons with NiBi synthesized using other low-temperature methods. We also have preliminary data suggesting that NbGa_3 forms using this strategy, providing evidence that the intermetallic Nb-Ga and Nb-Sn superconductors might be accessible using this low-temperature chemistry, as proposed.

Finally, as a first step toward accessing the metal carbides and borides described in our proposal, we have learned how to make phase-pure Ni_3B using polyol chemistry at temperatures below 300 °C (Figure 4). Boron is known to incorporate into Ni when preparing Ni nanoparticles using NaBH_4 in water,⁴ but polyol chemistry provides greater synthetic flexibility, and also yields Ni_3B directly in pure crystalline form. This is in contrast to the formation of metal borides using other methods, which produce amorphous solids and require annealing to crystallize.

As a side project, our synthetic explorations inspired some developments in an area outside of the original focus of our proposal, but highly germane to the issue of synthetic advances related to superconductivity. We discovered a multi-step solid-state pathway for accessing perovskite-type $\text{Eu}_2\text{Ti}_2\text{O}_7$ at 750 °C and ambient pressure, which is facilitated by exploiting a solid-state precursor (EuTiO_3) that contains the same structural motif that is present in the desired product (Figure 5).⁵ Perovskite-type $\text{Eu}_2\text{Ti}_2\text{O}_7$ has previously been synthesized only by high-temperature high-pressure techniques (> 2000 K, 4 GPa).⁶ We find that perovskite-type $\text{Eu}_2\text{Ti}_2\text{O}_7$ is active for second harmonic generation with efficiencies of $80 \times \text{SiO}_2$.

Future Plans

Our immediate plans, in line with our goal of understanding how the synthetic pathway influences the key superconducting properties for our new low-temperature routes, are to (a) synthesize NiBi , Bi_2Pd , and BiIn_2 using several distinct routes (low-temperature powder, low-temperature solution, traditional high-temperature), (b) measuring H_c and J_c for all samples, and (c) characterizing the microstructure and nanostructure in detail (electron microprobe, STEM), focusing on the characterization and identification of impurities, percolation networks, and grain size. Efforts to carefully control size, shape, and dispersity of key superconducting intermetallics (looking toward possible size-

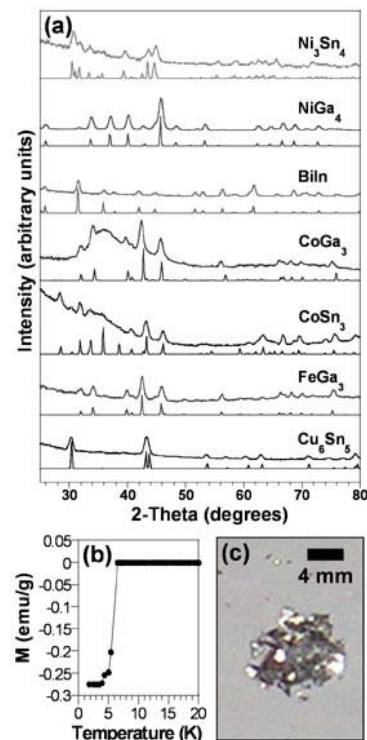


Figure 3. (a) XRD data for intermetallics synthesized via the polyol-mediated reaction of metal powders. (b) Magnetization data and (c) digital photograph of superconducting BiIn_2 .

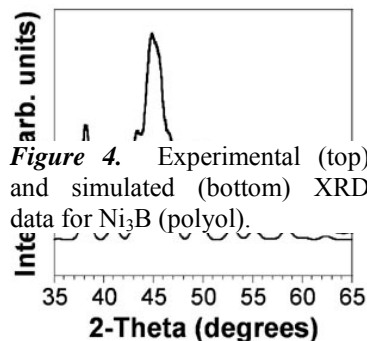


Figure 4. Experimental (top) and simulated (bottom) XRD data for Ni_3B (polyol).

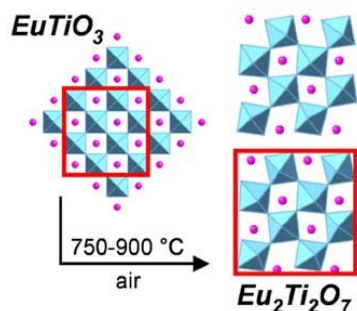


Figure 5. Schematic describing the low-temperature ambient-pressure synthesis of the SHG active perovskite $\text{Eu}_2\text{Ti}_2\text{O}_7$.

dependent property studies) will also be explored. We will simultaneously focus on the Nb-Ga system, building on our preliminary evidence that NbGa_3 forms using our new low-temperature polyol strategy. The first challenge will be to synthesize Nb_3Ga , and while we do not expect this (or other Nb-rich intermetallics) to form using simple one-pot reactions, we will approach this from other pathways, for example by reaction of NbGa_3 with reactive Nb precursors (NbCl_5 under strongly reducing conditions, zero-valent and low-valent organometallic Nb complexes). We will approach the Nb-Sn system in a similar manner.

We will also expand significantly on our initial work with metal borides and carbides. Building on our successful formation of Ni_3B , we will explore the formation and physical properties of other binary metal borides using low-temperature solution strategies. We will also use nanocrystalline Ni_3B (and other related borides that we anticipate being able to prepare) as a reactive low-temperature precursor to ternary metal borides, in analogy to “nanocrystal conversion chemistry” routes that we have reported previously.³ For example, by reacting nanocrystalline Ni_3B with activated magnesium (work in progress), we should be able to form MgNi_3B , the boron analogue of the non-oxide perovskite superconductor MgNi_3C .⁷ While MgNi_3B is not expected to be superconducting, other similar targets may be. We have already begun work to access Mg-based intermetallics using chemistry described in our proposal, and we will continue in that area. As a longer-term goal, we will also work toward preparing $\text{YNi}_2\text{B}_2\text{C}$ and $\text{YPd}_2\text{B}_2\text{C}$ ($T_c = 23$ K, previously inaccessible in pure form)⁸ using a combination of the strategies outlined above, as well as new techniques in development.

References

1. (a) Matthias, B.T. *Phys. Rev.* **1953**, *92*, 874; (b) Jones, R.E.; Ittner, W.B. *Phys. Rev.* **1959**, *113*, 1520; (c) Alekseevskii, N.E.; Lifanov, I.I. *Sov. Phys. JEPT* **1956**, *3*, 294.
2. Park, S.; Kang, W.Q.; Han, W.Q.; Vogt, T. *J. Alloys Compounds* **2005**, *400*, 88.
3. (a) Leonard, B.M.; Schaak, R.E. *J. Am. Chem. Soc.* **2006**, *128*, 11475; (b) Cable, R.E.; Schaak, R.E. *J. Am. Chem. Soc.* **2006**, *128*, 9588; (c) Henkes, A.E.; Vasquez, Y.; Schaak, R.E. *J. Am. Chem. Soc.* **2007**, *129*, 1896; (d) Chou, N.H.; Schaak, R.E. *J. Am. Chem. Soc.* **2007**, submitted [in revision]; (e) Cable, R.E.; Schaak, R.E., manuscript in preparation for *Chem. Mater.*
4. Glavee, G.N.; Klabunde, K.J.; Sorensen, C.M.; Hadjipanayis, G.C. *Langmuir* **1994**, *10*, 4726.
5. Henderson, N.L.; Baek, J.; Halasyamani, P.S.; Schaak, R.E. *Chem. Mater.* **2007**, *19*, 1883.
6. (a) Bondarenko, T.N. et al. *J. Korean Phys. Soc.* **1998**, *32*, S65; (b) Sycj, A.M.; Stafanovich, S.Y.; Titov, Y.A.; Bondarenko, T.N.; Mel'nik, V.M. *Inorg. Mater.* **1991**, *27*, 2229.
7. He, T.; Cava, R.J. et al. *Nature* **2001**, *411*, 54.
8. (a) Cava, R.J. et al. *Nature* **1994**, *367*, 146; (b) Gupta, L.C. *Phil. Mag. B* **1998**, *77*, 717.

Publications (last two years)

- N. Henderson, J. Baek, P.S. Halasyamani, and R.E. Schaak, “Ambient Pressure Synthesis of SHG-Active $\text{Eu}_2\text{Ti}_2\text{O}_7$ with a [110] Layered Perovskite Structure: Suppressing Pyrochlore Formation by Oxidation of Perovskite-Type EuTiO_3 ,” *Chem. Mater.* **2007**, *19*, 1883-1885.
- N. Henderson and R.E. Schaak, “Solution-Mediated Synthesis of Polycrystalline Intermetallic Compounds using Bulk Metal Powders as Precursors,” manuscript in preparation.

Nanoscale Morphology Evolution Under Ion Irradiation

Michael J. Aziz, Harvard School of Engineering and Applied Sciences, Cambridge MA

I. Scope of the program

The ability to understand and control the properties of matter on nanometer length scales is a major thrust in materials chemistry and physics today. Mastery of fundamental science at this length scale will have profound implications for a wide variety of future discoveries and applications in the chemical and biological sciences as well as in materials science and condensed matter physics. This program is a combined experimental and theoretical study of the fundamental physical principles governing nanoscale surface morphology evolution during sputter erosion using ions with energies roughly in the range 0.1 to 30 keV.

Nanoscale surface morphologies spontaneously develop from uniform ion irradiation of an initially flat surface in a non-equilibrium self-organization process termed “sputter patterning”. Spontaneous self-organization processes such as this have no fundamental throughput limitations and have been used to create nanometer-scale patterns with good short-range order as shown in Fig. 1. As in most self-organization processes, the major challenge is the flexibility one has over the resulting pattern. A combination of “top-down” approaches for flexibility and “bottom-up” approaches for size and throughput is likely to be a successful strategy for mass production of functional nanoscale devices. The importance of the “bottom-up” approaches will be determined to a significant degree by the answer to the question, “how much control do we have over the morphology?” A great deal of fundamental work must be done before this question can be answered directly.

There is a significant body of experimental and theoretical work on ion-stimulated formation and relaxation of self-organized topographic features on solid surfaces^{2,3}. For sputter patterns on Si, on which we will focus, the in-plane length scales (wavelengths) are typically of order 100 nm, and the out-of-plane length scales (amplitudes) are of order 10 nm. Spontaneously self-organized ripples and dots as small as 15 nm have been formed in other materials systems such as GaSb⁴ and SiO₂⁵. We are studying the larger lateral length scales in Si because of the ready availability of *in-situ* probes, e.g. optical diffraction techniques⁶ and Focused Ion Beam (FIB)-Scanning Electron Microscopy (SEM)⁷ and because Si is a monatomic system highly amenable to atomistic modeling. With measurements at these length scales, we hope to rapidly develop a deep understanding of the fundamental aspects of the phenomenon. Ultimately we expect to develop sufficient understanding to design and guide experiments at sub-lithographic length scales that permits us to answer the question, “How much morphology control can be attained without having to write each individual feature?”

To this end we are trying to develop a new paradigm of morphology evolution under ion sputter erosion. It will start with local morphology changes observable in AFM images or mo-

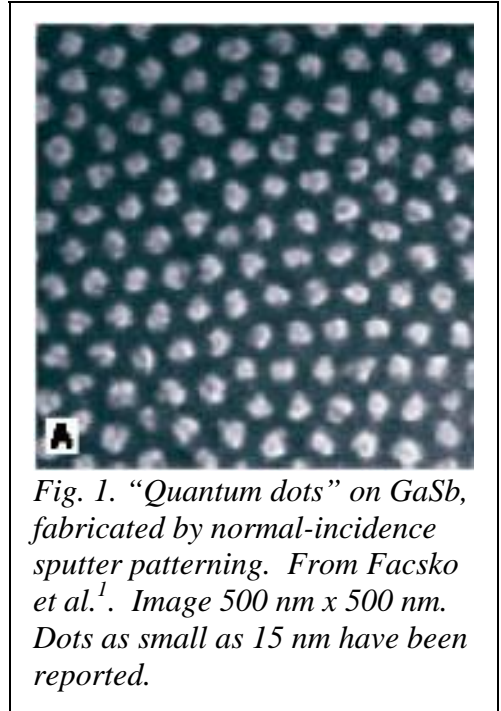


Fig. 1. “Quantum dots” on GaSb, fabricated by normal-incidence sputter patterning. From Facsko et al.¹. Image 500 nm x 500 nm. Dots as small as 15 nm have been reported.

lecular dynamics simulations of topographical changes due to individual ion impacts and will build these events into a continuum theory for morphology evolution. A linear stability analysis will reveal conditions for experimental testing of the stability of a planar surface to uniform ion irradiation. Experiments employ unfocused and focused ion beams to manipulate sputter patterning, for example by creating an initial morphology designed to test a particular theoretical prediction and then measuring the evolution directly⁸. Beyond linear stability, a new experimental approach using amplitude saturation is expected to determine the dominant nonlinear effect from among a zoo of proposed effects. These results will permit the development of predictive models for ion-stimulated morphology evolution and make significant advances toward the utility of simple, wafer-compatible methods to fabricate a wide variety of functional nanostructures.

II. Recent progress

Lateral Templating for Guided Self-Organization of Nanoscale Topographies. Due to their potential for the fabrication of large areas of nanoscale features with controlled period and intra-period organization for high-throughput mass production of nanoscale devices, much recent attention has been devoted to self-organization processes. Although the short-range order can be quite high, some envisaged applications require long-range order, which is destroyed by uncontrolled topological defects arising spontaneously from the self-organization process. A potentially successful hierarchical fabrication strategy is the fabrication of controlled features at a small, but lithographically tractable, length scale by methods such as conventional mask or optical standing wave lithography, in order to guide a self-organization process at the finest length scale¹⁰.

We measured the influence of patterned boundaries on a Si(001) substrate in guiding self-organized sputter ripples⁹. We showed that the long-range order of the features can be greatly enhanced by this lateral templating approach (Fig. 2). The emerging pattern can be manipulated by changing the boundary spacing and misorientation with respect to the projected ion beam direction. At small boundary separation, the greatest order is observed when the separation is near an integer multiple of the spontaneously arising feature size. The density of topological defects is exceedingly low up to a critical misorientation angle, beyond which defects develop in proportion to the incremental misorientation. No theory is known to predict the lateral templating effect and the documented behavior of the defect density, or to address the maximum distance between template boundaries over which it is possible to deterministically set the pattern that evolves within the intervening area. These remain open questions.

Shocks in Sputter Erosion Sharpen Surface Features. We discovered a new regime of ion beam sputtering that occurs for sufficiently steep slopes⁸. High slopes propagate over large distances without dissipating the steepest features. Both the propagation velocity and the dynamically selected slope are universal, independent of the details of the initial shape of the surface.

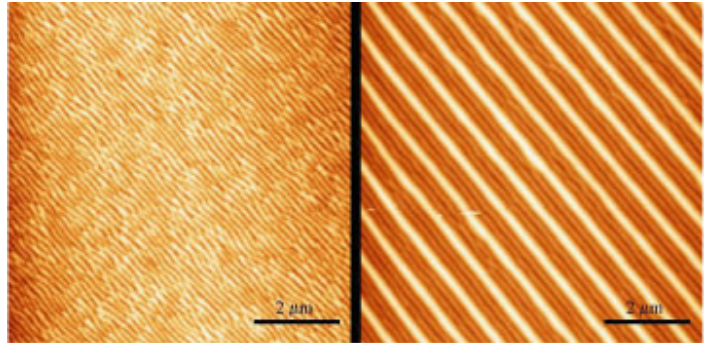


Fig. 2. Lateral templating under ion beam sputtering⁹. AFM topographs of sputter-rippled Si(001) just outside (left) and inside (right) lithographically templated region of same sample. High regions are white.

The left panel of Fig. 3 shows predictions of the new theory of sputter morphology evolution for an initial shape consisting of a high-slope step at $t = 0$. Under uniform ion irradiation the step propagates laterally and, for this particular set of conditions, evolves to maintain a uniform slope that is steeper than the original slope. The theory also predicts that sufficiently shallow

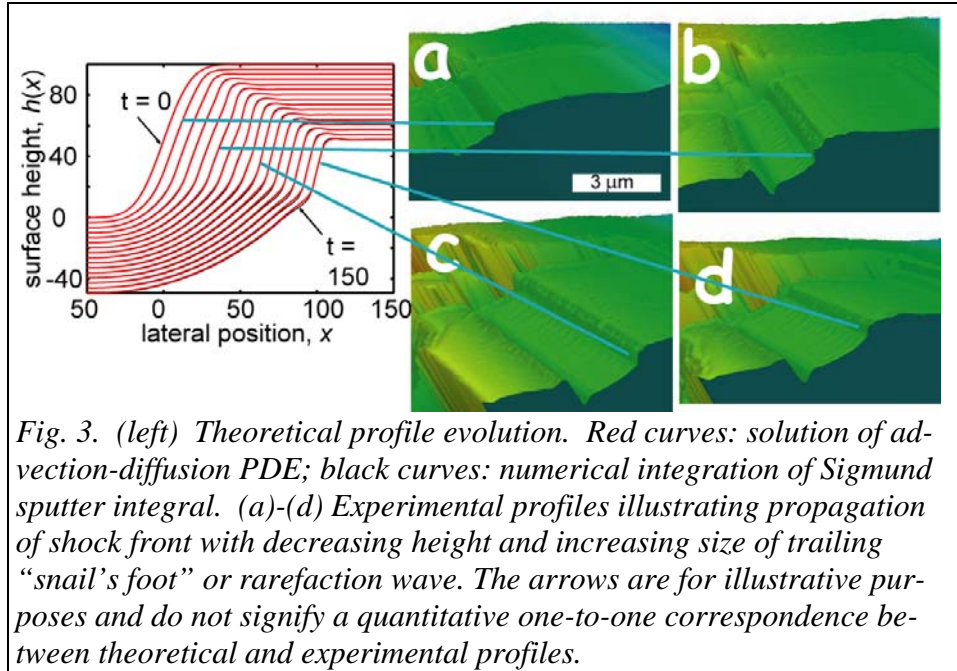


Fig. 3. (left) Theoretical profile evolution. Red curves: solution of advection-diffusion PDE; black curves: numerical integration of Sigmund sputter integral. (a)-(d) Experimental profiles illustrating propagation of shock front with decreasing height and increasing size of trailing “snail’s foot” or rarefaction wave. The arrows are for illustrative purposes and do not signify a quantitative one-to-one correspondence between theoretical and experimental profiles.

slopes dissipate, which is the conventionally observed behavior. The experimental sequence in Fig. 3, obtained with a confocal optical profilometer, shows striking confirmation of the predictions of the theory. An important implication of the transition from dissipative behavior to propagative behavior at high slopes is that a structure (e.g. line or dot) can be fabricated at a large length scale and, with uniform ion irradiation, reduced to a smaller length scale while preserving, or even sharpening, the steepest features.

Stability Theory: Beyond Gaussian Ellipsoids. The Bradley-Harper linear stability theory² for a flat surface under uniform ion irradiation is the widely accepted starting point for understanding self-organized nanoscale pattern formation. Through this theory, the linear instability of a flat surface of arbitrary slope to a sinusoidal modulation of some wave vector is a direct consequence of the assumption of Gaussian ellipsoids of nuclear energy deposition in the ion collision cascade. Our experiments for 250-1200 eV Ar^+ irradiation of amorphous silicon show regimes of linear instability but also regimes of complete stability of a flat surface -- the latter contradicts Bradley-Harper theory.

Theoretically, we have shown¹¹ that for any localized response of the surface to an ion impact that displays a certain symmetry (a subset of which is Bradley's and Harper's Gaussian ellipsoidal response), the surface remains linearly unstable to some wave vector. However, with other response functions we have found conditions that predict a window of linear stability, as is seen in experiment. This can happen if the ion impact creates craters with rims¹², or if there is momentum transfer driving target atoms "downhill" from the ion impact point¹³. This is the first theory predicting stability for any conditions.

III. Future Plans

We have begun an experimental test of conditions for stability and instability of sputter-patterned silicon surfaces at temperatures where the surface layer should be amorphous and isotropic. We will use the results to determine the important factors determining linear stability of flat surfaces. After the linear stability is understood satisfactorily, we will then be able to exam-

ine non-linear behavior and determine the important elements of a non-linear description. Only after a satisfactory nonlinear description is developed will we obtain an understanding of pattern formation and the limits to the flexibility and manipulability of self-organized patterns. At that time we will also be poised to incorporate the singularities in surface energetics and kinetics arising from crystallographic anisotropy which is important for crystalline surfaces below the thermodynamic roughening transition.

IV. References

- ¹S. Facsko, T. Dekorsy, C. Koerdts, C. Trappe, H. Kurz, A. Vogt, and H.L. Hartnagel, *Science* **285**, 1551 (1999).
- ²R.M. Bradley and J.M. Harper, *J. Vac. Sci. Technol. A* **6**, 2390 (1988).
- ³S. Habenicht, *Phys. Rev. B* **63**, 125419 (2001); M.A. Makeev, R. Cuerno, and A.-L. Barabasi, *Nucl. Instrum. Meth. B* **197**, 185 (2002); U. Valbusa, C. Boragno, and F.B. de Mongeot, *Mater. Sci. Eng. C* **23**, 201 (2003); M.J. Aziz, *Mat. Fys. Medd. Dan. Vid. Selsk.* **52**, 187 (2006).
- ⁴S. Facsko, T. Bobek, T. Dekorsy, and H. Kurz, *Physica Status Solidi B* **224**, 537 (2001).
- ⁵T.M. Mayer, E. Chason, and A.J. Howard, *J. Appl. Phys.* **76**, 1633 (1994).
- ⁶E. Chason, M.B. Sinclair, J.A. Floro, J.A. Hunter, and R.Q. Hwang, *Appl. Phys. Lett.* **72**, 3276 (1998); J. Erlebacher, M. Aziz, E. Chason, M. Sinclair, and J. Floro, *Phys. Rev. Lett.* **82**, 2330 (1999).
- ⁷W. Zhou, A. Cuenat, and M.J. Aziz, in *Proceedings of the 13th International Conference on Microscopy of Semiconducting Materials*, edited by A.G. Cullis and P.A. Midgley (IOP, 2003).
- ⁸H.H. Chen, O.A. Urquidez, S. Ichim, L.H. Rodriguez, M.P. Brenner, and M.J. Aziz, *Science* **310**, 294 (2005).
- ⁹A. Cuenat, H.B. George, K.C. Chang, J. Blakely, and M.J. Aziz, *Advanced Materials* **17**, 2845 (2005).
- ¹⁰R.D. Peters, X.M. Yang, Q. Wang, J.J. de Pablo, and P.F. Nealey, *J. Vac. Sci. Technol. B* **18**, 3530 (2000); J.Y. Cheng, A.M. Mayes, and C.A. Ross, *Nature Materials* **3**, 823 (2004).
- ¹¹B. Davidovitch, M.J. Aziz, and M.P. Brenner, *unpublished* (2007).
- ¹²G. Costantini, F. Buatier de Mongeot, C. Boragno, and U. Valbusa, *Phys. Rev. Lett.* **86**, 838 (2001); E.M. Bringa, K. Nordlund, and J. Keinonen, *Phys. Rev. B* **64**, 235426 (2001).
- ¹³G. Carter and V. Vishnyakov, *Phys. Rev. B* **54**, 17647 (1996); M. Moseler, P. Gumbsch, C. Casiraghi, A.C. Ferrari, and J. Robertson, *Science* **309**, 1545 (2005).

V. Recent Publications

- A. Cuenat, H.B. George, K.-C. Chang, J.M. Blakely and M.J. Aziz, "Lateral Templating for Guided Self-Organization of Sputter Morphologies", *Advanced Materials* **17**, 2845 (2005).
- S. Ichim and M.J. Aziz, "Lateral templating of self-organized ripple morphologies during focused ion beam milling of Ge", *J. Vac. Sci. Technol. B* **23**, 1068-1071 (2005).
- H.A. Stone, D. Margetis and M.J. Aziz, "Grooving of a Grain Boundary by Evaporation-Condensation below the Roughening Transition", *J. Appl. Phys.* **97**, 113535 (2005).
- H.B. George, A.-D. Brown, M.R. McGrath, J. Erlebacher, and M.J. Aziz, "Quantifying the order of spontaneous ripple patterns on ion-irradiated Si(111)", *MRS. Proc.* **908E**, OO2.4 (2005).
- M.J. Aziz, "Nanoscale Morphology Control Using Ion Beams", *Matematisk-Fysiske Meddelelser / udg. af Det Kongelige Danske Videnskabernes Selskab* **52**, 187 (2006).
- D.P. Adams, M.J. Aziz, G. Hobler, W.J. MoberlyChan, T. Schenkel, "Fundamentals of FIB Nanostructural Processing: Below, At and Above the Surface", *MRS Bulletin* (in press)

- N.H. Chou and R.E. Schaak, “Modified Polyol Synthesis and Superconducting Properties of β -Sn Nanospheres, Nanocubes, and Nanorods,” manuscript in preparation.
- F.A. Dawood, B.M. Leonard, and R.E. Schaak, “Solution Synthesis of Superconducting NiBi Powders, Films, and Patterned Microstructures,” manuscript in preparation.

This page is intentionally blank

One-dimensional Mesosstructures of NbSe₂ and NbN Superconductors

Zhili Xiao (Principal Investigator), Umesh Patel (Ph.D. student) and Curt DeCaro (M.S. student)

Department of Physics, Northern Illinois University, DeKalb, Illinois 60115

i) Program Scope

One dimensional (1D) mesostructures in the form of free-standing wires, ribbons and tubes have been the subject of intensive research in recent years due to their novel properties and intriguing applications [1-4]. Free-standing 1D superconducting mesostructures will be highly desirable in future electronic nanodevices as interconnects since they circumvent the damaging heat produced by energy dissipation in a normal nanoconductor whose high resistance is inversely proportional to its cross-section area. Furthermore, when Cooper pairs are squeezed into a small volume, their wave functions are strongly modified, and therefore, mesoscale superconductors are expected to exhibit properties that are different from bulk materials. Due to the confinement of Cooper pairs, new phenomena such as vortex-antivortex pairs and fractional flux quanta have been observed in 2D superconducting microstructures [5-8]. With further reduction of the dimensionality from 2D to 1D, a fundamental question arises as to how the collective properties of superconductors are affected. This issue is also of practical importance in defining the size limit of a superconducting wire with regards to potential applications in electronic circuits.

We aim to develop novel approaches to synthesize a new class of mesoscale 1D superconductors based on NbSe₂ and NbN and to explore their electronic properties. The materials are much more robust than currently available 1D superconductors. We also aim to extend the studies on 1D superconductors from nanoscale to microscale where interesting physics are expected and new applications may arise. The exploration of other geometries besides wires (e.g. ribbons) will also be pursued as a goal in this project. Vortex physics and nanoscale junctions are also our research focus. The size effect on the anisotropy of the nanostructures will be investigated with transport measurements in variable magnetic field directions.

ii) Recent Progress

The synthesis approach we have been developing is comprised of two-steps: first, to synthesize 1D mesostructures of NbSe₃ and second, to convert these into desired 1D superconducting mesostructures of NbSe₂ and NbN by adjusting their composition while maintaining their shapes. Due to the chain-like crystalline structure, NbSe₃ mesostructures including mesowires and mesoribbons can be achieved by simply sintering a mixture niobium and selenium powders at appropriate temperatures [9]. Thus, the essential part of the synthesis procedure is to transform NbSe₃ mesostructures into superconducting NbSe₂ and NbN while preserving their shapes. Since the reaction between nitrogen and niobium can only take place at extremely high temperature while the decomposition temperature of NbSe₃ is about 700 °C [9,10], it is extremely challenging to convert the NbSe₃ mesowires and mesoribbons into NbN without destroying their shapes. In the past months we tackled this problem on synthesis of NbN mesowires and mesoribbons. The synthesized NbN mesostructures were characterized with scanning electron microscopy, x-ray diffraction, magnetization and transport measurements. The main progresses are elaborated below:

1. Synthesis of NbN mesowires and mesoribbons

For the synthesis of NbSe₃ mesostructure precursors, stoichiometric quantities of high purity (>99.99%) niobium and selenium powders with particle sizes of several micrometers were combined. The mixture was ground and sealed in an evacuated quartz ampoule of 17 mm in inner diameter and ~15 cm in length, after purging repeatedly with high purity Ar gas to ensure an oxygen free environment [9]. By sintering the mixtures at appropriate temperatures NbSe₃ mesostructures were synthesized. In the conversion process, we tried two synthesis routes: annealing NbSe₃ nanostructures in a flowing ultrahigh purity (>99.999%) nitrogen gas with 4% hydrogen and in a flowing gas of ammonia. The first route, with annealing temperatures between 700 °C ~ 1000 °C produced white and yellow powders which showed no superconductivity at temperatures above 1.8 Kelvin. The white powder was identified as Nb₂O₅ and the

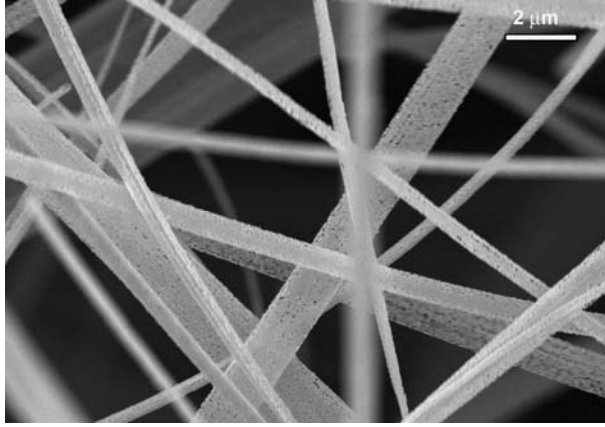


Fig.1. SEM micrograph of superconducting NbN mesowires and mesoribbons synthesized by annealing NbSe₃ mesostructure precursors in flowing ammonia gas at 950 °C for 2 hrs.

morphological analyses were performed with a scanning electron microscope (SEM) (Hitachi S-4700-II). Figure 1 shows a typical SEM micrograph for the NbN mesowires and mesoribbons synthesized through this route, where the annealing temperature was 950 °C and the annealing time was 2 hours. Although the annealing temperature is higher than the decomposition temperature of NbSe₃, the shape of NbSe₃ nanostructures did not collapse. This could mean that either the ammonia decomposed at low temperatures and NbN formed below the NbSe₃ decomposition temperature or the extremely active ionic hydrogen reduced the niobium oxide formed in low temperatures which enabled the ionic nitrogen to react with niobium. Systematic investigation on the formation mechanism is still underway.

2. Mechanism for the destruction of superconductivity in mesowires

The four-probe transport measurement is a convenient way to study superconducting properties of individual nanowires and nanoribbons. For potential applications as interconnects in nanodevices, one of the important properties for a nanowire is its capacity to carry transport currents. For this purpose, four-probe transport measurements of current-voltage (I - V) characteristics need to be done. Sudden voltage

yellow powder is composing of various phases of niobium oxides. This is consistent with the fact that the reaction between Nb and molecular nitrogen can only take place at extremely high temperatures and niobium is very reactive with oxygen. The second route, annealing NbSe₃ nanostructures in flowing ammonia gas at 700°C - 1000 °C, resulted gray products which showed superconductivity up to 11 Kelvin, as measured with both SQUID magnetometer (mesostructure bundle) and transport measurements (individual mesowire). X-ray diffraction analysis revealed that the gray products are mainly a NbN phase with a Nb to N ratio close to 1:1.2, i.e. the Nb₅N₆ phase. The formation of niobium nitride in flowing ammonia gas indicates that the ammonia was probably decomposed and ionic nitrogen replaced selenium in NbSe₃ mesostructures. The

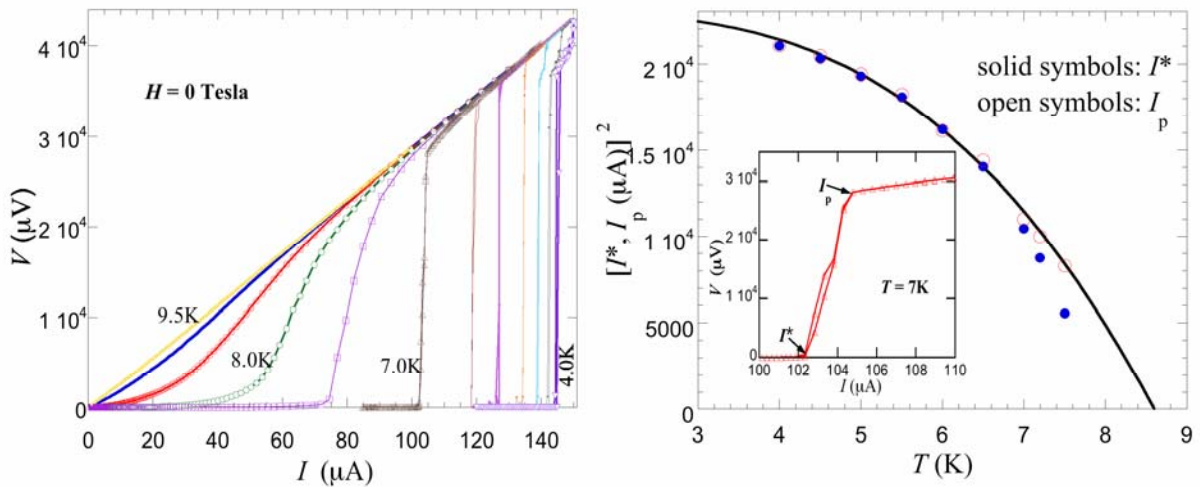


Fig.2. Left panel: voltage-current (I - V) characteristics of a NbN nanowire at zero field and various temperatures (the temperature interval is 0.5K). Sharp voltage increases can be identified in I - V curves obtained at temperatures below 7.5K. Right panel: temperature dependence of the characteristic current I^* and I_p as defined in the inset. The solid curve represents a fitting based on a self-heating mechanism.

increases have been observed in I - V characteristics of other superconducting nanowires in two-probe transport measurements [11] and qualitatively understood with a phase slip mechanism. However, other mechanisms such as self-heating and Josephson junctions can also induce voltage jumps in I - V curves. Furthermore, contact resistance can also cause complexity in two-probe transport measurements. By applying photolithography techniques we were able to make four contacts to NbN mesowires of various diameters and measured their I - V characteristics. As given in the left panel of Fig.2, voltage jumps appeared in I - V curves obtained at temperatures not very close to the critical temperature. Although the feature is similar to those reported in literature, a quantitative analysis indicates that self-heating is the origin for the voltage jumps observed in the I - V characteristics of our NbN mesowires.

3. Dynamics of few-row vortex lattices

When a type-II superconductor is placed in a magnetic field, the magnetic flux lines can penetrate in the form of vortices. Past research in vortex physics mainly focused on the collective properties of large numbers of strong interacting vortices in bulk superconductors where vortices form the well-known Abrikosov lattice and each vortex carries one flux quantum Φ_0 . Taking advantage of the progress in nanotechnology, scientists were very interested and able to study the vortex phenomena in so-called “few-flux-quanta” superconductors in which the superconductivity is destroyed by only a few vortices [5-8]. The NbN superconducting mesowires and mesoribbons provide unique platforms to study the “few-vortex-rows” superconductors [12] which contain only a few rows of vortices and the entrance and exit of each row can be detected, for example, as resistance oscillations with increasing magnetic fields in transport measurements. We carried out four-probe transport measurements on NbN mesowires/mesoribbons of various sizes in magnetic fields perpendicular to the wire axis. Oscillations were observed in the magnetic field dependence of both critical current and resistance as given in the left and right panels of Fig.3, respectively.

Efforts have also been made to carry out four-probe transport measurements on NbSe₂ mesowires and mesoribbons synthesized through sintering NbSe₃ mesostructure precursors with stoichiometrical Nb powder in evacuated quartz tubes. Related results will be presented at this workshop.

In addition to the progresses made in our research group at Northern Illinois University, we also provided mesowires and mesoribbons samples to our collaborators: Prof. Eva Andrei at Rutgers University, Dr. Rongying Jin at Oak Ridge National Laboratory and Prof. Milind Kunchur at South Carolina University. The Oak Ridge group recently submitted a manuscript entitled “Evidence for two Distinct Gaps in Superconducting NbSe₂ Nanowires” to *Physical Review Letters*.

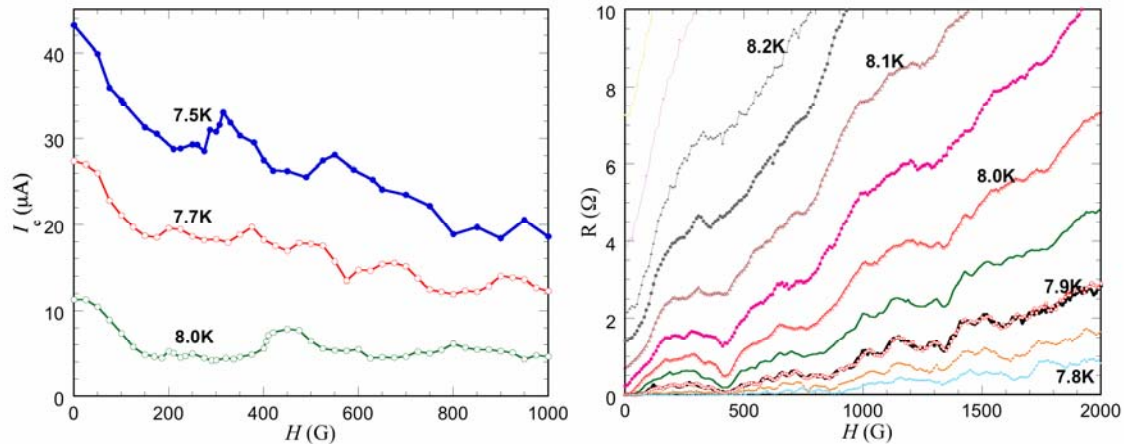


Fig.3. Magnetic field dependences of the critical current (left panel) and the magnetoresistance (right panel) at various temperatures. The magnetic field direction was perpendicular to the current which flows in the axis direction of the nanowire. The voltage criterion used to define the critical current is 1 μV .

iii) Future Plans

This project just started in August 2006, we will continue the research which has showed promising results, for example, the critical current and resistance oscillations in magnetic fields. Other planned research activities for the near future include:

Optimizing the synthesis parameters: so far we succeeded in obtaining both NbSe₂ and NbN mesowires and mesoribbons. However, efforts are needed to improve the quality of the synthesized samples. For example, the critical temperature (11 Kelvin) of the NbN mesostructures is lower than that (~16 Kelvin) of the bulk samples. It is also extremely challenging to precisely control the Nb:N ratio.

Andreev reflection at nanoscale junctions: by utilizing our mesowires we can achieve small junctions that enable us to pursue Andreev reflection at the nanoscale. We will study normal metal (e.g. Au)-superconductor (N-S) and ferromagnet (i.e. Fe)-superconductor (F-S) junctions. Superconductor-superconductor (S*-S) nanoscale junctions, which showed intriguing anti-proximity effect can also be conveniently obtained by forming the contact leads with superconductors (e.g. Nb).

Size effect on superconducting anisotropy: We will conduct studies on the anisotropy of the synthesized NbSe₂ and NbN mesostructures. It is especially interesting to probe the NbSe₂ mesostructures because NbSe₂ itself is a layered material with strong anisotropy. Furthermore, surface superconductivity will also dominate in these tiny superconductors that will make the investigations more challenging.

iv) References

1. J. T. Hu, T. W. Odom, and Ch. M. Lieber, *Acc. Chem. Res.* **32**, 435 (1999).
2. M. S. Dresselhaus et al., *Mater. Sci. Eng. C* **23**, 129 (2003).
3. Z. L. Wang, *J. Phys.-Cond. Mat.* **16**, R829-R858 (2004).
4. Y. N. Xia et al., *Adv. Mater.* **15**, 353 (2003).
5. A. K. Geim et al., *Nature* **390**, 259 (1997).
6. C. A. Bolle et al., *Nature* **399**, 43 (2000).
7. A. K. Geim et al., *Nature* **407**, 55 (2000).
8. L. F. Chibotaru, A. Ceulemans, V. Bruyndoncx, and V. V. Moshchalkov, *Nature* **408**, 833 (2000).
9. Y. S. Hor et al., *Nano Lett.* **5**, 397 (2005).
10. Y. S. Hor et al., *Appl. Phys. Lett.* **87**, 142506 (2005).
11. M. L. Tian et al., *Phys. Rev. B* **71**, 104521 (2005).
12. J. J. Palacios, Vortex lattices in strong type-II superconducting two-dimensional strips, *Phys. Rev. B* **57**, 10873 (1998).

v) Publications in the last two years

1. Zhixian Zhou, R. Jin, Gyula Eres, D. Mandrus, Victor Barzykin, P. Schlottmann, Y. S. Hor, Z. L. Xiao, and J. F. Mitchell, Evidence for two Distinct Gaps in Superconducting NbSe₂ Nanowires, *Physical Review Letters* (submitted, 2007).
2. J. Hua, Z. L. Xiao, D. Rosenmann, I. Beloborodov, U. Welp, W. K. Kwok, and G. W. Crabtree, Resistance anomaly in Disordered Superconducting Films, *Applied Physics Letters* **90**, 072507 (2007).
3. G. H. Li, E. Y. Andrei, Z. L. Xiao, P. Shuk, and M. Greenblatt, Onset of motion and dynamic reordering of a vortex lattice, *Physical Review Letters* **96**, 084502 (2006).
4. Y. S. Hor, U. Welp, Y. Ito, Z. L. Xiao, U. Patel, J. F. Mitchell, W. K. Kwok and G. W. Crabtree, Superconducting NbSe₂ nanowires and nanoribbons converted from NbSe₃ nanostructures, *Applied Physical Letters* **87**, 142506 (2005).
5. T. Xu, M. P. Zach, Z. L. Xiao, D. Rosenmann, U. Welp, W. K. Kwok and G. W. Crabtree, Self-assembled monolayer promoted hydrogen sensing of ultra-thin palladium films, *Applied Physical Letters* **86**, 203104 (2005).
6. Y. S. Hor, Z. L. Xiao, U. Welp, Y. Ito, J. F. Mitchell, R. E. Cook, W. K. Kwok, and G. W. Crabtree, Nanowires and nanoribbons of charge-density-wave conductor NbSe₃, *Nano Letters* **5**, 397 (2005).
7. U. Welp, Z. L. Xiao, V. Novasad, and V. K. Vlasko-Vlasov, Commensurability and strong vortex pinning in nanopatterned Nb films, *Physical Review B* **71**, 014505 (2005).

Plasmonic Dispersion Engineering for Light-Emission Efficiency Enhancement

R. Paiella

Department of Electrical and Computer Engineering, Boston University, 8 St. Mary's Street, Boston, Massachusetts 02215
Phone: 617-353-8883, Fax: 617-353-1283, Email: rpaiella@bu.edu

1. Program Scope

Surface plasmon polaritons (SPPs) at metal/dielectric interfaces are promising for many applications in sub-wavelength integrated optics, sensing, and optoelectronics, due to their unique optical properties. The broader goal of this research program is to design and develop nanoscale metallo-dielectric multiple-layer structures in which the SPP dispersion characteristics can be engineered to optimally meet these applications. Specifically, our focus is on the use of SPPs to enhance the efficiency of solid-state light emitting diodes (LEDs) – an application that has attracted considerable interest following recent experimental demonstrations with (In)GaN, ZnO, and dye-doped polymer devices [1-3].

SPPs are bound electromagnetic modes guided at metal-dielectric interfaces, whose fields are strongly localized near the interface and whose density of states (DOS) is highly enhanced near their resonance frequency ω_{SPP} . Due to these features, if a metal film is deposited in close proximity of an LED active layer, the device internal quantum efficiency can be strongly increased through the emission of SPPs [4,5]. These guided modes can then be converted into radiative waves with a grating, or even by the roughness of the metal surface [1-3]. However, for this approach to be effective the LED emission frequency needs to be closely matched to the SPP resonance ω_{SPP} , which for a single metal film is entirely determined by the dielectric functions of the metal and emitter material. If the emission frequency differs from ω_{SPP} the SPP efficiency enhancement is strongly reduced [1]. Thus the practical development of SPP-enhanced LEDs will require a technique to effectively tune by design the SPP resonance to match the desired LED output wavelength.

A possible solution recently proposed by the author is the use of strongly coupled SPP modes in metallo-dielectric multiple layers [6]. These structures allow to tailor the SPP dispersion curves $\omega(k)$ so as to introduce tunable singularities in the SPP-DOS (which is inversely proportional to the slope $d\omega/dk$), and hence in the quantum efficiency enhancement of nearby emissive layers. An example of this approach is illustrated in Fig. 1, where we plot the SPP dispersion curves for a single 100-nm-thick Ag film (Fig. 1a) and for a Ag(8nm)/TiO₂(12nm)/Au(23nm)/TiO₂ stack (Fig. 1b) deposited on GaN LED substrates. These curves were computed from Maxwell's equations using a Drude model of Ag and Au for simplicity. In Fig. 1a the slope $d\omega/dk$ rapidly increases as the photon energy is decreased below ω_{SPP} (~ 2.9 eV for Ag on GaN); as a result the SPP-DOS and the quantum efficiency enhancement are peaked near ω_{SPP} and rapidly drop off away from this resonance. Thus the use of a single Ag film on nitride LEDs is suitable for devices emitting near 2.9 eV (in the blue-violet spectral region), consistent with experiments [1].

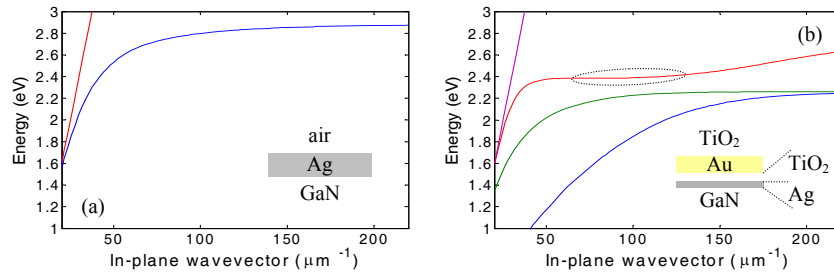


Fig. 1: SPP dispersion curves of a single Ag film (a) and a Ag(8nm)/TiO₂(12nm)/Au(23nm)/TiO₂ stack (b) on GaN substrates. The dashed straight line in each plot is the light line in GaN.

In the case of the Ag/TiO₂/Au/TiO₂ stack, the SPP dispersion curves can be substantially modified by properly selecting the layer thicknesses. In particular, through the mixing and anticrossing of SPP modes localized at neighboring interfaces it is possible to cause a flattening of these curves, and hence singularities in the SPP-DOS, at photon energies that are tunable by design. An example of such flattening is indicated by the circle in Fig. 1b. The SPP modes within this region are delocalized across the entire stack and have relatively large penetration depth in

the GaN LED substrate; combined with their large DOS, this leads to a strongly enhanced SPP emission rate in the spectral vicinity of these modes (in the green spectral region around 2.4 eV). We emphasize that the photon energy of peak enhancement can be tuned over a relatively wide range by varying the thicknesses of the metal and dielectric layers.

The goal of this research program is to develop and investigate these and similar metallo-dielectric multiple-layer structures, and use them to demonstrate large light emission efficiency enhancements in nitride-based LEDs. It should be mentioned that these structures also have promising applications in the areas of sub-wavelength waveguides, slow light, and negative refraction, as discussed in recent theoretical publications [7,8]. The experimental platform developed in this program – where SPPs are excited over a wide range of k values by the near-field of the LED active-layer emission – will also contribute to enable these other applications of metallo-dielectric multiple layers by advancing our understanding of their SPP dispersion characteristics.

2. Recent Progress

In this initial phase of the program we have carried out a more rigorous theoretical study of SPP emission in the proposed structures, using a model that allows for a more realistic description and hence more accurate design of these structures. Additionally, we have fabricated and characterized a first batch of samples based on GaN/AlGaIn quantum-well substrates emitting in the near UV.

In our previous work [6], the dispersion characteristics of SPPs in metallo-dielectric stacks were modeled by treating all metal films as ideal free-electron gases, and the excitation of these modes by a nearby LED active layer was studied using Fermi golden rule. This treatment provides a simple and intuitive description of the resulting quantum efficiency enhancement [5]; however it does not account for the spectral broadening resulting from the SPP damping losses in the metals, a simplification which can be expected to limit its quantitative predictive accuracy. To improve upon this initial analysis we have employed a more rigorous theoretical model, which was developed to study molecular fluorescence near metal surfaces [9,10] and which allows computing the spontaneous emission rate over the entire k - ω plane. Additionally, in these new calculations we describe all metals by means of their experimentally determined complex dielectric functions (as reported in refs. 11 and 12) rather than an elementary Drude response.

The details of this theoretical model can be found, e.g., in refs. 9 and 10. The emitter is treated as an electric dipole source of frequency ω whose radiated field is expanded in a sum of plane or evanescent waves over all values of the in-plane wavevector k . For all these component waves, the correspondingly reflected waves from the metallo-dielectric stack are calculated using a matrix technique and their amplitudes added. The spontaneous emission rate is then computed from the scalar product of the dipole moment with the total (emitted plus reflected) field at the dipole location. The resulting rate is finally divided by the same quantity in the absence of any metallo-dielectric layers to yield the spontaneous emission rate enhancement $F_r(\omega)$ (analogous to the Purcell factor).

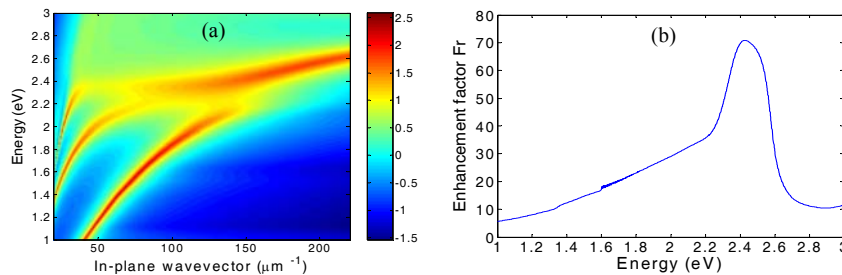


Fig. 2: Spontaneous emission rate enhancement of the metallo-dielectric stack of Fig. 1b, plotted as a log10-scale color map on the k - ω plane (a) and integrated over k and plotted versus ω (b). An 8-nm separation between the emissive layer (e.g. an InGaIn quantum well) and the Ag film is assumed in these calculations.

Shown in Fig. 2 are the results of this analysis for the Ag/TiO₂/Au/TiO₂ stack on GaN of Fig. 1b. The log10-scale color map of Fig. 2a gives the contribution to $F_r(\omega)$ from the component wave of in-plane wavevector k , plotted over the relevant range of the k - ω plane. The SPP modes of the dispersion curves of Fig. 1b are clearly seen to produce a large enhancement in the spontaneous emission rate, by an amount that depends on their damping rate and their penetration depth into the emissive layer. Fig. 2b gives the overall enhancement $F_r(\omega)$, which displays a pronounced peak near 2.4 eV as expected from the large SPP-DOS at this photon energy. A very large peak value of $F_r = 71$ is computed in this example, resulting in a strong enhancement of the LED overall efficiency by an

amount that depends on the nonradiative recombination rate [6]. Shown in Fig. 3 are similar results for an Al(4nm)/HfO₂(10nm)/Ag(10nm)/HfO₂ stack on AlGa_N, designed for maximum enhancement near 3.6 eV in the near UV. While smaller than in the previous example (due to the larger SPP damping rate in Al compared to Ag), the computed peak value of $F_r = 42$ is also large enough to produce a substantial enhancement of the overall light emission efficiency.

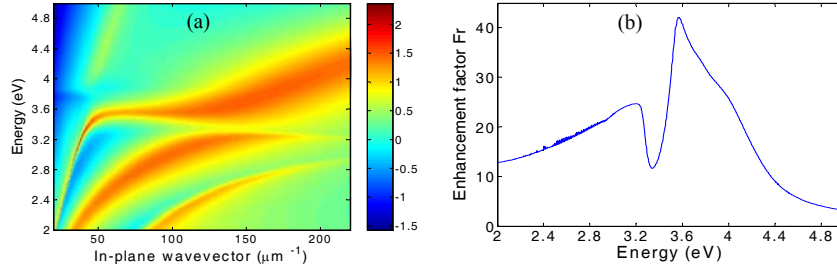


Fig. 3: same as Fig. 2 for the case of an Al(4nm)/HfO₂(10nm)/Ag(10nm)/HfO₂ stack on an AlGa_N substrate, with a 5-nm separation between the emissive layer and the Al film.

On the experimental side, we have fabricated and tested a few samples involving either single Al films or Al/HfO₂/Ag/HfO₂ stacks on GaN/AlGa_N quantum-well substrates emitting in the near UV. The semiconductor material was grown by molecular beam epitaxy (MBE) by Dr. Moustakas' group at Boston University. The metal and dielectric films were deposited by electron-beam evaporation, and the samples were characterized with photoluminescence measurements at room temperature. In the fabrication of these initial samples, no effort was devoted to intentionally introduce roughness in the deposited layers. The presence of roughness (or alternatively of a lithographically defined grating) is however essential to out-couple the emitted SPPs to radiation [1-3], or else the presence of a metal film near the emissive layer would actually result in a decrease of the LED output light [5]. Thus the investigation of the optimal deposition conditions to introduce the required roughness (at least in the uppermost layer) is an important aspect of this research, currently being explored.

In any case, as shown in Fig. 4 we have observed in one sample an increase in the overall light emission efficiency near 340 nm mediated by the emission and subsequent out-coupling of SPPs in a single Al film. In this figure, the solid black and dashed blue lines are the emission spectra of a reference uncoated sample and a sample coated with an Al layer, respectively, originating from two adjacent pieces on a same wafer (the measured wavelength range is limited on the short end by the wavelength of the HeCd pump laser). The integrated intensity emitted from the Al-coated sample is about 2.7 times larger than that from the reference sample. This is a sizable enhancement although it is smaller than in previous reports with other light-emitting materials and/or metals [1-3], which can be ascribed to the mismatch between the emitted photon energy of 3.6 eV and the resonance ω_{SPP} of over 5 eV for Al on AlGa_N.

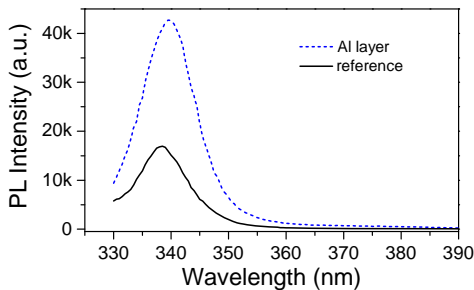


Fig. 4: emission spectra providing evidence of SPP-induced efficiency enhancement

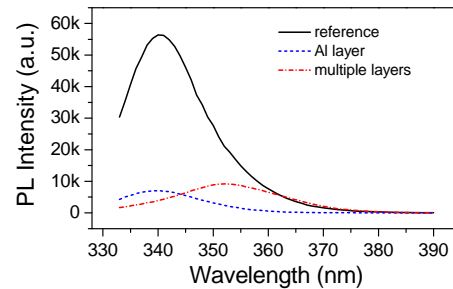


Fig. 5: emission spectra providing evidence of dispersion-engineered SPPs in an Al/HfO₂/Ag/HfO₂ stack on an AlGa_N substrate

Shown in Fig. 5 are the measured emission spectra of three adjacent pieces from another wafer, one with no metal coverage (solid black line), one capped with a single Al film (dashed blue line), and one coated with an Al/HfO₂/Ag/HfO₂ stack (dash-dotted red line). The nominal layer thicknesses of the latter structure (5, 14, 11, and 50 nm respectively) were selected based on a previous version of our design model so as to introduce a resonance peak in the SPP-DOS near 340 nm. No SPP-induced light emission efficiency enhancement is observed with these samples, which is ascribed to insufficient roughness in these deposited films and semiconductor substrate to

effectively out-couple the emitted SPPs. However, while the emission spectrum of the sample with the single Al film is simply a reduced replica of the reference spectrum (consistent with the relatively flat low-energy tail of $F_r(\omega)$ for a single metal layer), the emission spectrum of the sample with the multiple layers is substantially shifted, i.e. it peaks at about 352 nm instead of 340 nm. This is also consistent with expectations since by design the SPP emission rate in this sample is maximum near 340 nm; thus at this wavelength a particularly large number of SPPs are emitted and eventually lost in the flat metal films, at the expense of radiative waves at the same wavelength. Therefore, these data provide experimental evidence of the modification of the SPP dispersion characteristics and DOS allowed by the proposed metallo-dielectric stacks.

3. Future Plans

Following these promising results, we now plan to fully demonstrate the use of dispersion-engineered SPPs for light emission efficiency enhancement. To that purpose, we are currently carrying out a systematic study of layer thickness control and intentionally introduced roughness versus e-beam evaporation conditions. At the same time, we are further refining our design model to explicitly include the SPP out-coupling efficiency into radiation. We will then develop and characterize SPP-enhanced LEDs based on various configurations, beginning with single metal films of varying thicknesses and then progressing to more sophisticated metallo-dielectric stacks as described in the previous sections. The use of gratings (e.g. in the uppermost dielectric layer) fabricated by e-beam lithography will also be explored if needed to obtain more reproducible SPP out-coupling.

In these experiments we will employ nitride-based samples consisting of InGaN/GaN and GaN/AlGaIn quantum wells, emitting in the green and near-UV respectively (two spectral regions where substantial margins of improvement exist with respect to LED quantum efficiency). Several combinations of quantum-well design (i.e. LED emission wavelength) and metallo-dielectric stack design will be investigated, so as to fully demonstrate the tunability of the proposed approach. At the same time, the results of these measurements will allow us to infer quantitative information about the dispersion and damping properties of SPPs in strongly coupled metallo-dielectric multiple layers, which will potentially benefit other applications of these surface waves. Additionally, in the final phase of this program, we will pursue the use of the proposed approach to improve the performance of electrically-injected LEDs.

4. References

- [1] K. Okamoto, I. Niki, A. Shvartser, Y. Narukawa, T. Mukai, and A. Scherer, "Surface-plasmon-enhanced light emitters based on InGaN quantum wells," *Nature Materials* **3**, 601-605 (2004).
- [2] C. W. Lai, J. An, and H. C. Ong, "Surface-plasmon-mediated emission from metal-capped ZnO thin films," *Appl. Phys. Lett.* **86**, 251105 (2005).
- [3] T. D. Neal, K. Okamoto, and A. Scherer, "Surface plasmon enhanced emission from dye doped polymer layers," *Opt. Express* **13**, 5522-5527 (2005).
- [4] W. L. Barnes, "Electromagnetic crystals for surface plasmon polaritons and the extraction of light from emissive devices," *J. Lightwave Technol.* **17**, 2170-2182 (1999).
- [5] I. Gontijo, M. Boroditsky, E. Yablonovitch, S. Keller, U. K. Mishra, and S. P. DenBaars, "Coupling of InGaN quantum-well photoluminescence to silver surface plasmons," *Phys. Rev. B* **60**, 11564-11567 (1999).
- [6] R. Paiella, "Tunable surface plasmons in coupled metallo-dielectric multiple layers for light-emission efficiency enhancement," *Appl. Phys. Lett.* **87**, 111104 (2005).
- [7] A. Karalis, E. Lidorikis, M. Ibanescu, J. D. Joannopoulos, and M. Soljacic, "Surface-plasmon-assisted guiding of broadband slow and subwavelength light in air," *Phys. Rev. Lett.* **95**, 063901 (2005).
- [8] H. Shin and S. Fan, "All-angle negative refraction for surface plasmon waves using a metal-dielectric-metal structure," *Phys. Rev. Lett.* **96**, 073907 (2006).
- [9] G. W. Ford and W. H. Weber, "Electromagnetic interactions of molecules with metal surfaces," *Phys. Rep.* **113**, 195-287 (1984).
- [10] W. L. Barnes, "Fluorescence near interfaces: the role of photonic mode density," *J. Mod. Opt.* **45**, 661-699 (1998).
- [11] P. B. Johnson and R. W. Christy, "Optical constants of noble metals," *Phys. Rev. B* **6**, 4370-4379 (1972).
- [12] E. D. Palik, ed., *Handbook of Optical Constants of Solids* (Academic Press, New York, 1985).

5. Publications related to this project

- [1] R. Paiella, "Tunable surface plasmons in coupled metallo-dielectric multiple layers for light-emission efficiency enhancement," *Appl. Phys. Lett.* **87**, 111104 (2005).
- [2] R. Paiella and M. Cunha, "Plasmonic dispersion engineering for light emission efficiency enhancement," *IEEE Conference on Lasers and Electro-Optics*, paper CWB2, Long Beach (CA), 2006.

Investigations into the Electronic and Magnetic Behavior of Semiconductor-Transition
Metal Clusters via Velocity Map Imaging

S.J. Peppernick and A.W. Castleman, Jr.

The Pennsylvania State University

University Park, PA 16802

Recently, a Velocity map imaging (VMI) instrument has been constructed by the Castleman Group to investigate the electronic properties of atoms, molecules and clusters. The VMI technique essentially takes digitized pictures, via a charged coupled device camera, of expanding electrons from a photodetachment event. These electron snapshots can then be converted to photoelectron spectra from which electron affinities, HOMO-LUMO gaps, and vibrational separations (useful for structural analysis) can be measured. Moreover, VMI can also simultaneously measure the angular distribution of the detached electrons, whereby a quantity called the anisotropy parameter can be calculated. This anisotropy parameter is useful for inferring the nature of the atomic or molecular orbital the ejected electron came from. Silicon clusters can form fullerene like cages with the addition of a single or multiple endohedral transition metals. Elucidating both the electronic and magnetic properties of these silicon transition metal clusters (Si_xM_y where $\text{M} = \text{Cr}, \text{Mb}, \text{W}$) via the VMI technique is paramount in understanding these clusters for their potential technological applications as building blocks in cluster assembled solids. The latest experimental findings will be presented.

We gratefully acknowledge funding from the U. S. Department of Energy, Building Blocks: DE-FG02-02ER46009.

This page is intentionally blank

Al_4H_7^- : A Resilient Building Block for Aluminum Hydrogen Cluster Materials

P. J. Roach, W. H. Woodward, and A.W. Castleman, Jr.

*The Pennsylvania State University, Department of Chemistry and Physics,
Chemistry Research Building, University Park PA, 16802*

A.C. Reber and S.N. Khanna

*Department of Physics, Virginia Commonwealth University,
Richmond, VA 23284, USA.*

The electronic structure of aluminum clusters can be described by a jellium shell model, allowing the chemical behavior of specific clusters to be explained in a superatom context. Because the number, identity and hybridization behavior of the atoms that constitute a free-electronic cluster dictate its outward chemical reactivity, it is necessary to understand the factors that result in a superatomic chemical identity. Furthermore, a realization of the exploitation of superatoms as building blocks in cluster-assembled materials will only come concomitantly with an understanding of the extent and limitations of the outward manifestation of superatomic chemical behavior. Current investigations have been directed at understanding evolution of the electronic structure of small aluminum clusters with hydrogen addition to understand how and why a specific cluster can absorb and store hydrogen. Special attention is being given toward intermediate species that may be formed in “bottom-up” synthetic attempts of a stable high energy density cluster-assembled material.

We gratefully acknowledge financial support from the United States Department of Energy; DOE Building Blocks DE-FG02-02-ER46009

This page is intentionally blank

Asymmetric Hybrid Nanoparticles

Stephen Hudson and George Chumanov
shudson@clemson.edu, gchumak@clemson.edu
Department of Chemistry, Clemson University, Clemson, SC 209634

Program Scope

Asymmetric Hybrid Nanoparticles (AHNs) are rationally-designed multifunctional nanostructures and novel building blocks for the next generation of advanced materials and devices.

Nanoscale materials attract considerable interest because of their unusual properties and potential for practical applications. Most of the activity in this field is focused on the synthesis of homogeneous nanoparticles from metals, metal oxides, semiconductors, and polymers. It is well recognized that properties of nanoparticles can be further enhanced if they are made as hybrid structures. This program is concerned with the synthesis, characterization, and application of such hybrid structures termed AHNs. AHNs are composed of a homogeneous core and several caps of different materials deposited on its surface (**Fig. 1**). Combined properties of the core and the caps as well as new properties that arise from core-cap and cap-cap interactions render AHNs multifunctional. In addition, specific chemical reactivity of the caps enables directional self-assembly of AHNs into complex architectures that are not possible with only spherical nanoparticles.

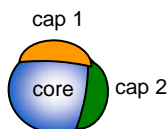


Fig. 1 A general structure of AHNs with two caps

The specific focus is on plasmonic AHNs and their application in photovoltaic devices, for capturing and storing of light energy, and as nonlinear optical materials. Plasmonic AHNs will have Ag cores with multilayered semiconductor, dielectric, and magnetic caps. Ag nanoparticles (Ag NPs) exhibit unique optical properties arising from the excitation of plasmon resonances. Plasmon resonances can be tuned across the visible spectral range by varying the particle size, shape, and dielectric environment.¹ Their excitation in Ag NPs represents the most efficient mechanism by which light interacts with matter¹. Because of this efficiency, tunability, and photochemical robustness, plasmonic AHNs are ideal for applications involving interaction with light.

Recent Progress

The main focus during the first 6 month in the program was on the development of the instrumentation and methodology for depositing caps on the surface of Ag NPs. Thermo-evaporation of materials in vacuum was selected as first technique. This technique was previously used to deposit caps from gold²⁻⁷, platinum, palladium², nickel⁴, Ag, Cu, Cr³, and Al^{3,8} on submicron glass and polystyrene beads. The beads, however, played a passive role of a structural support for the caps and their properties were not included into the hybrid nanostructures. In this work, plasmonic AHNs were synthesized for the first time and optical properties of the core constitute an inherent part of the multifunctional structure.

The following procedure for synthesizing AHNs was developed. Ag NPs were first assembled onto glass substrates modified with poly(4-vinylpyridine) that was previously demonstrated to be a 'universal surface modifier' for immobilization of NPs. The assembly took place from suspensions of low ionic strength in order to provide electrostatic repulsion between the electric double layers associated with the metal NPs. This repulsion is required to maintain large separation between the particles so that the deposited caps on neighboring particles do not overlap. Deposition of the caps was carried out in a vacuum chamber equipped with a custom designed substrate holder that allows changing the deposition angle and utilizing both

sides of substrate. After the deposition the AHNs were stripped into different solutions using mild sonication.

One of the goals of these initial studies was to demonstrate the fabrication of AHNs with different caps and to investigate the effect of the caps of the plasmon resonance in the plasmonic core. One of the concerns related to the adhesion of the caps to the surface of Ag NPs. The adhesion should be sufficiently to at least be capable of withstanding of sonication during the removal the AHNs from the substrates. The two polymers, poly(4-vinylpyridine) and poly(dimethylallylamine), were tested for an adhesion layer between the core and of different caps. Both polymers gave positive results, however, many caps adhered sufficiently strong to Ag NPs even without the polymers adhesion layer.

Caps of different materials, specifically of SiO, LiF, Ti, Al, Cr, Ni, and Fe were successfully deposited onto Ag NPs. These represent high (SiO) and low (LiF) refractive index materials, two metals (Ti, Al) that can be deposited in the metallic form but oxidize upon exposure to ambient atmosphere, and the three metals (Cr, Ni, and Fe) as magnetic materials. The effect of these caps on plasmon resonance in Ag cores can be summarized as following. As was expected, depending upon the value of the real and imaginary parts of the refractive index of the cap materials the shift of the frequency and damping of the plasmon resonance occurred. For the large real and small imaginary parts, both dipole and quadrupole components of the resonance shifted to the red spectral range for AHNs as compared to the same Ag NPs without the caps. All measurements were performed with particles suspended in water. An unexpected result, potentially representing a new phenomenon was encountered with LiF caps. Even though the refractive index of this material is larger than that of water, a blue shift of the plasmon resonance was observed as opposed to an expected red shift. This behavior was attributed to the presence of a large dipole moment (6.3 Debye) in LiF molecules. When these molecules are vectorially oriented on the Ag NP surface they produce local electrostatic field that can 'push' the electron density from the surface layer more into the interior of the core. This redistribution of the electrons increases the electron density in the core or, in other words, reduces the effective size of the plasmonic particle, the two factors that could lead to the observed blue shift of the plasmon resonance frequency. Partial damping of the plasmon resonance was observed for cap materials that have large imaginary part of the refractive index.

The AHNs technology provides an opportunity to add magnetic properties to otherwise nonmagnetic nanoparticles. Out of the three metals tested for this purpose, Cr caps did not produce AHNs with noticeable magnetic response. The lack of the magnetic response was attributed to the oxidation of the Cr cap to its nonmagnetic oxide form. Both Ni and Fe caps produced plasmonic AHNs that responded to a magnetic field. Although the response of Fe AHNs was several times stronger than that of Ni AHNs, the Fe cap produced significant plasmon damping. This damping was attributed to the large imaginary part of the refractive index of the paramagnetic iron oxide that was formed after exposing the Fe AHNs to water. Also the direct electronic coupling between the Ag core and the oxide cap contributed to plasmon damping. Two strategies were implemented to minimize the plasmon damping. A thin

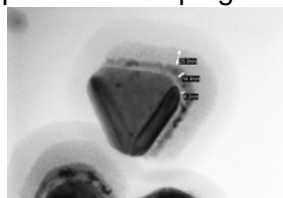


Fig. 2 Triple layered magnetic plasmonic AHNs composed of 90 nm Ag core, 8.2 nm SiO spacer, 14.4 nm Fe cap, and 25 nm SiO overlayer to protect oxidation of Fe.

layer of SiO was deposited onto Ag NPs prior to the deposition of the Fe caps to act as an insulating spacer and to reduce plasmon damping. In addition, another SiO layer was deposited on top of the Fe cap to prevent Fe from oxidation. Smaller losses in the visible spectral range were expected from the Fe metal as compared to its oxides because the latter (Fe_2O_3) is known to be a semiconductor with ca. 2.2 eV band gap. Also, the Fe cap can render the AHNs to be ferromagnetic where as iron oxide caps are superparamagnetic in the form of nanosize particles. Implementation of these approaches practically eliminated plasmon dumping. As a result, triple layered plasmonic AHNs were synthesized that exhibit strong

magnetic properties and strong unattenuated plasmon resonance in the visible spectral range **Fig. 2**. Extended optimization of the spacer layer thickness between the Ag core and the Fe cap was performed and its effect on the resonance was studied and compared to the same AHNs without Fe caps **Fig. 3**. Plasmonic AHNs with magnetic properties were synthesized for the first time.

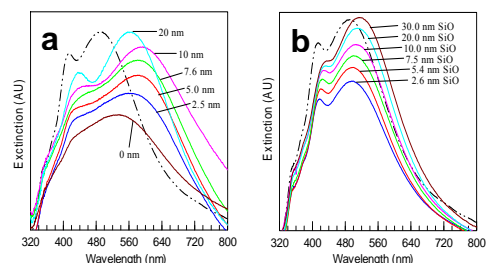


Fig. 3 Effect of the spacer layer thickness (SiO) on the plasmon resonance of (a) Fe plasmonic AHNs and (b) plasmonic AHNs without Fe caps.

Future Plans

Near-future work will proceed along several venues.

First we will continue to study magnetic plasmonic AHNs. Their magnetic properties and the oxidation state of the Fe and Ni caps will be characterized using SQUID and XPS, respectively. Experiment will be performed to vectorially orient these AHNs on substrate using a uniform magnetic field. The ability to vectorially orient these particles is required for nonlinear optical materials based on AHNs that are proposed in this program. In addition, the combination of magnetic properties with strong plasmon resonances in the visible spectral range, specifically when the core and the cap are weakly electronically coupled (partial plasmon damping) may result in novel magneto-optical materials of practical importance. Magneto-optical activity in suspensions of iron oxide nanoparticles were previously demonstrated.⁹ Here, the addition of plasmon resonance is expected to enhance magneto-optical activity due to the strong resonance interaction with light. We aim to detect the Faraday effect in the suspension of magnetic plasmonic AHNs.

Second, using the substrate holder that permits the deposition at different angles, SiO caps of varying size will be deposited onto Ag NPs. The caps will partially coat the surface of Ag NPs while the exposed metal surface will be subjected to chemical modification to induce interaction between the particles. With this approach, spontaneous formation of dimers, trimers and oligomers is expected in suspension. This type of assembly is termed site-selective self-assembly and its development is also a part of this program. This work will be extended to include two caps from different materials with distinctly different chemical properties. Interaction between different caps and between the caps and the exposed Ag surface will be exploited to drive the self-assembly to yield more complex clusters. Optical resonance in these clusters will be drastically different because of the plasmon coupling between particles. Plasmon coupling will be studied as a function of the interparticle spacing and the shape of the clusters. This approach based on the controlled manipulation of the plasmon coupling can potentially lead to novel optical properties of practical importance.

Once conditions for the site-directed self-assembly are established and enough experience with this technique is gained, experiment will be initiated to synthesize ring clusters of plasmonic AHNs. These clusters are proposed for storing of electromagnetic energy in the form of circulating plasmon modes.

Third, we will extend the range of materials for caps to include semiconductors. Our first choice is NiO, nonstoichiometric form of which is known to be a p-type semiconductor. Even though that, according to literature¹⁰, the films of this semiconductor were previously fabricated using plasma sputtering techniques, we will start our experiment with thermal evaporation of Ni metal in vacuum with partial pressure of oxygen to form NiO caps with semiconductor properties. The initial experiments will be performed on plane substrates without Ag NPs to find optimum conditions for the formation of the semiconductor films. Once these conditions are found, the deposition will be carried out onto Ag NPs to produce semiconductor plasmonic AHNs. Semiconductor plasmonic AHNs will be used in the future work for the development of photovoltaic devices that utilize plasmon resonances.

References

1. Evanoff, Jr. D. D.; Chumanov, G. *ChemPhysChem* 2005, **6**, 1221-1231.
2. Love, J. C.; Gates, Wolfe, D. B.; Paul, K. E.; Whitesides, G. M. *Nano Lett.* 2002, **2**, 891.
3. Cortie, M. B.; Liu, J.; Maarof, A. I.; Wieczorek, L. *Adv. Mater.* 2005, **17**, 1276-1281.
4. Correa-Duarte, M. A.; Salgueirino-Maciera, V.; Rodriguez-Gonzales, B.; Liz-Marzan, L. M.; Kosiorek, A.; Kandulski, W.; Giersig, M. *Adv. Mater.* 2005, **17**, 2014-2018.
5. Lu, Y.; Liu, G. L.; Kim, J.; Mejia, Y. X.; Lee, L. P. *Nano Lett.* 2005, **5**, 119-124.
6. Agayan, R. R.; Horvath, T.; McNaughton, B. H.; Anker, J. N.; Kopelman, R. *Proc. SPIE* 2004, **5514**, 502-513.
7. Himmelhaus, M.; Takei, H. *Phys. Chem. Chem. Phys.* 2002, **4**, 496-506.
8. Anker, J. N.; Kopelman, R. *Appl. Phys. Lett.* 2003, **82**, 1102-1104.
9. Royer, F.; Jamon, D.; Rousseau, J. J.; Cabuil, V.; Zins, D.; Roux, H.; Bovier, C. *The European Physical Journal*, 2003, **AP22**, 83-87.
10. Zhang, X.; Chen, G. *Thin Solid Films*, 1997, **298**, 53-56.

DOE Sponsored Publications, September 2006 - April 2007

Stephen D. Hudson, George Chumanov, "Synthesis and Characterization of Plasmonic Asymmetric Hybrid Nanoparticles" *Chemistry of Materials*, 2007, submitted.

Subtask Title: **ARTIFICIALLY STRUCTURED SEMICONDUCTORS for BIOPHOTONICS**

P.I. Paul Gourley, Sandia National Laboratories, Albuquerque, NM

Project Scope

This subtask project investigates biocompatible semiconductors and photonic physics of the material/biosystem interface. The scope of the program includes semiconductor material design, surface functionalization for biocompatibility, processing into micro/nanocavities, and study of optical transduction of biomolecules, pathogens, organelles, and whole biological cells on material surfaces. The goal is to investigate emerging physics of optical transduction of biological species integrated with material structures, and to identify and mitigate problems arising at the biosystem/semiconductor interface. We have recently focused attention on statistical physics of soft biological matter. These studies rely heavily on techniques borrowed from condensed matter physics and material optics and exploit the discoveries and innovations of nanolaser spectroscopy, laser correlation microscopy, and ultra-dark field light scattering to study spatial, spectral, and temporal correlation of the organization of biomatter in cells and bioparticles as it relates to bioenergetics and metabolism. A challenge arising from this work is to develop an understanding of the transduction mechanism of light generation in a microcavity with micron- or submicron-sized biological species. The particle geometry, dielectric properties, correlation, and their interaction with the semiconductor influence the spontaneous and stimulated light emitted. The appearance of quantum optical effects is expected when the particle size diminishes below the wavelength of the light emitted. Another challenge is to understand the physics of nanobio-transduction, how biological matter may be probed by photonic techniques that may lead to novel methods for detecting pathogens like virus particles and bacterial spores, and may have implications for assessing energy production of ethanol by fermentation processes in mitochondria.

Recent Progress

This project recently innovated nanolaser spectroscopy,¹ a unique and powerful new tool for the rapid analysis of biophysical properties of cells and submicron bioparticles like mitochondria. The nanolaser permits the precise measurement of a powerful new parameter $\Delta\lambda$ of cells and mitochondria. Unlike any other single chemical or biophysical measurement, $\Delta\lambda$ is a measure of the overall biophysical state of the cell and mitochondria. The biophysical state of a cell is a reflection of its “omic” profile--genomics, proteomics, lipidomics, glycomics, and metabolomics--which in turn results from the sum total of changes in biomolecular composition and subcellular organization of structures within the cell. The laser is illustrated in Fig. 1. showing a magnified view of a mitochondrion in the laser microcavity and an exploded view of a semiconductor/biomaterial interface. Whole cells, organelles, biomaterial layers or biomolecular solutions can be studied in the laser cavity, either in a static or flowing mode. Spectra generated from the laser can be used to characterize the flowing specimens or study the interaction of the flowing specimen with the material surface. Biocompatibility of the material/biofluid interface can also be studied by measuring changes in flow rate and particle adherence that occurs with different surface chemistries or functional groups.

The nanolaser can be configured with stationary or flow of individual cells, organelles, or bioparticles to measure $\Delta\lambda$ that is a function of the refractive index, a quantity that is closely related to the cell biomolecular composition, concentration, and particle size. When the internal refractive index is increased by the addition of a particle to the cavity the emitted light wavelength will experience a red shift

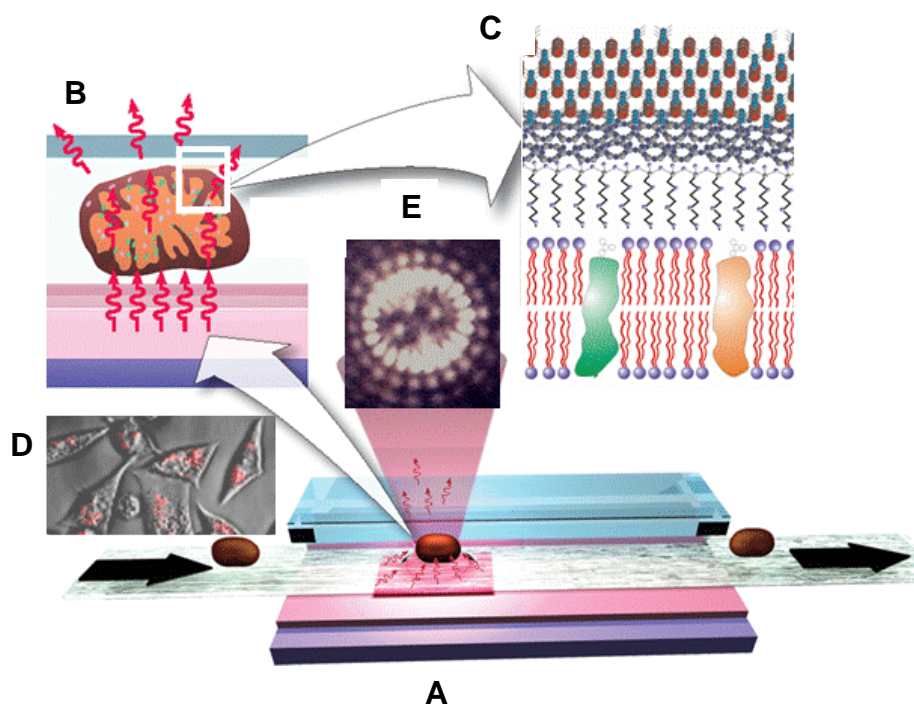


Fig. 1. (A) Schematic of flow system within a nanolaser. (B) Magnified view of a mitochondrion in the laser microcavity. (C) exploded view of material/biofluid interface comprising semiconductor, oxide layer, self-assembled monolayer, and bilipid layer of cell. (D) Cell culture with fluorescently labeled mitochondria that are isolated and flowed one by one through the laser cavity. With no special surface coating, whole cells tend to stick and limit flow time. In contrast, surface layers allow whole cells or mitochondria to flow for extended periods. The mitochondria interact with a submicron gain region (pink square) to produce a lasing mode (photo E) and spectrum used to analyze the mitochondrion biomolecular makeup.

in proportion to the index change. The red shift is a function of the cell and cavity geometry and optical parameters. The red shift is given approximately by $\Delta\lambda = \Gamma_m \Delta n d \lambda / n L$, where Δn is the refractive index difference of the cell relative to the index n of the fluid, d is the cell diameter, λ the laser wavelength, L the effective cavity length and Γ_m is an electromagnetic volume fraction for the particle. The red shift is proportional to Δn which in turn is a sum over the particle biomolecular contributions. The statistical variation of $\Delta\lambda$ within a population of bioparticles can be measured and studied to gain insight into their biomolecular makeup and biophysical behavior.

The laser technique has two important features. First, it is sensitive to very small changes in biomolecular composition of cells. Tiny changes in laser wavelength can be detected since the laser linewidth is very narrow, on the order of 0.01 nm. So, we expect to be able to detect small biomolecular changes that occur with genetic manipulation. Second, the laser is sensitive to very small objects like mitochondria and exploits a newly discovered nano-optical transduction method. Basically, this ultrasensitive detection of submicron particles uses “nano-squeezing” of light into photon modes imposed by submicron dimensions of a particle in a laser cavity. The condition for nano-squeezing is that the organelle must be approximately smaller than the wavelength of light. With these conditions met, the laser signal is amplified by spectral squeezing into a single intense optical mode, enhancing signal-to-noise ratio and making spectral analysis simple. This is an enabling critical advantage of the laser. Because the mitochondria are so tiny (0.4-0.7 μm in diameter), it has been difficult to study them using standard light microscope or flow cytometry techniques. And, electron or atomic force microscopies are limited to nonviable, fixed organelles so they cannot reproduce noninvasive physiologic measurements. Thus the nanolaser is an ideal tool for studying biomolecular changes in metabolically active mitochondria.

Ongoing and Future work

Very recently, we have responded to the need for basic research on renewable energy sources to lessen the U. S. dependence on foreign petroleum. Alternative energy sources abundant in North America are

grain crops for production of ethanol by fermentation. Ethanol production from plant starches occurs by anaerobic respiration (fermentation) by yeast fungi growing symbiotically with the plant or selected yeast fungi added later by design. Unfortunately, this inefficient process is limited by low tolerance of yeast metabolism to high alcohol concentration in culture. Ways to genetically alter this limitation by manipulating yeast metabolism would be highly desirable. We have begun studying the effects of genetic alteration of the electron transport chain and measurement of statistical physics of the yeast cells and their isolated mitochondria. Keys to this bioscience are biophysical/material tools to rapidly probe cell culture using the critical enabling tools of ultrafast nanolaser spectroscopy and nanoscopic imaging methods. Recently, Öner, et al.² showed that a petite strain of Baker's yeast—one in which the respiratory capacity of mitochondria is eliminated in ways that eliminate certain cellular cytochromes—produced over 40% higher ethanol concentrations (17% vs. 12%) than its parental, non-petite control strain. We will analyze similar normal and yeast mutants using nanolaser spectroscopy and fluorescent imaging by laser correlation microscopy. We will use a wild-type (ρ^+) strain of common baker's yeast, *Saccharomyces cerevisiae*. The altered strain will be derived from the wild strain by removal of its mitochondrial DNA (mtDNA).³

Approach

We will analyze 2 yeast cell mutants using nanolaser spectroscopy. The two yeast strains will differ only by the presence or absence of mitochondrial DNA. Strain 104 is a wild-type (ρ^+) strain of the baker's yeast, *Saccharomyces cerevisiae*. Strain 110 will be derived from strain 104 by removal of its mitochondrial DNA (mtDNA). Removal of mtDNA causes strain 110 to grow as a "petite" (ρ^-), named because it forms small colonies (of fewer cells because it grows more slowly) on agar plates supplemented with a variety of different carbon sources. The absence of mitochondrial DNA results in the complete loss of all the mtDNA-encoded proteins and RNAs, and loss of the pigmented, heme-containing cytochromes a and b. These cells have mitochondria, but the mitochondria lack the normal respiratory chain complexes I, III, IV, and V. Complex II is preserved because its subunits are encoded by genes located in nuclear DNA.

The nanolaser will be used to measure $\Delta\lambda$, a laser wavelength shift arising from the optical density of a cell or mitochondrion that is a unique biophysical property that reflects their physical size and biomolecular composition through the refractive index. For theoretical computation, the laser shift can be viewed as a frequency detuning of the cavity resonance in dimensionless units as $\delta = \Delta\lambda/\lambda = \Delta\omega/\omega$ where λ and ω are the fluid-filled cavity (without cell) resonance wavelength and frequency, respectively. Experimentally, $\Delta\lambda$ is measured in nanometers as the difference between a longitudinal laser mode of the fluid-filled cavity and the red-shifted laser wavelength produced by flowing cells or mitochondria through the cavity. The statistical variation of $\Delta\lambda$ within each population will be studied and modeled.

The biophysical parameter of statistical interest is the refractive index. We will model the refractive index of cells and mitochondria with the following equation:

$$\Delta n_i = \sum_i \alpha_i C_i = \sum_{\text{cytochromes}} \alpha_{ci} C_{ci} + \sum_{\text{proteins}} \alpha_{pi} C_{pi} + \sum_{\text{lipids}} \alpha_{li} C_{li} + \dots \quad (1)$$

Where α_i is the specific refractive increment for biomolecule i and C_i its concentration and the sum is over all biomolecules. If the C_i are normally distributed variables the distribution then takes the form of a convolution integral of variables d (which will have to be measured separately) and $\Delta n = \Delta\lambda/kd$, measured by laser spectra. We will use this result to provide the best, self-consistent fitting function to laser data to provide an explanation of the shapes of the distribution functions arising from a physical optics interpretation.

Summary

Nanolaser spectroscopy represents a unique and powerful new tool for the rapid analysis of biophysical properties of cells and submicron bioparticles like mitochondria. The spectra enable the precise measurement of a powerful new parameter $\Delta\lambda$ of cells and mitochondria. Unlike any other single chemical or biophysical measurement, $\Delta\lambda$ is a measure of the overall biophysical state of the cell and mitochondria. This tool is unique in its ability to probe statistical thermodynamics and to allow quantitative testing of new biophysical models of the optics of cells, isolated mitochondria, and other biomaterials. In the work proposed here, we will use both microscopy and spectroscopy to study mitochondria that have been manipulated by physical, chemical, and genetic means to form biomaterials with unique biophysical and optical properties.

References

1. "Nano-squeezed Light for Probing Mitochondrial Membrane Swelling and Study of Neuroprotectants," P. L. Gourley, P. Chen, R. G. Copeland, J. D. Cox, J. K. Hendricks, A. E. McDonald, and D. Y. Sasaki, *Proc. Conference on Microfluidics, BioMEMS, and Medical Microsystems SPIE* **5345**, 51-60 (2004).
2. "Production of ethanol from starch by respiration-deficient recombinant *Saccharomyces cerevisiae*," E. T. Öner, S. G. Oliver, B. Kirdar, *App Environ Microbiol* **2005**;71:6443-6445.
3. "Two nuclear mutations that block mitochondrial protein import in yeast.," M.P. Yaffe and G. Schatz, *Proc. Natl. Acad. Sci. USA* **81**, 4819-4823 (1984).

Publications

1. "Biomolecular Divergence in Genetically Altered Yeast and Isolated Mitochondria as Measured by Nanolaser Spectroscopy," Paul L. Gourley, Judy K. Hendricks, Anthony E. McDonald, R. Guild Copeland, Michael P. Yaffe, Robert K. Naviaux, *J. Biomedical Optics*, submitted Dec. 2006.
2. "Biocavity Laser Spectroscopy of Genetically-altered Yeast Cells and Isolated Yeast Mitochondria," Paul L. Gourley, Judy K. Hendricks, Anthony E. McDonald, R. Guild Copeland, Robert K. Naviaux, Michael P. Yaffe, *Proceedings of SPIE conference on Imaging, Spectroscopy, and Manipulation of Molecules, Organelles and Cells*, San Jose, CA, Jan. 23-25, 2006. published 5/06.
3. "Mitochondrial Correlation Microscopy and Nanolaser Spectroscopy," P. L. Gourley, J. K. Hendricks, A. E. McDonald, R. G. Copeland, K. E. Barrett, C. R. Gourley, K. K. Singh, R. K. Naviaux, *NanoTechnology in Cancer Research & Treatment* **4**, Adenine Press (2005), p. 585-592, invited paper, journal cover article.
4. "Optical Phenotyping of Human Mitochondria in a Biocavity Laser," P. L. Gourley and R. K. Naviaux, *Special Issue on Biophotonics, IEEE J. of Selected Topics in Quantum Electron.* **11**, July/August 2005, p. 818-826.
5. "Ultrafast Nanolaser for Detection of Cancer in Individual Cells," P. L. Gourley, J. K. Hendricks, A. E. McDonald, R. G. Copeland, K. E. Barrett, and C. R. Gourley, and R. K. Naviaux, *J. Biomed. MicroDevices.* **7**, 2005, Springer Science, p. 331-339.
6. "Nanolaser Spectroscopy for Detecting Abnormal Cells," P. L. Gourley, Conf. Chair, Symposium on BioMicroNano and Medicine, Sandia National Laboratories, Albuquerque, NM, Nov. 4, 2005.
7. "Brief Overview of BioMicroNanoTechnologies," P. L. Gourley, *Biotechnology Progress*, Am. Chem. Soc. Feb 2, 2005.
8. "Mitochondrial Correlation As A Biophotonic Marker For Detecting Cancer In A Single Cell," P. L. Gourley, J. K. Hendricks, A. E. McDonald, R. G. Copeland, K. E. Barrett, and C. R. Gourley, and R. K. Naviaux, *proceedings of the Biomedical Optical Society*, Photonics West conf. 5699A, San Jose Jan 24-26, 2005.
9. "Poly(dimethylsiloxane) thin films as biocompatible coatings for microfluidic devices: Cell culture and flow studies with glial cells," S. L. Peterson, A. E. McDonald, P. L. Gourley, D. Y. Sasaki, *J. Biomed. Mater. Res.* **2005**, *72A*, 10 - 18.

Project: “Modification of Thermal Emission via Metallic Photonic Crystals”

David J. Norris,¹ Steven M. George,² and Andreas Stein³

¹*Department of Chemical Engineering & Materials Science, University of Minnesota*

²*Department of Chemistry & Biochemistry, Department of Chemical Engineering, University of Colorado*

³*Department of Chemistry, University of Minnesota*

Program Manager: Tim Fitzsimmons
Project Start Date: September 1, 2006

Award: DE-FG02-06ER46348
End Date: August 30, 2010

Scope: The aim of this project is to study metallic photonic crystals and their ability to modify thermal emission. Photonic crystals are structured solids that are three-dimensionally patterned on an optical length scale [1]. Recent research has indicated that this structure can alter the “glow” from heated metallic photonic crystals [2-5]. This may allow the elimination of unwanted heat from thermal emission sources, such as the tungsten filament in a conventional light bulb. Furthermore, these materials may be important for obtaining improved thermophotovoltaic devices (for converting heat into electricity) and novel thermal barriers for applications such as fuel cells. To clarify the underlying physical phenomena, fundamental research is necessary. However, a full examination has been limited by difficulties in fabricating the appropriate structures. Here, self-assembly approaches are being used to obtain metallic photonic crystals in several formats (including monoliths, thin films, and filaments). Namely, micrometer-scale spheres made from polymers or silica can be synthesized and induced to organize spontaneously on a substrate [6]. Such structures, shown in Fig. 1, are often called “synthetic opals” due to their similarity to the natural gemstone. These opals can then be infiltrated with a variety of materials and the spheres removed to obtain a photonic crystal, known as an inverse opal, in which an array of bubbles is embedded in a film (see Fig. 2) [7-10]. We are utilizing this general approach to fabricate and study several types of metallic photonic crystals for thermal emission. The project is a collaboration between the University of Minnesota (Norris and Stein) and the University of Colorado (George).

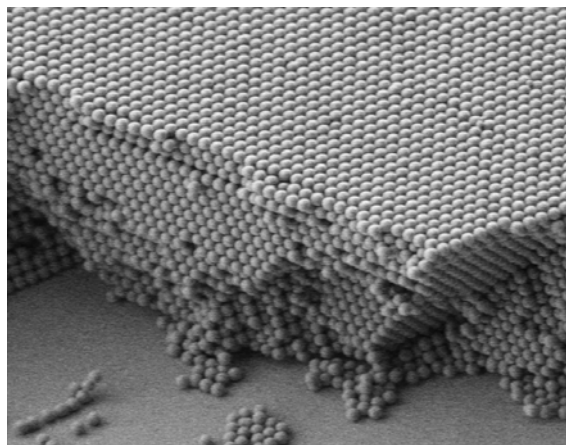


Fig. 1 Cross-sectional electron micrograph of a thin synthetic opal (made from 1000 nm silica spheres).

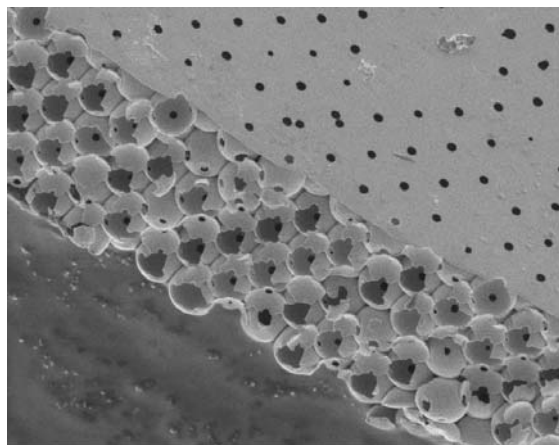


Fig. 2 Cross-sectional electron micrograph of a tungsten inverse opal made from a film as in Fig. 1 using atomic layer deposition (ALD).

Recent Progress: We have developed the capability to synthesize tungsten inverse opals using several different approaches, including atomic layer deposition (ALD), chemical vapor deposition (CVD) and solution chemistry. However, one important and immediate concern of our project was whether such structures would be suitable to modify thermal emission. Tungsten inverse opals had previously been reported [11], however experiments on these crystals also revealed that they suffered from extremely strong optical absorption. Essentially, the propagating light was absorbed before it could sense the periodic structure. This eliminated the influence of the photonic crystal. While Kirchhoff's law states that absorption is needed for thermal emission, clearly the absorption should not be severe. In that case, modification of thermal emission by the photonic crystal would not be expected. Thus, previous measurements on tungsten inverse opals suggested that they were not suitable for studying this phenomenon.

We have performed a theoretical analysis of this conclusion and our calculations show that the severe absorption is not intrinsic to these materials but rather can be moderated by properly tailoring the structure [12]. Indeed, slight alterations to the tungsten inverse opal can lead to optical properties that are very similar to a particular photonic crystal known as the tungsten woodpile. This is important because the tungsten woodpile has previously shown modified thermal emission [3-5]. A computer-generated rendition of our new self-assembled structure is shown in Fig. 3.

Furthermore, we have also demonstrated through solution chemistry that such structures can be synthesized [13]. A tungsten inverse opal has been prepared as shown in Fig. 4 via solution chemistry. These structures can also be obtained via atomic layer deposition by adapting a recent procedure for realizing TiO_2 inverse opals [14]. Thus, self-assembly techniques should provide tungsten photonic crystals that are relatively simple to prepare and suitable for both fundamental and applied studies of thermal emission.

Future Plans: As the project moves forward, we are building upon the initial results described above in the following ways: First, the thermal emission properties of the tungsten photonic crystals shown in Fig. 4 will be examined experimentally to determine the influence of the structure on their emission spectra. Second, our theoretical analysis will move beyond tungsten to probe whether other metals with high melting temperatures can yield modified thermal

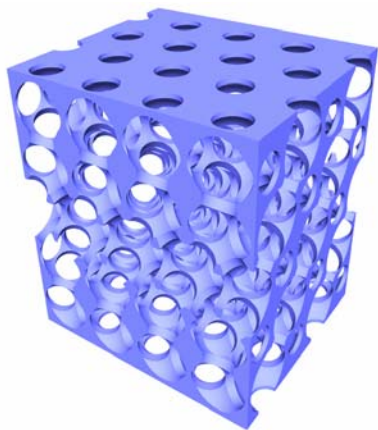


Fig. 3 Computer-generated rendition of altered inverse opal structure with optimized absorption properties.

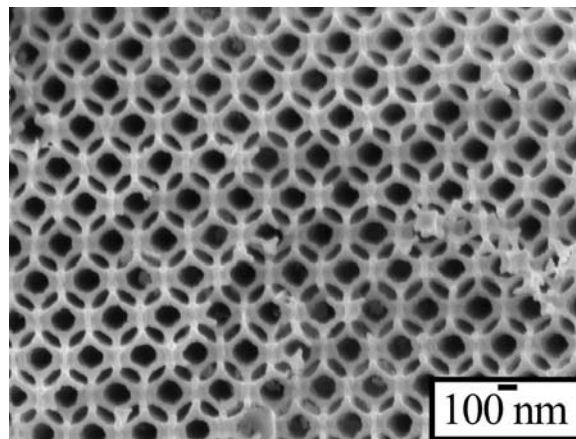


Fig. 4 Electron micrograph of a monolithic tungsten inverse opal made via solution chemistry that has the appropriate structure.

emission. Third, we will continue to develop our synthetic abilities to obtain not only improved tungsten photonic crystals, but also other structures guided by our theoretical analyses. Finally, we will explore other approaches to metallic photonic crystal fabrication, such as direct laser writing [15-17]. Preliminary work in all of these areas has already begun.

Publication List for Project (since start date of 09/01/2006):

- S. E. Han, A. Stein, and D. J. Norris, "Tailoring Tungsten Inverse Opals for Modified Thermal Emission," Phys. Rev. Lett. (submitted).

Cited References:

- [1] J. D. Joannopoulos, R. D. Meade, and J. N. Winn, *Photonic Crystals* (Princeton University Press, Princeton, 1995).
- [2] C. M. Cornelius, and J. P. Dowling, Phys. Rev. A **59**, 4736 (1999).
- [3] J. G. Fleming, S. Y. Lin, I. El-Kady, R. Biswas, and K. M. Ho, Nature **417**, 52 (2002).
- [4] S. Y. Lin, J. G. Fleming, and I. El-Kady, Opt. Lett. **28**, 1683 (2003).
- [5] S. Y. Lin, J. G. Fleming, and I. El-Kady, Appl. Phys. Lett. **83**, 593 (2003).
- [6] P. Jiang, J. F. Bertone, K. S. Hwang, and V. L. Colvin, Chem. Mater. **11**, 2132 (1999).
- [7] B. T. Holland, C. F. Blanford, and A. Stein, Science **281**, 538 (1998).
- [8] J. E. G. J. Wijnhoven, and W. L. Vos, Science **281**, 802 (1998).
- [9] A. Blanco, E. Chomski, S. Grachtchak, M. Ibisate, S. John, S. W. Leonard, C. López, F. Meseguer, H. Míguez, J. P. Mondia, G. A. Ozin, O. Toader, and H. M. van Driel, Nature **405**, 437 (2000).
- [10] Yu. A. Vlasov, X. Z. Bo, J. C. Sturm, and D. J. Norris, Nature **414**, 289 (2001).
- [11] G. von Freymann, S. John, M. Schulz-Dobrick, E. Vekris, N. Tetreault, S. Wong, V. Kitaev, and G. A. Ozin, Appl. Phys. Lett. **84**, 224 (2004).
- [12] S. E. Han, A. Stein, and D. J. Norris, Phys. Rev. Lett. (submitted).
- [13] N. R. Denny, S. Han, R. T. Turgeon, J. C. Lytle, D. J. Norris, and A. Stein, SPIE Proc. **6005**, 60050501 (2005).
- [14] J. S. King, E. Graugnard, and C. J. Summers, Adv. Mater. **17**, 1010 (2005).
- [15] B. H. Cumpston, S. P. Ananthavel, S. Barlow, D. L. Dyer, J. E. Ehrlich, L. L. Erskine, A. A. Heikal, S. M. Kuebler, I.-Y. S. Lee, D. McCord-Maughon, J. Qin, H. Röckel, M. Rumi, X.-L. Wu, S. R. Marder, and J. W. Perry, Nature **398**, 51 (1999).
- [16] S. Kawata, H. B. Sun, T. Tanaka, and K. Takada, Nature **412**, 697 (2001).
- [17] M. Deubel, G. v. Freymann, M. Wegener, S. Pereira, K. Busch, and C. M. Soukoulis, Nature Mater. **3**, 444 (2004).

This page is intentionally blank

Photo-Directed Molecular Assembly of Multifunctional Inorganic Materials

B.G. Potter, Jr.* and K. Simmons-Potter**

*Materials Science and Engineering Dept.

**Electrical and Computer Engineering Dept. and the College of Optical Sciences
University of Arizona
Tucson, AZ 85721

Program Scope:

Control of molecular assembly during the chemical synthesis of inorganic and molecular hybrid materials can strongly influence the evolution of nanostructure in these systems, furnishing fundamental insight into the influence of such processes on the development of higher-order structure and properties. Such a capability, for example, could be used to provide new options for steric and chemical character manipulation of nano- and meso-scale structures (sensor and separation membranes, bioactive scaffolds) or new opportunities for nanoparticle morphological control (quantum structures for optical and electronic functions). In prior work, intermolecular reaction kinetics, during the sol-gel processing of inorganic materials, have been influenced through the synthesis of metal alkoxide precursors containing sterically bulky ligand groups to inhibit hydrolysis [1]. Other methods of control include the photoinduced modulation of local pH, and the associated catalysis of hydrolysis/condensation reactions, via the introduction of photoacid generators in conventional sol-gel chemistries [2]. In addition, photo-disruption of unreactive alkoxide ligands has been used to complete network formation late in the gelation process in otherwise conventionally synthesized materials [3-7].

The focus of the present program integrates photoinduced structural modification with the rational design of complex metal alkoxide precursors to control the solution-based synthesis of

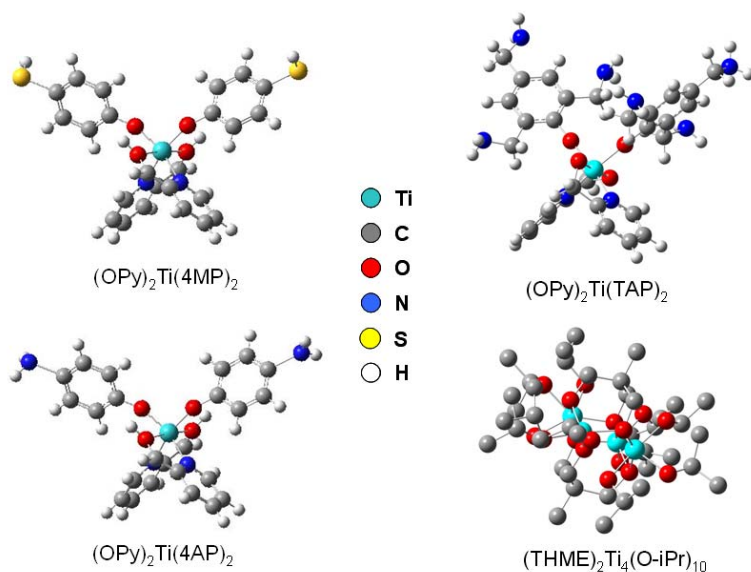


Figure 1: Heteroleptic Ti-alkoxide structures. Hydrogen atoms removed from THME structure for increased clarity. (OPy=C₆H₆NO, 4MP=OC₆H₄SH, 4AP=OC₆H₄NH₂, TAP = OC₆H₂(CH₂NH₂)₃, THME = C₅H₁₂O₃)

metal oxides at the onset of material assembly. Photo-activation of reaction sites about the metal center is expected to influence the development of intermolecular bonding, its geometry, and the ensuing higher-order structure. With the overall intent being to optically modify reaction kinetics that result in such bonding (e.g. hydrolysis rates in sol-gel systems), precursor selection in the present study has been predicated on the desire to preferentially access a targeted ligand (via

excitation wavelength tuning) and on the need to produce a photoinduced structural state for the site that enhances chemical reactivity. Thus, by appropriate molecular design and optical processing conditions, the strategy is intended to bias the selection of intermolecular reaction

sites and influence the morphological development of multimolecular aggregate structures. Moreover, it is intended that micro-scale patterning of the optical exposure will effectively combine bottom-up and top-down processes to achieve multilength-scale structural control in a single methodology.

Consistent with these goals, heteroleptic, metal-alkoxide precursor molecules are under investigation as a means to produce dissimilar photoresponses (and reactivities) at sites about the metal center. Experimental activities in the present program involve photoactive Ti-alkoxides with mono- and bidentate ligands of varied steric character and optical behavior (see Figure 1). Ligand selection is used to manipulate the electronic structure of the molecule (influencing absorption transitions arising from charge-transfer and conjugated ligand states) and the overall sterics of the molecule (modifying conventional hydrolysis kinetics). The photoresponse of the molecule is evaluated under a range of local environment conditions (e.g. in dilute solution, in the solid-state, and during thin film deposition) whose characteristics are anticipated to impact the photoexcitation mechanism and the subsequent assembly process through changes in local chemistry, structure and intermolecular dynamics. Photostructural modification of the alkoxides under these conditions is examined using optical (electronic, vibrational) and nuclear magnetic resonance spectroscopies. Density Functional Theory (DFT) computations are integrated with experiment to elucidate the structural basis for the vibrational resonances observed through a normal mode analysis of energy-minimized molecular structure.

The project enjoys a close collaboration with the group of T.J. Boyle at Sandia National Laboratories for the synthesis of the complex precursor structures under study. Computational activities will also benefit from an ongoing collaboration with L.R. Corrales (UA, formerly Pacific Northwest National Laboratories).

Recent Progress:

Efforts to-date have focused on photoinduced effects in mononuclear Ti-precursors based on bidentate pyridinecarbinol ($(\text{NC}_5\text{H}_4(\text{CH}_2\text{O})) = \text{OPy}$) and monodentate, derivatized-phenol ligands (Figure 1). Derivatization of the monodentate phenol moiety (e.g. amino- (4-AP), mercapto (4-MP), and triamino- (TAP) groups) has resulted in molecules exhibiting varied optical absorption responses and stabilities to conventional hydrolysis kinetics.

Photoexcitation of $(\text{OPy})_2\text{Ti}(\text{4MP})_2$, at energies resonant with a metal-to-ligand charge transfer band in the molecule [8] ($\lambda_{\text{exc}} = 337.1$ and 360 nm), resulted in preferential modification of the 4MP ligand. The effect was observed using vibrational spectroscopy (FTIR, micro-Raman), in both in pyridine solution and in a solution-cast film. All sample preparation and handling was performed under glove box conditions (dry Ar-atmosphere) and control samples were subjected to identical handling (without photoexposure) to isolate photoinduced changes in vibrational structure from the effects of conventional or “dark” chemistries.

Figure 2 depicts two IR-active vibrational resonances associated with in-plane 4-MP vibrational modes after UV-exposure. A clear reduction in intensity, distinct from that observed in an unexposed sample, is exhibited. Results of photoexposure studies under dry-Ar and ambient air (40% RH) exhibited an enhancement of photostructural modification at the

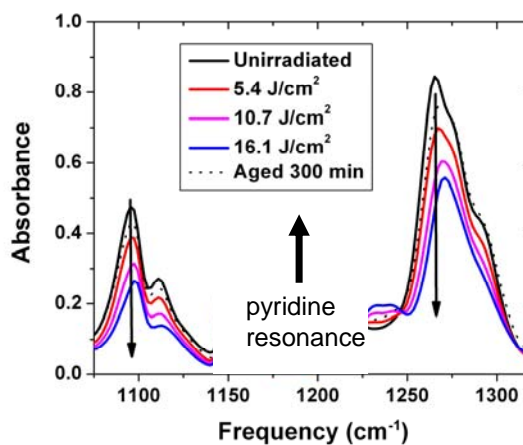


Figure 2: FTIR absorption spectrum of 0.48 M $(\text{OPy})_2\text{Ti}(\text{4MP})_2$ solution (in pyridine) as a function of total accumulated UV-fluence at $\lambda = 337.1$ nm. A large solvent-related resonance feature (location indicated) has been removed for clarity. The response of an unexposed control sample (denoted “aged”) is also provided

4MP ligand under the moist-air conditions. These trends, and the appearance of weak hydroxyl related resonances in the Raman spectra of solution-cast film samples in air, led to association of stable photoinduced changes in structure with an optically enhanced hydrolysis reaction at these ligands involving atmospheric water [9].

The greater steric bulk of the TAP ligand in the $(\text{OPy})_2\text{Ti}(\text{TAP})_2$ molecule, effectively arrests conventional hydrolysis at this site, enabling dissolution of the material in water without reaction and the clear isolation of photomediated effects from those of conventional reaction kinetics. The enhanced stability afforded by this system allowed the study of photoresponse in solutions with controlled addition of water. Photoexposure of an $\text{H}_2\text{O}:\text{Ti}$ (4:1) pyridine solution at wavelengths near-resonant with the conjugated ligand groups ($\lambda_{\text{exc}} = 248 \text{ nm}$) resulted in the formation of particulates exhibiting marked optical scattering. Identical exposures of a dry-pyridine solution of the precursor do not produce such an effect. Raman spectroscopy of the recovered particulates supported the presence of hydrolyzed species and the preferential modification of the TAP ligand group, similar to the effects observed in the 4MP system.

In addition to the particulate formation, photo-induced deposition of a highly scattering film of insoluble material on the inner vertical surface of the fused silica cuvette used to contain the water-pyridine solution was also observed. Film formation only occurred on the cuvette surface area illuminated with the excitation beam, indicating a material formation process associated with photoexposure of solution in the near surface region of the fused silica. Raman analysis of this photodeposited film revealed marked changes in the vibrational structure of this material, compared with that of the starting precursor, that support the preferential modification of the TAP ligand group. Spectroscopic studies to-date also confirm the presence of hydroxyl resonances in this photoproduct. Further investigation of the photomediated film deposition phenomena in the context of optical exposure conditions (wavelength, pulse energy) and solution parameters (precursor concentration, water content) are underway to more fully evaluate the nature of the photoreaction process and its role in the formation of the precipitate.

Future Plans:

Studies thus far support the presence of a photocatalyzed hydrolysis reaction, preferentially localized on monodentate ligand sites in these mononuclear-Ti alkoxide molecules. Results also indicate that the accompanying formation of a chemically distinct phase, appearing as both a colloidal precipitant in solution and, under suitable excitation conditions, as a film deposited on the inner surface of the solution container within the illuminated area. Such results confirm the selective ligand excitation and photoinitiated material formation effects central to the project. Future work will furnish additional insight into the nature of these photoexcitation and assembly phenomena through the investigation of alternative precursor chemistries and excitation conditions, and as mentioned above, the photoprocessing of these molecules under varied solution conditions (water content, precursor dilution).

Based on the current findings, new polynuclear Ti clusters (e.g. see Figure 1, THME-based structure) are now being synthesized by the Boyle group at Sandia that will enable further modification of photoexcitation energetics and the manipulation of intermolecular bond geometry in systems with inherent stability against conventional hydrolysis. A new computational thrust (in collaboration with L.R Corrales at UA) will utilize DFT techniques to evaluate excited-state molecular conformations providing additional insight into the photophysics of the excitation process and the link to increased reactivity. Solution studies will lead to the optical “pre-processing” of sols to investigate the impact of multimolecular aggregate size/morphology on the microstructural development of thin films and to the introduction of *in-situ* optical exposure during thin film dip-coating.

References:

1. for example: T.J. Boyle, J.M. Segall, T.M. Alam, M.A. Rodriguez, and J.M. Santana: Chemistry of a novel family of tridentate alkoxy tin(II) clusters *J. Am. Chem. Soc.* 124, 6904 (2002).
2. D. Dhoshi, N.K Huesing, M. Lu, H. Fan, K. Simmons-Potter, B.G. Potter, Jr., A.J. Hurd, and C.J. Brinker: Optically, defined multifunctional patterning of photosensitive thin-film silica mesophases. *Science* 290, 107 (2000).
3. H. Segawa, K. Tateishi, Y. Arai, K. Yoshida, and H. Kaji: Patterning of hybrid titania film using photopolymerization. *Thin Solid Films* 466, 48 (2004).
4. T. Ohya, A. Nakayama, T. Ban, Y. Ohya, and Y. Takahashi: Effect of photoirradiation on the properties of layered titanate thin films from transparent aqueous titanate sols. *Bull. Chem. Soc. Jpn.* 76, 429 (2003).
5. N. Asakuma, H. Hirashima, H. Imai, T. Fukui, A. Maruta, M. Toki, and K. Awazu: Photocrystallization of amorphous ZnO. *J. Appl. Phys.* 92, 5705 (2002).
6. H.-R. Kim, O.-H. Park, Y.-K. Choi, and B.-S. Bae: Photobleaching of gamma-glycidoxypropyltrimethoxysilane-chelated metal alkoxide gel films. *J. Sol-Gel Sci. Technol.* 19, 607 (2000).
7. H. Segawa, S. Adachi, Y. Arai, and K. Yoshida: Fine patterning of hybrid titania films by ultraviolet irradiation. *J. Am. Ceram. Soc.* 86, 761 (2003).
8. T.J. Boyle, R.M. Sewell, L.A.M. Ottley, H.D. Pratt, C.J. Quintana, and S.D. Bunge: Controlled Synthesis of a Structurally Characterized Family of Sterically Constrained Heterocyclic Alkoxy-Modified Titanium Alkoxides. *J. Inorg. Chem.* 2007 (in press).
9. J.D. Musgraves, B.G. Potter, Jr., R. Sewell, and T.J. Boyle: Preferential Photostructural Modification of Heteroleptic Titanium Alkoxides for Molecular Assembly. *J. Mat. Res.*, to appear: June, 2007

Publications:

1. J.D. Musgraves, B.G. Potter, Jr., R. Sewell, T.J. Boyle, and L.R. Corrales: Photo-Induced Structural Changes in Titanium Alkoxides for Directing Molecular Assembly. *MRS Proceedings of the Self Assembly of Nanostructures Aided by Ion- or Photo-Beam Irradiation – Fundamentals and Applications, Symposium N, MRS Fall Meeting, 2006.* accepted for publication.
2. J.D. Musgraves, B.G. Potter, Jr., R. Sewell, and T.J. Boyle: Preferential Photostructural Modification of Heteroleptic Titanium Alkoxides for Molecular Assembly. *J. Mat. Res.*, to appear: June, 2007.

Surface-Initiated Ionomer Films Based on Modified Poly(n-alkylnorbornene)s

G. Kane Jennings (PI) and Brad Berron, Vanderbilt University, Department of Chemical Engineering, Nashville, TN 37235

I. Program Scope

By integrating catalyst, ionomer, and gas diffusion layer into a nanoporous architecture, the proposed research project seeks to molecularly optimize the cathode side of a proton exchange membrane fuel cell. This new cathode will consist of a porous alumina membrane with metal-lined pores that function as gas diffusion conduits while supporting a catalyst layer and ionomer. The ionomer chains will be grown from the surface of the pore walls and are designed to encapsulate the catalyst particles to provide a well-defined three-phase boundary for gas, proton, and electron transfer. Two new classes of ionomer will be investigated, including non-fluorinated and a partially fluorinated polymers prepared by the surface-initiated ring-opening metathesis polymerization (ROMP) of a functionalized norbornene and subsequent sulfonation. The norbornene will contain either fluorocarbon or hydrocarbon side chains of controlled length that promote self-organization of the polymer chains to create a hydrophobic matrix for gas transport and hydrophilic channels for proton conduction.

In the initial stage, the proposed research will investigate the effect of the chain length and composition of the hydrophobic side groups on the self-organizing structure of the ionomer film and the effect of this structure on proton conduction and the rate of the oxygen reduction reaction. Through these experiments on 2-D surfaces, ionomer composition will be molecularly optimized to facilitate self-organization into well-defined nanostructured materials. These optimized ionomers will then be grown from catalyst-lined pore walls to study intramembrane proton transport and gas diffusion. Diblock copolymers will be used to create well-defined ion-conducting channels at the center of the pores while maintaining radially oriented ionic pathways to the adsorbed catalyst particles on the pore walls. The composition of this integrated ionomer/catalyst/diffusion network will be tuned to optimize the power density of the cathode while furthering the basic understanding of the three-phase boundary in fuel cell electrodes.

Recent Progress

A. Surface-Initiated Growth of Polymer Thin Films on 2-D Surfaces.

We have developed a surface-initiated polymer film composed of poly(*n*-alkylnorbornene)s. Our approach (Figure 1) begins by preparing a vinyl-terminated monolayer on a gold substrate via exposure to allyl mercaptan. The terminal vinyl group is then reacted with a metathesis catalyst, immobilizing the catalyst on the substrate. The bound catalyst is then reacted with the desired monomer through ring-opening metathesis

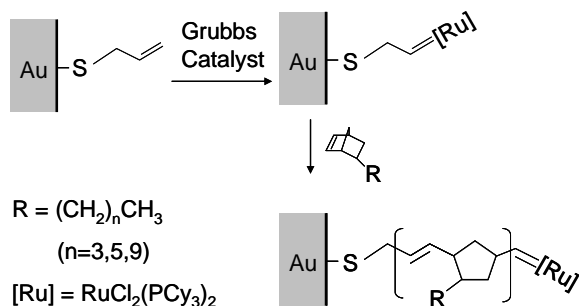


Figure 1. Schematic illustration of the gold surface preparation by attachment of allyl mercaptan, attachment of Grubbs' catalyst, and the ring-opening metathesis polymerization of alkylnorbornenes.

polymerization (ROMP) to create a surface-tethered poly(*n*-alkylnorbornene) film. The kinetic rates of polymerization are slowed by use of longer *n*-alkyl side chains, but films in the range of 10 – 100 nm can easily be produced from polymerization of butylnorborne (C4NB) and hexylnorbornene (C6NB) monomers. This research represents the first surface-initiated growth of poly(*n*-alkylnorbornene) films as well as the first use of allyl mercaptan as a linkage between a substrate and a metathesis catalyst.

We used RAIRS to probe the composition and structure of poly(*n*-alkylnorbornene) films (~45 nm) as compared to a film of polynorbornene (pNB; R = H) of similar thickness (Figure 2). The addition of an *n*-alkyl side chain to the 5 position of the norbornene monomer alters the composition and structure of the resulting polymer. The polymer films with longer alkyl substituents exhibit increased *n*-alkyl functionality in the RAIR spectra with diminished polynorbornene functionality when compared to their shorter chained analogues. Specifically, the contribution of the acyclic methylene stretching ($\nu_{\text{as}} = 2926\text{-}28\text{ cm}^{-1}$, $\nu_{\text{s}} = 2854\text{-}58\text{ cm}^{-1}$) increases while the contributions of the cyclic methylene stretching ($\nu_{\text{as}} = 2948\text{-}2955\text{ cm}^{-1}$, $\nu_{\text{s}} = 2866\text{-}71\text{ cm}^{-1}$) and the trans C=CH out of plane bending ($968\text{-}9\text{ cm}^{-1}$) decrease in an inversely proportional fashion. The shift of the methylene

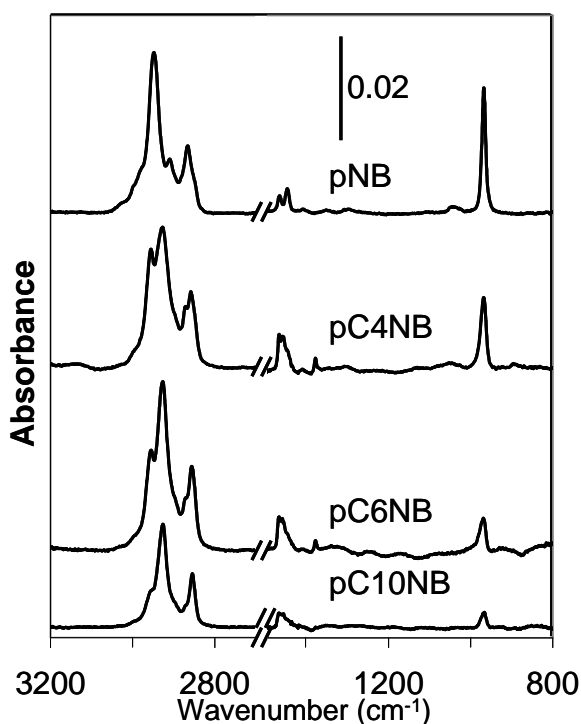


Figure 2. Reflectance-absorption infrared spectra of the indicated polymer films. The spectra have been offset vertically for clarity.

scissoring peak with the addition of the alkyl side chain is indicative of a deviation from a purely cyclic methylene component (1447 cm^{-1}) toward a largely acyclic film (1467 cm^{-1}). The position of the cyclic methylene stretching peaks in the poly(alkylnorbornene)s are shifted towards higher wavenumbers ($\nu_{\text{as}} = \sim 2955\text{ cm}^{-1}$, $\nu_{\text{s}} = \sim 2870\text{ cm}^{-1}$) indicative of a less crystalline conformation of the cyclopentane groups as compared to those in the original poly(norbornene) film.

The increased liquid character, as shown in RAIRS, as well as the greater volume per chain of the resulting pC4NB and pC6NB polymer films, likely allows these films to form more conformal films at reduced overall thicknesses. This observation is supported by 100-fold improvements in the resistance of $\sim 45\text{ nm}$ pC4NB and pC6NB films against ion transfer as compared to pNB films of similar thickness. Of course, sulfonation of the pC4NB and pC6NB films will greatly diminish their resistance against proton transfer, while yielding a lower (more favorable) ion exchange content than similarly sulfonated pNB films.

B. Sulfonation of Surface-Initiated Films

Upon exposure of a 70 nm pNB film to 0.1 M acetyl sulfate in dichloromethane for 5 min , the RAIR spectrum (Figure 3) indicates $\sim 98\%$ diminution of the trans C=CH out of plane bending peak (968 cm^{-1}) and reduction of all peaks associated with olefin functionality. The introduction of sulfonate functionality is observed through the appearance of asymmetric and symmetric S=O stretching (~ 1359 and $\sim 1204\text{ cm}^{-1}$) and S-OH stretching (903 cm^{-1}) modes. The crisp asymmetric and symmetric CH_2 (2948 cm^{-1} and 2866 cm^{-1}) and CH stretching (2911 cm^{-1}) peaks of the pNB spectrum are distorted upon sulfonation. This distortion of the peaks is attributed to the alteration of the intensities and positions of peaks as the chains reorganize due to the additional sulfonate and hydroxyl functionality. The position of the CH_2 scissoring peak ($\sim 1450\text{ cm}^{-1}$) is indicative of the conservation of the cyclic CH_2 functionality after sulfonation. Similarly, we have sulfonated the pC4NB and pC6NB films via a 5 min reaction with 0.1 M acetyl sulfate and achieved analogous results.

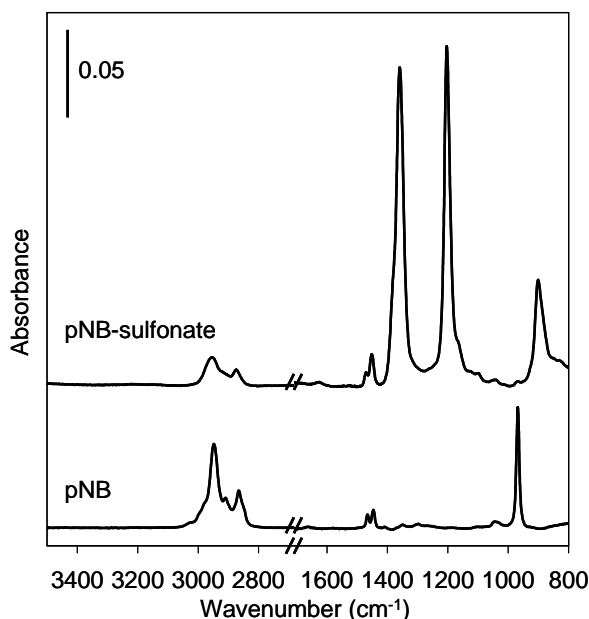


Figure 3. Reflectance-absorption infrared spectra of polynorbornene and sulfonated polynorbornene films. The spectra have been offset vertically for clarity.

II. Future Plans

There are several tasks that we plan to complete by the end of September, 2007. These include the following: 1) Modify the norbornene monomer with fluorocarbon side chains prior to polymerization and sulfonation to investigate the effect of ionomer composition on structure, and the effect of film structure on proton conductivity. 2) Upon growing these films from 2-D surfaces that contain catalytic Pt nanoparticles, determine the effect of ionomer composition and structure on the rate of the oxygen reduction reaction. 3) Define target or optimum ionomer film compositions from work on 2-D surfaces to aid the design of 3-D systems. We will begin growing these films within nanoporous electrode supports in the third year of the project.

III. Publications from Project

Brad J. Berron, Evan P. Graybill, and G. Kane Jennings, "Growth and Structure of Surface-Initiated Poly(n-alkylnorbornene) Films," *Macromolecules*, submitted in March, 2007.

Spatially Controlled Atomic Layer Deposition in Porous Supports*

J. A. Libera, J. W. Elam, and M. J. Pellin

Argonne National Laboratory, Argonne, Illinois 60439

An advancement of conventional ALD techniques has been developed for depositing materials at controlled depth locations within porous substrates. This technique uses the passivating effect produced by the saturated adsorption of one ALD precursor to prevent the adsorption of a second ALD precursor. For example, a surface exposed to trimethyl aluminum is not reactive towards diethyl zinc. This effect, combined with Knudsen diffusion in which the reactant exposure time dictates the depth of penetration of the ALD layer, enables spatially controlled “stripe coating” within porous supports such as anodic aluminum oxide (AAO) membranes or spherical silica gel particles. In this study, the ALD precursors trimethyl aluminum (TMA), diethyl zinc (DEZ), niobium ethoxide ($\text{Nb}(\text{OEt})_5$), and titanium tetrachloride (TiCl_4) were used to deposit stripes of Al_2O_3 , ZnO , Nb_2O_5 , and TiO_2 , respectively, at specified depths in AAO membranes. The results were analyzed by cross-sectional elemental mapping using energy dispersive analysis of X-rays. It was found that trimethyl aluminum is very effective at passivating surfaces towards adsorption of the other ALD precursors, whereas the converse was not true, i.e., the trimethyl aluminum was found to etch the material deposited by the preceding DEZ or TiCl_4 exposures. The stripe locations and profiles have been successfully modeled using Monte-Carlo simulations in the Knudsen flow regime. This new technique enables the deposition of ALD coatings at controlled depths within nanoporous AAO membranes and opens up potential applications in sensors, separation devices, and multi-step catalysts.

*** Work at Argonne is supported by the U.S. Department of Energy, BES-Materials Sciences under Contract W-31-109-ENG-38.**

This page is intentionally blank

STRESS IN CONFINED FLUIDS

DE-FG02-97ER45642

George Scherer

Princeton University

i) Program scope

The goal of this project is to develop a fundamental understanding of the interaction between a fluid in a nanometric pore and the solid phase that confines it. We are engaged in an integrated program of computer simulations and novel experimental methods that focus on two phenomena that can lead to damaging stresses in the solid: anomalous thermal expansion of the pore liquid and disjoining pressure. Recent work in our lab has shown that the thermal expansion coefficient of confined liquids increases rapidly as the pore diameter decreases below ~15 nm. The expansion of the pore liquid has been shown to cause cracking of materials as diverse as silica gels and Portland cement paste. Molecular dynamics (MD) simulations, based on an improved intermolecular potential for water, are being used to explore the structure of water in the pores and the change in structure with temperature. Alteration of ordering of molecules adjacent to the pore walls as temperature decreases may be responsible for the anomalously high thermal contraction observed experimentally. Solvent ordering is also believed to be a primary cause of disjoining pressure (repulsive force) between growing crystals and confining surfaces. It is generally observed, as in frost heave of soils or crystal growth in gels, that growing crystals push objects out of their way. Direct contact between the crystal and the obstacle is prevented by a film of liquid attracted to the solid surface. We have devised a method for measuring the crystallization pressure exerted by salt, and will compare the results with simulations. MD will be used to reveal the structure of the layer of solution between the crystal of salt and the confining mineral surface. Understanding the origin of the repulsive forces may suggest methods for reducing them, and thereby decreasing the tens of billions of dollars worth of damage done by ice and salt to the infrastructure. In particular, we have demonstrated that chemical modification of the mineral surface (e.g., by adsorption of low molecular weight polyacrylic acid) can reduce the disjoining pressure between sodium sulfate and calcium carbonate to the point that damage is avoided.

ii) Recent progress

We had originally proposed a variety of experiments to acquire more data regarding the anomalous expansion of water in small pores. However, we decided that there is already a sufficient body of data, so it is more important to push the molecular dynamics modeling. Therefore, the graduate student (Melanie Webb) who had begun to do the experiments has turned her attention to MD. While Prof. Garofalini and his student refined the potentials for water and silica, Melanie made excellent progress on potentials for Na⁺ and Cl⁻, both in the crystal and as hydrated ions. That will enable us to simulate the disjoining pressure between a crystal of salt and the confining pore wall. We had also proposed to measure the disjoining force by growing a salt crystal in a void within a nanoporous host (*viz.*, a partially sintered aerogel). A great deal of effort was put into that project this year, but the experiment turned out to be far more difficult than anticipated, so we have abandoned it in favor of two other methods: atomic force microscopy and a novel warping experiment.

With the help of Dr. Andrea Hamilton, a post-doctoral researcher working with Prof. Hall in Edinburgh, we are now pursuing a novel approach: a salt crystal is attached to the tip of an AFM and is brought into contact with a different crystal (e.g., quartz). This has the disadvantage of imposing a uniaxial force on the crystal, but it provides the whole force-distance curve for the disjoining force, and it can be done quickly enough to prevent substantial changes in supersaturation. To obtain the disjoining pressure, it is necessary to subtract the electrostatic and van der Waals components of the force using DLVO theory. We plan to expand this work in the coming year. Dr. Hamilton has applied for a fellowship that will allow her to come to Princeton this year to continue the AFM studies.

Another fruitful experiment is to glue a porous layer onto a nonporous glass layer, then induce crystallization in the pores. The photo below shows a plate of Indiana limestone epoxied to glass (with two holes into which thermocouples will be inserted). The stone is impregnated with sodium sulfate (thenardite), then water is poured on the top, which causes dissolution of thenardite and precipitation of mirabilite (sodium sulfate decahydrate). The resulting stress causes the stone to expand, and the constraint imposed by the glass causes the composite to bend; the deflection can be used to calculate the stress in the stone; typical results are presented in the plot below.

DRAFT COPY
FOR INFORMATIONAL PURPOSES ONLY
DO NOT REPRODUCE OR CITE

Figure 1. Sample of Indiana limestone epoxied onto a glass plate; the pores in the stone contain thenardite.

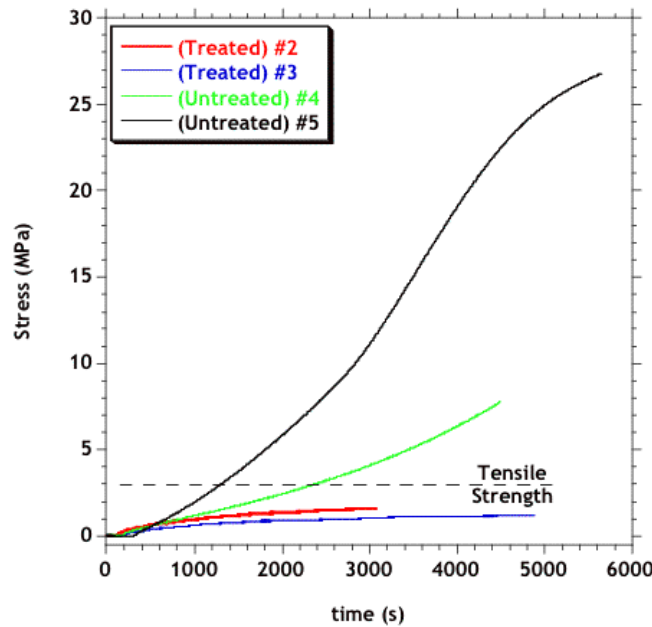
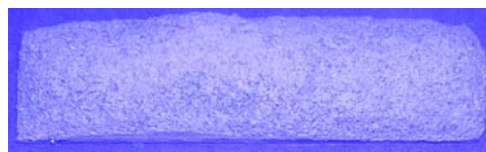


Figure 2. Stress calculated from deflection of composite plate when water is added to stone. The upper curves show that the stress generated in bare (untreated) stone exceeds its tensile stress. The lower curves show the consequences of treating the stone with low molecular weight polyacrylic acid, which adsorbs on the stone and reduces the disjoining force between the stone and the salt. The stress in treated stone is lower than the tensile strength, so damage is avoided, as indicated in the following photos.



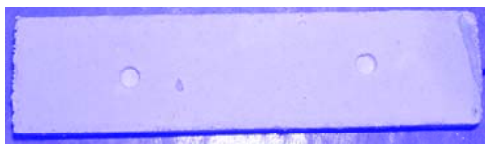


Figure 3. Upper plate shows damage after a single crystallization cycle of mirabilite in Indiana limestone; lower plate was pre-treated with polyacrylic acid, and it shows no damage.

A new dissociative water interatomic potential was developed in order to account for the reactions that occur at the water-silica interface (hydroxylation) as well as reproduce the density-temperature curve between 263K and 373K at 1 atm. Reproduction of the equation of state of water is vital to the application of the MD simulations in this project, where density variations with temperature must be accurately simulated in order to evaluate the anomalous expansion of water confined to small pores. Figure 4 shows the comparison between simulations and experimental data for the density-temperature curve for bulk water. Various properties of the simulated water, such as structure, energy, diffusion constants, and vibrational spectra are accurately described in the simulations using this potential.

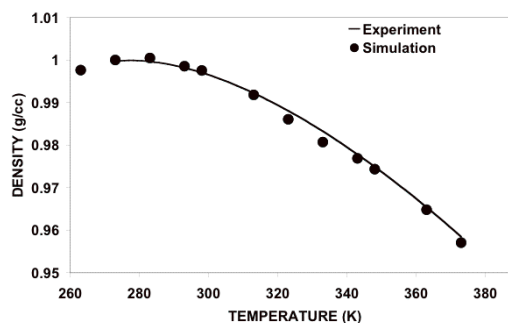


Figure 4. Comparison between simulated density-temperature data at 1 atm with experimental data.

Figure 5 shows the results of simulations done using the dissociative water potential that reproduces the experimentally observed volume with temperature. Details of the role of surface reactions, interface densities, and dipole moments as a function of location in the water are being

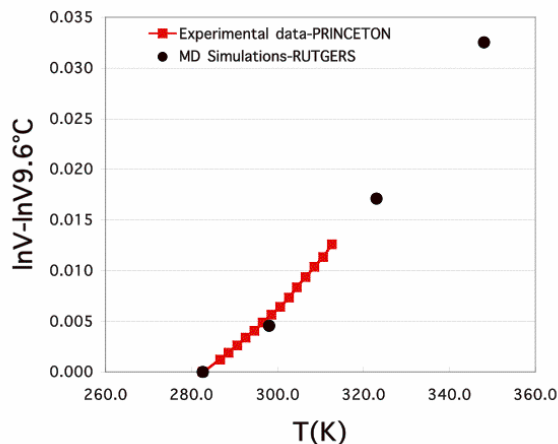


Figure 5. Comparison between experimental and simulation data for the volume of water confined to 3nm pores as a function of temperature

analyzed.

In order to simulate sodium chloride crystals and these ions in solution, interatomic potentials consistent with the new dissociative water potential were required. These were developed using

comparison of the simulated crystal to bulk crystal structure and simulations of each ion in small water clusters, with comparison to ab-initio calculations. The cluster simulations resulted in low energy structures consistent with the ab-initio data, several of which are shown below in figure 6.

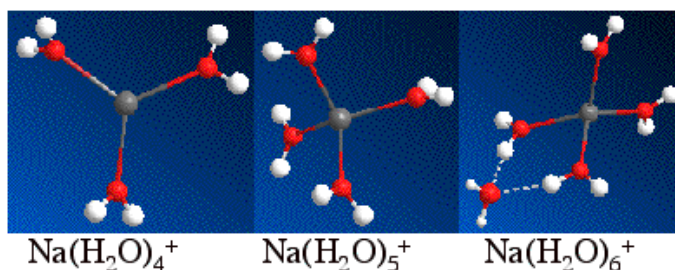


Figure 6. Low energy configurations of Na⁺ ion interactions with water clusters.

iii) Future plans

The experimental program will focus on measurement of disjoining pressure using the AFM, which yields force-displacement curves that can be directly compared to MD simulations. Warping experiments will be used to explore surface treatments that reduce the disjoining pressure and prevent damage to the porous host. The MD simulations will continue with the evaluation of the cause of the anomalous expansion of water in confined pores using detailed analysis of atom positions, surface reactions, local interface densities, dipole moment variations, and forces. The successful development of the NaCl potential that is consistent with the dissociative water potential will enable simulations of the salt-mineral interfaces in contact with reactive water. These will give us a more accurate evaluation of atomistic structure, energies, and forces occurring at these interfaces and their role in disjoining pressure.

v) Publications

1. T. S. Mahadavan and S. Garofalini, Dissociative water potential for molecular dynamics simulations, *J. Phys. Chem.* (submitted)
2. T. S. Mahadavan and S. Garofalini, The structure of water confined in 3 nanometer pores in silica (in prep for *J Chem Phys*)
3. S. Xu, G. Simmons, T. Mahadavan, S. Garofalini, G.W. Scherer, Effect of confinement on the anomalous expansion of water in small pores (in preparation)
4. A. Hamilton, AFM (submitted)
5. J.J. Valenza & G.W. Scherer, "Control of Crystallization Pressure by Surface Modification of Stone: 2. Warping test" (in prep for *J. Crystal Growth*)
6. A. Hamilton, C. Hall, and V. Koutsos, "Investigations of surface forces between soluble metal sulphates and silica in electrolyte solutions", in preparation

The Evolution of Topologically Complex Structures: Coarsening of Dendritic Mixtures

P.W. Voorhees* and K. Thornton**

*Department of Materials Science and Engineering
Northwestern University, Evanston, IL

**Department of Materials Science and Engineering
University of Michigan, Ann Arbor, MI

Program Scope

Dendrites frequently form during solidification into an undercooled melt. These dendrites possess secondary and sometimes even tertiary arms. While the tip radius and tip velocity of the dendrite are set by the growth conditions, the side branches behind the tip undergo a coarsening process under nearly isothermal conditions. This coarsening process sets an arm thickness and distances between dendrite arms in the solidified structure that are almost independent of the length-scale given by the dendrite tip. Since there is a close relationship between the size scale of the dendrites and the mechanical properties of the material, the coarsening process in dendritic solid-liquid systems has received much attention.

Despite the clear importance of the coarsening process, measurements of the morphology of the two-phase mixture during coarsening that capture the full three-dimensional nature of the structure are in their infancy. In addition, since calculations of the evolution of such topologically complex systems are challenging, existing models of this coarsening process involve significant simplifications of the microstructure.

To address these deficiencies in our understanding of the coarsening process, we study the coarsening process in topologically complex systems using three-dimensional reconstructions of the microstructure in concert with phase-field calculations of systems undergoing coarsening.

Recent Progress

The coarsening process was examined in a Pb-Sn alloy with three volume fractions of solid: 43%, 58% and 81%. The morphological evolution process at these three volume fractions was markedly different. In the system with a low volume fraction of solid, Figure 1, the earliest time shows clearly a dendritic structure. As coarsening proceeds there is a marked change in morphology to a microstructure consisting of a series of solid cylindrical-like objects. It is important to note that the cylinders are oriented in the direction along which the samples were originally directionally solidified. In contrast, the samples with a higher volume fraction of solid do not form solid cylindrical objects. In this case, liquid cylinder-like domains form within the solid, as well as nearly planar thin films of liquid. This result with a high volume fraction of solid is consistent with our work in the Al-Cu alloy system. Thus *the formation of liquid cylinders is not specific to the alloy system employed to study the coarsening process*. Solid cylinders, at low volume fractions, and liquid cylinders, at high volume fractions, form as a result of the underlying microstructural anisotropy that follows from the manner in which these

samples were initially prepared. The directional solidification process orients the trunks of the dendrites or the thin liquid films along the z-direction. This yields the highly non-self-similar coarsening process. The microstructures have been characterized using interface shape distributions, the distributions of interface normals, and the fractions of mean and Gauss curvature as a function of time.

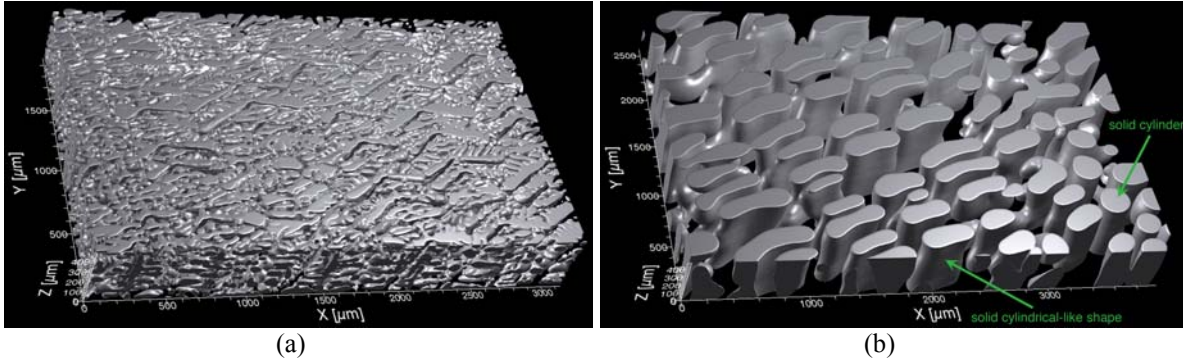


Figure 1. Three-dimensional reconstruction of a 43% volume fraction solid system: (a) 3 minutes and (b) 2 days of coarsening. The drastic change in the structure due to coarsening is evident. The liquid is transparent.

We have also assessed the effect of the initial state of the system by examining the coarsening process in Al-Cu alloys prepared by equiaxed solidification. In this case a liquid droplet was undercooled and solid dendrites nucleated randomly in the droplet to form an equiaxed structure. Thus there is no underlying directionality in the system. The volume fraction of solid in this system was 49%. We observed from the three-dimensional reconstructions that cylindrical domains do not form during coarsening; the microstructural evolution in this case is dramatically different from those of the directionally solidified samples. Most remarkably, the morphological evolution is much closer to self-similar evolution than in the directionally solidified samples, as quantified by the probability of finding a patch of interface with a given pair of principle curvatures, κ_1, κ_2 , shown in Figure 2 and discussed below.

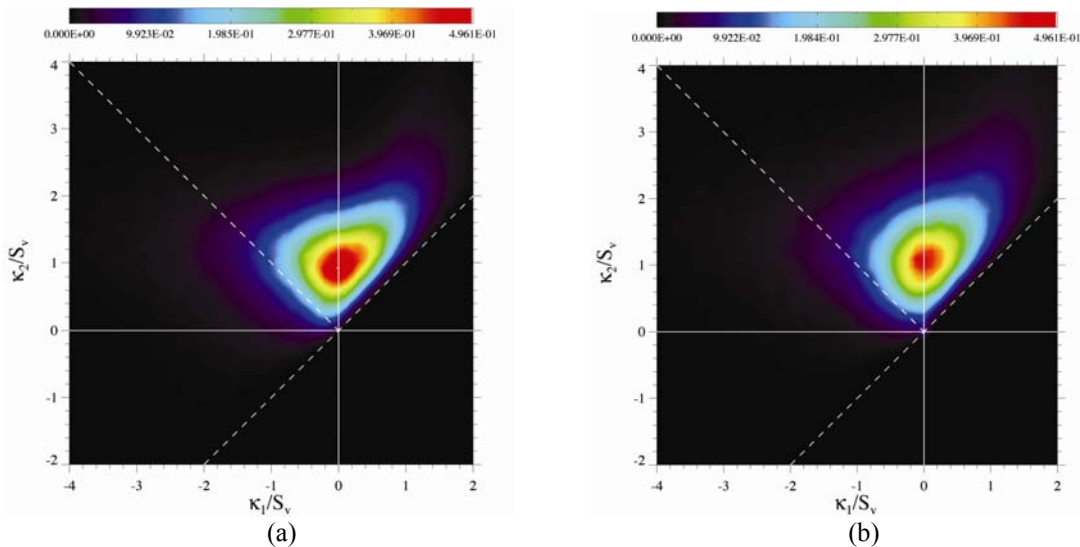


Figure 2. The interfacial shape distribution. High probability is red, low probability is black. The principle curvatures are scaled by the surface area per unit volume, S_v . (a) 17 hours of coarsening, (b) 4 days of coarsening.

Since the principle curvatures are scaled by the inverse of a time-dependent characteristic length, the interface shape distributions should be time-independent if the microstructure is self-similar. While the interfacial shape distributions in Figure 2 show some evolution, the changes are much less prominent than those in the directionally solidified samples. Thus if the initial structure is equiaxed, as is the case in the central region of most castings, the evolution of the microstructure is much closer to self-similar than those of directionally solidified samples we obtained earlier. Thus, we conclude that the initial state of the microstructure has a major effect on the manner in which coarsening proceeds in these solid-liquid systems. Interestingly, we again observe no tendency for the structure to break up into an array of spherical domains of solid, as would be expected since a sphere minimizes the surface energy per unit volume. While a breakup may occur at longer coarsening times, the absence of spherical domains of the minority phase appears to be generic to coarsening processes in a wide range of initially dendritic microstructures. The analysis of this fascinating data is continuing.

On the theoretical front, we made a first step toward developing a theory of coarsening in morphologically complex systems. To that end, we examined coarsening following phase decomposition of mixtures with equal volume fractions of phases evolving by conserved and nonconserved dynamics. These microstructures are bicontinuous and have intricately interpenetrating phase domains. Using large-scale simulations (Figure 3), we have established that unique scaled microstructures exist. We have characterized their morphologies by the interfacial shape distribution, and their topologies by the genus. We find that the two dynamics result in unique, but different, scaled interfacial shape distributions, with conserved dynamics yielding a narrower distribution around zero mean curvature. In contrast, the two scaled structures are topologically similar, having nearly equal values of the scaled genus. Using these systems, we are developing a theoretical framework to describe morphological evolution in highly complicated microstructures.

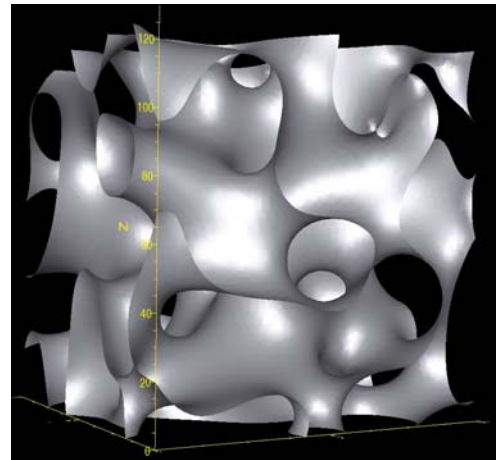


Figure 3. A typical microstructure during coarsening following phase separation.

Future Plans

We have begun using our phase-field code that accounts for the difference in diffusivity between the solid and liquid, to explore the flow in probability space using the many experimentally measured microstructures. We will employ the experimentally measured microstructures from both the initially directionally and equiaxed solidified structures. Since the evolution of these structures differs greatly, this will serve as a particularly stringent test of our simulation approach. The insights obtained from the simulations will be applied to develop the theoretical understanding of the coarsening in systems with complex microstructures.

We will continue our work on measuring the evolution of the microstructure during coarsening in systems that were initially solidified in an equiaxed structure. In particular, we will examine a

higher volume fraction of solid to determine if cylindrical domains of liquid form, as was the case in the directionally solidified samples.

In collaboration with Erik Lauridsen of RISO laboratory in Denmark, we will measure *in situ* the three-dimensional evolution of the solid-liquid microstructure in the Al-Cu system during coarsening. This will be done using x-ray tomography at a synchrotron light source. We will be searching, in particular, for the dynamics of topological singularities. We have postulated that cylinders of liquid form in this system via hole formation in walls of liquid. These *in situ* experiments will provide important insights into this process.

Publications

R. Mendoza, I. Savin, K. Thornton and P.W. Voorhees, *Topological Complexity and the Dynamics of Coarsening*, Nature Materials, **3** 386 (2004).

R. Mendoza, J. Alkemper and P.W. Voorhees, *The Topology of Coarsened Microstructures*, in Solidification Processes and Microstructures: A Symposium in Honor of Wilfried Kurz, M. Rappaz, C. Beckerman and R. Trivedi eds, TMS pp. 123-129 (2004).

R. Mendoza, J. Alkemper and P.W. Voorhees, *Z. fur Metallkunde, Three-Dimensional Morphological Characterization of Coarsening Microstructures*, **96** (2005).

D. Kammer, R. Mendoza, and P.W. Voorhees, *Cylindrical Domain Formation in Topologically Complex Structures*, Scripta Mater. **55**, 17-22 (2006) in viewpoint set no. 41 “3D Characterization and Analysis of Materials”.

D. Kammer and P.W. Voorhees, *The Morphological Evolution of Dendritic Microstructures During Coarsening*, Acta Mater. **54**, 1549-1558 (2006).

Y. Kwon, K. Thornton, and P.W. Voorhees, *Coarsening of Bicontinuous Structures via Conserved and Nonconserved Dynamics*, Physical Review E, **75**, 021120 (2007).

D. Kammer and P.W. Voorhees, *The Effect of Volume Fraction on Coarsening in Dendritic Microstructures*, submitted.

Y. Kwon, K. Thornton and P.W. Voorhees, *The Topology and Morphology of Bicontinuous Interfaces Following Phase Separation*, submitted.

Self-organized nanostructured superhard materials

Ivan Petrov

petrov@uiuc.edu

Fredrick-Seitz Materials Research Laboratory

University of Illinois at Urbana-Champaign, Urbana, IL-61801

Program Scope

We use an innovative non-equilibrium synthesis methods developed by us combined with in-situ atomistic surface science studies to make progress in the understanding and the development of novel self-organized nanostructured superhard materials. Nanostructured thin films constitute some of the most promising candidates for new coating materials displaying hardness comparable to diamond. These materials consist of a set of precipitated nanometer-sized grains, which small size hinders dislocation nucleation and glide, embedded in a strong intergranular tissue-phase that inhibits grain boundary sliding. One commonly exploited route to achieve such structures is to take advantage of thermodynamically-driven spinodal decomposition of metastable mixtures of immiscible nitrides during growth or afterwards, which results in the phenomenon of age-hardening. As with any nanostructured system, the final properties of the system are largely determined by the structure of the internal interfaces, which remains largely unknown due to the inherent difficulty of applying TEM and other standard analytical techniques to study such high curvature interfaces.

The goals of this project are: [1] To study the structure of the internal interfaces in nanocomposites and its effect on film properties. [2] To understand the atomic mechanisms occurring during low-energy ion induced nanostructure formation during film growth. [3] To apply this knowledge to develop new coating materials with enhanced chemical stability and mechanical properties.

Recent Progress

We have developed an innovative magnetically-unbalanced UHV magnetron reactive sputter deposition system that allows *independent* control of ion energy E_i and ion to metal flux density ratio J_i/J_{Me} . In particular, the method allows ion-to-neutral flux ratios J_i/J_{Me} incident at the growing film to be varied over extremely wide ranges (up to > 50) at very low ion energies (e.g. below the bulk displacement energies $\sim 10-20$ eV) and achieve regimes of ion-assisted growth that had not been explored.

Our previous work on complex nanostructured transition metal (TM) nitrides resulted in the discovery of $\simeq 2$ nm wavelength equiaxed and nanocolumnar phases of $Ti_{1-x}Al_xN$ (2) and $Ti_{1-x}Ce_xN$ (3), originating via surface-initiated spinodal decomposition of the quasi-binary alloys during growth. Continuing this work, we choose $Hf_{1-x}Al_xN$ as a model system to study film nanostructuring because [1] HfN is the highest melting point and highest elastic modulus TM nitride; [2] cubic HfN and hexagonal AlN are immiscible in equilibrium, a prerequisite for the formation of the nanostructures of interest; and [3] our previous experience allows us to routinely synthesize high-quality epitaxial HfN_x films of controlled composition x (4,5).

We deposited a series of epitaxial metastable $Hf_{1-x}Al_xN$ layers deposited on MgO(001) using UHV reactive magnetron sputter deposition in mixed Ar/N₂ discharges

with $f_{N_2} = 0.10$, at a total pressure of 7 mTorr, and a substrate temperature of 600°C. The combination of Rutherford backscattering spectroscopy (RBS), high-resolution x-ray diffraction (HR-XRD), and high-resolution cross-sectional transmission electron microscopy (HR-XTEM) shows that $Hf_{1-x}Al_xN(001)$ layers with Al compositions x between 0.00 and 0.50 are metastable B1-NaC structure single crystals. The relaxed lattice constant a_0 ranges from 0.4519 nm for $x = 0$ to 0.4438 nm for $x = 0.50$. Analyses of high-resolution reciprocal lattice maps (HR-RLMs) show that the films are nearly fully relaxed with mild residual in-plane compressive strain ranging from -0.70% for $x = 0$ to -1.69% for $x = 0.50$. Nanoindentation analyses reveal that the elastic modulus of $Hf_{1-x}Al_xN$ decreases continuously with increasing x , 405 ± 6 to 336 ± 7 GPa, while the hardness remains essentially constant at 24.7 ± 0.8 GPa until approximately $x = 0.25$, at which point the hardness increases about 30% to 32.4 ± 0.7 GPa. This abrupt sample hardness increase corresponds to the onset of a 3D compositional modulation of ≈ 2 nm wavelength, as evidenced by Z-contrast XTEM. Thus the increased film hardness can be qualitatively explained by the Koehler effect (6), as the composition modulation results in a lattice constant modulation (strain field) in the film, hindering dislocation glide.

Koehler hardening is also active in nc-SiN_x/TiN, the archetypical superhard nanocomposite, although in this case the presence of an abrupt interface between two distinct components (commonly assumed to be amorphous Si₃N₄ and crystalline TiN) needs to be taken into account. Previous results by our international cooperators uncovered the existence of a metastable SiN phase, with B1-NaCl structure and low lattice mismatch ($\approx 1\%$) with TiN (7,8). This phase was shown to be stabilized in planar TiN/SiN nanolaminates for SiN layer thicknesses $\lesssim 2$ ML, the same regime where maximum hardness is attained in both nanolaminate and nanocomposite films.

We approach the problem of isolating and probing SiN_x/TiN interface chemistry and structure by preparing planar interfaces in the form of bilayers starting with well-defined TiN(001) and TiN(111) surfaces. In order to minimize contamination effects, film growth experiments are performed in ultra-high-vacuum. In situ UHV variable-temperature scanning tunneling microscopy (VT-STM), low-energy electron diffraction (LEED), and ab initio DFT calculations are used to provide atomistic information regarding bonding and crystallographic order at SiN_x/TiN interfaces.

LEED analysis of layers with SiN_x coverages $\theta_{SiN} < 0.30$ ML reveals the coexistence of $c\text{-}3\times 3$ and 1×5 surface phases. As θ_{SiN} approaches 0.30 ML, the intensity of the $c\text{-}3\times 3$ reconstruction spots decrease and the 1×5 pattern dominates. At $\theta_{SiN} = 0.5$ ML, the 1×5 spots become streaks along (110) reflections. STM images corresponding to the 1×5 reconstructed domains reveal a characteristic “corn-cob” atomic-scale morphology exhibiting a height modulation of ~ 1 Å peak-to-peak. The width of the five-row repeat structure, four “corn rows” and a missing row, along both [110] and $[1\bar{1}0]$ is 14.4 ± 1.1 Å, which is in agreement with the TiN interplanar spacing of ~ 3 Å.

We explored the atomic structure of the SiN/TiN(001) interface further using ab-initio DFT to determine minimum energy structures as a function of θ_{SiN} . We constructed initial corn-like trial structures placing Si and N on TiN lattice positions (Si on top of N_{TiN} and N on top of Ti_{TiN}) leaving every fifth Si $[1\bar{1}0]$ row empty. Full geometrical relaxation of these trial structures indicates that SiN surface coverages ≥ 1 ML result in tetrahedral environments, while lower θ_{SiN} values favor octahedral environments. The

range of Si and N bond lengths with $\theta_{\text{SiN}} = 1$ ML is 1.60-1.87 Å, close to the reported value for Si-N compounds, 1.74 Å (9). Si-N_{TiN} bonds have a strong covalent character and a high local electron density (between 0.45 and 1.01 electrons/bond), comparable to diamond (1 electron/bond). These results suggest that the interfacial structure of superhard TiN-SiN_x nanocomposites and nanolaminates are much more complex and play a more important role in controlling film properties than was previously thought.

Future Plans

Recent results demonstrate the existence of ordered metastable SiN_x phases on TiN(001). In the near future, we will characterize the SiN_x-induced reconstructions on both TiN(001) and TiN(111), for the full coverage range up to the amorphization of the SiN_x layer, which is expected to occur between 1 and 2 ML. These reconstructions will be mapped using both atomic-resolution STM and LEED, and we will extend the scope of our DFT calculations to gain detailed atomistic information regarding every experimentally observed reconstruction. The result of this work will be a set of trial structural models that will be used, in conjunction with DFT calculations to investigate the bonding structure, detailed morphology, and interfacial energy of nc-TiN-SiN_x.

DFT calculations will also be applied to the detailed understanding of the properties and growth of Hf_{1-x}Al_xN. Full geometrical relaxation of trial Hf_{1-x}Al_xN cells, as a function of both composition and lattice constant, will provide insight into the ground state energies of metastable and equilibrium structures, which can be used to study the thermodynamics leading to cation clustering and the development of compositional modulations in the film. Furthermore, electronic structure calculations will be used in conjunction with ellipsometry measurements to understand the dependence on composition of the optical properties of Hf_{1-x}Al_xN. Finally, the compositional range of the Hf_{1-x}Al_xN will be extended beyond the single-phase stability limit into the composition range where precipitation of wurtzite AlN grains occurs (estimated to occur beyond $x = 0.5$).

Reference

- (1) F. Adibi, I. Petrov, L. Hultman, U. Wahlström, T. Shimazu, D. McIntyre, J. E. Greene, J.-E. Sundgren, *J. Appl. Phys.*, **69** 6437 (1991)
- (2) T.-Y. Lee, S. Kodambaka, J. G. Wen, R. Twisten, J. E. Greene, and I. Petrov, *Appl. Phys. Lett.*, **84** 2796 (2004)
- (3) H.-S. Seo, T.-Y. Lee, J. G. Wen, I. Petrov, J. E. Greene, and D. Gall, *J. Appl. Phys.* **96**, 878 (2004)
- (4) H.-S. Seo, T.-Y. Lee, I. Petrov, and J. E. Greene, *J. Appl. Phys.* **97**, 83521 (2005)
- (5) J.S. Koehler, *Phys. Rev. B* **2**, 547 (1970)
- (6) H. Söderberg, J. Molina-Aldareguia, L. Hultman, and M. Odén, *J. Appl. Phys.* **97**, 114327-1 (2005)
- (7) A. Flink, T. Larsson, J. Sjöln, L. Karlsson, and L. Hultman, *Surf. Coat. Technol.* **200**, 1535 (2005)
- (8) A. Aylward and T. Findlay, in *Si Chemical Data*, edited by P. Store (Wiley & Sons, Milton, 3rd Edition, 1994)

Recent DOE-sponsored publications

L. Hultman, J. Bareño, A. Flink, H. Söderberg K. Larsson, V. Petrova, M. Odén, J. E. Greene, and I. Petrov, “Interface structure in superhard TiN-SiN nanolaminates and nanocomposites: Film growth experiments and ab initio calculations”, *Physical Review B* (accepted)

B. Howe, J. Bareño, M. Sardela, J.G. Wen, A.A. Voevodin, and I. Petrov, Growth and physical properties of epitaxial metastable $\text{Hf}_{1-x}\text{Al}_x\text{N}$ alloys grown on MgO(001) by ultrahigh vacuum reactive magnetron sputtering. *Thin Solid Films* (accepted).

M. Stoehr, H.-S. Seo, I. Petrov, J.E Greene, “Raman scattering from epitaxial HfN layers grown on MgO(001),” *J. Appl. Phys.* 99, 043507 (2006)

C.W. Lim, J.E. Greene, I. Petrov, CoSi_2 growth on Si(001) by reactive deposition epitaxy: Effects of high-flux, low-energy ion irradiation, *J. Appl. Phys.* 100, 013510 (2006)

J. Bareno, S. Kodambaka, S.V. Khare, W. Swiech, I. Petrov, J.E.Greene, Orientation-dependent mobilities from analyses of two-dimensional TiN(111) island decay kinetics, *Thin Solid Films*, 510, 339 (2006)

C.W. Lim, I. Petrov, and J.E. Greene, “Epitaxial growth of CoSi_2 on Si(001) by reactive deposition epitaxy: island growth and coalescence,” *Thin Solid Films*, 515, 1340 (2006).

P. H. Mayrhofer, C. Mitterer, J. G. Wen, I. Petrov, and J. E. Greene, “Thermally induced self-hardening of nanocrystalline Ti–B–N thin films,” *J. Appl. Phys.* 100, 044301 (2006)

S Kodambaka., S.V. Khare, I. Petrov, and J.E. Greene, “Two-dimensional island dynamics: role of step energy anisotropy,” *Surf. Sci. Repts.*, 60, 55-77 (2006).

A.P. Ehiasarian, J.G. Wen, I. Petrov, Interface microstructure engineering by high power impulse magnetron sputtering for the enhancement of adhesion, *J. Appl. Phys.* 101, 054301 (2007)

P. O. Å. Persson, S. Kodambaka, I. Petrov, and L. Hultman, Epitaxial Ti_2AlN (0001) Thin Film Deposition by Dual Target Reactive Magnetron Sputtering, *Acta Materialia*, (in press)

Solidification Dynamics and Selection Principles

R.E. Napolitano, R. Trivedi, S. Liu, M. Mendeleev
Materials and Engineering Physics, Ames Laboratory

Program Scope

The objective of this program is to achieve a basic understanding of the fundamental principles of competition and dynamical selection governing phase transitions from alloy melts in weakly and strongly driven systems. This entails bringing together computation and simulation methods together with theory-critical experiments to investigate the evolution of structure and chemistry at all relevant length scales. Computational efforts here include first-principle methods, classical molecular dynamics using both pair-wise and many-body interatomic potentials, solution-based thermodynamic modeling, and phase-field approaches. Experimental efforts include various techniques accessing a wide range of solidification conditions, including gradient-zone directional solidification, levitation melting, melt-spinning, and atomization. Characterization of phase selection, chemical segregation, and microstructural evolution is carried out using a wide range of e-beam and X-ray methods. The effort also includes measurement of critical fundamental thermo-physical and kinetic parameters using various calorimetric methods. The program is logically divided into three principal areas of solidification dynamics. These are (i) Fundamental behavior of crystal-melt interfaces, (ii) Thermodynamics of phase selection, and (iii) Multiscale structural selection.

Recent Progress

Anisotropic interfacial free energy is a critical factor in any predictive theory or computational treatment of the evolution of solidification microstructures, and its quantification is essential to the development of such treatments. In this project, we have used several approaches to quantify the anisotropic behavior of crystal-melt interfaces and to understand its influence on the dynamics of crystalline phases growing from the melt. We have developed a method for experimentally determining the 3-D equilibrium (Wulff) surface by directly measuring the shape of intragranular liquid droplets. In addition, we have computed the theoretical shape of coupled crystal-melt interfacial grain boundary grooves as a function of anisotropy, orientation of the solid-liquid interface, and orientation mismatch between the grains. Finally, we have examined the utility of the solvability theory with regard to its prediction of the influence of anisotropy on the selection of dendrite tip morphology.

The mobility of crystal-melt interfaces is also a fundamental property critical to solidification selection dynamics. We have used an embedded-atom method (EAM) potential to determine the crystal-melt interface mobility in pure Al. The method employs a simulation cell with periodic lateral boundaries open surfaces in the growth direction. A constant strain is applied at the melting temperature, altering the free energy of crystal relative to the liquid, consequently driving the interface. Velocity-driving force relationships were found to be linear at all applied strains, yielding mobility values.

Prediction and control of phase selection requires accurate quantification of driving forces for stable and metastable phases. This is particularly true in highly driven systems, where metastable crystalline and/or amorphous phases may be competitive. We have used CALPHAD methods to model the thermodynamic properties and phase equilibria in several Al-RE (Rare-earth) glass forming systems (La, Ce, Gd, Ho, Nd, Y, Dy). These methods incorporate experimental data (e-beam, X-ray, and calorimetry) and first principles calculations into comprehensive self-consistent thermodynamic models.

Nonequilibrium partitioning and glass formation become important at high undercooling. In treating the Al-La and Al-Sm binary systems, we have used a two-state model for the pure component liquid in the sub-melting temperature regime and a three-species association model

to describe the solution or mixing properties of the liquid phase. The resulting liquidus boundaries show better agreement with experimental observation than previously reported models. In addition, we model both terminal and intermediate phases as solid solutions and compute the values of T_L , T_0 , and T_k , corresponding to the conditions $\mu_i^{liq} = \mu_i^\phi$, $G^{liq} = G^\phi$, and $S^{liq} = S^\phi$, respectively. Results are compared with experimental observations of glass formation. Employing a Baker-Cahn approach, we also use our thermodynamic models to compute the range of compositions permissible for the solidification of a single crystalline phase or a two-phase mixture, from any given liquid. These include regions of nonequilibrium chemical partitioning, indicating the limits of crystalline phase solidification that must be investigated through kinetic analysis. (c)

Although significant studies are devoted to solidification microstructures as a function of processing conditions, microstructural evolution is significantly influenced by the size of the system. Specifically, when solidification is carried out in micron or submicron systems, the stability conditions for different morphologies are significantly altered. We have investigated this effect of system size on solidification microstructures through directional solidification of SCN-0.7wt%Salol and have found that the growth morphology changes significantly as the sample thickness becomes very small. For example, in a 12 μm thick sample, only dendritic structures are formed even at very low velocity where planar front stability is predicted for the bulk. The altered stability conditions give rise to larger tip radii and enable more effective investigation of dendrite tip kinetics. Using this feature, we have observed an oscillating dendritic growth mode, with each oscillation generating a pair of side arms.

Small ternary additions to Al-Si alloys have been shown to significantly alter or “modify” the morphology of the silicon phase within the eutectic constituent. While an interfacial mechanism involving twinning has been proposed as is generally accepted, there is very little detailed evidence to compel any conclusive statements concerning the interfacial mechanisms behind this well-known phenomenon. With recent advances in atomistic simulation techniques aimed at the investigation of such mechanisms, we have initiated an experimental effort to identify the important characteristics of this modification behavior. We have investigated the impurity modification of Al-Si eutectics with levels of strontium varying from 0 to 1 wt.%. Our preliminary experimental results have shown that the onset of the modification behavior occurs at compositions less than 0.01 wt.% Sr. In addition, we have performed liquid diffusion couple experiments followed by directional solidification and have estimated that the modification transition occurs between 0.002 and 0.006 wt% Sr. Establishing a critical threshold for the modification behavior is an essential step toward understanding the atomistic mechanisms involved in this growth mode transition. Indeed, the interaction between solutes, impurities and interfacial defects (e.g., twins) is likely to be a principal contributor to various observed growth behaviors that remain poorly understood and not well-predicted by existing theory.

The prediction of microstructure in which two or more solid phases form from the liquid is generally quite complex since both the nucleation characteristics and the dynamics of growth competition of the phases play critical roles. In this work, the fundamental physics that govern the complex microstructure is examined through critical experiments in a peritectic system of Sn-Cd, and theoretical models have been developed to analyze the results. Experiments are carried out in capillary samples to obtain diffusive growth conditions. When a peritectic system is directionally solidified, initially a primary phase forms. Before it reaches the steady-state, the peritectic phase nucleates, and the growth competition between the two phases will generate a complex microstructure. We have observed experimentally that the nucleation of the peritectic phase in thin samples occurs at the wall, and the undercooling at which the nucleation occurs is measured precisely through temperature and composition measurements. A detailed model of nucleation at the triple junction at the wall is developed in terms of three contact angles. A theoretical model, based on these contact angles and dynamics of interface propagation has been

developed to obtain the differences in the physics of two widely differing morphologies, one being an oscillatory or “banded” structure, the other being a eutectic-like structure.

Multiphase coupled growth morphologies are ubiquitous in nature and many fundamental questions remain outstanding regarding the related competition and selection. In this effort, we are investigating several important issues related to stability of various coupled morphologies and the dynamics of growth mode transitions. Issues here include (i) fundamental criteria for spacing selection, (ii) mechanisms for spacing adjustment, (iii) the boundaries for rod and lamellar stability ranges, coexistence, and transition dynamics, and (iv) coupled growth under rapid solidification conditions. Accurate thermodynamics and three-dimensional analysis of microstructure are important in all of these efforts.

Morphological selection during growth of faceted phases is an area that is currently not well understood, even though many crystalline phases with interesting functionality are highly anisotropic and exhibit faceted growth morphologies. Using serial milling and 3D image reconstruction, we have investigated the growth mechanisms that lead to the observed rapid lateral propagation of the bicrystalline dendritic twin-grains and have shown the critical role of twinning in the formation of the sideplates, a necessary feature for selection of this diffusive growth morphology. The migration of twin boundaries within the dendritic core enables efficient twin boundary reconfiguration, permitting diffusion-based evolution of sideplate structures, new primary core formation, and the associated selection of primary array spacing. With direct evidence from high resolution TEM imaging to support our claim, we have proposed a structure for the dendritic core that includes a combination of {310} and {210} symmetric coherent twins and have described an associated twin boundary migration mechanism, at the atomistic level, which would facilitate reconfiguration of the core structure and the sideplate generation required for efficient response to radial supersaturation gradients. We are currently using phase-field modeling to investigate the associated dendrite tip kinetics and selection.

Future Plans

We will continue to investigate the three stated areas related to solidification selection dynamics. With regard to the fundamental behavior of interfacial properties, we will investigate the role of anisotropy in dendrite selection in Al-Mg system. Here, we will use the experimental methods we have recently developed(1-3) in addition to new techniques to test recent theories of orientation selection, based on solvability and phase-field modeling (4). We will continue to develop thermodynamic models to examine phase stability and selection in highly undercooled systems, focusing on nonequilibrium partitioning, metastable crystalline phases, and glass formation. We will continue to focus on the mechanisms and dynamics of three-dimensional morphological selection in single phase and multi-phase growth modes. Here, we will address the limitations of current theories and modeling strategies (5-8) and develop analytical and computational models for microstructural prediction. We will investigate further the mechanism of growth in bicrystalline faceted primary Si in Al-Si alloys (9), look for similar behavior in other anisotropic materials, and continue to develop phase-field methods for modeling this behavior.

References

1. R. E. Napolitano, S. Liu, *Physical Review B* **70**, 214103 (2004).
2. R. E. Napolitano, S. Liu, R. Trivedi, *Interface Science* **10**, 217 (2002).
3. S. Liu, R. E. Napolitano, R. Trivedi, *Acta Materialia* **49**, 4271 (2001).
4. T. Haxhimali, A. Karma, F. Gonzales, M. Rappaz, *Nature Materials* **5**, 660 (Aug, 2006).
5. H. Kasajima, E. Nagano, T. Suzuki, S. G. Kim, W. T. Kim, *Science and Technology of Advanced Materials* **4**, 553 (2003).
6. S. G. Kim, W. T. Kim, *Journal of Crystal Growth* **275**, e355 (2005).
7. T. Suzuki, S. G. Kim, W. T. Kim, *Materials Science and Engineering A* **449-451**, 99 (2007).
8. J. M. Debierre, A. Karma, F. Celestini, R. Guerin, *PRE* **68**, 041604(1) (2003).

9. R. E. Napolitano, C. Jung, H. Meco, in *Solidification Processes and Microstructures: A symposium in Honor of W. Kurz* M. Rappaz, Ed. (The Minerals, Metals, and Materials Society, Charlotte, N.C., 2004) pp. 245-250.

Publications 2005-2007

1. S.H. Zhou and R.E. Napolitano, "The stability of Al₁₁Sm₃ compounds, *Met. Mat. Trans.*, (accepted, in press) 2007.
2. H. Walker, S. Liu, J.H. Lee, and R.K. Trivedi, "Eutectic Growth in Three Dimensions", *Metall. Mater. Trans.* (accepted, in press).
3. N. Wang, S. David, H. Walker, and R. Trivedi, "Eutectic Instability and Phase Selection in the Al-Sm Systems" *Trans. Ind. Inst. Metals* (accepted, in press).
4. Y.E. Kalay, L.S. Chumbley, I.E. Anderson, R.E. Napolitano, "Characterization of Hypereutectic Al-Si powders solidified under far from equilibrium conditions", *Met. Trans.* (accepted, in press) 2007.
5. S.H. Zhou and R.E. Napolitano, "Thermodynamic treatment of undercooled Cu-Mg liquid and the limits for partitionless crystallization", *J. Phase Equil. Diff.*, (accepted, in press) 2007.
6. S. Zhou, Y. Wang, F.G. Shi, F. Sommer, L.Q. Chen, Z.K. Liu, and R.E. Napolitano, "Thermodynamic assessment and modeling of phase equilibria for the Cu-Mg binary system", *J. Phase Equil. Diff.*, (accepted, in press) 2007.
7. H. Meco and R.E. Napolitano, "Nonequilibrium chemical partitioning and phase formation in rapidly solidified Al-Sm and Ag-Sm binary alloys", *Mat. Sci. Forum* **539-543** (2007) 2810-2815.
8. B.P. Athreya, J. Dantzig, S. Liu, and R. Trivedi, "On the Role of Confinement on Solidification in Pure Materials and Binary Alloys", *Philos. Mag.*, **86**, 3739 (2006).
9. R.E. Napolitano and J.R. Morris, "Frontiers in Solidification Science: Preface to the special issue", *Phil. Mag.* **86** (2006) 3647-3649.
10. S. Liu and R.K. Trivedi, "The Effect of Thermosolutal Convection on Microstructure Formation in the Pb-Bi Peritectic System", *Metall. Mater. Trans. A*, **37A**, 3293 (2006).
11. S. Liu, J. Li, J.H. Lee, and R.K. Trivedi, "Spatio-Temporal Microstructure Evolution in Directional Solidification Processes", *Philos. Mag.*, **86** (24), 3717 (2006).
12. S. Zhou and R.E. Napolitano, "Phase equilibria and thermodynamic limits for partitionless crystallization in the Al-La binary system, *Acta Materialia*, **54** (2006) 831-840.
13. R.E. Napolitano and J.R. Morris, "Frontiers in Solidification Science: Preface to the Special Issue", *Philos. Mag.*, **86**, 3647 (2006).
14. H. Meco and R. E. Napolitano, "Liquidus and solidus boundaries in the vicinity of order-disorder transitions in the Fe-Si system", *Scripta Materialia*, **52** (2005) 221-226.
15. J.H. Lee, S. Liu, and R. Trivedi, "The Effect of Fluid Flow on Eutectic Growth", *Metall. Mater. Trans. A*, **36A**, 3111 (2005).
16. J.H. Lee, H.C. Kim, C.Y. Jo, S.K. Kim, J.H. Shin, S. Liu, and R. Trivedi, "Microstructure Evolution in Directionally Solidified Fe-18Cr Stainless Steels", *J. Mater. Sci. Eng.*, **A**, **413**, 306 (2005).
17. H. Meco and R.E. Napolitano, "Liquidus and Solidus Boundaries in the Vicinity of Order-Disorder Transitions in the Fe-Si System", *Scripta Mater.*, **52**, 221 (2005).
18. R. Trivedi and J.H. Shin, "Modeling of Microstructure in Peritectic Systems", *J. Mater. Sci. Eng.*, **A**, **413**, 288 (2005).

Session IV

Hybrid Materials and Assembly

Session Chair: Paul Gourley, Sandia National Laboratories

Invited Speaker: Paul Chaikin, New York University

This page is intentionally blank

Hybrid Nanoscale Synthesis and Assembly using Atomic Layer Deposition

Michael J. Pellin¹ and Jeff Elam²
Pellin@anl.gov

¹Materials Science Division, ²Energy Systems Division, Argonne National Laboratory,
Argonne, IL 60439

Program Scope

Atomic Layer Deposition (ALD) is a precision synthesis method providing a facile, flexible route for the functionalization of the interior surfaces of nanoporous materials. This method of synthesizing functional architectures takes advantage of the wide range of nano-scaffolds currently available to produce functional architectures with a wide range of energy relevant physical properties. Atomic Layer Deposition has a broad palate with demonstrated synthetic precursors for the growth oxides, carbides, nitrides, and elemental films. The films synthesized are conformal with a demonstrated ability to coat materials with aspect ratios exceeding 5000. In recent work we have demonstrated that pin-hole free multiple oxide layers of nm thickness can be used to functionalize nanoporous solids to produce dye-sensitized solar cell structures with significantly reduced dimensionality (and consequentially much reduced electron transport differences). These solar cells demonstrate both record photovoltages and fill factors (for ZnO).

Recent Progress

We have developed Atomic Layer Deposition (ALD) synthesis methods to functionalize two nanoporous solids, anodic alumina and aerogels (silica and C), with thin conformal pin-hole free layers of wide band gap oxides (ZnO and TiO₂), transparent conducting oxides (ITO and AZO) and metals (W and Pd). In the case of carbon aerogels, for instance, The resulting material has a filamentous structure in which the W completely encapsulates the carbon aerogel strands. The material mass increases nonlinearly with W coating, achieving a tenfold increase following ten ALD cycles. The aerogel surface area increases by nearly a factor of 2 after ten W ALD cycles. This conformal metal coating of extremely high aspect ratio nanoporous materials by ALD represents a unique route to forming metal functionalized high surface area materials.

Nanostructured membrane structures have been fabricated by a combination of anodic aluminum oxide (AAO) and ALD for use as platforms for the synthesis of highly uniform heterogeneous catalysts. The ALD method makes it possible to control pore diameters on the Angstrom scale even when the overall pore diameter is 10's to 100's of nanometers. AAO membranes imbedded in an aluminum sealing ring have been tested for flow properties and found to follow Knudsen diffusion behavior. Vanadia-coated membranes have been tested for the catalytic oxidative dehydrogenation of cyclohexane and show improved selectivity at the same conversion compared to conventional powdered alumina supported vanadia catalysts with significant improvement in both reactivity and specificity. An example of the functionalize AAO structures can be found in **Fig. 1**.

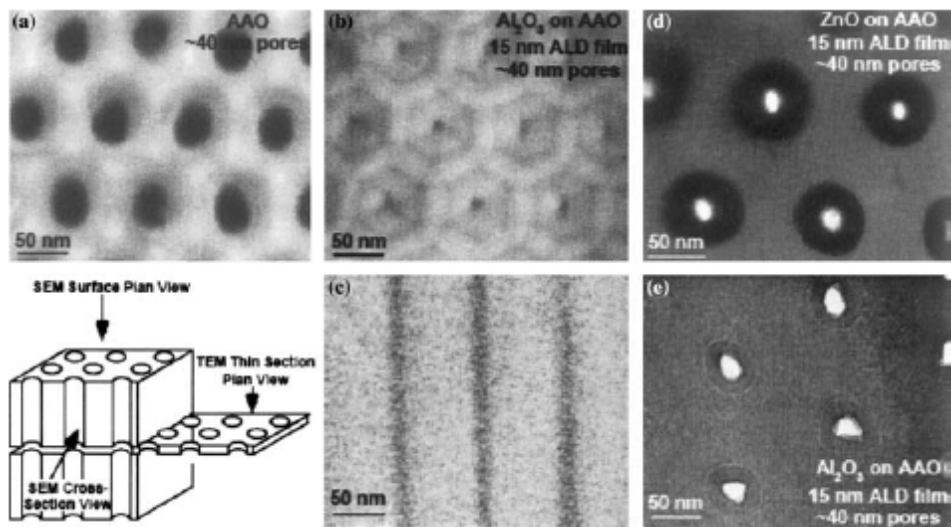


Figure 1. (a) Plan view SEM image of surface of the original 40 nm AAO material. (b) Plan view SEM image of the surface of the 40 nm AAO material coated with 15 nm of alumina. (c) Cross sectional view of 40 nm AAO material coated with 15 nm of alumina taken from the center of the AAO membrane (note that the coating is uniform despite the high aspect ratio). (d) Plan view TEM thin section image taken from the center of a 40 nm AAO membrane coated with 15 nm of ZnO. (e) Plan view TEM thin section image taken from the center of a 40 nm AAO membrane coated with 15 nm of Al₂O₃ (note that the ALD coating conformally coats pores with eccentric pore shapes).

Finally in joint work with Northwestern University (Hupp et al), this method has been used to assemble a new photoanode structure featuring very high aspect ratio substructures with roughness factors (RF) greater than 1000. The design implementation strategy combines anodic aluminum oxide (AAO) templating and atomic layer deposition (ALD) to yield oriented arrays of electrically interconnected semiconductor nanotubes. Because it is both a stepwise and conformal coating technique, ALD provides exceptional control over nanoscale device composition and architecture. The large number of metal oxides accessible by ALD (including, but not limited to, TiO₂, ZnO, SnO₂, ZrO₂, and NiO) makes the technique potentially very widely applicable for the development of new photoelectrodes. Here we demonstrate the viability of ZnO versions of these structures as dye sensitized electrodes by characterizing their morphology, light harvesting efficiency, and photovoltaic performance. The photoanode produced in the synthesis process is displayed in **Fig. 2**. Among the breakthroughs demonstrated in this study was an ability to use the pulse sequence times inherent in the ALD method to produce either thin, pinhole free conformal coatings (conductive at thickness down to 1 nm) or thick pore sealing TCO films such as the 1 micron thick conducting electrode film on the right of **Fig 2**.

Construction of a dye sensitized solar cell using these photoanodes following attachment of a dye to the ZnO surface was possible. The subsequent solar cells achieved the highest photovoltage and the largest fill factor (for ZnO). These results demonstrate the quality of the nanostructured photoanode. Moreover the precision synthesis method allowed for the first time the thickness dependence of the photoanode films on photovoltage and photocurrent.

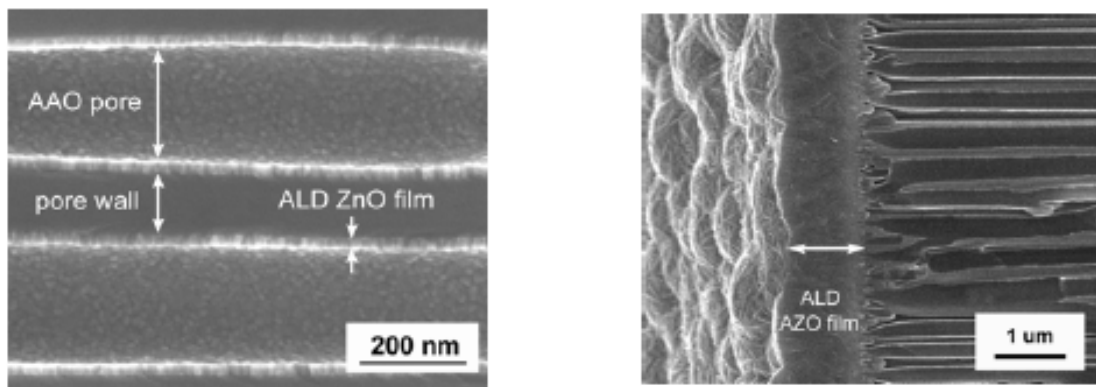


Figure 2. At left is a cross-sectional SEM image of commercial AAO membrane pores coated with 20 nm of ZnO by ALD. At right is a cross-sectional SEM image of commercial AAO face coated with transparent conductive oxide AZO.

Future Plans

More complicated photoanode structures interdigitating a TCO and wide band gap oxides are being constructed. These structures provide a greatly reduced dimensionality to the DSSC cells. Consequently the electron collection distance can be reduced by nearly 3 orders of magnitude. Electron transport times should be reduced by 6 orders of magnitude providing significant opportunities for efficiency increases.

References

DOE Sponsored Publications in 2005-2007

Transparent Conducting Oxides at High Aspect Ratios by ALD, M. J. Pellin, J. W. Elam, J. A. Libera, A. B. F. Martinson and J. T. Hupp, *Journal of the Electrochemical Society* **2007**, accepted.

ZnO Nanotube Dye-Sensitized Solar Cells, A. B. F. Martinson, J. W. Elam, J. T. Hupp and M. J. Pellin, *Nanoletters* **2007**, in revision.

Novel Photoanode Architectures and Tunneling Barriers, T. W. Hamann, A. B. F. Martinson, J. W. Elam, M. J. Pellin and J. T. Hupp, *Preprints of Symposia - American Chemical Society, Division of Fuel Chemistry* **2007**, 52, accepted.

Supported gold clusters and cluster-based nanomaterials: characterization, stability and growth studies by in situ GISAXS under vacuum conditions and in the presence of hydrogen, S. Vajda, R. E. Winans, J. W. Elam, B. Lee, M. J. Pellin, S. Seifert, G. Y. Tikhonov and N. A. Tomczyk, *Topics in Catalysis* **2006**, 39, 161-166.

Novel, Uniform Nanostructured Catalytic Membranes, P. C. Stair, C. Marshall, G. Xiong, H. Feng, M. J. Pellin, J. W. Elam, L. Curtiss, L. Iton, H. Kung, M. Kung and H. H. Wang, *Topics in Catalysis* **2006**, 39, 181-186.

Imaging of Atomic Layer Deposited (ALD) Tungsten Monolayers on α -TiO₂(110) by X-ray Standing Wave Fourier Inversion, C.-Y. Kim, J. W. Elam, M. J. Pellin, D. K. Goswami, S. T. Christensen, M. C. Hersam, P. C. Stair and M. J. Bedzyk, *Journal of Physical Chemistry B* **2006**, 110, 12616-12620.

Atomic layer deposition of palladium films on Al₂O₃ surfaces, J. W. Elam, A. Zinovev, C. Y. Han, H. H. Wang, U. Welp, J. N. Hryn and M. J. Pellin, *Thin Solid Films* **2006**, 515, 1664-1673.

Atomic Layer Deposition for the Conformal Coating of Nanoporous Materials, J. W. Elam, G. Xiong, C. Y. Han, H. H. Wang, J. P. Birrell, J. N. Hryn, M. J. Pellin, J. F. Poco and J. Joe H. Satcher, *Journal of Nanomaterials* **2006**, 2006, 64501-1 - 64501-5.

Atomic Layer Deposition of In₂O₃ Using Cyclopentadienyl Indium: A New Synthetic Route to Transparent Conducting Oxide Films, J. W. Elam, A. B. F. Martinson, M. J. Pellin and J. T. Hupp, *Chemistry of Materials* **2006**, 18, 3571-3578.

Atomic layer deposition of W on nanoporous carbon aerogels, J. W. Elam, J. A. Libera, M. J. Pellin, A. V. Zinovev, J. P. Greene and J. A. Nolen, *Applied Physics Letters* **2006**, 89, 053124-1 - 053124-3.

Atomic layer deposition of uniform metal coatings on highly porous aerogel substrates, T. F. Baumann, J. Biener, Y. M. Wang, S. O. Kucheyev, E. J. Nelson, J. H. Satcher, Jr., J. W. Elam, M. J. Pellin and A. V. Hamza, *Chemistry of Materials* **2006**, 18, 6106-6108.

Effect of Atomic Layer Deposition Coatings on the Surface Structure of Anodic Aluminum Oxide Membranes, G. Xiong, J. W. Elam, H. Feng, C. Y. Han, H.-H. Wang, L. E. Iton, L. A. Curtiss, M. J. Pellin, M. Kung, H. Kung and P. C. Stair, *Journal of Physical Chemistry B* **2005**, 109, 14059-14063.

Mesoporous catalytic membranes: Synthetic control of pore size and wall composition, M. J. Pellin, P. C. Stair, G. Xiong, J. W. Elam, J. Birell, L. Curtiss, S. M. George, C. Y. Han, L. Iton, H. Kung, M. Kung and H. H. Wang, *Catalysis Letters* **2005**, 102, 127-130.

Atomic layer deposition of ZnO on ultralow-density nanoporous silica aerogel monoliths, S. O. Kucheyev, J. Biener, Y. M. Wang, T. F. Baumann, K. J. Wu, T. Van Buuren, A. V. Hamza, J. H. Satcher, Jr., J. W. Elam and M. J. Pellin, *Applied Physics Letters* **2005**, 86, 083108/1-083108/3.

GaPO₄ Sensors for Gravimetric Monitoring During Atomic Layer Deposition at High Temperatures, J. W. Elam and M. J. Pellin, *Analytical Chemistry* **2005**, 77, 3531-3535.

Carbohydrate Templates for Engineering Nanostructures

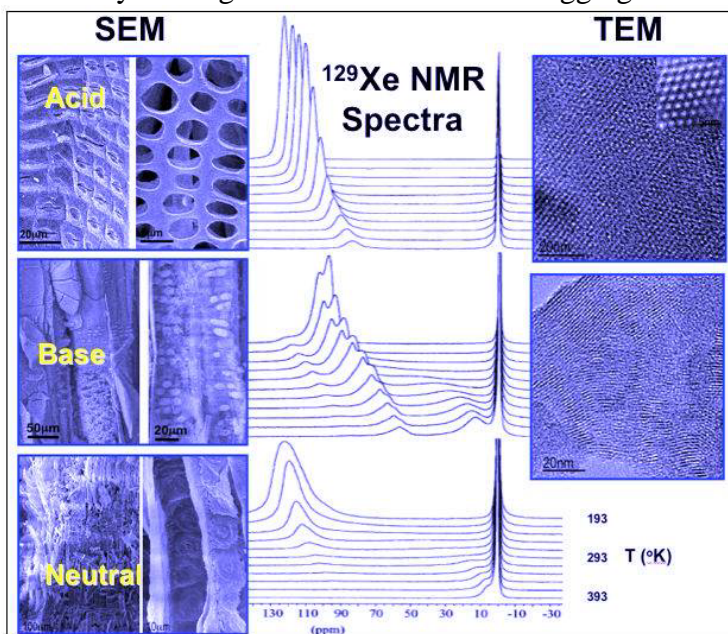
Gregory J. Exarhos, William D. Samuels, Yongsoon Shin, Li Qiong Wang, PNNL
Chunhua Yao, William M. Risen, Jr., Brown University

I. Program Scope

Both porous and anisotropic nanoarchitectures are generated using an array of solution templated growth and post growth modification approaches that invoke chemical control of molecular self-assembly at interfaces. Synthesis strategies are designed based upon a fundamental understanding of coupled formation reactions that drive the self-assembly process and that can be manipulated kinetically by altering reaction rates. Templated growth processes pursued in this research include: ceramic micelle assisted mineralization of wood; hydrothermal dehydration of carbohydrates to form carbon nanospheres; and, interface-driven reduction of metal cations along fixed directions in nano-crystalline cellulose. Materials derived from these solution approaches are characterized with respect to phase composition, homogeneity, structural anisotropy, pore structure and pore interconnectivity, and attendant molecular structure by means of non-conventional magnetic resonance measurements that are complemented by traditional electron microscopy, diffraction, and scattering approaches.

II. Recent Progress

Hierarchically ordered silica-based materials that emulate wood cellular structures have been synthesized by means of surfactant-directed *in-situ* mineralization.⁽¹⁾ Under low pH conditions that favor preferential leaching of lignin from the wood, surfactant combines with an organosilicate precursor to form micelles that penetrate the porous structure of wood eventually coating all interfaces without clogging the resident wood pores as seen to the left.

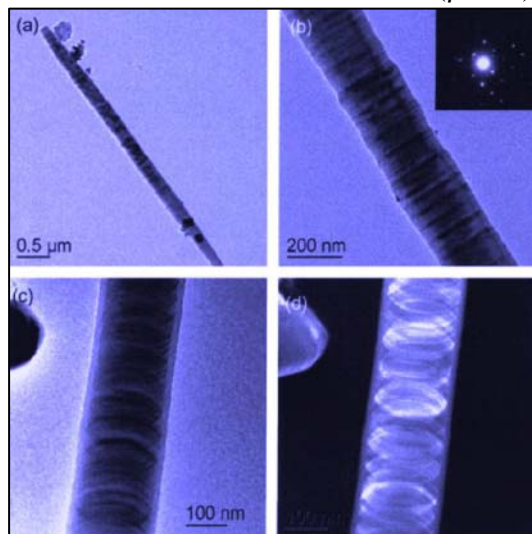


This ‘molecular paint’ uniformly nucleates on all buried interfaces.

Following subsequent heating in air, the organic constituents are oxidized to form silica. However, under high pH conditions, silica particles nucleate rapidly and coalesce to fill the open cells and pits within the structure thereby forming a dense negative replicate. This figure shows temperature-dependent continuous flow HP ^{129}Xe NMR spectra and associated SEM (left) and TEM (right) images for poplar samples treated under acid (top) base (middle) and neutral (bottom) conditions.⁽²⁾ The spectra can be interpreted in terms

of pore distribution and pore connectivity. Surfactant-templated mineralization at low pH not only preserves structural integrity, but also integrates hexagonally ordered nanoporosity into the structure of the cell walls as a result of the micelle ordering that occurs at the interfaces.

Carbothermal reduction of wood mineralized with transition metal oxide precursors produces metal carbides. Biomimetic cellular metal carbides have been prepared through selective control of resident metal oxide content, and appropriate choice of reaction temperature. XRD patterns of SiC fibers derived from a mineralized wood/silica composite at 1400°C in Ar confirm the cubic (β -SiC) phase. SEM and TEM measurements (left) reveal the presence of both whisker and oriented nano-



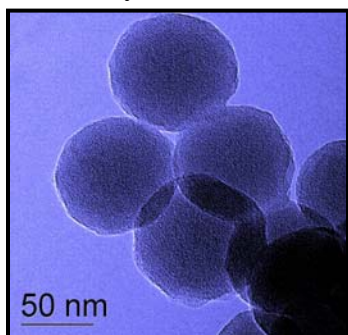
crystalline silicon carbide platelet morphologies.⁽³⁾

Using an alkoxy titanium precursor in the wood mineralization step leads to formation of phase-pure, face-centered cubic TiC replicas after subsequent thermal processing. Micrographs of the crystalline TiC that results, confirm that the initial cellulose structures have indeed been reproduced.

Temperature dependent xenon magnetic resonance spectroscopy was shown in this work to be a powerful probe of micro- and meso-porosity and pore interconnectivity in high surface area materials including mineralized wood, metal oxide framework structures, and ultraporous polymer networks. These first measurements supplement

structural information available from neutron and x-ray scattering approaches. Operando proton and hyperpolarized xenon NMR measurement protocols developed here have been extended in related research to understand flow processes and water partitioning in porous polymer membranes that govern energy conversion efficiency in PEM fuel cells.⁽⁴⁾

A related research area examines the remarkable transformation of sugars and certain chemically similar, $(\text{CH}_2\text{O})_x$, carbohydrates into homogeneous carbon spheres in a closed system.⁽⁵⁾ The reaction occurs readily via a dehydration

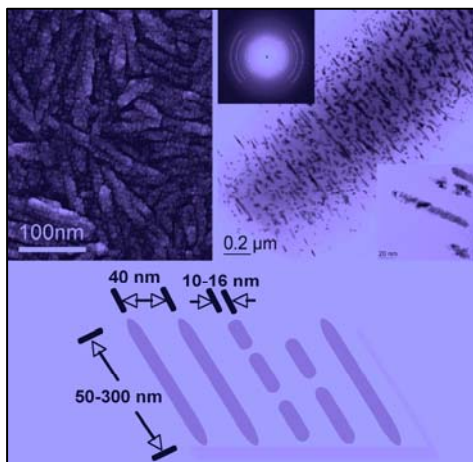


mechanism and subsequent molecular assembly in aqueous solutions that are heated to about 130°C in a pressurized vessel. *In situ* Raman measurements confirm that the sugar molecules actually dehydrate even though they are dissolved in water.

Glucose molecules in solution condense (polymerize) via an intermolecular dehydration route. Subsequent loss of water leads to formation of hydrophobic regions of the molecule that partition from the hydrophilic solution and rearrange into spheres (left). In contrast, the fructose isomer initially degrades to form 5-hydroxymethyl-2-furaldehyde by means of intramolecular dehydration. Hydrophobic partitioning then drives formation of microscopic carbon-containing spheres that subsequently coalesce into a golf-ball-like morphology seen in SEM and TEM images. The use of derivitized sugar molecules containing acid functionality (glucuronic acid), amine (glucosamine), or phosphate (glucose-6-phosphate) groups to modify the surface chemistry generates functionalized carbon for prospective applications including sequestration of contaminants, catalyst supports, and electrically conducting hybrid phases for energy conversion devices including fuel cells.

We have recently found that nanocrystalline cellulose, which is easily isolated from paper or cotton, behaves as an anisotropic reduction template as evidenced by textured growth of metal nanoparticles and nanorods when placed in contact with aqueous solutions of certain

metal cations, Ag^+ , Pd^{+2} , Au^{+3} , and Ni^{+2} . Preferential cation (Pt^{+4}) reduction as shown in the figure below occurs along crystalline planes where oriented hydroxyl groups reside.



III. Future Plans

Ongoing research continues to investigate molecular templating approaches in carbohydrate systems that often proceed by means of at least two coupled chemical reactions where rate constants and ensuing self-assembled structures can be altered by the processing chemistry. Experiments aim to discover and understand the major factors that influence the formation kinetics of nanostructured media and their attendant structural modifications. Concepts and characterization tools developed in this project propel new research avenues that address structural modification in supramolecular cage-like hydrocarbon-based structures (foldamers) with

Professor Alex Li at Washington State University and metal oxide nanotubes (ZnO) where variations in processing chemistry drive structural modification perturb associated properties.

IV. References

- (1) Y Shin, J Liu, J-H Chang, Z Nie, and GJ Exarhos, 2001. *Adv. Mater.* 13(10) 728.
- (2) L-Q Wang, Y Shin, WD Samuels, GJ Exarhos, IL Moudrakovski, VV Terskikh, and JA Ripmeester. 2003. *J. Phys. Chem. B* 107(50):13793.
- (3) Y Shin, C Wang, and GJ Exarhos, 2005. *Adv. Mater.* 17(1) 73.
- (4) KR Minard, VV Vishwanathan, PD Majors, LQ Wang, and PC Rieke, 2006. *Journal of Power Sources* 161(2):856-863.
- (5) Q Wang, H Li, L Chen, and X Huang, 2002. *Solid. State Ionics.* 152-153, 43.

V. Publications (previous 2 years)

- Shin Y, CM Wang, XS Li, and GJ Exarhos, 2005. "Synthesis of supported carbon nanotubes in mineralized silica-composites." *Carbon* 43(5):1096-1098.
- Y Shin, LQ Wang, GE Fryxell, and GJ Exarhos, 2005. "Hygroscopic growth of self-assembled layered surfactant molecules at the interface between air and organic salts." *J. Coll. and Interfac. Sci.* 284(1):278-281.
- Shin Y, CM Wang, and GJ Exarhos, 2005. "Synthesis of SiC ceramics by the carbothermal reduction of mineralized wood with silica." *Adv. Mater.* 17(1):73-77.
- Moudrakovski IL, CI Ratcliffe, JA Ripmeester, LQ Wang, GJ Exarhos, T Baumann, and JH Satcher, 2005. "Nuclear magnetic Resonance studies of resorcinol-formaldehyde aerogels." *J. Phys. Chem B* 109(22):11215-11222 .
- Wang LQ, SV Mattigod, KE Parker, DT Hobbs, and DE McCready, 2005. "Nuclear magnetic resonance studies of aluminosilicate gels prepared in high-alkaline and salt-concentrated solutions." *J. Non-Crys. Sol.* 351(43-45):3435-3442.
- Dabbs DM, U Ramachandran, S Lu, J Liu, LQ Wang, and IA Aksay, 2005. "Inhibition of aluminum oxyhydroxide precipitation with citric acid." *Langmuir* 21(25):11690-11695.

- JH Chang, CH Shim, BJ Kim, Y Shin, GJ Exarhos, and KJ Kim, 2005. "Bicontinuous, thermoresponsive, L-3-phase silica nanocomposites and their smart drug-delivery applications." *Adv. Mater.* 17(5):634-637.
- L Qi, BI Lee, S Chen, WD Samuels, and GJ Exarhos, 2005. "High-dielectric-constant silver-epoxy composites as embedded dielectrics." *Adv. Mater.* 17(14):1777-1781.
- CF Windisch Jr, Y Shin, and GJ Exarhos, 2005. "Chemical and biological point sensors for homeland defense", In *Chemical and Biological Standoff Detection II. Proceedings of the SPIE*, vol. 5585, pp. 79-87. International Society for Optical Engineering, Bellingham, WA.
- CF Windisch, Jr., GJ Exarhos, and SK Sharma, 2005. "Viscosity by fluorescence depolarization of probe molecules. A Physical Chemistry Laboratory Experiment." *J. Chem. Ed.* 82(6):916-918.
- BI Lee, M Wang, D Yoon, P Badheka, L Qi. and L-Q Wang, 2005. "Synthesis of nanoparticle barium titanate", Chapter 7 in *Chemical Processing of Ceramics*, 2nd edition, CRC Press, Taylor & Francis Books, Inc, Boca Raton, FL, p.173.
- JH Chang, GJ Exarhos, and Y Shin, 2005. "Biomimetic catalysis of tailored mesoporous materials with self-assembled multifunctional monolayers." *J. Ind. Eng. Chem.* 11(3):375-380.
- L Qi, BI Lee, WD Samuels, GJ Exarhos, and SG Parker, Jr., 2006. "Three-phase percolative silver-BaTiO₃-epoxy nanocomposites with high dielectric constants." *J. Appl. Poly. Sci.* 102:967-971.
- L Qi, BI Lee, P Badheka, LQ Wang, P Gilmour, WD Samuels, and GJ Exarhos, 2006. "Low-Temperature paraelectric-ferroelectric phase transformation in hydrothermal BaTiO particles." *Mat. Lett.* 59(22):2794 – 2798.
- J Kim, H Jia, C Lee, S Chung, J Kwak, Y Shin, A Dohnalkova, B Kim, P Wang, and JW Grate, 2006. "Single enzyme nanoparticles in nanoporous silica: A hierarchical approach to enzyme stabilization and immobilization." *Enzyme and Microbial Technology* 39:474-480.
- A Gutowska, L Li, Y Shin, CM Wang, XS Li, JC Linehan, RS Smith, BD Kay, BA Schmid, WJ Shaw, MS Gutowski, and T Autrey, 2006. "Nano-scaffold mediates hydrogen release and reactivity of ammonia borane." *Angewandte Chemie International Edition* 44(23):3578-3582.
- JD Torrey, RK Bordia, CH Henager, JR, Y Blum, Y Shin, and WD Samuels, 2006. "Composite polymer derived ceramic system for oxidizing environments." *J. Mat. Sci.* 41(14):4617-4622.
- C Lei, Y Shin, JK Magnuson, GE Fryxell, LL Lasure, DC Elliott, J Liu, and EJ Ackerman, 2006. "Characterization of functionalized nanoporous supports for protein confinement" *Nanotech.* 17(22):5531-5538.
- SV Mattigod, BP McGrail, DE McCready, LQ Wang, KE Parker, and JS Young, 2006. "Synthesis and structure of perhenate sodalite." *Microporous and Mesoporous Materials* 91(1-3):139-144.
- Q. Huo, J Liu, LQ Wang, Y Jiang, TN Lambert, and E Fang, 2006. "A new class of silica cross-linked micellular core-shell nanoparticles" *JACS* 128(19):6447-6453.
- KR Minard, VV Vishwanathan, PD Majors, LQ Wang, and PC Rieke, 2006. "Magnetic resonance imaging (MRI) of PEM dehydration and gas manifold flooding during continuous fuel cell operation." *Journal of Power Sources* 161(2):856-863.
- Y Shin, JM Blackwood, I Bae, BW Arey, and GJ Exarhos, 2007. "Synthesis and stabilization of selenium nanoparticles on cellulose nanocrystal ." *Mat. Lett.* [In Press].

Active Assembly of Dynamic and Adaptable Materials

Bruce C. Bunker, Sandia National Laboratories, Albuquerque, NM 87185

Program Scope

The objective of this project is to exploit key strategies used by living systems to develop materials whose transport, assembly, reconfiguration, and disassembly can be programmed or “self-directed” in controlled environments. These strategies are based on the exploitation of two energy-consuming proteins, the motor protein kinesin and the fiber-forming protein tubulin, in artificial systems for the manipulation of man-made nanomaterials. Components of the overall effort include: 1) **Dynamic Assembly**, which involves manipulating the behavior of tubulin-based microtubules to create fiber networks, mobile shuttles, and programmable materials, 2) **Active Transport**, which involves the use of motor proteins to transport and reconfigure nanomaterials, either by walking along microtubules (normal motility) or by having arrays of microtubules propel microtubule shuttles and their associated cargo (inverted motility), 3) **Multicomponent Materials**, which explores the behavior of ordered arrays of particles, microtubules, and motor proteins, and 4) **Theory and Modeling**, which is used to both visualize and predict the complex behavior of active assembly, transport, and reconfiguration processes.

Recent Progress

Dynamic Assembly – We have conducted in-depth investigations of the use of chemical crosslinking to stabilize microtubules against dynamic instability for use in active transport systems. Due to dynamic instability, native microtubules typically exhibit lifetimes of less than one hour. With appropriate crosslinking, we have been able to extend lifetimes out to over one week, as well as stabilizing the microtubules to the adverse effects of temperature fluctuations and chemical destabilization in the presence of calcium and other divalent cations (Fig. 1).

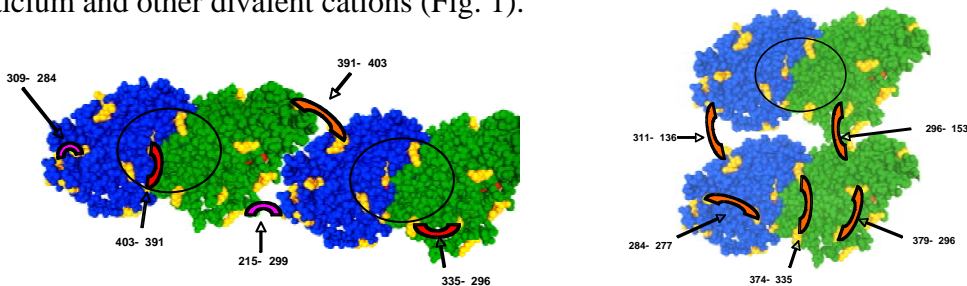


Fig. 1 Mapping of crosslinks between lysine residues (yellow) on a microtubule surface comprised of a- (blue) and b- (green) tubulin dimers¹¹. The most effective crosslinks are sufficiently short (pink) that they only connect tubulin units along protofilaments (left) without blocking the motor protein binding site (inside circle). Crosslinks that are long enough to bridge between protofilaments (right) eventually transform rigid microtubules into flexible sheets that exhibit poor interactions with motor proteins.

Active Transport - Recently, we have taken the first step toward creating programmable motors by genetically engineering a molecular “on-off” switch into the neck linker region of kinesin. The switch is based on “molecular shackles” controlled by metal chelates. When metal cations bind to chelates incorporated into the linker region, the mobile heads are tied together and are not able to respond to the presence of ATP fuel. Removal of the metal cations “unlocks” the shackles, allowing transport to occur. The first demonstration of the “molecular shackles” concept has been achieved by genetically engineering zinc-binding domains into five distinct locations in the linker region. One of these mutants can be reversibly switched “off” via addition of Zn^{2+} or other divalent cations (Ni^{2+} , Cu^{2+} , and Co^{2+}). Transport can be switched back “on” via addition of metal chelates in the solution (e.g. cysteine or 1,10 phenanthroline).

Multicomponent Materials – A major emphasis of our activities in particulate composites involves the synthesis and use of artificial microtubule organizing centers (AMOCs) that mimic the most common constructs used by organisms to exploit microtubules and motor proteins. MOCs consist of a central organizing particle to which an array of microtubules is attached. One successful strategy for making AMOCs involves the use of segmented microtubule seeds containing biotin-rich and biotin free segments. The biotinylated segment is used to attach the microtubule to the central particle, while the biotin-free segment is left free as a nucleation center for subsequent microtubule growth. As the biotin-containing segment can be produced at either the + or – end of the polar microtubule, AMOCs can be created in which either + or – ends radiate out into solution, controlling the radial polarity of the AMOC (Fig. 2).

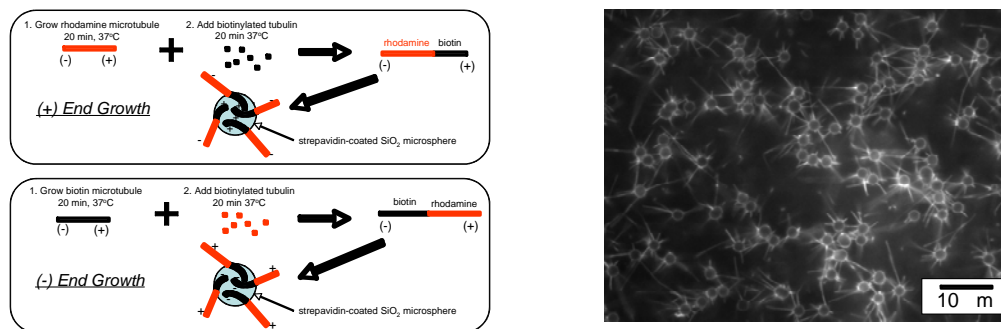


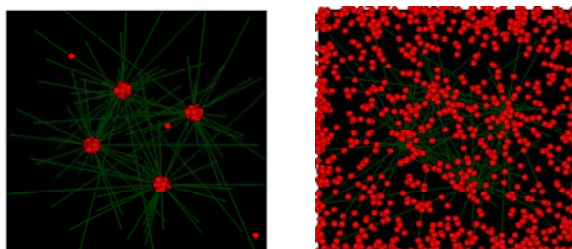
Fig. 2 Left – Representations of a polar oriented microtubule organizing centers created via adsorption of microtubules containing biotin-rich segments. Right – Optical micrograph of an array of artificial microtubule organizing centers.

Theory/Modeling

Stochastic methods have been developed to explore potential applications of motor proteins and microtubules for assembly and reconfiguration of nanomaterials. The new models capture both the statistical and temporal properties of active proteins, allowing us to visualize and predict complex behavior patterns associated with active assembly processes. Recently, the models have been applied to study materials assembly and

reconfiguration processes associated with microtubule organizing centers. For example, simulations have been performed to guide our efforts to create artificial melanophores (the color changing system used by organisms such as chameleons)(Fig. 3).

Fig. 3 Snapshots taken from simulated movies of the behavior of an array of artificial melanophores showing (a) the concentration of all particles on microtubule organizing centers when only inward-walking motors are activated (green microtubules radiate outward from each center), and (b) the equilibrium distribution of dye particles resulting from the tug of war between inward and outward walking motors.



The results show that we should be able to create artificial color changing centers if we can attach both inward and outward-walking motors to quantum dots, and have the ability to switch the outward-walking motors on and off (as we have achieved with kinesin).

Future Plans

Dynamic Assembly – Our modeling efforts indicate that there are many exciting assembly and transport functions that we can achieve if we can learn to exploit the polymerization and depolymerization of microtubules. We will explore the use of parameters such as temperature, tubulin and GTP concentrations, solution ions, and microtubule-associated proteins to control microtubule growth and collapse rates.

Active Transport – We plan to extend our genetic engineering efforts to incorporate molecular switches that are electrochemically-activated for controlling both transport and cargo loading and unloading functions. We also plan to study the behavior of motors such as dynein that move in the opposite direction to our current kinesin motors.

Multicomponent Materials – Now that we have successfully produced artificial microtubule organizing centers, our plan is to try to replicate the materials assembly and reconfiguration functions represented by diatom skeletal assembly and the color changing systems (Fig. 4). Preliminary results on single microtubules suggest that the diatom assembly process can be achieved if we can learn to control the “stringing of pearls” phenomena that we have observed with polystyrene particles (Fig. 4).

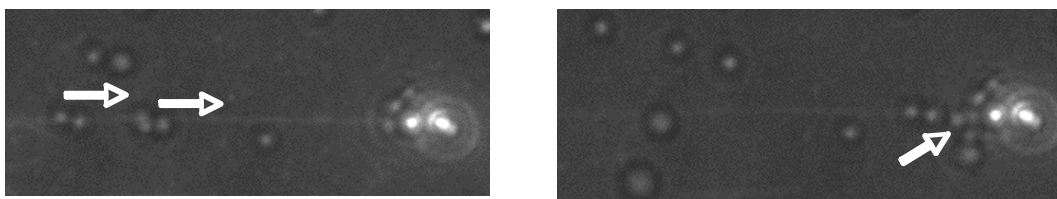


Fig. 4 Frames from a fluorescence micrograph movie showing the transport and collection of a series of polystyrene beads along a single microtubule to form a short particulate string in analogy to diatom skeleton assembly. Left – Five particles in transit, moving from left to right. Right – The five particles have been collected in a string at the right end of the microtubule.

Theory/Modeling – A major focus of the modeling effort will be on guiding our experimental efforts in exploiting dynamic instability processes. For example, preliminary analyses show that clear shifts between conditions favoring growth and depolymerization will require a temperature difference of around 10°C, guiding our development of microheaters to control network formation in microfluidic systems.

Publications

1. H. Hess and G. D. Bachand, “Biomolecular Motors to Power Nanotechnology,” *Materials Today*, **8**, 22 (2005) (invited review)
2. H. Hess, G. D. Bachand, and V. Vogel, “Powering Nanodevices with Biomolecular Motors,” *Chemistry – A European Journal*, **10**, 2110 (2004)
3. H. Hess, G. D. Bachand, and V. Vogel, “Motor Proteins in Synthetic Materials and Devices,” *Encyclopedia of Nanoscience and Nanotechnology*, American Science Publishers, pp. 2201-2209
4. G. D. Bachand, S. B. Rivera, A. K. Boal, J. M. Bauer, S. J. Koch, R. P. Manginell, J. Liu, and B. C. Bunker, “Developing Nanoscale Materials Using Biomimetic Assembly Processes,” *Mat. Res. Soc. Symp. Proc.: Micro- and Nanosystems*, **782**, A1.1.1 (2004)
5. J. Clemmens, H. Hess, R. Doot, C. M. Matzke, G. D. Bachand, and V. Vogel, “Motor-Protein Roundabouts: Microtubules Moving on Kinesin-Coated Tracks through Engineered Networks,” *Lab on a Chip*, **4**, 83 (2004)
6. A. K. Boal, H. Tellez, S. B. Rivera, N. Miller, G. D. Bachand, and B. C. Bunker, “The Stability and Functionality of Crosslinked Microtubules,” *Small*, **2**, 793 (2006)
7. G. D. Bachand, S. B. Rivera, A. K. Boal, J. Gaudioso, J. Liu, and B. C. Bunker, “Assembly and Transport of Nanocrystal CdSe Quantum Dot Nanocomposites using Microtubules and Kinesin Motor Proteins,” *Nano Lett.* **4**, 817 (2004)
8. A. K. Boal, T. J. Headley, R. G. Tissot, and B. C. Bunker, “Microtubule-Templated Biomimetic Mineralization of Lepidocrocite,” *Adv. Funct. Mater.*, **14**, 19 (2004) (cover story)
9. S. B. Rivera, S. J. Koch, J. M. Bauer, J. M. Edwards, and G. D. Bachand, “Temperature-dependent Properties of a KIF1/Unc104-like Kinesin from *Thermomyces Lanuginosus*,” *FEBS J.*, in review (2006)
10. A. K. Boal, J. M. Bauer, S. B. Rivera, R. G. Manley, R. P. Manginell, G. D. Bachand, and B. C. Bunker, “Monolayer Engineered Microchannels for Motor Protein Transport Platforms,” submitted to *Langmuir*
11. M. Bachand, A. M. Trent, B. C. Bunker, and G. D. Bachand, “Physical Factors Affecting Kinesin-Based Transport of Synthetic Nanoparticle Cargo,” *J. Nanoscience Nanotech.*, **5**, 718 (2005)
12. A. K. Boal, G. D. Bachand, S. B. Rivera, and B. C. Bunker, “Interactions between Cargo-Carrying Biomolecular Shuttles,” *Nanotechnology*, **17**, 349 (2006)
13. A. M. Bouchard, C. E. Warrender, and G. C. Osbourn, “Harnessing Microtubule Dynamic Instability for Nanostructure Assembly,” *Phys. Rev. E*, **74**, 041902 (2006)

Combing with Light to Create Defect-Free, Hierarchically Ordered Polymeric Materials

Anna C. Balazs
Chemical Engineering Department
Univ. of Pittsburgh, Pittsburgh, PA 15261

I. Program Scope

One of the current grand challenges in the physical sciences is the fabrication of materials that are spatially ordered on the sub-micron scale and are defect-free on the *mm* to *cm* length scale. The development of facile techniques for creating such defect-free materials would enable the efficient production of a vast variety of opto-electronic and magnetic components for the next generation of devices. Currently, there is a tremendous drive to use polymeric materials in the fabrication of components for memory or logic devices, opto-electronic interconnects, displays, and photovoltaic cells since polymers are lightweight, flexible and relatively inexpensive. These polymer materials commonly involve a blend of multiple homopolymers or copolymers since the blending process allows one to fine-tune the properties by tailoring the amount and type of the constituents. Polymer blends, however, phase-separate and coarsen into highly disordered structures and not the spatially periodic, defect-free morphologies that are needed for photonic, electronic or magnetic devices. This poses a significant stumbling block to achieving the goal of manufacturing high quality polymeric devices in a low-cost, efficient manner.

The aim of the proposed research is to exploit photosensitive chemical reactions in polymeric mixtures to create hierarchically ordered materials that are defect-free on relatively large length scales. In particular, we will use a uniform “background” light source to initiate a reversible chemical reaction in a polymeric mixture. We then introduce a higher intensity, spatially localized beam that locally increases the rate of reaction. This, in turn, increases the interfacial energy in the regions irradiated with the secondary light source. We exploit this fact in two ways. First, for an AB binary blend, by rastering over the sample with the secondary light, we effectively “comb” out any defects in the material and create highly regular structures. Second, for ternary blends, we can drive a third component, C, to the region of higher light intensity and thereby “write” onto the AB binary system.

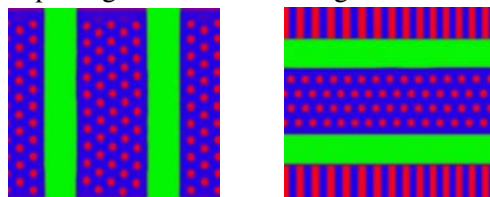
II. Recent Progress

We first carried out computer simulations in two dimensions to demonstrate how photoinduced chemical reactions in polymeric mixtures can be exploited to create long-range order in materials with features that range from the submicron to the nanoscale (1). The process is initiated by shining a spatially uniform light on a photosensitive AB binary blend, which thereby undergoes both a reversible chemical reaction and a phase separation. When a well-collimated, higher intensity light is rastered over the sample, the system forms defect-free, spatially periodic structures. If a nonreactive homopolymer C is added to the system, this component localizes in regions that are irradiated with a higher intensity light, and one can effectively “write” a pattern of C onto the AB film. Rastering over the ternary blend with the collimated light now leads to hierarchically ordered patterns of A, B, and C. Because our approach involves homopolymers, it significantly expands the range of materials that can be fashioned into a periodic pattern. The findings point to a facile process for manufacturing high-quality polymeric components in an efficient manner.

After these preliminary computational studies, we carried more in depth investigations (2). In particular, we measured the regularity of the ordered structures as a function of the relative reaction rates for different values of the rastering speed and determined the optimal conditions for creating defect-free structures in the binary systems. We carried out these calculations for both lamellar and hexagonal

structures. We also carried out more in depth calculations for the ABC ternary structures. In particular, we established design rules for designing a variety of defect-free morphologies, as shown in Fig. 1.

Fig. 1 Defect-free ternary morphologies formed from the ABC mixture. Note the combination of lamellar and hexagonal symmetries in one structure.



Having carried out these 2D studies, we modeled the effects of illuminating a *three-dimensional* sample with spatially and temporally dependent light irradiation (3). We again considered ABC ternary blends where the A and B components undergo a reversible photochemical reaction, which leads to phase-separation between A and B. In addition, the non-reactive C component is assumed to be immiscible with both A and B. Using computer simulations, we have shown that this ternary mixture can be ordered into regular, periodic *three-dimensional* structures by exposing the system to both spatially and time dependent light irradiation. We first focused on the effects of illuminating the system with just the spatially dependent light irradiation. Experimentally, this would correspond to using both a uniform background light and a localized, well-collimated light source. We assumed that the well-collimated light has a higher intensity than the background light. To model this scenario, we utilized a three-dimensional simulation box that contains two distinct regions, where each region is characterized by a different reaction rate coefficient. For the region illuminated by the background light, the rate coefficient is given by k_1 , while the region illuminated by the well-collimated, higher intensity light is characterized by a rate coefficient of $k_2 > k_1$. (Here, we assumed that the forward and reverse rate coefficients for the reversible photochemical reaction are equal.)

We found that the reactive AB mixture will diffuse out of the k_2 regions, while the non-reactive C component will diffuse into these regions. Thus, by directing the collimated, higher intensity light onto selected regions, one can write a *three-dimensional* pattern of C onto the AB reactive blend. This approach provides a non-invasive, robust means of writing with the C “ink” and is effective for a wide range of system parameters.

A necessary condition for successfully writing the desired C pattern is that the amount of C within the system is such that the C effectively fills the higher intensity region (or regions). We derived an additional criterion that allows us to predict, for different system parameters, the sharpness of the written pattern (i.e., how closely the shape of the C domain replicates the geometry of the k_2 region). We showed that the writing is sharper for relatively high values of k_2 and relatively low values of the interfacial tension between the A(B) and C components.

We then demonstrated how moving the k_2 region through the 3D sample could lead to spatially ordered binary and ternary blends. In experiments, such motion would correspond to rastering over the sample with the well-collimated light source. We first showed that for a specified range of the rastering velocities, the moving, higher intensity light “combs out” defects within the AB lamellar domains and the system becomes ordered along the combing direction. This ordering occurs because the moving k_2 region creates a moving “neutral” boundary, which drives the re-orientation of the AB domains perpendicular to this interface (that is, along the rastering direction). The results also reveal that the binary blend can be ordered in *all three directions* by applying the proposed technique twice, i.e., by rastering the higher intensity light along z and then along x .

By combining the two effects described above (the migration of C to stationary k_2 domains, and

the combing of the AB domains with the moving λ_2 regions), one can create a variety of defect-free, hierarchically ordered multi-component materials. For example, one can create defect-free materials that exhibit a periodicity over two distinct length scales, where one length scale is defined by the thickness of the AB lamellae, and the second length scale is defined by the size of the C-filled stationary λ_2 regions. Our approach could potentially provide advantages over current photolithographic techniques since the proposed process is fully reversible, non-invasive, and points to a novel means of writing patterns in *three dimensions*.

III. Future Plans

In the next phase of the theoretical work, we will use the above concepts to design synthetic polymeric films that undergo a transformation from a two-dimensional sheet to a three-dimensionally structured object when the system is exposed to light. In the systems to be considered here, the light initiates a chemical reaction, which in turn alters the mechanical forces in the system. Figure 2 shows an example of a system of interest. As a function of time, the system goes from a flat layer to textured film. As can be seen in the last image in Fig. 2, the features or corrugations in the vertical direction have a well-defined size. This system is formed from a reactive, AB binary polymeric mixture. More complex architectures can be formed from a ternary ABC blend, as seen in Fig. 3. In the latter image, the C domains form well-defined craters in the A/B hills.

As in the previous studies, the A and B components are assumed to be immiscible and thus, are undergoing phase separation. We also assume that the A and B domains exhibit different curvatures in the film. Such films could represent a polymeric bilayer and A might be a group of lipids or biomolecules that exhibit a particular curvature, while B might be another group that induces a different curvature. Alternatively, the A domains could be formed from the *cis* isomers of a compound, while the B domains comprise the *trans* isomers (e.g., the domains can contain isomers of an amphiphilic azobenzene derivative). Due to these differences in local curvature, the elastic properties (bending rigidity) will play a central role in the behavior of the film.

We now introduce an applied light that initiates a chemical reaction that inter-converts A and B, i.e., $A \leftrightarrow B$. The reaction can be understood as an isomerization-like chemical transformation. Since A and B have different curvatures, the chemical reaction will cause a stretching or bending of the film; in other words, the induced reactive process locally "kicks" the film. The latter distortions exert local mechanical forces, which lead to modifications in the shape of the film.

The structural features in Figs. 2 and 3 (which are the result of preliminary studies (4)) form relatively simple patterns and the patterns themselves are relatively disordered. Our first goal is to establish guidelines for creating vertically (in the z direction) patterned films with highly ordered and well-defined structural features. Our second aim is to isolate conditions where the structure formation is reversible, with the topographically patterned layers collapsing into a flat sheet in a controllable manner. Our ultimate objective is to design a system where an external stimulus can drive an entire 2D film to form a 3D entity, e.g., transforming from a sheet into a box. In effect, we are striving to design reactive, deformable surfaces that can be readily fashioned into specified structures.

In the next phase of the research, we will investigate how phase-separation and chemical reactions can be harnessed to control the domain formation and how these processes can be regulated by light to yield the textured films. We will also examine polymeric composites that contain electrically conducting or magnetic nanoparticles and determine how applied fields can be used to promote the formation of ordered textures or regular folds.

On a fundamental level, the findings can significantly extend our understanding of how to exploit local stimuli to control the collective properties of the material. Since we are coupling external stimuli to multi-component materials that are undergoing, for example, chemical reactions and mechanical

deformation, we anticipate the emergence of highly complex behavior, where the properties and behavior of the system cannot be understood merely by understanding the individual components. On a more applied level, the results can significantly alter the way nano- and micron-scale patterned surfaces are fabricated. In particular, the methods can provide an alternative to or augment current soft lithography techniques to create surfaces with small-scale features. The idea is to potentially reduce the number of processing steps to form three-dimensionally patterned or textured substrates. Ultimately, the ability to transform a 2D objects into well-defined 3D structures can significantly alter the way in which components are self-assembled and fabricated.

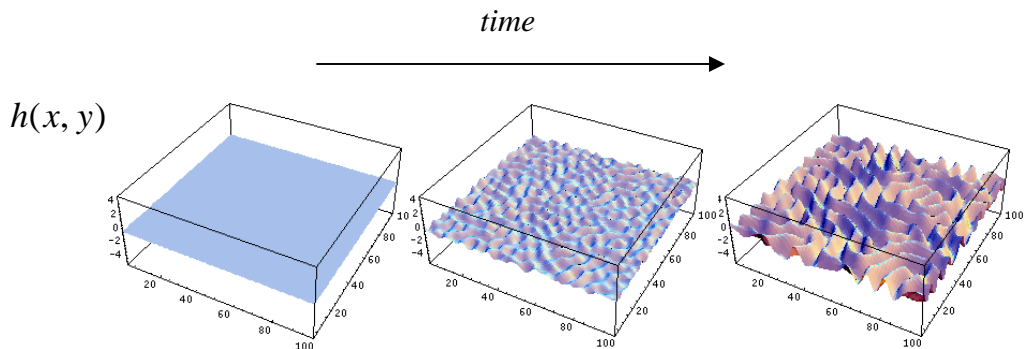


Fig 2. Time evolution of the height, $h(x, y)$ of the reactive binary film

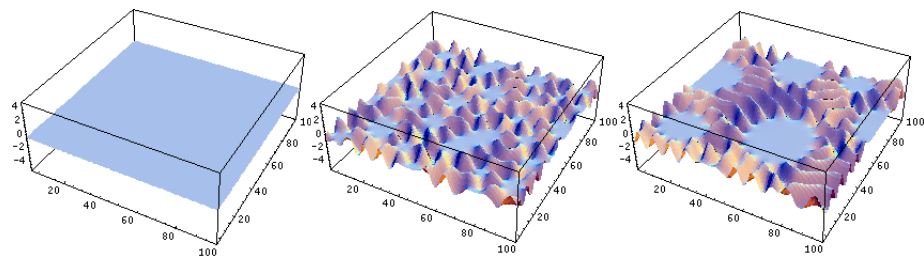


Fig. 3. Time evolution of the height, $h(x, y)$, of the reactive ternary film

IV-V References and Our DOE-Supported Publications on this Topic (Last Two Years)

- (1) Travasso RDM, Kuksenok O, Balazs AC “Harnessing light to create defect-free, hierarchically structured polymeric materials”, *LANGMUIR* 21 (2005) 10912-10915
- (2) Travasso RDM, Kuksenok O, Balazs AC “Exploiting photoinduced reactions in polymer blends to create hierarchically ordered, defect-free materials” *LANGMUIR* 22 (2006) 2620-2628.
- (3) Kuksenok, O, Travasso RDM, Balazs, AC, “Dynamics of Ternary Mixtures with Photosensitive Chemical Reactions: Creating Three Dimensionally Ordered Blends“ *PHYS. REV. E*, 74 (2006) 011502.
- (4) Kuksenok, O, Balazs, AC, Kuksenok, O. and Balazs, A. C., “Modeling Multi-Component Reactive Membranes”, *PHYS. REV. E*, in press.

Invited Speaker Presentation

Title: Self-Replication with Colloids

Author: Paul Chaikin, New York University

Abstract:

We want to make a non-“biokleptic” system which can self-replicate. The idea is to design colloids with specific, reversible and irreversible interactions, introduce seed motifs, and cycle the system in such a way that a copy is made. Repeating the cycle would double the number of offspring in each generation leading to exponential growth. We're not there yet! We use colloidal particles with bound DNA sequences for reversible recognition. They now "work" - recognize, cycle and can be permanently attached as well. So the talk will be on where we are, how we got there and where we're going.

This page is intentionally blank

Session V

Tools for Synthesis and Novel Approaches

Session Chair: P.W. Voorhees, Northwestern University

This page is intentionally blank

Atomistic Structure, Strength, and Kinetic Properties of Intergranular Films in Ceramics
DOE GRANT NUMBER: DE-FG02-06ER46336
Stephen H. Garofalini, Rutgers University

I: Scope

Polycrystalline ceramics often contain thin (1-5nm) glassy intergranular films (IGFs) between the crystals that occupy only a small volume percentage of the bulk ceramic, but can strongly influence various mechanical, thermal, chemical, and optical properties. As such, there have been a large number of studies to determine the structure and behavior of these IGFs, of which only a few are referenced here¹⁻¹⁰. Although significant progress has been made experimentally in recent years⁶⁻⁸, the glassy nature of the IGF and its very thin width between crystals makes understanding the atomistic structure and fundamental behavior of IGFs experimentally formidable and we have been applying molecular dynamics (MD) computer simulations to the problem that offer an important complementary approach to understanding these intergranular films.

Several major results from our previous work relate to the ordering into the IGF induced by the crystal surfaces^{11,12} (subsequently corroborated experimentally⁸) and the ion specific nature of that ordering, the effect of composition of the IGF on growth behavior along specific crystal orientations (consistent with experimental observations), the atomistic structure of an IGF/crystal system (subsequently corroborated by large-scale VASP ab-initio calculations¹³), and an atomistic description of adsorption and growth that helps to clarify the role of the composition of the IGF on normal, abnormal, and anisotropic grain growth in alumina^{14,15}.

The current research is designed to capitalize and expand on these important results in order to address additional questions regarding atomistic behavior in IGFs. The simulations can be used to provide guides for kinetically controlled design of the IGFs (and hence the material) via processing. The relevant systems in our work include alumina (α -Al₂O₃) and silicon nitride (β -Si₃N₄) crystals because these two systems show important differences in behavior. Composition of the silicate-based IGFs include species such as Ca, Al, Mg, and rare earths (REs) in the alumina case and Ca, Al, N, and REs in the nitride case because of the major influence these different species in the IGF have on properties. Our research includes: (1) a computational analysis of the effect of experimentally observed composition and thickness of the IGF and different crystallographic orientations on atomistic structure and properties as well as variations from these values to mimic kinetically varying compositions during sintering; (2) the effect of both compositional variations of the crystal surfaces (interface mixing with the IGF) and topographic roughening of the crystal surfaces on ordering into the IGF, bonding, and composition at the interfaces; (3) elevated temperature studies to evaluate dissolution and growth of the different crystal surfaces in contact with the IGF and the effect of composition of the IGF on this behavior; (4) mechanical properties of two-crystal systems as well as multigrain nanoparticle systems and the role of local structure and composition on these properties.

II. Recent Progress

1. Dissolution Behavior:

We have taken alumina crystals with two low energy surfaces, the (0001) basal plane ($\sim 2.0\text{J/m}^2$) and the (11 $\bar{2}$ 0) prism surface ($\sim 2.5\text{J/m}^2$) as the initial crystal orientations in contact with the silicate IGFs. Previous work showed preferential adsorption and crystal growth along the surface normal on the (11 $\bar{2}$ 0) surface at certain IGF compositions, with slower growth on the

basal orientation (which is consistent with experimentally observed anisotropic grain growth in alumina). However, at elevated temperatures, we expect preferential dissolution of the higher energy $(11\bar{2}0)$ surface into the silicate melt in comparison to the (0001) surface. To test this, we simulated crystal/vacuum interfaces followed by crystal/silicate melt interfaces to see the effect of T and melt composition on crystal surface stability.

Using a temperature at which both crystal orientations were stable in simulations of crystal/vacuum interfaces, simulations of these orientations in contact with silicate melts showed quite different results. Figure 1 a schematic of the system configuration. Figure 2 shows the number density of Al ions in the original crystals with the basal and prism orientations as well as those crystals in contact with two different silicate melts (no other ions shown in the figures). Arrow in each figure locates the original terminal Al plane in each crystal.

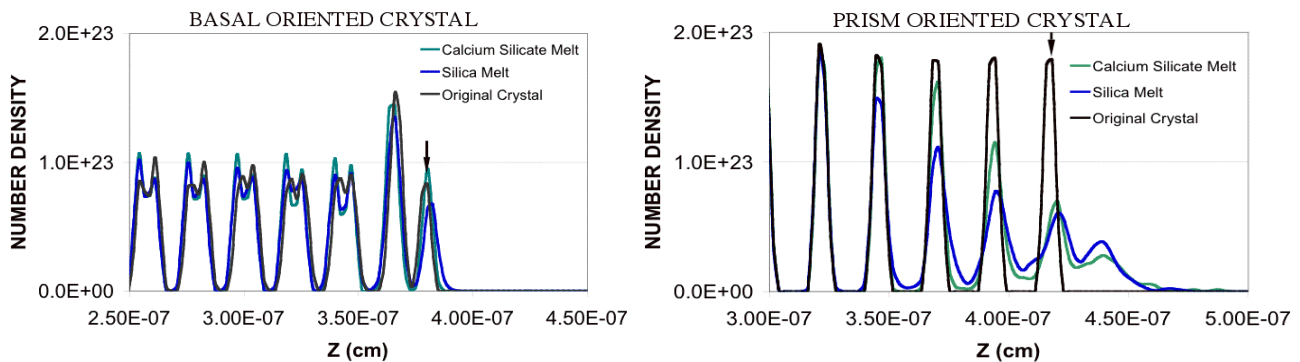


Figure 2. Al ion distribution in basal oriented crystal (left) and prism oriented crystal (right) in contact with melts.

Clearly, under the same conditions of melt composition and time at temperature, the (0001) basal surface remained stable while the $(11\bar{2}0)$ prism surface showed dissolution into the melt. Therefore, during liquid phase sintering (LPS) at this equivalent temperature, the prism oriented surfaces preferentially dissolve into the silica(te) melts while the basal oriented surfaces are more stable. However, as our earlier work showed, at lower temperatures during cooling from the melt state, adsorption and growth on the prism surface occurs more rapidly than on the basal surface. Therefore, there are competing kinetics in LPS during which the prism surface dissolves, providing Al (and O) ions into the melt at certain temperatures, but preferentially grows at other lower temperatures and compositions. Additional temperatures and melt compositions will be used to determine the critical temperature separating dissolution from adsorption and growth.

2. Rare Earth Additions to IGF:

We are currently adding Y to the IGFs to compare its behavior with that of Al and Ca ions in IGFs between alumina crystals and silicon nitride crystals. Ca ions preferentially segregate to the basal surface in alumina, but to the prism surface in the nitride (poisoning each and affecting adsorption and growth). Based on our knowledge of silicate glass structure and the role of ‘modifiers’ in silicate glasses, we can associate the adsorption of Ca ions onto certain sites on the prism oriented nitride crystal that we see in our simulations to similar behavior of

rare earth ions observed in HAADF-STEM. The use of Y and other rare earth ions will make the association between the simulations and the experiments more direct. It will also enable better comparison to the fracture studies done experimentally.

3. Fracture Behavior:

Fracture of IGF systems is being accomplished by straining the sample in the direction perpendicular to the IGF/crystal interfaces. Film thickness has been shown in our simulations to affect fracture strength. Because of the role of void formation and coalescence during fracture of bulk glasses, we are evaluating void formation in these confined films using analysis of the ring structures. Formation of larger rings implies larger ‘voids’ in the glass, with accompanying weakening of the material. Figure 3 shows the concentration of different ring structures during fracture of the 1nm film between silicon nitride crystals, as well as the stress (black line, 0.02*stress to fit on scale). Arrows point to (1) increase of very large 9-membered rings at first decrease in stress and (2) maximum stress followed by increase in 7- and 9-membered rings, plus increase in 3- and 4-membered rings (latter two structural features are consistent with formation of new surface), as well as a large decrease in 6-membered rings.

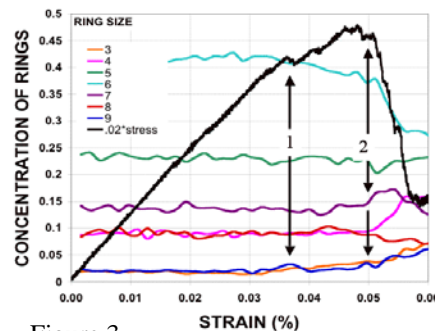


Figure 3.

Figure 3 shows the concentration of different ring structures during fracture of the 1nm film between silicon nitride crystals, as well as the stress (black line, 0.02*stress to fit on scale). Arrows point to (1) increase of very large 9-membered rings at first decrease in stress and (2) maximum stress followed by increase in 7- and 9-membered rings, plus increase in 3- and 4-membered rings (latter two structural features are consistent with formation of new surface), as well as a large decrease in 6-membered rings.

4. Equilibrium Structures and Compositions:

We had originally planned to do Grand Canonical MD (GCMD) to help in determining equilibrium compositions in the IGF because it has been well known that the composition of the bulk glass in a polycrystalline ceramic is **not** the same as the composition in the IGF³. However, GCMD is computationally very difficult and expensive for condensed phases, especially ones as complicated as those we are studying, although some success exists¹⁶. However, we are taking a different approach at this stage. We are using a recent development in the so-called ‘atomic density function’ (ADF) phase field approach¹⁷, also known as the ‘phase field crystal’ (PFC) model¹⁸. We are doing this in collaboration with our colleague at Rutgers, Professor Khachatryan. ADF offers the potential of more rapid equilibration of a condensed liquid phase into the space between crystals than would be possible with MD simulations or even GCMD. Khachatryan’s recent work looked at crystal growth in a liquid using an arbitrary harmonic potential¹⁷. We have begun using simple pair potentials to develop code and methodology, with plans to move to our more realistic multi-body potentials that describe our oxides and nitrides.

5. Diffusion in IGFs

Because of its importance in sintering densification and local compositional variations, diffusion of species within the IGFs as a function of film thickness is currently being analyzed. Results are showing that film thickness appears to play an important role in altering diffusion coefficients of species in calcium aluminosilicate IGFs. These data will be correlated with the structural data that we have obtained from previous simulations.

III. Future Plans

We will continue with our studies of the dissolution of different crystallographic orientations of the crystals into silicate melts as a function of temperature to determine the role of the competing kinetics of dissolution and adsorption that change with cooling temperature.

We will also continue with our simulations of fracture and determine the causes of the change in fracture stress as a function of the thickness of the IGF that we have been observing. We are also observing the role of additives on fracture strength and will similarly evaluate the details of this behavior. We will add Y and then other RE (La, Lu) and evaluate their location in the IGF and at the IGF/crystal interface in order to compare directly to recent HAADF-STEM and ab-initio cluster results. Fracture of these systems will also be studied to determine fracture location (interface or within the glassy film).

We will introduce the more realistic multibody interatomic potential used in our simulations into our ADF calculations in order to determine equilibrium IGF compositions and thicknesses.

IV. Publications

“Molecular dynamic simulations of the dissolution of (0001) and (1120) oriented alumina grains in contact with silicate melts”, S. Zhang and S. H. Garofalini, *J. Chem. Phys.* (to be submitted)

“Fracture of silicate intergranular films in silicon nitride-a molecular dynamics study”, S. Zhang and S. H. Garofalini, *J. Am. Ceram. Soc.* (to be submitted)

“Molecular dynamics simulations of fracture of multicomponent silicate intergranular films in alumina”, S. Zhang and S. H. Garofalini, *J. Am. Ceram. Soc.* (to be submitted)

“Effect of composition and film thickness on diffusion in intergranular films”, N. Michaluk, S. Zhang, and S. H. Garofalini, *J. Matls. Sci.* (in preparation)

V. References

- (1) Kleebe, H.-J.; Cinibulk, M. K.; Cannon, R. M.; Rühle, M. *J. Am. Ceram. Soc.* **1993**, *76*, 1969.
- (2) Tanaka, I., et al., *M. J. Am. Ceram. Soc.* **1994**, *77*, 911.
- (3) Gu, H.; Pan, X.; Cannon, R. M.; Rühle, M. *J. Am. Ceram. Soc.* **1998**, *81*, 3125.
- (4) Becher, P. F. et al., *J. Am. Ceram. Soc.* **2000**, *48*, 4493.
- (5) McBride, W.; Cockayne, D. J. H. *J. of Non-Cryst. Sol.* **2003**, *318*, 233.
- (6) Ziegler, A.; Kisielowski, C.; Hoffmann, M. J.; Ritchie, R. O. *J. Am. Ceram. Soc.* **2003**, *86*, 1777.
- (7) Shibata, N.; Pennycook, S. J.; Gosnell, T. R.; Painter, G. S.; Shelton, W. A.; Becher, P. F. *Nature* **2004**, *428*, 730.
- (8) Winkelman, G. B.; Dwyer, C.; Hudson, T. S.; Nguyen-Mahn, D.; Doblinger, M.; Satet, R. L.; Hoffmann, M. J.; Cockayne, D. J. H. *Appl. Phys. Lett.* **2005**, *87*, 061911.
- (9) Satet, R. L.; Hoffmann, M. J.; Cannon, R. M. *J. Mat. Sci. Eng. A* **2006**, *422*, 66.
- (10) Becher, P. F.; Painter, G. S.; Shibata, N.; Satet, R. L.; Hoffmann, M. J.; Pennycook, S. J. *Matl. Sci. Eng. A* **2006**, *422*, 85.
- (11) Garofalini, S. H.; Luo, W. *J. Am. Ceram. Soc.* **2003**, *86*, 1741.
- (12) Su, X.; Garofalini, S. H. *J. Mat. Res.* **2004**, *19*, 752.
- (13) Rulis, P.; Chen, J.; Ouyang, L.; Ching, W.-Y.; Su, X.; Garofalini, S. H. *Phys.Rev. B* **2005**, *71*, 235317.
- (14) Zhang, S.; Garofalini, S. H. *J. Phys. Chem. B* **2006**, *110*, 2233.
- (15) Garofalini, S. H. *Mater. Sci. Eng. A* **2006**, *422*, 115.
- (16) Hudson, T. S. et al., *Mater. Sci. and Eng. A* **2006**, *422*, 123..
- (17) Jin, Y. M.; Khachatryan, A. G. *J. Appl. Phys.* **2006**, *100*, 013519.
- (18) Elder, K. R.; Grant, M. *Phys. Rev. E* **2004**, *70*, 051605

Rational Growth, Control and Manipulation of Novel Materials

T. A. Lograsso, R. W. McCallum and P. C. Canfield
Materials and Engineering Physics, Ames Laboratory, Ames IA 50010

Program Scope

The design, synthesis and characterization of new materials that lead to important discoveries, both expected and unexpected, as well as new knowledge and techniques, within and across traditional disciplinary boundaries, are critical components of the DOE, Basic Energy Sciences' mission. In support of this mission, the *Rational Growth, Control and Modification of Novel Materials* effort will advance Ames Laboratory's capabilities to synthesize and characterize high purity, high quality materials, primarily in single crystal form, spanning a range of sizes. This will involve research focused on quantifying and controlling the processing-structure-property relationship of responsive materials as well as examining promising phase spaces (either physical or chemical) that we identify as compelling based upon advances in synthesis and / or control of novel materials.

During the next three years, this effort will advance both the Bridgman and solution growth techniques by implementing greater control over the nucleation and growth processes so as to improve overall homogeneity and volume. In addition, we will augment our suite of growth capabilities and develop a wide range of new fluxes, primarily for light, reactive and/or volatile elements. These advances in synthesis will allow us to develop model systems which exhibit a high degree of sensitivity to controllable chemical and structural imperfection. These model systems will allow for the systematic study of the dominant mechanisms that lead to or affect responsive behaviors. In specific, we will focus on behaviors controlled by twin boundary motion, clustering in solid solutions, defect density and fine-scale phase heterogeneity.

Recent Progress

An example of early synergy between our research groups was joint efforts on the physics, metallurgy and surface science of quasicrystalline materials. Each group utilized their individual growth and characterization methods to produce a wide range of large single grain quasicrystalline compounds, e.g., Al-Pd-Mn, R-Zn-Mg Al-Cu-Fe, Al-Ni-Co and, most recently, binary Cd-Yb quasicrystals and their approximant phases. The availability of these materials as single grains from the Ames Laboratory has had significant impact on the scientific understanding of this new class of materials. For instance, our large, highly perfected, single grains challenged the idea that these materials were inherently disordered due to their aperiodic structure. High resolution TEM studies (Figure 1) of solution grown R-Zn-Mg found that these quasicrystals had the lowest density of phason strain (gross equivalent of defect density) of any known quasicrystals [1].

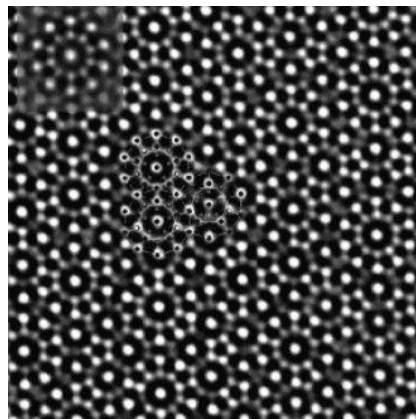


Figure 1 HRTEM image taken along the 5f (10×10 nm) for the Y–Mg–Zn face centered icosahedral and model structure (near center) with small inset showing the multi-slice calculation for a single cluster.

Although being able to grow “lots of really big” crystals is a fine accomplishment, it is vital to keep in mind that issues of purity, stoichiometry, and structural perfection are ubiquitous problems in new materials physics. The *Rational Growth* group has been, and will continue to be, active in clarifying such issues on a wide range of new materials that are either of direct interest to the group, or are of particular interest to other groups within the Ames Laboratory and elsewhere. Recent examples include preparation of Ni-Mn-Ga ferromagnetic shape memory alloys with low enough defect densities to allow for the high

mobility of twin boundaries. These highly mobile twin boundaries are necessary for achieving the full theoretical value (6%) of magnetic field induced strain [2]. Other examples of this are the relationship between transport properties and boron purity in MgB_2 (the intermetallic superconductor with the current highest T_c) [3] and the establishment of an extreme sensitivity of the temperature dependent resistivity of single crystalline $\text{YbNi}_2\text{B}_2\text{C}$ (a model heavy fermion compound) to the dislocation line density [4]. In this latter case, we were able to control the dislocation density via judicious post growth annealing and we were able to quantify the dislocation density using TEM. In these examples, the establishment of clear and controllable relations between the sample preparation, growth and processing, and the physical properties allowed for a clearer understanding of the underlying physics.

As part of our effort to define and manipulate the tuning and requisite control parameters, we have also found it necessary to push the frontiers of new materials growth and design. This has taken the form of modifying existing growth techniques to allow for better control of growth and processing conditions; creating new growth techniques to allow for new combinations of control parameters; devising new types of solutions for the growth of samples, and new types of crucibles for their containment and manipulation. In order to improve phase purity and reduce physical cracking in $\text{R}_5(\text{Si}_{1-x}\text{Ge}_x)_4$ compounds, we implemented tri-arc crystal pulling methods [5] to avoid crucible interactions encountered in the Bridgman methods. In order to produce single crystals of complex Pr-Ni-Si compounds with very narrow exposed liquid solidus surfaces we devised a solution growth / Bridgman hybrid growth technique [6]. In order to grow single grain of R-Mg-Zn quasicrystals, we developed sealed Ta crucibles with a fully enclosed filter that allowed for the use and decanting of volatile Mg-rich solutions [7].

Future Plans

The goals of the *Rational Growth, Control and Modification of Novel Materials* group are to:

- Advance the ability to synthesize and characterize high purity, high quality materials, primarily in single crystal form, spanning a range of sizes;
- Quantify and control processing-structure-property relationships: the basic science of how chemical inhomogeneities and structural defects affect the properties of highly responsive materials;
- Explore promising phase spaces (either physical or chemical) that we identify as compelling based upon advances in synthesis and / or control of novel materials.

We will address these goals through work on a number of activities. In the area of growth capabilities, we will advance both Bridgman and solution growth techniques by implementing greater control over the nucleation and growth processes so as to improve overall sample homogeneity and volume. In addition, we propose to augment our suite of growth capabilities by implementing vapor transport methods. Quantification and control of twin boundaries, clustering in solid solutions and defect density will be systematically studied in a number of model systems that have become accessible to us through our wide range of growth techniques. Finally, we will explore promising phase spaces by (i) developing a wide range of new fluxes, primarily for light, reactive and/or volatile elements and (ii) studying the effects of chemical and phase inhomogeneities on the wide range of groundstates existing in the Heusler/half-Heusler structural families.

For this meeting, we will discuss our ongoing research on clusters in solid solutions. Recently, Fe-Ga alloys were discovered to possess the highest single crystalline magnetostrictive strain (~13x that of pure Fe) of binary alloys. Our ability to prepare single crystals via several growth methods with controlled compositions over a large composition range ($0 < x < 35$) and through several different, but similar phase fields, has directly allowed for extensive property measurements and structural studies to be conducted. Based on these single crystal investigations, there is growing theoretical and experimental evidence suggesting non-random distributions or clustering of Ga atoms within the Fe lattice plays an important role in enhancing the magnetoelasticity. Specifically, the nature of non-random Ga clusters and how they

affect the strain, elasticity and magnetic moment distributions within the Fe Lattice are open questions. How does Ga substitution and clustering affect the band structure of Fe? What is the nature of Ga short range order? What lattice distortions are created by the short range order (type, crystallographic nature, magnitude of strains) and do these and/or other types of distortions or chemical ordering lead to enhanced magnetoelasticity?

We will continue to investigate Fe-X alloys to understand the role of clustering (random and non-random) of solute atoms on the magnetoelastic coupling of Fe and, more broadly, on the magnetic and transport properties in solid solutions. In the course of this investigation we will directly address the question of how non-random clustering can be analyzed and controlled through physical property measurement and structural characterization. We will extend these studies to other binary Fe-X systems where clustering of solute is reported to occur (e.g. Al, Si, Ti, Mn, Mo) to examine the effect of atomic size and electronic structure on the effectiveness of the clusters to control magnetoelastic interactions. We will utilize X-ray diffraction during in-situ heating/cooling with applied magnetic fields to examine the structural evolution and distortions arising from magnetically induced strains, evolution of two-phase mixtures during thermal processing and quantification of the phase distributions. Phase identification will also be confirmed by TEM investigations and time resolved single crystal diffraction at the Advanced Photon Source. Detailed TEM convergent beam studies will examine localized lattice distortions and symmetry associated with short range order. When coupled with unique *in-situ* heating, we will link microstructural evolution associated with phase distribution, domain and defect structure, and crystallography with magnetic properties and processing. This detailed characterization of clusters and their influence on properties will lead to the ability to tailor the synthesis routes and chemistry to optimize the magnetoelastic response of existing alloys and to provide intelligent search criteria for discovering new compounds or alloys.

References

1. M. J. Kramer, S. T. Hong, P. C. Canfield, I.R. Fisher, J. D. Corbett, Y. Zhu, and A. I. Goldman, *J. Alloys and Comp.*, **342**, 82 (2002).
2. S. J. Murray, M. Marioni, S. M. Allen, R. C. O'Handley and T. A. Lograsso, *Appl. Phys. Lett.*, **77**, 886 (2000).
3. R. A. Ribeiro, S. L. Bud'ko, C. Petrovic, and P. C. Canfield, *Physica C*, **382**, 194 (2002).
4. M. A. Avila, Y.Q. Wu, C. L. Condron, S. L. Bud'ko, M. Kramer, G. J. Miller and P. C. Canfield, *Phys. Rev. B*, **69**, 205107 (2004).
5. T. A. Lograsso, D. L. Schlagel and A. O. Pecharsky, *J. Alloy Comp.*, **393**, 141 (2005).
6. D. Wu, R. W. McCallum and T. A. Lograsso, Unpublished Research (2004).
7. I. R. Fischer, M. J. Kramer, Z. Islam, T. A. Wiener, A. Kracher, A. R. Ross, T. A. Lograsso, A. I. Goldman and P. C. Canfield, *Mat Sci. Eng. A*, **294-296**, 10 (2000).

Publications (last 2 years)

- T. A. Lograsso, D. L. Schlagel and A. O. Pecharsky, "**Synthesis and Characterization of Single Crystalline $Gd_5(Si_xGe_{1-x})_4$ by the Bridgman Method**", *J. Alloy Comp.*, **393**, 141 (2005).
- H. Wende, A. Scherz, C. Sorg, Z. Li, P. Pouloupoulos, K. Baberschke, A. Ankudinov, J. J. Rehr, F. Wilhelm, N. Jaouen, A. Rogalev, D. L. Schlagel and T. A. Lograsso, "**Temperature Dependence of Magnetic EXAFS for Rare Earth Elements**", *Physica Scripta*, **T115**, 600 (2005).
- M. Huang and T. A. Lograsso, "**Experimental Investigation and Thermodynamic Modeling of the Ni-Pr System**", *J. Alloy Comp.*, **395**, 75 (2005).

- A. E. Clark, J. B. Restorff, M. Wun-Fogle, K. W. Dennis, T. A. Lograsso, and R. W. McCallum, “**Temperature Dependence of the Magnetic Anisotropy Constants of Fe_{100-x}Ga_x, x=8.6, 16.6, 28.5**”, J. Appl. Phys., **97**, 10M316 (2005).
- M. Huang, R. W. McCallum and T. A. Lograsso, “**Experimental Investigation and Thermodynamic Modeling of the Nd-Ni System**”, J. Alloy Comp., **398**, 127 (2005).
- M. Huang, D. Wu, K. W. Dennis, R. W. McCallum and T. A. Lograsso, “**Revised Phase Diagram for the Ni-Pr System in Pr-rich Region**”, J. Phase Equil. Diff., **26**, 209 (2005).
- L. Tan, A. Kreyssig, J. W. Kim, A. I. Goldman, R. J. McQueeney, D. Wermeille, B. Sieve, T. A. Lograsso, D. L. Schlager, S. L. Budko, V. K. Pecharsky and K. A. Gschneidner, Jr., “**The Magnetic Structure of Gd₅Ge₄**”, Phys. Rev. B, **71**, 214408 (2005).
- A. L. Lima, A. O. Tsokol, K. A. Gschneidner, Jr., V. K. Pecharsky, T. A. Lograsso, and D. L. Schlager, “**The Magnetic Properties of Single Crystal DyAl₂**”, Phys. Rev. B, **71**, 024403 (2005).
- M. J. Kramer, D. J. Sordelet and T. A. Lograsso, “**Solid and Liquid Thermal Expansion and Structural Observations in the Quasicrystalline Cd₈₄Yb₁₆ Compound**”, Phil Mag. Lett., **85**, 151 (2005).
- M. Pasquale, C. P. Sasso, L. H. Lewis, L. Giudici, T. Lograsso and D. Schlager, “**Magneto-structural Transition and Magnetocaloric Effect in Ni₅₅Mn₂₀Ga₂₅ Single Crystals**”, Phys. Rev. B., **72**, 094435 (2005).
- J. L. Zarestky, V. O. Garlea, T. A. Lograsso, D. L. Schlager and C. Stassis, “**Compositional Variation of the Phonon Dispersion Curves of bcc Fe-Ga Alloys**”, Phys. Rev. B, **72**, 180408 (2005).
- Y. Janssen, M. Angst, K. W. Dennis, P. C. Canfield and R. W. McCallum, “**Differential Thermal Analysis and Solution Growth of Intermetallic Compounds.**”, J. Crystal Growth, **285**, 670 (2005).
- D. Wu, O. Ugurlu, L. S. Chumbley, M. J. Kramer and T. A. Lograsso, “**Synthesis and Characterization of Hexagonal Cd₅₁Yb₁₄ Single Crystals**”, Phil. Mag., **86**, 381 (2006).
- O. Ugurlu, L. S. Chumbley, D. L. Schlager and T. A. Lograsso, “**Orientation and Formation of Atypical Widmanstätten Plates in the Gd₅(Si_xGe_{1-x})₄ System**”, Acta Mat., **54**, 1211 (2006).
- X. Moya, L. Manosa, A. Planes, T. Krenke, M. Acet, O. Garlea, T. Lograsso and J. Zarestky, “**Lattice Dynamics of Ni-Mn-Al Shape Memory Alloys**”, Phys. Rev. B, **73**, 064401 (2006).
- Y. Janssen, S. Chang, B. K. Cho, A. Llobet, K. W. Dennis, R. W. McCallum, R. J. McQueeney, and P. C. Canfield, “**YbGaGe: Normal Thermal Expansion**”, J. Alloys Comp., **389**, 10 (2005).
- Z. Islam, D. Haskel, J. C. Lang, G. Srajer, Y. Lee, B. N. Harmon, A. I. Goldman, D. L. Schlager and T. A. Lograsso, “**An X-Ray Study of Non-Zero Nickel Moment in a Ferromagnetic Shape-Memory Alloy**”, J. Mag. Magn. Mat., **303**, 20 (2006).
- X. Moya, L. Mañosa, A. Planes, T. Krenke, M. Acet, M. Morin, J. L. Zarestky, and T. A. Lograsso, “**Temperature and Magnetic-field Dependence of the Elastic Constants of Ni-Mn-Al Magnetic Heusler Alloys**”, Phys. Rev. B, 024109 (2006).
- Y. Janssen, M. Angst, K. W. Dennis, P. C. Canfield and R. W. McCallum, “**Small Sealed Ta Crucible for Thermal Analysis of Volatile Metallic Samples**”, Rev. Sci. Instr., **77**, 056104 (2006).
- J. L. Zarestky, O. Moze, J. W. Lynn, Y. Chen, T. A. Lograsso and D. L. Schlager, “**Spin Wave Dispersion in Magnetostrictive Fe-Ga Alloys**”, Phys. Rev. B, **75**, 052406 (2007).

Vibrational Entropy Studies Using Inelastic Neutron Scattering

DE-FG02-03ER46055

Brent Fultz btf@caltech.edu
California Institute of Technology, mail 138-78
Pasadena, California 91125

1. Program Scope

Thermal excitations of phonons, spins, and electrons contribute to the entropy of a material. These "dynamical" sources of entropy have been known for about a century, but the question for phase transitions is a bit subtler. For example, "Can differences between the phonon entropies of two phases affect their relative stabilities?"

Inelastic neutron scattering has proved invaluable for showing how and why solid phases differ in their phonon entropies, and for showing when these differences are important for the thermodynamic stability of the phases. Most of our experiments are designed to measure the density-of-states, $g(E)$, of elementary excitations in solids, especially phonons. For a probability of a set of states in an energy interval ΔE , in the harmonic approximation the thermodynamic partition function, Z , is:

$$Z = \prod_i^m \left(\frac{1}{1 - e^{-E_i/k_B T}} \right)^{3N g(E_i) \Delta E}$$

from which all phonon thermodynamics information (free energy, entropy, etc.) can be derived. The core quantity needed for the partition function is the phonon DOS $g(E)$. Any temperature-dependence of the phonon DOS can give a window on the anharmonic behavior of materials. In our BES program we measure the dynamical sources of entropy, and deduce their origin from the structure of materials. Most of the measurements are performed at the neutron scattering facilities operated by DOE.

2. Recent Progress

Charge Redistribution and Phonon Entropy of Vanadium Alloys

[O. Delaire and B. Fultz, "Charge Redistribution and Phonon Entropy of Vanadium Alloys", Phys. Rev. Lett. 97, 245701 (2006).]

The effects of alloying on the lattice dynamics of vanadium were investigated using inelastic neutron scattering. A good correlation was found between the vibrational entropy of alloying and the electronegativity of transition metal solutes across the $3d$ row and down columns of the periodic table (Fig. 1). First-principles calculations on supercells matching the experimental compositions predicted a systematic charge redistribution in the nearest-neighbor shell around the solute atoms, also following the Pauling and Watson electronegativity scales.

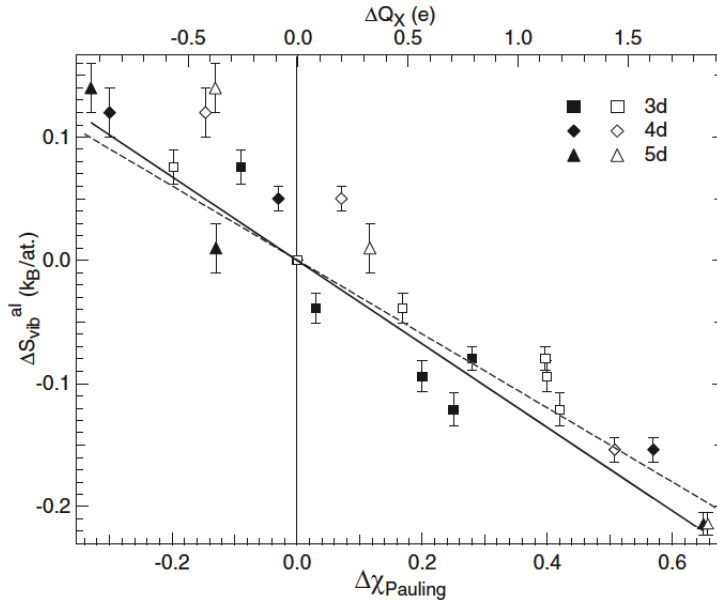


Fig. 1. Neutron-weighted vibrational entropy of alloying, $\Delta S_{\text{vib}}^{\text{al}}$, plotted versus difference in Pauling electronegativity, $\Delta\chi$ (solid symbols) between solute and V, and Bader charge transfer on solute Q_X (open symbols). The solid (dashed) line is a linear fit of $\Delta S_{\text{vib}}^{\text{al}}$ vs. Q_X .

Neutron scattering measurements of phonons at elevated temperatures

[M. Kresch, et al. "Neutron scattering measurements of phonons in nickel at elevated temperature", Phys. Rev. B 75, 104301 (2007).]

Measurements of elastic and inelastic neutron scatterings from elemental nickel were made at 10, 300, 575, 875, and 1275 K. The phonon densities of states (DOSs) were calculated from the inelastic scattering and were fit with Born–von Kármán models of the lattice dynamics. We accounted for the classical effect of thermal expansion, explained as an energy penalty for expansion against the bulk modulus, compensated at higher temperature by phonon softening and its higher entropy. This classical "quasiharmonic" contribution was removed from the heat capacity, as was the big contribution from harmonic entropy and a modest contribution from electronic entropy. The residual is the "anharmonic entropy." We used this to place bounds on the magnetic entropy of nickel. A significant broadening of the phonon DOS at elevated temperatures, another indication of anharmonicity, was also measured and quantified.

In a separate set of measurements, being written for publication, we also investigated Al metal at high temperatures by neutron inelastic scattering and by calorimetry. We found an anharmonic contribution of similar size to that of Ni.

Partial phonon densities of states of ^{57}Fe in Fe-Cr: Analysis by a local-order cluster expansion

[M.S. Lucas, et al. "Partial Phonon Densities of States of ^{57}Fe in Fe-Cr: Analysis by a Local-Order Cluster Expansion", Phys. Rev. B 75, 054307 (2007).]

Nuclear resonant inelastic x-ray scattering spectra were measured for ^{57}Fe in disordered

body-centered-cubic alloys of Fe-Cr. Partial phonon density of states DOS curves were obtained from these data. These results, in conjunction with the results of Ruckert *et al.* [Hyperfine Interact. **126**, 363 (2000)] on Fe-Cr thin-film multilayers and alloys, were analyzed with a "local-order cluster expansion method." This is an original approach that expresses a real phonon DOS, $g^m(E)$, in terms of "interaction phonon DOS" functions, $g_n(E)$, on the right side of this equation:

$$g^{m'}(E) = \sum_{n=0}^{\nu-1} g_n(E) \xi_{n,m'}$$

Here $\xi_{nm'}$ is a geometrical correlation function expressing how frequently the cluster n is in m' . This method is useful only if there are not too many important interaction phonon DOS functions, and they are applicable over a wide range of compositions and structures. We found that they were. We know that the vibrational entropy depends on the atom configurations in an alloy. The implication here is that we may be able to understand the thermodynamic trends of vibrational entropy from rather local information about atom arrangements in solids.

3. Future Plans

Electronic Origin of the Phonon Entropy of Vanadium Alloys

The systematic stiffening of the phonons with late transition-metal solutes correlates with the charge transfer as shown in Figure 1, but the Coulomb effects of individual charge transfers would cause much stronger forces than are actually observed. An important modification is how the conduction electrons screen the charge around the solute atom and its neighbors. We will follow this direction next year. From electronic structure calculations we know that the late transition metals such as Ni cause a substantial decrease in the electron density of states at the Fermi level. This is evidence that fewer conduction electrons are available to participate in the screening, so the local bonding becomes more Coulombic, or ionic, and stiffer.

Cluster Expansions and the Neutron Weight Correction

A longstanding problem in inelastic neutron scattering of alloys is the difference in scattering efficiencies by different elements in the material. For example, Ni atoms scatter phonons with much greater efficiency than Al atoms, so high-frequency vibrations that are associated primarily with Al motions are under-weighted in a phonon spectrum measured by inelastic neutron scattering. We have recently found that if we know the local atomic structure of a set of samples of different composition, we can find the interaction phonon DOS curves $g_n(E)$ above, and correct the neutron scattering for the weights of individual atoms. This method works if the range of the phonon DOS depends primarily on short-range interactions between atoms.

Neutron Scattering Studies of High-Temperature Thermodynamics

We upgraded the calorimetry facility at Caltech. We can now make measurements of sufficient accuracy to sort out the origin of the anharmonic contributions to the heat capacity in metals such as Ni, Al, V, and their alloys. The idea is that with neutron scattering data of sufficient quality, we can account for all of the phonon contribution to the entropy and heat

capacity. (Pharos at Lujan is good enough for this, and the ARCS instrument at the SNS will make this routine.) With electronic structure calculations such as the VASP pseudopotential code or the WIEN full-potential calculation, we obtain the electronic entropy. If we cannot account for the heat capacity with these contributions, other degrees of freedom, such as from electron-phonon contributions, must be responsible. We have acquired new inelastic neutron scattering data on A15 superconductors at high temperature that may show interesting anharmonic effects, but these data are not yet analyzed.

New Laboratory for Raman Spectroscopy on Materials in Excited States

In the late summer of 2006, the Engineering and Applied Science Division of Caltech provided k\$ 140 in funds to rehabilitate a laboratory space of approximately 560 sq. ft. in the Steele Building for our new effort on Raman spectroscopy on materials in excited states. The construction has been underway since late 2006, and is expected to be complete in April.

All of the optical components for this lab facility are in procurement, and many have arrived at Caltech. The last components are expected to arrive in late March, 2007. Of the k\$ 300 for this equipment, approximately k\$ 255 has been encumbered for procurements to date.

Some samples have been selected for preliminary study, and first results are expected before the summer of 2007. A computational effort is also underway to understand the Raman spectra of materials in their ground state.

4. References and Publications

- R. J. McQueeney, A. C. Lawson, A. Migliori, T. M. Kelley, B. Fultz, M. Ramos, B. Martinez, J.C. Lashley and S. Vogel, , "Unusual phonon softening in δ -phase plutonium ", Phys. Rev. Lett. 92(14) (2004) 146401.
- A. F. Yue, A. B. Papandrew, O. Delaire, B. Fultz, Z. Chowdhuri, R. Dimeo and D. A. Neumann, "Vibrations of micro-eV energies in nanocrystalline microstructures", Phys. Rev. Lett., 93 (20): Art. No. 205501 Nov. 12, 2004.
- O. Delaire, T. Swan-Wood, and B. Fultz, "Negative entropy of mixing for solutions of vanadium-platinum ", Phys. Rev. Lett., 93 (18): Art. No. 185704 Oct. 29, 2004.
- T. Swan-Wood, O. Delaire, and B. Fultz, "Vibrational Entropy of Spinodal Decomposition in FeCr", Phys. Rev. B, 72 (2): Art. No. 024305 July 2005.
- O. Delaire, M. Kresch, and B. Fultz, "Vibrational entropy of the γ - α martensitic transformation in Fe₇₁Ni₂₉", Philos. Mag. 85 (2005) 3567-3583.
- O. Delaire and B. Fultz, "Charge Redistribution and Phonon Entropy of Vanadium Alloys", Phys. Rev. Lett. 97, 245701 (2006).
- B. Fultz "Materials Science Applications of Inelastic Neutron Scattering", JOM, 58 (3): 58-63 Mar. 2006.
- Matthew S. Lucas, A. Papandrew, B. Fultz and M.Y. Hu "Partial Phonon Densities of States of ⁵⁷Fe in Fe-Cr: Analysis by a Local-Order Cluster Expansion", Phys. Rev. B 75, 054307 (2007).
- M. Kresch, O. Delaire, R. Stevens, J.Y.Y. Lin, and B. Fultz "Neutron scattering measurements of phonons in nickel at elevated temperature", Phys. Rev. B 75, 104301 (2007).
- O. Prytz, J. Taftø, C.C. Ahn, and B. Fultz, "Transition metal d-band occupancy in skutterudites studied by electron energy-loss spectroscopy" Physical Review B, in press.
- Olivier Delaire, "The Phonon Entropy of BCC Transition Metals and Alloys: Effects of Impurities and of a Martensitic Phase Transition" Ph.D. in Materials Science, May 12, 2006.

Real-Time X-ray Studies of Surface and Thin Film Processes

DE-FG02-03ER46037

Karl F. Ludwig, Jr.
Department of Physics
Boston University

Collaborators:

Boston University

Ludwig Group:

Nathalie Bouet

Yiyi Wang

Gozde Ozaydin

Christopher Sanborn

Ted Moustakas Group:

Anirban Bhattacharya

Ramya Chandrasekaran

University of Vermont

Randy Headrick Group:

Hua Zhou

Arizona State University

David Smith Group:

Lin Zhou

Brookhaven National Lab

D. Peter Siddons

I. PROGRAM SCOPE

Real-time investigations of surface and thin film processes have natural advantages over *post facto* studies. In real-time studies, there is a complete temporal record and no concern about sample changes in the period between the end of processing and the *post facto* measurement. This is of particular importance if the processes of interest occur at high temperature where surface relaxation can be relatively rapid. In addition, in building a quantitative kinetic record of the sample evolution for a given set of experimental parameters, real-time studies do not suffer from run-to-run variations that can occur if the kinetic evolution is instead reconstructed through *post facto* measurements made on samples from different runs. In many cases, x-ray techniques are the natural choice for real-time studies because of their ability to examine atomic-level structure as well as morphology on larger length scales. In addition, x-rays penetrate most ambient environments and can probe below the surface to examine buried

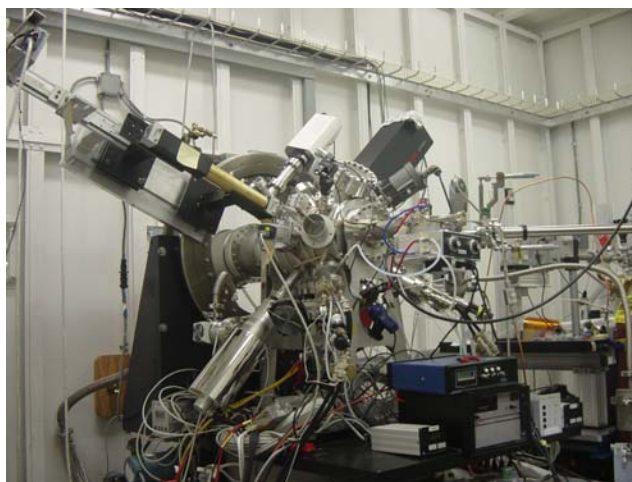
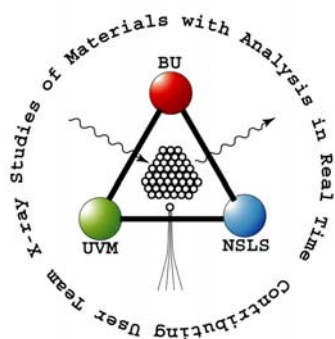


Fig. 1: Facility for real-time studies of surface and thin film processes on NSLS X21.

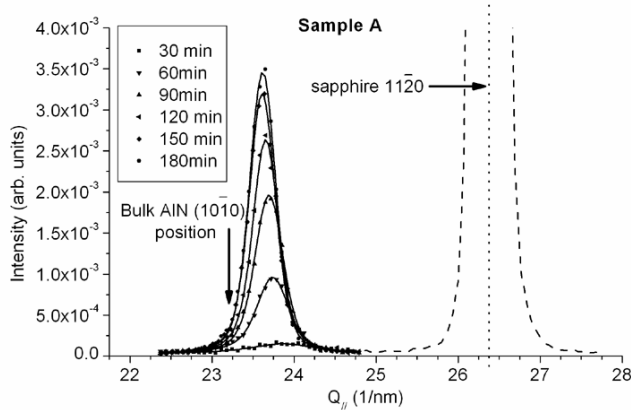


Fig. 2: X-ray GID patterns along the AlN [10 $\bar{1}$ 0] direction during low-temperature nitridation of sapphire. The sapphire (11 $\bar{2}$ 0) peak is plotted in dashed line.

interfaces. In collaboration with Prof. Randall Headrick of the University of Vermont, we have constructed a facility for real-time studies of surface and thin film processes at the National Synchrotron Light Source (NSLS) insertion-device beamline X21.

To promote flexibility, the base spectrometer is designed so that modest-sized processing/vacuum chambers can be rolled onto it. This design allows multiple specialized chambers to be constructed, optimized for experimentation, and then moved onto the diffractometer for x-ray studies. The experimental geometry enables the use of a wide range of x-ray techniques to be employed, including grazing-incidence small-angle x-ray scattering (GISAXS) to study surface morphology development, grazing-incidence diffraction (GID) to examine phase content, strain and lateral domain sizes, and x-ray reflectivity to measure density profiles perpendicular to the surface.

The facility currently has a suite of instrumentation for surface modification and characterization during real-time x-ray study, including: Thermionics sample manipulator with BN heating element, Oxford Scientific OSPrey ECR plasma source, Applied Epi UNI-bulb RF plasma source, Applied Epi SUMO effusion cells, US Inc. sputter deposition source, Balzers mass spectrometer, Staib RHEED system, and Ircon infrared pyrometer. As part of our Contributing User status at the NSLS, we make the facility available for outside users under the NSLS General User Program.

II. RECENT PROGRESS

Our recent focus has been on issues related to the growth of wide-bandgap group III-nitride semiconductors by plasma-assisted MBE (PA-MBE) and the development of nanoscale surface morphologies during low-energy ion bombardment:

Low- and high-temperature nitridation of *c*-plane sapphire

The plasma nitridation kinetics of *c*-plane sapphire at both low (200-300°C) and high (750°C) substrate temperatures was examined using real-time GISAXS, GID, x-ray reflectivity and RHEED. These monitored the evolution of the nitride thickness, strain and surface structure during nitridation. We have developed a model of the nitridation with initial nucleating islands consisting of several monolayers which grow laterally. By fitting the x-ray data, we extract nucleation densities and growth velocities both laterally along the surface and vertically into the sapphire.

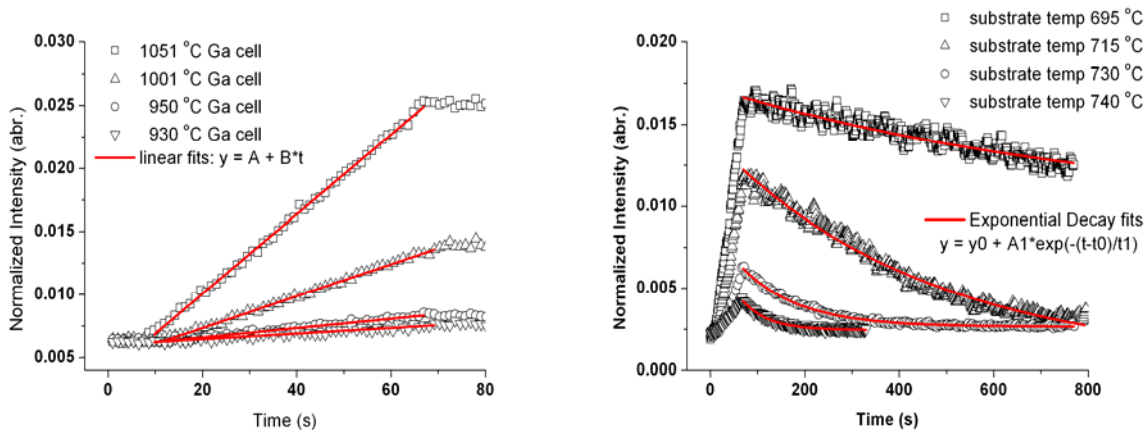


Fig. 3: Adsorption and desorption of Ga on sapphire as monitored by x-ray fluorescence. Fits to the curves yield adsorption and desorption rates.

Gallium adsorption/desorption kinetics on sapphire and GaN

Real-time GISAXS and x-ray fluorescence was used to study Ga adsorption/desorption kinetics on sapphire and GaN surfaces. Formation and coarsening of liquid Ga nanodroplets was observed on sapphire. For identical processing conditions, significantly different Ga adsorption/desorption rates were observed on sapphire and GaN surfaces.

Gallium Nitride Nanodot Formation by Droplet Heteroepitaxy

Epitaxial self-organized gallium nitride nanodots have been fabricated using droplet heteroepitaxy on *c*-plane sapphire by plasma-assisted molecular beam epitaxy at different substrate temperatures and Ga fluxes. Nanoscale Ga droplets were initially formed on the sapphire substrate at high temperatures by Ga deposition from an effusion cell in an ultra-high vacuum growth chamber. Subsequently, the droplets were converted into GaN nanodots using a nitrogen plasma source. The process was monitored and controlled using real-time GISAXS. X-ray diffraction indicated that the wurtzite phase was dominant at higher substrate temperature (710°C), but a mixture of wurtzite and zincblende phases was present at a substrate temperature of 620°C. A thin GaN continuous layer of ~ 3ML thick was observed by transmission electron microscopy on the sample grown at a substrate temperature of 620°C, but no such layer was observed for

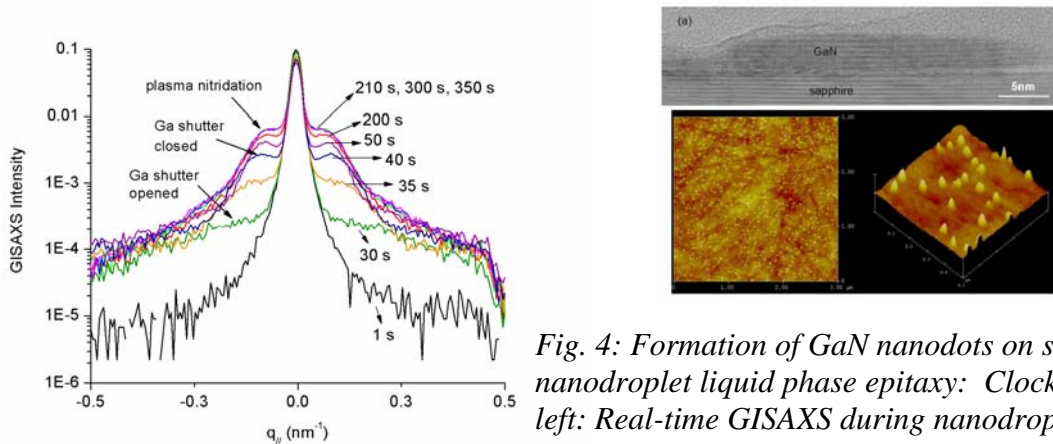


Fig. 4: Formation of GaN nanodots on sapphire by nanodroplet liquid phase epitaxy: Clockwise from left: Real-time GISAXS during nanodroplet formation and subsequent nitridation; cross-section TEM; AFM topograph of dots.

the substrate temperature of 710°C. This suggests that at the lower temperature there is little mobility of Ga atoms in contact with the sapphire substrate so that they cannot easily diffuse to nearby droplets and instead form a thin layer covering the surface.

Incommensurate ordering in Al_{0.72}Ga_{0.28}N thin films

Novel structures with incommensurate ordering along the [0001] direction are observed in wurtzite Al_{0.72}Ga_{0.28}N alloys grown by plasma-assisted molecular beam epitaxy on *c*-plane sapphire. The increasing complexity of the ordering with increasing Ga-rich growth environment suggests that the ordering is related to the presence of a Ga overlayer believed to exist on the surface of the growing film. The ordering may depend on the kinetics of cation incorporation from the highly mobile overlayer into the film.

Surface morphology evolution of Si(100) during low-energy normal-incidence Ar⁺ ion bombardment

The temperature dependence of the surface morphology evolution during 1000 eV Ar⁺ normal incidence ion bombardment of Si(100) surfaces is studied in real time. At room temperature the surface remains smooth. However, at the fluxes used here, surface roughening occurs above 400C and in the range of 450C to 500C a transition region from amorphous to crystalline surface is observed. Above 500C, the surface remains crystalline and the growing corrugations exhibit dynamic scaling with power law growth in amplitude and characteristic length scale.

Effects of Mo seeding on the formation of Si nanodots

Although Si surfaces remain smooth during low-energy normal-incidence bombardment at room temperature, when a small amount of Mo atoms was supplied to the surface during ion bombardment, the development of correlated structures was observed. Stress measurements show that initially a compressive stress develops during bombardment, likely due to amorphization of the surface. However seeding causes a larger tensile stress to develop with further bombardment, possibly due to the formation of higher density regions around the Mo seed atoms on the surface. This large tensile stress may play a dominant role in the dot formation.

Recent Publications:

- 1) "Real-Time X-ray Studies of Mo-Seeded Self-Organized Si Nanodot Formation During Low Energy Ar⁺ Ion Bombardment", G. Ozaydin, A.S. Özcan, Y. Wang, Karl F. Ludwig, H. Zhou, R. L. Headrick and D.P. Siddons, *Appl. Phys. Lett.* **87**, 163104 (2005).
- 2) "Complex and Incommensurate Ordering in Al_{0.72}Ga_{0.28}N Thin Films Grown by Plasma Assisted Molecular Beam Epitaxy", Y. Wang, A. Özcan, K. Ludwig, A. Bhattacharyya, T.D. Moustakas, L. Zhou and D. J. Smith, *Appl. Phys. Lett.* **88**, 181915 (2006).
- 3) "Real-Time X-Ray Studies of Gallium Adsorption and Desorption", Ahmet S. Özcan, Yiyi Wang, Gozde Ozaydin, Karl F. Ludwig, Anirban Bhattacharyya, Theodore D. Moustakas and D. Peter Siddons, *J. Appl. Phys.* **100**, 084307 (2006).
- 4) "Real-time synchrotron x-ray studies of low and high temperature nitridation of *c*-plane sapphire", Yiyi Wang, Ahmet S. Özcan, Gözde Özaydin, Karl F. Ludwig, Jr., Anirban Bhattacharyya, Theodore D. Moustakas, Hua Zhou and Randall L. Headrick, and D. Peter Siddons, *Phys. Rev. B* **74**, 235304 (2006).
- 5) "Wavelength Tunability of Ion-bombardment Induced Ripples on Sapphire investigated with small-angle x-ray scattering and atomic force microscopy", Hua Zhou, Yiping Wang, Lan Zhou, Randall L. Headrick, Ahmet S. Ozcan, Yiyi Wang, Gozde Ozaydin, and Karl F. Ludwig Jr., and D. Peter Siddons, *Phys. Rev. B*, in press.

In Situ Synchrotron X-ray Studies of Growth and Ferroelectricity in Ultrathin Perovskite Films

G. B. Stephenson^{1,2}, D. D. Fong¹, S. K. Streiffer^{1,2}, R.-V. Wang^{1,2}, F. Jiang¹,
Carol Thompson³, J. A. Eastman¹, P.H. Fuoss¹

¹Materials Science Division, Argonne National Laboratory, Argonne, Illinois, USA

²Center for Nanoscale Materials, Argonne National Laboratory, Argonne, Illinois, USA

³Dept. of Physics, Northern Illinois Univ., DeKalb, Illinois, USA

Program Scope

As part of a larger effort to bring forefront synchrotron x-ray techniques to bear on key problems in materials science, we have been using *in situ* x-ray scattering and fluorescence to study synthesis and processing of ultrathin films of perovskite-structure ferroelectric materials. X rays provide an excellent atomic-scale probe of non-vacuum processes such as metal-organic chemical vapor deposition (MOCVD). We have developed a growth chamber mounted on a z-axis surface diffractometer optimized for these studies at beamline 12-ID-D of the Advanced Photon Source. The ability to perform x-ray studies in the film growth chamber allows us to determine optimum growth conditions, to control the thickness of the films to sub-unit-cell accuracy, and to control surface and film stoichiometry during high temperature study [1-3]. X-ray energies of 24 to 30 keV are used to penetrate the 2-mm-thick quartz wall of the deposition chamber. Here we give examples of our *in situ* synchrotron x-ray scattering and fluorescence studies of processes occurring during MOCVD growth, and the effects of controlled environment on ferroelectricity in ultrathin films following growth.

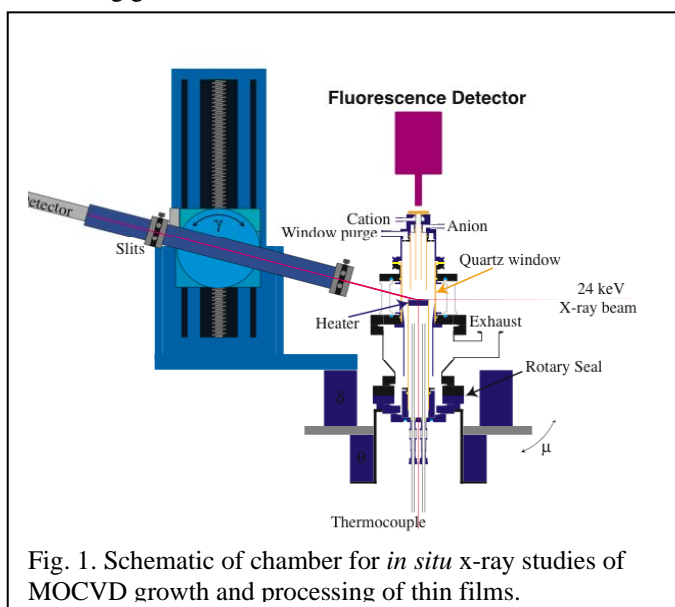


Fig. 1. Schematic of chamber for *in situ* x-ray studies of MOCVD growth and processing of thin films.

Recent Progress

Lattice pulling during growth of PZT

We have recently performed studies of the initial stages of epitaxial growth of $\text{Pb}(\text{Zr},\text{Ti})\text{O}_3$ (PZT) films on (001) SrTiO_3 using simultaneous *in situ* grazing-incidence x-ray scattering and fluorescence [4]. Figures 1 and 2 show simultaneous measurements of the strain and composition of the film surface during growth. We observe that the Zr content increases dramatically as strain relaxation occurs, resulting in a compositional non-uniformity in the growth direction. Such non-uniformity is especially critical in ferroelectric thin films, since both film strain and composition strongly influence ferroelectric properties. The results are consistent with the model of “lattice pulling” developed to describe growth of epitaxial

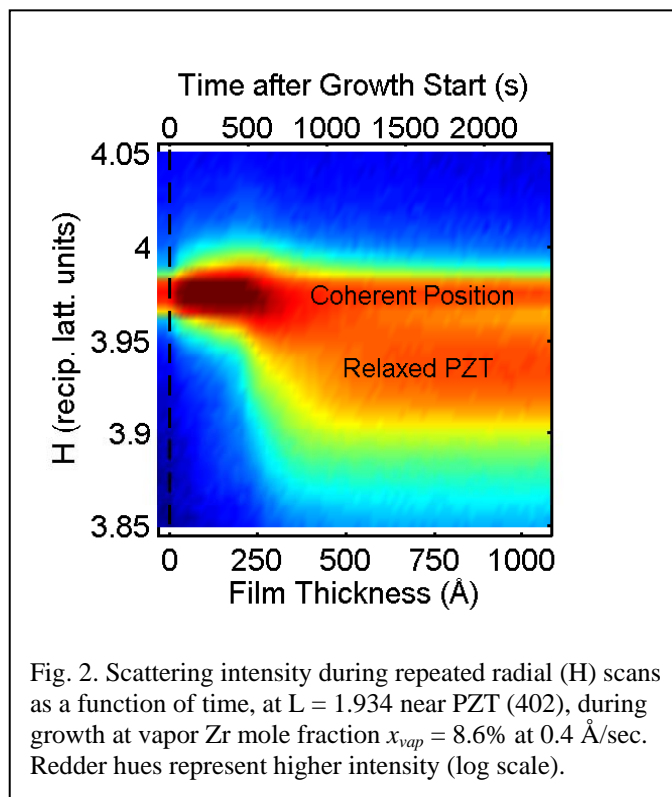


Fig. 2. Scattering intensity during repeated radial (H) scans as a function of time, at $L = 1.934$ near PZT (402), during growth at vapor Zr mole fraction $x_{\text{vap}} = 8.6\%$ at $0.4 \text{ \AA}/\text{sec}$. Redder hues represent higher intensity (log scale).

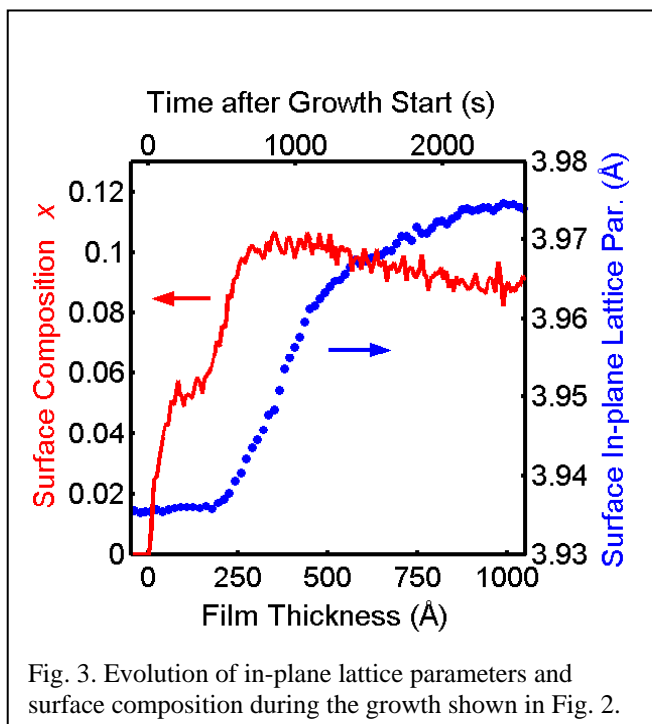


Fig. 3. Evolution of in-plane lattice parameters and surface composition during the growth shown in Fig. 2.

semiconductor alloy films [5], which assumes that the evolving surface composition is determined by the equilibrium between the vapor and the film in its current strain state. This indicates that MOCVD of PZT is not transport-limited, but is surprisingly near equilibrium. The model can be used to predict growth procedures that would give uniform composition films.

Ferroelectricity in ultrathin $PbTiO_3$ films

In situ x-ray scattering provides a powerful tool for observing the phase transition, domain structure, and surface structure of ultrathin ferroelectric films [6-10]. The paraelectric-to-ferroelectric phase transition in ultrathin films displays complex behavior driven by a fascinating competition between polarization, strain, electric field, domain wall energy, and surface chemistry. For decades, researchers have found that ferroelectric behavior is typically suppressed in films that are sufficiently thin. Various explanations have been put forward: intrinsic suppression of polarization at surfaces, the effect of depolarizing electric fields, or extrinsic effects of composition or strain. As a result, the factors responsible for the size dependence of the paraelectric-to-ferroelectric phase transition have remained unresolved, in particular for the technologically important perovskites.

We have investigated the ferroelectric properties of ultrathin, coherently strained epitaxial films of $PbTiO_3$ as a function of film thickness, temperature, vapor ambient, and electrical boundary conditions. We find that the transition temperature T_C and domain structure depend

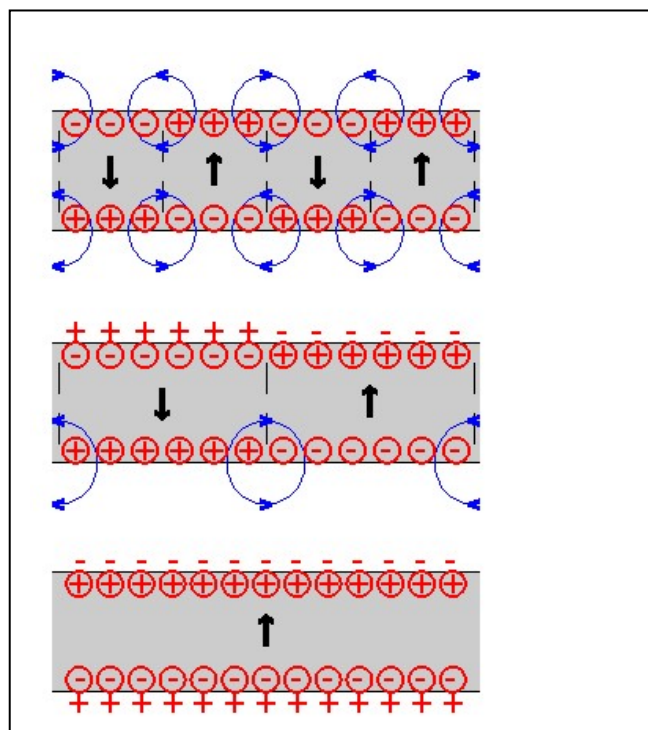


Fig. 4. Schematic of domain structures in thin ferroelectric films determined by surface compensation. Equilibrium 180° stripe domains form to reduce the depolarization field (top two cases) unless both interfaces are compensated by free charge (bottom case).

sensitively on the electrical boundary conditions, as illustrated in Fig. 4. When films are grown on insulating $SrTiO_3$, the polar phase forms as nanoscale 180° stripe domains [6-9]. Such equilibrium stripe domains minimize the depolarizing field. They produce strong satellites around the $PbTiO_3$ Bragg peaks having non-zero L , as shown in Fig. 5. When films are grown on conducting $SrRuO_3$ layers on $SrTiO_3$, the polar phase forms in a single domain with no satellites [10]. This implies that the interface of the film exposed to the vapor is compensated by free charge, as well as the interface in contact with the conducting $SrRuO_3$. Density functional theory modeling [10] indicates that adsorbed ions may provide sufficient compensation at the surface to stabilize the polar phase. Although we observe a thickness-dependent T_C (Fig. 6), in both cases the polar phase is stable at room temperature in films with thicknesses as small as three unit cells (1.2 nm). The thickness dependence of T_C for $PbTiO_3$ films on $SrTiO_3$ is compared with Landau theory for stripe domains [11] in Fig. 7. Theory predicts a greater suppression of T_C from the residual depolarizing field than actually observed, indicating that any intrinsic surface effect enhances

(rather than suppresses) polarization, contrary to some previous models.

Future Directions

We plan to study the effects of the vapor environment on the ferroelectric transition in ultrathin films. Can the polarization be controlled by varying the chemistry of the environment? Can surface chemistry be manipulated by changing the film polarization? Such effects could lead to new types of sensors, chemical actuators, or active catalytic devices.

Work supported by the U. S. Department of Energy, Office of Science (BES), under Contract No. DE-AC02-06CH11357.

Contributing author: Brian Stephenson, stephenson@anl.gov

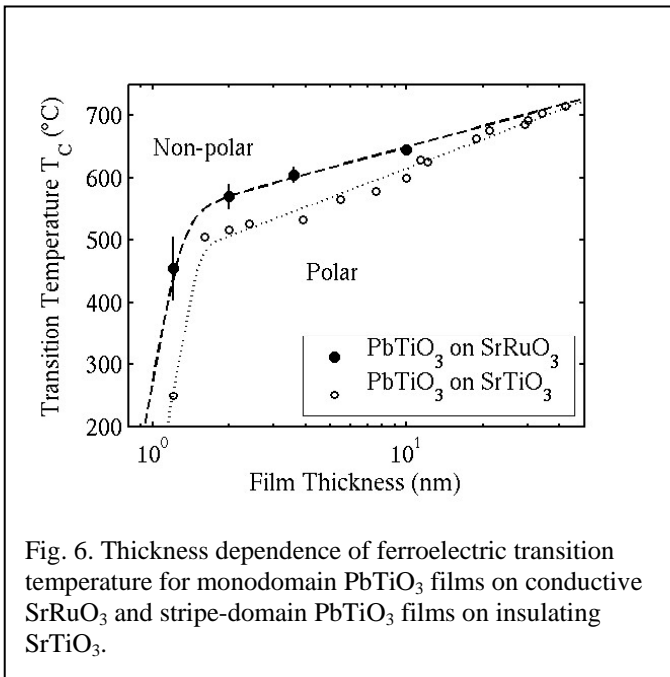


Fig. 6. Thickness dependence of ferroelectric transition temperature for monodomain PbTiO_3 films on conductive SrRuO_3 and stripe-domain PbTiO_3 films on insulating SrTiO_3 .

References

- [1] A. Munkholm *et al.*, *Phys. Rev. Lett.* **88**, 016101 (2002).
- [2] M.V. Ramana Murty *et al.*, *Appl. Phys. Lett.* **80**, 1809 (2002).
- [3] G.B. Stephenson *et al.*, *Physica B* **336**, 81 (2003).
- [4] R.-V. Wang *et al.*, *Appl. Phys. Lett.* **89**, 221914 (2006).
- [5] F.C. Larché and J. W. Cahn, *J. Appl. Phys.* **62**, 1232 (1987)
- [6] S.K. Streiffer *et al.*, *Phys. Rev. Lett.* **89**, 067601 (2002).
- [7] D.D. Fong *et al.*, *Ann. Phys. (Leipzig)* **13**, 27 (2004).
- [8] D.D. Fong *et al.*, *Science* **304**, 1650 (2004).

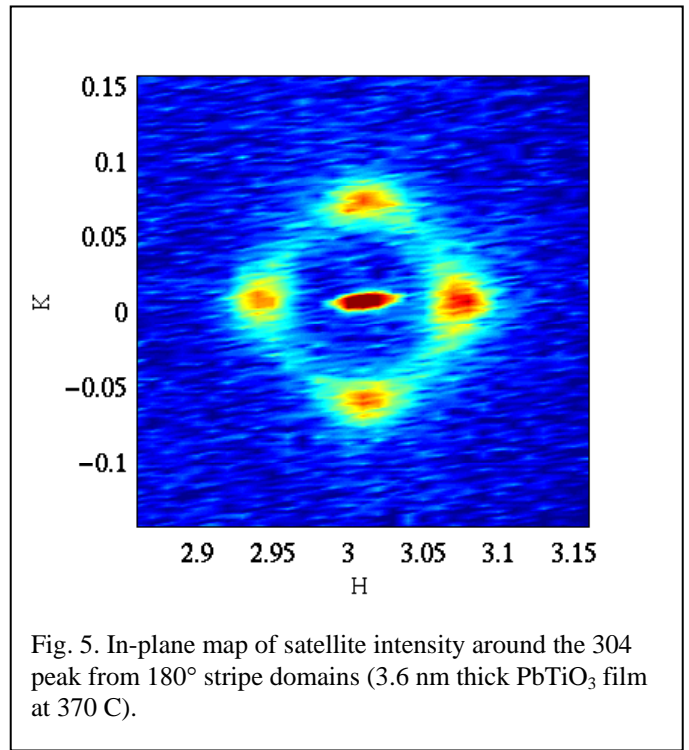


Fig. 5. In-plane map of satellite intensity around the 304 peak from 180° stripe domains (3.6 nm thick PbTiO_3 film at 370 C).

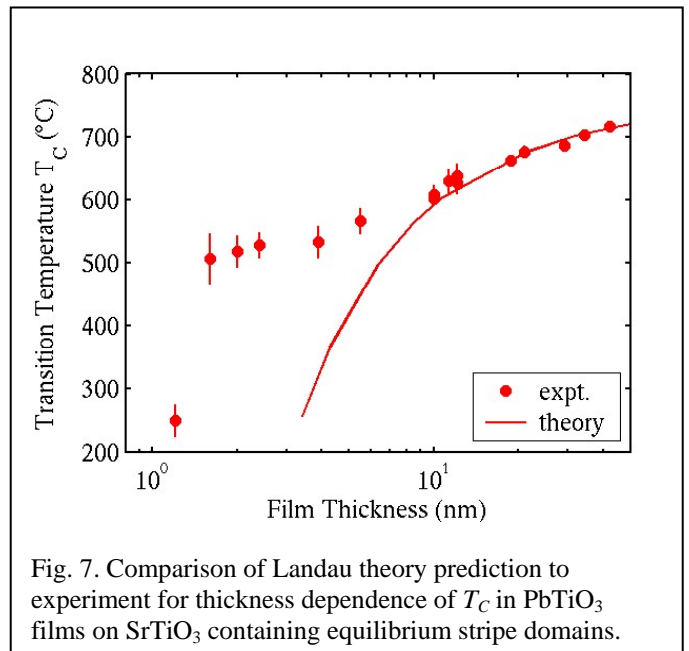


Fig. 7. Comparison of Landau theory prediction to experiment for thickness dependence of T_C in PbTiO_3 films on SrTiO_3 containing equilibrium stripe domains.

- [9] D.D. Fong *et al.*, *J. Synchrotron Rad.* **12**, 163 (2005).
- [10] D.D. Fong *et al.*, *Phys. Rev. Lett.* **96**, 127601 (2006).
- [11] G.B. Stephenson and K.R. Elder, *J. Appl. Phys.* **100**, 051601 (2006)

Publications 2004 to present:

1. "Ferroelectricity in Ultrathin Perovskite Films," D.D. Fong, G. B. Stephenson, S.K. Streiffer, J. A. Eastman, O. Auciello, P.H. Fuoss, and C. Thompson, *Science* **304**, 1650-1653 (2004).
2. "In-Situ Synchrotron X-ray Studies of PbTiO₃ Thin Films," D.D. Fong, C. Thompson, S.K. Streiffer, J.A. Eastman, O. Auciello, P.H. Fuoss and G.B. Stephenson, *Proc. 10th Int. Workshop on Oxide Electronics* (Augsburg, Germany, September 11-13, 2003), *Annalen der Physik* **13**, 27-30 (2004).
3. "Beyond High-K: Ferroelectric Ultrathin Films and Nanostructures," S. K. Streiffer, G. B. Stephenson, D. D. Fong, J. A. Eastman, C. Thompson, M. Zurbuchen, M. Biegalski, O. Auciello, P. H. Fuoss, D. M. Kim, K. J. Choi, C. B. Eom, *Proc. of International Workshop on Dielectric Thin Films*, Tokyo, Japan, May 26-28 (2004).
4. "In-Situ Synchrotron X-ray Studies of Processing and Physics of Ferroelectric Thin Films," G.B. Stephenson, S.K. Streiffer, D.D. Fong, M.V. Ramana Murty, O. Auciello, P.H. Fuoss, J.A. Eastman, A. Munkholm, and C. Thompson, in *Polar Oxides: Properties, Characterization, and Imaging*, ed. R. Waser, U. Bottger, and S. Tiedke (Wiley-VCH, Weinheim, 2005), ch. 8, pp 151-160.
5. "In Situ Synchrotron X-Ray Studies of Ferroelectric Thin Films," D.D. Fong, J. A. Eastman, G. B. Stephenson, P.H. Fuoss, S.K. Streiffer, C. Thompson, and O. Auciello, *Journal of Synchrotron Radiation* **12**, 163-167 (2005).
6. "Direct Structure Determination in Ultrathin Ferroelectric Films by Analysis of Synchrotron X-Ray Scattering Measurements," D.D. Fong, C. Cionca, Y. Yacoby, G.B. Stephenson, J.A. Eastman, P.H. Fuoss, S.K. Streiffer, C. Thompson, R. Clarke, R. Pindak, and E.A. Stern, *Physical Review B* **71**, 144112 (2005).
7. "In situ X-Ray Analysis of Materials Growth and Processing," P.H. Fuoss, R.-V. Wang, J.A. Eastman, D.D. Fong, G.B. Stephenson, S.K. Streiffer, Carol Thompson, F. Jiang, G.-W. Zhou, L.E. Rehn, P.M. Baldo and L.J. Thompson, *Journal of the Taiwan Vacuum Society*, **18**, 69 (2005).
8. "In-Situ X-Ray Scattering Studies of Electroded Epitaxial PbTiO₃ Thin Films," S.K. Streiffer, G.B. Stephenson, D.D. Fong, P.H. Fuoss, J.A. Eastman, R.-V. Wang, F. Jiang, K. Latifi, and Carol Thompson, *Proceedings of the 12th US-Japan Seminar on Dielectric and Piezoelectric Ceramics*, held Annapolis, MD, Nov. 6-9, 2005, (2005).
9. "Stabilization of Monodomain Polarization in Ultrathin PbTiO₃ Films," D. D. Fong, A. M. Kolpak, J. A. Eastman, S. K. Streiffer, P. H. Fuoss, G. B. Stephenson, Carol Thompson, D. M. Kim, K. J. Choi, C. B. Eom, I. Grinberg, A. M. Rappe, *Physical Review Letters* **96**, 127601 (2006).
10. "Indium adsorption on GaN under metal-organic chemical vapor deposition conditions," F. Jiang, R.-V. Wang, A. Munkholm, S. K. Streiffer, G. B. Stephenson, P. H. Fuoss, K. Latifi and Carol Thompson, *Applied Physics Letters* **89**, 161915 (2006).
11. "Ferroelectric thin films: Review of materials, properties, and applications," N. Setter, D. Damjanovic, L. Eng, G. Fox, S. Gevorgian, S. Hong, A. Kingon, H. Kohlstedt, N. Y. Park, G. B. Stephenson, I. Stolitchnov, A. K. TagansteV, D. V. Taylor, T. Yamada, and S. Streiffer, *Journal of Applied Physics* **100**, 051606/1-46 (2006).
12. "In Situ Synchrotron X-Ray Studies of Ferroelectric Thin Films," D. D. Fong and Carol Thompson, *Annual Review of Materials Research* **36**, 431-465 (2006).
13. "Real Time X-Ray Observation of Lattice Pulling During Growth of Epitaxial Pb(Zr,Ti)O₃ Films," R.-V. Wang, G. B. Stephenson, D. D. Fong, F. Jiang, P. H. Fuoss, J. A. Eastman, S. K. Streiffer, K. Latifi and Carol Thompson, *Applied Physics Letters* **89**, 221914 (2006).
14. "Theory for Equilibrium 180° Stripe Domains in PbTiO₃ Films," G. B. Stephenson and K. R. Elder, *Journal of Applied Physics* **100**, 051601 (2006).
15. "In situ X-ray Studies of Metal Organic Chemical Vapor Deposition of Pb(Zr,Ti)O₃," R.-V. Wang, F. Jiang, D. D. Fong, G. B. Stephenson, P. H. Fuoss, J. A. Eastman, S. K. Streiffer, K. Latifi, and C. Thompson, Proc. of Ninth Int. Conf. on Surface X-ray and Neutron Scattering, Taipei, Taiwan May 23-26 2006, to appear in *Thin Solid Films* (2007), available online January 19, 2007.

Author Index

This page is intentionally blank

Author Index

Anderson, I.....	51	Fowlkes, J.	123
Ashbaugh, Henry	55	Fuentes-Cabrera, M.....	123
Aziz, Michael.....	139	Fultz, Brent	225
Bader, Samuel.....	11	Fuoss, P.	233
Balazs, Anna	209	Garofalini, Stephen	217
Banerjee, Sanjay	99	Garrett, M.....	127
Barisic, Neven.....	25	Geohegan, D.	127
Berron, Brad.....	173	George, Steven.....	165
Bhattacharya, Anand.....	11	Gong, Yinyan.....	87
Bhattacharya, Anirban	229	Gourley, Paul	161
Bollinger, A.....	33	Gozar, A.....	33
Bouet, Nathalie	229	Greven, Martin.....	25
Bourges, Philippe.....	25	Grigoropoulos, Costas.....	7
Bozovic, I.....	33	Gu, Genda	41
Bunker, Bruce	205	Heald, Steven	95
Burger, Christian.....	15, 63	Hensley, D.....	123
Butko, V.....	33	Horton, J.....	123
Canfield, P.....	37, 221	Hu, H.....	127
Castleman, Jr., A.....	111, 153, 155	Hu, Rongwei	19
Chabot-Couture, Guillaume	25	Huang, Hanchen.....	119
Chaikin, Paul	213	Huang, Rui	99
Chambers, Scott.....	95	Hücker, Markus.....	41
Chandrasekaran, Ramya	229	Hudson, Stephen	157
Chason, Eric	77	Israelachvili, Jacob.....	69
Chen, Gang	7	Ivanov, I.	127
Cheng, M.-D.	127	Jackson, J.	127
Cheung, Irene.....	95	Jennings, G.....	173
Cho, Yong-Chan	25	Jiang, F.....	233
Chu, Benjamin	15, 63	John, Vijay	55
Chumanov, George	157	Jones, Camille	55
Clement, Teresa	65	Jones, L.	51
Cui, H.....	127	Kaneko, Nobuhisa.....	25
Dailey, Eric	65	Kaspar, Tiffany	95
DeCaro, Curt.....	145	Khanna, S.....	111, 155
Di, Zengfeng.....	73	Klein, K.....	123
Dresselhaus, Mildred	7	Krishnan, Chirakkal	15, 63
Droubay, Timothy.....	95	Kuskovsky, Igor.....	87
Drucker, Jeff	65	Lagally, Max	81, 91
Eastman, J.	233	Lee, Jung-Kun.....	73
Eckstein, J.	11	Li, Yuan	25
Elam, Jeff.....	177, 197	Libera, J.....	177
Eres, G.....	127	Liu, Feng.....	129
Exarhos, Gregory	201	Liu, S.....	191
Fong, D.	233	Liu, Ying.....	47

Liu, Z.....	127	Shen, Aidong.....	87
Lograsso, T.	37, 51, 221	Shin, Yongsoon.....	201
Logvenov, G.	33	Shutthanandan, V.....	95
Lu, Li.....	25	Siddons, D.....	229
Ludwig, Jr., Karl.....	229	Simmons-Potter, K.....	169
Madras, Prashanth.....	65	Simpson, M.....	123
Mao, Samuel.....	7	Smith, Dave.....	65
McCallum, R.....	37, 221	Sordelet, D.	51
McMillan, Paul.....	3	Sorgey, K.	123
McPherson, Gary.....	55	Stein, Andreas.....	165
Melechko, A.....	123	Stephenson, G.....	233
Mendeleev, M.....	191	Stocks, G.....	123
Misewich, J.....	107	Streiffer, S.....	233
Motoyama, Eugene.....	25	Styers-Barnett, D.....	127
Mukherjee, P.....	59	Swadener, Greg.....	73
Muñoz-Espí, Rafael.....	15, 63	Tamargo, Maria.....	87
Nachimuthu, P.....	95	Thompson, Carol.....	233
Napolitano, R.....	191	Thornton, K.....	183
Nastasi, Michael.....	73	Tirrell, Matthew.....	69
Navrotsky, Alexandra.....	29	Tranquada, John.....	41
Neumark, Gertrude.....	87	Trivedi, R.....	191
Nolas, G.	59	Vajk, Owen.....	25
Norris, David.....	165	Voorhees, P.....	183
Ozaydin, Gozde.....	229	Wang, Chongmin.....	95
Paiella, R.....	149	Wang, Li.....	201
Pang, Yaoyu.....	99	Wang, R.-V.....	233
Pannala, S.....	127	Wang, Yiyi.....	229
Patel, Umesh.....	145	Wang, Yongqiang.....	73
Pellin, Michael.....	177, 197	Wells, J.....	127
Peng, Xiaogang.....	105	Witanachchi, S.....	59
Peppernick, S.....	153	Wong, S.....	107
Petrov, Ivan.....	187	Wood, R.....	127
Petrovic, Cedomir.....	19	Woodward, W.....	155
Picraux, Tom.....	65	Wu, Judy.....	115
Potter, Jr., B.	169	Xiang, Xiaodong.....	7
Puretzky, A.	127	Xiao, K.....	127
Rack, P.....	123	Xiao, Zhili.....	145
Randolph, S.....	123	Yao, Chunhua.....	201
Reber, A.....	155	Yoon, M.....	127
Risen, Jr., William.....	201	Yu, Guichuan.....	25
Roach, P.....	155	Zeng, Hongbo.....	69
Rouleau, C.....	127	Zeng, Taofang.....	7
Samuels, William.....	201	Zhao, B.....	127
Sanborn, Christopher.....	229	Zhao, Xudong.....	25
Schaak, R.....	135	Zhong, J.....	123
Scherer, George.....	179	Zhou, Hua.....	229
Scott, S.....	81	Zhou, Lin.....	229
Shao, Lin.....	73		

Participants

This page is intentionally blank

**US DOE Program Meeting on Fundamental Synthesis
Research Challenges for 21st Century Materials:
Mechanism and Methods
Participants**

Firstname	Lastname	Organization	Phone	Email
Christie	Ashton	US DOE Office of Basic Energy Sciences	301-903-0511	christie.ashton@science.doe.gov
Michael	Aziz	Harvard University	617-495-9884	maziz@harvard.edu
Anna	Balazs	University of Pittsburgh	412-648-9250	balazs1@engr.pitt.edu
Sanjay	Banerjee	The University of Texas, Austin	512-471-6730	j.toll@mer.utexas.edu, banerjee@ece.utexas.edu
Javier	Bareno	University of Illinois	217-333-3481	bareno@mrl.uiuc.edu
Bradley	Berron	Vanderbilt University	314-952-8995	brad.berron@vanderbilt.edu
Anand	Bhattacharya	Argonne National Laboratory	630-252-3996	anand@anl.gov
Nathalie	Bouet	Boston University	617-416-9386	bouet@bu.edu
Ivan	Bozovic	Brookhaven National Laboratory	631-344-4973	bozovic@bnl.gov
Bruce	Bunker	Sandia National Laboratories	505-284-6892	bcbunke@sandia.gov
Paul	Canfield	Ames Laboratory	515-294-6271	canfield@ameslab.gov
A. Welford	Castleman	Pennsylvania State University	814-865-7242	awc@psu.edu
Paul	Chaikin	New York University	212-998-7694	chaikin@nyu.edu
Scott	Chambers	Pacific Northwest National Laboratory	509-376-1766	sa.chambers@pnl.gov
Eric	Chason	Brown University	401-863-2317	eric_chason@brown.edu
Gang	Chen	Massachusetts Institute of Technology	617-253-0006	gchen2@mit.edu
Benjamin	Chu	Stony Brook University	631-632-7928	bchu@notes.cc.sunysb.edu
George	Chumanov	Clemson University	864-656-2339	gchumak@clemson.edu
Eric	Dailey	Arizona State University	602-317-0526	eric.j.dailey@asu.edu
Satyen	Deb	National Renewable Energy Laboratory	303-384-6405	satyen_deb@nrel.gov
Jianjun	Dong	Auburn University	334-844-2943	jjdong@physics.auburn.edu

**US DOE Program Meeting on Fundamental Synthesis
Research Challenges for 21st Century Materials:
Mechanism and Methods
Participants**

Firstname	Lastname	Organization	Phone	Email
Jeff	Drucker	Arizona State University	480-965-9658	jeff.drucker@asu.edu
Gregory	Exarhos	Pacific Northwest National Laboratory	509-376-4125	greg.exarhos@pnl.gov
Julie	Fife	Northwestern University	847-491-3425	jfife@northwestern.edu
Timothy	Fitzsimmons	US DOE Office of Basic Energy Sciences	301-903-9830	tim.fitzsimmons@science.doe.gov
Brent	Fultz	California Institute of Technology	626-395-2170	btf@caltech.edu
Stephen	Garofalini	Rutgers University	732-445-2216	shg@rutgers.edu
David	Geohagan	Oak Ridge National Laboratory	865-576-5097	odg@ornl.gov
Bonnie	Gersten	US DOE Office of Basic Energy Sciences	301-903-0002	Bonnie.Gersten@science.doe.gov
Paul	Gourley	Sandia National Laboratories	505-844-5806	plgourl@sandia.gov
Martin	Greven	Stanford University	650-725-8978	greven@stanford.edu
Hanchen	Huang	Rensselaer Polytechnic Institute	518-276-2020	hanchen@rpi.edu
Rui	Huang	University of Texas, Austin	512-471-7558	ruihuang@mail.utexas.edu
James	Horwitz	US DOE Office of Basic Energy Sciences	301-903-4894	james.horwitz@science.doe.gov
Vijay	John	Tulane University	504-865-5883	vj@tulane.edu
Lawrence	Jones	Ames Laboratory	515-294-5236	jonesll@ameslab.gov
Camille	Jones	Hamilton College	315-859-4209	cyjones@hamilton.edu
Shiv	Khanna	Virginia Commonwealth University	804-828-1820	snkhanna@vcu.edu
Harriet	Kung	US DOE Office of Basic Energy Sciences	301-903-0497	harriet.kung@science.doe.gov
Igor	Kuskovsky	Queens College of CUNY	718-997-3367	Igor.Kuskovsky@qc.cuny.edu
Max G.	Lagally	University of Wisconsin-Madison	608-263-2078	lagally@engr.wisc.edu
Young	Lee	Massachusetts Institute of Technology	617-253-7834	younglee@mit.edu

**US DOE Program Meeting on Fundamental Synthesis
Research Challenges for 21st Century Materials:
Mechanism and Methods
Participants**

Firstname	Lastname	Organization	Phone	Email
Joseph	Libera	Argonne National Laboratory	630-252-7124	jlibera@anl.gov
Feng	Liu	University of Utah	801-587-7719	fliu@eng.utah.edu
Ying	Liu	Pennsylvania State University	814-863-0090	liu@phys.psu.edu
Thomas	Lograsso	Ames Laboratory	515-294-8425	lograsso@ameslab.gov
Karl	Ludwig	Boston University	617-353-9346	ludwig@bu.edu
Prashanth	Madras	Arizona State University	480-457-0185	ppm@asu.edu
R. William	McCallum	Ames Laboratory	515-294-4736	mccallum@ameslab.gov
Paul	McMillan	University College London	44-0-20-7679-4610	p.f.mcmillan@ucl.ac.uk
Anatoli	Melechko	Oak Ridge National Laboratory	865-566-2713	acm@ornl.gov
James	Misewich	Brookhaven National Laboratory	631-344-3501	misewich@bnl.gov
Rafael	Munoz-Espi	Stony Brook University	631-632-1315	rmunozespi@sunysb.edu
Ralph	Napolitano	Ames Laboratory	515-294-9101	ralphniastate.edu
Michael	Nastasi	Los Alamos National Laboratory	505-667-7007	nasty@LANL.gov
Alexandra	Navrotsky	University of California, Davis	530-752-3292	anavrotsky@ucdavis.edu
George	Nolas	University of South Florida	813-974-2233	gnolas@cas.usf.edu
Roberto	Paiella	Boston University	617-353-8883	rpaiella@bu.edu
Michael	Pellin	Argonne National Laboratory	630-252-3510	pellin@anl.gov
Xiaogang	Peng	University of Arkansas	479-575-4612	xpeng@uark.edu
Samuel	Peppernick	The Pennsylvania State University	814-863-3432	sjp185@psu.edu
Cedomir	Petrovic	Brookhaven National Laboratory	631-344-5065	petrovic@bnl.gov
Barrett	Potter	University of Arizona	520-322-2303	bgpotter@mse.arizona.edu

US DOE Program Meeting on Fundamental Synthesis
Research Challenges for 21st Century Materials:
Mechanism and Methods
Participants

Firstname	Lastname	Organization	Phone	Email
Longguang	Zhou	Rensselaer Polytechnic Institute	518-276-3943	lgzhou@gmail.com